

BLDSC no: - DX 97443

LOUGHBOROUGH
UNIVERSITY OF TECHNOLOGY
LIBRARY

AUTHOR/FILING TITLE	
ZANTOUT, B	
ACCESSION/COPY NO.	
008074/01	
VOL. NO.	CLASS MARK
	T

26 JUN 1998

25 JUN 1999

25 JUN 1999

14 JAN 2000

09 DEC 1997

20 NOV 1999

27 JUN 1997

5

000 8074 01



This book was bound by

Badminton Press

18 Half Croft, Syston, Leicester, LE7 8LD

Telephone: Leicester (0533) 602918.



THE PRODUCTION AND EVALUATION OF
SQUEEZE CAST Al-ALLOY MATRIX -
SHORT CERAMIC FIBRE COMPOSITES

by

B. ZANTOUT BSc (Damascus), MSc (Loughborough)

A Doctoral Thesis submitted in partial fulfilment
of the requirements for the award of
Doctor of Philosophy
of the Loughborough University of Technology

January 1986

Loughborough University of Technology Library	
Date	May '86
Class	T
Acc. No.	008074/01

ACKNOWLEDGEMENTS

The author is deeply indebted to the following:

Professor R J Sury, Head of the Department of Engineering Production and Director of Research, for providing the opportunity and facilities necessary to carry out this work.

Dr A A Das and Dr A J Clegg, Research Supervisors, for their kind encouragement and constructive guidance throughout their supervision of this investigation.

All members of the technical staff in the Department of Engineering Production, in particular Messrs B J Goodman, R Abrey, A Haigh, R Parker and J F Manning, for their assistance with experimental work. Dr D H Ross and Mr M F Page, Experimental Officers in the Department of Materials Engineering and Design, for conducting the Electron Microscopy work.

Dr A R Baker, at A.E. Developments Ltd for providing the SEM examination work reported in Appendix II.

SUMMARY

Research work on metal matrix-fibre composites has concentrated in the past on aligned fibre composites. The poor transverse strength of these composites is seen as a major hindrance to their practical use in the majority of engineering applications because stresses exist in more than one direction. Materials with isotropic properties are preferred and consequently reinforcement of composites in three dimensions will be necessary.

With this objective, an investigation was conducted to assess the method of fabrication and properties of Al-alloy reinforced with short fibres (SiC and Al_2O_3) randomly oriented in three dimensions. Two composite systems were examined: Al-4.5 Cu alloy reinforced with SiC fibre; and Al-3.75 Mg alloy reinforced with Al_2O_3 fibre.

The general approach was to establish a satisfactory manufacturing method for the composites before evaluating their mechanical properties. The vortex technique was used to introduce the fibres into the molten alloy. Pre-treatment of the fibres, to induce wetting, and the use of a specially designed device for fibre separation and introduction to the molten Al-alloys was found to be necessary so that a uniform distribution of fibres oriented in three dimensions could be achieved. The composites were squeeze cast, under conditions which were experimentally determined, to ensure the production of pore-free castings with fine equiaxed structures. The improvement in tensile strength and ductility of the cast metal, provided by squeeze casting, would be beneficial to composite properties.

Composite castings, with up to 10% volume fibre, were produced with a sound structure and with fibres that were uniformly distributed and randomly oriented in three dimensions.

It was found that the reaction between the fibres and the respective molten alloy must be closely controlled so that fibre reinforcement can be realised. In this respect the optimum time of contact between the fibres and the molten alloy was experimentally defined for both composite systems.

The tensile properties (UTS, 0.1% proof stress, and ductility) of the fibre-free alloys were substantially improved by squeeze casting. The addition of fibre produced further substantial improvement in the tensile properties of the squeeze cast composites, in particular elastic modulus and 0.1% proof stress. Furthermore, composite properties were isotropic. The improvement in the tensile properties of composite castings (as a result of the addition of fibre) was maintained at elevated temperatures. At 250°C, castings of both composite systems with 10% (volume) fibre had 0.1% proof stress and elastic modulus values similar to those for the fibre-free castings at room temperature..

The tensile properties of the composite castings were not affected by thermal cycling (at experimental conditions). The fatigue life of the squeeze cast composite was substantially improved over and above the initial improvement in fatigue life of the fibre-free castings produced by squeeze casting. Wear of cutting tools was adversely affected by the presence of fibres.

CONTENTS

	<u>Page No</u>
CHAPTER I: INTRODUCTION	1
1.1 The Project Objectives	3
CHAPTER II: BACKGROUND AND LITERATURE SURVEY	6
2.1 Definition of Composite	6
2.2 Basic Approach to the Design of Composite Systems	8
2.3 Principles of Fibre Reinforcement	9
2.3.1 Continuous Fibres	9
2.3.2 Discontinuous Fibres	14
2.3.3 Fibre Orientation	19
2.3.4 Effect of Fibre Ends	22
2.3.5 Three-dimensional Randomly Oriented Discontinuous Fibre Composite	25
2.4 Compatibility of Composite Constituents	28
2.5 Bonding and Interface Stability	29
2.5.1 Bonding	29
2.5.2 Interface Stability	30
2.6 Fabrication Methods	33
2.7 Squeeze Casting	35
2.7.1 Introduction	35
2.7.2 The Process	36
2.7.3 Advantages of Squeeze Casting	38
2.7.4 Process Parameters	39
2.7.5 Structure and Properties of Squeeze Castings	41
2.8 The Current Status of Metallic-Matrix Composites	42
2.8.1 Wettability of Ceramics by Liquid Metal	42
2.8.2 Composite Systems and their Properties	44
I Reinforced super-alloys	45
II Reinforced titanium	47
III Light-alloy composites	48

	<u>Page No.</u>
CHAPTER III: COMPOSITE PRODUCTION	56
3.1 The Design of Composite Systems	56
3.1.1 Selection of the Reinforcement Fibres	57
3.1.2 Selection of the Matrix Alloys	58
3.2 Exploratory Attempt to Produce Composites	59
3.2.1 Difficulties Met and Solved in the Production of Composites	61
3.3 Design and Manufacture of Equipment	65
3.3.1 Fibre Separation Device	65
3.3.2 Stirring Propeller and its Shaft	78
3.3.3 Modification of the Squeeze Casting Die and Punch	80
3.4 Experimental Set-up for the Production of Squeeze Cast Composites	84
3.4.1 The Set-up Used for the Production of Liquid Composites	84
3.4.2 Squeeze Casting Equipment	87
3.5 Method of Composite Production	89
3.5.1 Preparation of Matrix Materials and Fibres	89
3.5.2 Preparation of Liquid Composites	93
3.5.3 Squeeze Casting the Liquid Composite	95
3.6 Groups of Castings Produced	96
3.7 Heat Treatment of the Squeeze Cast Al-4.5 Cu Alloy	101
3.8 Observations on Composite Production	101
3.8.1 Fibre Rejection	101 *
3.8.2 Reaction of the LM5 Alloy with Atmos- phere	102
CHAPTER IV: COMPOSITE EVALUATION	104
4.1 Preview	104
4.2 Experimental Procedure and Techniques	105
4.2.1 Fibre Damage	105
4.2.2 Metallographic Examination	107
4.2.3 Electron Probe Microanalysis	108
4.2.4 Hardness Testing	109
4.2.5 Thermal Cycling	109

	<u>Page No.</u>
4.2.6 Room Temperature Tensile Test	111
4.2.7 High Temperature Tensile Test	112
4.2.8 Fatigue Testing.....	116
4.2.9 Fractured Surfaces Examinations....	118
4.2.10 Tool Wear Test	118
4.3 Thermal Stability of the Nicalon ^(R) Silicon Carbide Fibre	120
4.3.1 The Effect of Heat Treatment Conditions on the Tensile Strength of the Nicalon ^(R) Silicon Carbide Fibre	122
4.3.2 Differential Thermal Analysis (DTA)	126
CHAPTER V: RESULTS AND OBSERVATIONS	128
5.1 Macrostructure	128
5.2 Room Temperature Tensile Properties of the Cast Al-4.5 Cu and Al-3.75 Mg Matrix Alloys	128
5.3 Heat Treatment of the Squeeze Cast Al-4.5 Cu Matrix Alloy	129
5.4 Examination of the Fibre Surfaces	129
5.5 Fibre Breakage	130
5.6 Fibre Distribution and Orientation	130
5.6.1 Microscopic Examination	130
5.6.2 Tensile Properties of the Composite Parallel and Perpendicular to the Punch Movement	131
5.7 Electron Probe Microanalysis	132
5.8 Tensile Properties of the Squeeze Cast Composites	132
5.9 Fatigue Life	136
5.10 Fracture of Composites	136
5.10.1 Tensile Fracture	136
5.10.2 Fatigue Fracture	139
5.11 Tool Wear	140
5.12 Thermal Stability of Nicalon ^(R) Silicon Carbide Fibre	140
5.12.1 Tensile Strength (Room Temperature) of Fibre Subjected to Different Heating Cycles	140

	<u>Page No.</u>
5.12.2 Differential Thermal Analysis (DTA)	141
Tables 5-16 	142
Figures 37-85 	162
CHAPTER VI: DISCUSSION 	214
6.1 The Structure and Properties of the Squeeze Cast Matrix Alloys (Al-4.5 Cu and Al-3.75 Mg)	214
6.2 Heat Treatment of the Squeeze Cast Al-4.5 Cu Alloy 	217
6.3 Wetting of Fibres 	218
6.4 Structure of the Squeeze Cast Composites (Al-Cu/SiC and Al-Mg/Al ₂ O ₃) 	220
6.5 Method of Composite Production 	229
6.5.1 Viability of the Method of Production	228
6.5.2 Volume Content of Fibre 	230
6.5.3 Sources of Inclusion 	231
6.5.4 Reaction of the Al-3.75 Mg Molten Alloy with Atmosphere 	232
6.6 Effect of the Time of Contact Between the Fibre and the Molten Matrix on the Tensile Properties of the Al-Cu/SiC and Al-Mg/Al ₂ O ₃ Composites 	234
6.7 Tensile Properties of the Squeeze Cast Composites 	240
6.7.1 The Tensile Properties (Room Temperature) of the Composites of Section I (Casting Groups III, IV) 	240
6.7.2 The Tensile Properties of the Composites of Section III, Casting Groups VI and VII (Controlled Time of Contact), at Room and Elevated Temperatures	246
6.7.3 Comparison of the Experimental Results with the Theoretical Prediction of Composite Tensile Properties 	251
6.8 The Effect of Thermal Cycling on the Tensile Properties of the Composites 	259
6.9 Fatigue Life of the Composites 	260
6.10 Tool Wear 	264
6.11 Thermal Stability of Nicalon ^(R) SiC Fibre	265

	<u>Page No.</u>
CHAPTER VII: CONCLUSIONS	269
CHAPTER VIII: SUGGESTIONS FOR FURTHER WORK	274
REFERENCES	277
APPENDICES:	
I: A1.1 Press Load Test	291
A1.2 Flank Wear of a Turning Tool	292
II: Report on SEM Examination of Reaction Products of a Melt of LM5	294
III: Tables A3.1-A3.10	303
IV: Fibre Distribution, Figures A4.1-A4.4	321

CHAPTER I

INTRODUCTION

CHAPTER 1
INTRODUCTION

With the advance of modern technology, demands have increased on materials. The need for materials with improved properties is more urgent in the area of dynamic structures and machinery where high specific strength and modulus is more significant. The efficiency of dynamic structures such as aircraft, high-speed machinery, power generating equipment and aerospace equipment could be enhanced by improvement in the structural efficiency of the materials. In order to maintain the stiffness and strength of a structure or a component within minimum weight, materials with high specific strength and modulus are required. An extreme example to illustrate the significance of reduced weight of a structure or component, can be seen in the aerospace industry where the cost of lifting a unit of weight (1 kg) into space out of the atmosphere is of the order of \$25,000.

In addition to the critical stiffness and strength-to-weight ratio, many structures are limited in durability under service conditions. Those limitations relate to high temperature stress rupture, strength of the materials under fatigue loading, crack growth around notches and stress corrosion.

Engineering metals such as aluminium, cobalt, copper, chromium, iron, magnesium, nickel and titanium have specific moduli and strength in the range $1.3-3.5 \times 10^7$ cm and 2.5×10^6 cm respectively, while materials which are covalently bonded, such as boron and carbon, have a dramatically high specific modulus of 15×10^8 cm, and materials that have high covalent-bonding fractions, such as boron carbide, silicon carbide and aluminium oxide also have high specific modulus and strength (8×10^8 cm and 1×10^8 cm respectively).

The attractiveness of these materials is further enhanced by their low density and high melting points. These high values of strength and stiffness are attained when the materials are in the form of single crystal whiskers or fine fibres. These materials cannot be fabricated into large engineering structures, moreover they are brittle and therefore very sensitive to cracks and flaws, which make them weak in large section.

Although metal alloys have been strengthened considerably by various hardening mechanisms for improvements in static properties, they often sacrifice toughness and durability under dynamic service conditions. It appears that these materials have approached their limits and sharp increases in properties can no longer be anticipated by following the route of alloy development.

To utilise the exceptional properties of ceramics, it seems logical to incorporate the material in a matrix so as to achieve the desired structural shapes and properties. Such combinations are the composites of interest in this project. The most important aim in the design of composite materials is to increase the static and dynamic strength at both ambient and high temperature and reduce sensitivity to cracks and flaws. The concept of a composite material or system is to combine certain assets of the components of the composite system and suppress the shortcomings of the members in order to give the new synthesized composite unique and useful properties not obtainable from any member or component of the composite by itself.

A primary definition of a composite is a high strength and modulus material called the reinforcement, usually in the form of fibre or whisker (sometimes particulate), is combined with a second material called the matrix, which permits fabrication into the desired shape and transfer of the external loads onto the carrying reinforcement. Resin-matrix composites have received the widest recognition and acceptance in the area of high-modulus composites. In these composites the high-

modulus fibre (reinforcement) is combined with a matrix that has been selected for its ease of fabrication into a useful structural shape. In addition there is little chemical or mechanical interaction between the two phases at fabrication and service temperatures, which simplifies the matrix-fibre compatibility problem.

These two factors (ease of fabrication and compatibility), which are behind the success story of resin-matrix composites, are mainly responsible for the limited success in the case of metal-matrix composites. However, metal-matrix composites have advantages that are very important in the utilization of structural material. They include the combination of the following properties:

- higher service temperature
- higher strength and modulus
- higher toughness and impact properties
- low sensitivity to change in temperature and thermal shock
- higher electrical and thermal conductivity.

Although metal-matrix composites may have a higher density than resin composites, this disadvantage can be minimised by using a matrix of a light metal.

1.1 THE PROJECT OBJECTIVES

The availability of high strength ceramic whiskers and fibres and the proven concept of composite strengthening has challenged metallurgists and material scientists to develop metal-matrix composites. Consequently, large amounts of money and effort have been spent in developing fibre and whisker reinforced metal-matrix composites for possible use at both ambient and elevated temperatures.

The extent of work in this field on a world-wide scale has been considerable, which reflects the importance of and the need for these materials.

The potential importance and viability of metal-matrix fibrous composites and the challenge were the main attractions for undertaking an investigation into the reinforcement capability of ceramic fibres in a cast aluminium alloy matrix.

Most of the previous work on fibre reinforced metals has been mainly concerned with directional reinforcement of the matrix, which gives directional properties. Although those composites have their own applications, in the majority of engineering applications stresses exist in more than one direction and usually in three (triaxial stresses). Thermally induced stresses usually are triaxial. Under these conditions, the reinforcement should be designed to provide isotropic properties, i.e. reinforcement fibre should be randomly oriented in the matrix.

The absence of a satisfactory and cost effective technique for the production of metal-matrix composites is a major factor* behind the limited success so far in the field of metal-matrix composites. This is despite the considerable time and effort spent to develop these composites. Fabrication techniques have to be improved and costs reduced or a new satisfactory technique developed if any serious industrial market is to emerge.

With these views in mind the main objectives of this investigation were:

- to design a metal-matrix composite system with isotropic properties and improved specific strength and modulus and other properties at both ambient and moderately high temperature (300°C)

* Other factors are: the high cost of the reinforcement materials and compatibility problems between the two phases

- to establish a satisfactory manufacturing technique for producing this composite system
- to optimize fabrication conditions and control the quality of composite for optimum properties
- to evaluate the quality and mechanical properties of the composites produced at ambient and high temperatures.

CHAPTER II

BACKGROUND AND LITERATURE SURVEY

CHAPTER 2

BACKGROUND AND LITERATURE SURVEY

2.1 DEFINITION OF COMPOSITE

Before discussing the various aspects of composite materials, it is necessary from the beginning to define what is meant by a composite material. This necessity arises because there is some confusion concerning the definition of these materials even among materials scientists, some of whom attribute to these materials a very broad meaning, whilst others confine themselves to a much more specific definition.

According to Javitz¹:

"Theoretically, any material that is not a pure substance and contains more than one component, may be classified among the composite materials".

This definition includes nearly all natural material such as wood, bones, etc. and some synthetic materials such as certain powder metallurgy products, electrical insulators, porcelain-coated steel, etc. The weakness of this definition is that it allows one to classify among the composites any mixture of materials without indicating either its specificity or the laws which should govern it which distinguish it from other banal, meaningless mixtures².

Kelly³ clearly stressed that:

"The composite should not be regarded simply as a combination of two materials, it is still that, but in modern technology it has acquired a broader significance, the combination has its own distinctive properties, in terms of strength or resistance to heat or some other desirable quality, it is better than either of the components alone or radically different from either of them".

Berghezan⁴ stresses the difference between composites and alloys:

"The composites are compound materials which differ from alloys by the fact that the individual components retain their characteristics but are so incorporated into the composite as to take advantage only of their attributes and not of their shortcomings, in order to obtain an improved material".

Javitz¹ underlines composites' multifunctional service:

"Composites are multifunctional material systems that provide characteristics not obtainable from any discrete material. They are cohesive structures made by physically combining two or more compatible materials, differing in composition and characteristics and sometimes in form".

Berghezan⁵ insists more on a design philosophy in his definition of fibrous composites:

"The fibre reinforced composites are only those heterogeneous materials which are prepared by association and bonding in a single structure of materials possessing quite different properties and when these are complementary, give a composite material possessing additional and/or superior properties to the individual components either alone or mixed together".

Here one has to be careful since when two materials are combined together, each one possesses some good qualities as well as some defects, consequently it is possible that the new material may inherit, from the initial constituents either a mixture of qualities and defects, or at the extreme only qualities or only defects. So it is important to design the composite materials to possess the required qualities only and fulfil in service all the previously assigned functions.

2.2 BASIC APPROACH TO THE DESIGN OF COMPOSITE SYSTEMS

In 1947, Richard Young, an aeronautical engineer, by chance succeeded in obtaining a composite material composed of glass fibres and an epoxy resin. The measured properties of this first man-made true composite could not be explained by existing knowledge, so a new theory of fibre reinforcement was developed⁶⁻⁸. These new materials have revealed an entirely new approach to materials development, and we now possess an adequate but incomplete knowledge, which provides the basic principles which have to be obeyed when designing a composite system in order to achieve a material which possesses the desired properties, so that it can fulfil in service all assigned functions.

The most obvious design requirement is to select the most appropriate individual components based on previous assigned functions which each individual component has to fulfil in service. For instance, if the composite is designed to carry a load, then one of the components should be selected for strength to carry the load and the other must transfer the load to its stronger partner and that is why it should be able to yield elastically, and if necessary, plastically.

In addition to the mechanical properties, candidate components should be compatible with respect to: mechanical, chemical, and physical characteristics, so that when combined they function together in harmony.

Another requirement is that the components, to be able to fulfil in the final composite their specific assigned functions, need to be introduced in a certain geometrical shape, which is determined precisely by the functions they have to fulfil. Hence, the strongest constituent has to be introduced as long shapes, preferably as fibre, whisker, ribbons or foils, while the weaker constituent has to surround and bind the individual fibres in a single structure.

It is also essential that individual components have to retain their own properties and to be so associated in the new material that they

exploit in service only their qualities and not their defects.

2.3 PRINCIPLES OF FIBRE REINFORCEMENT

2.3.1 Continuous Fibres

Four stages in the stress-strain behaviour of a metal-matrix composite with continuous uniaxially aligned fibre when it is stressed parallel to the fibres were described by McDaniels et al (1963)⁹ and by Kelly and Davies (1965)¹⁰. In the region of the first stage both the fibres and the matrix deform elastically (Figure 1).

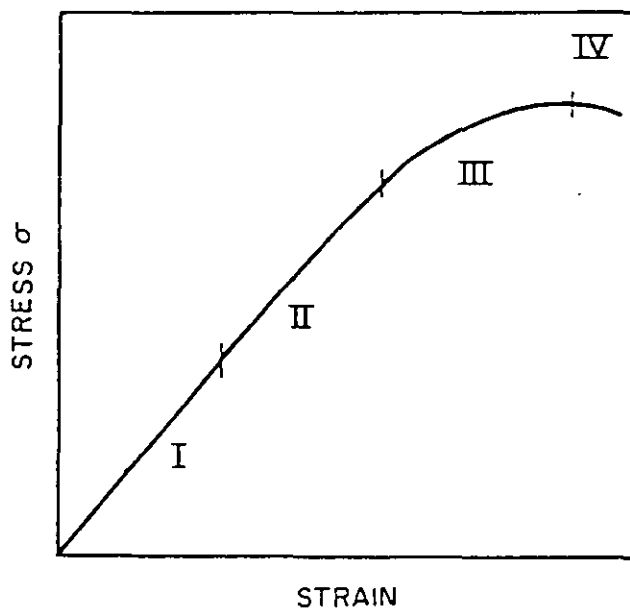


FIGURE 1: Schematic curve showing the stress-strain behaviour of a metal-matrix composite: (I) fibre elastic, matrix elastic; (II) fibre elastic, matrix plastic; (III) fibre plastic, matrix plastic; (IV) fibre fractured (ref 10)

Assuming a good bond exists between fibres and matrix, the load carried by a composite is simply the sum of the loads carried by the two components

$$L_c = L_m + L_f$$

where L refers to load and the subscripts c , m and f refer to composite, matrix and fibre respectively.

This equation can be expressed as:

$$\sigma_c \cdot A_c = \sigma_m \cdot A_m + \sigma_f \cdot A_f$$

We may substitute volume terms for the area terms:

$$\sigma_c \cdot V_c = \sigma_m \cdot V_m + \sigma_f \cdot V_f$$

and since $V_c = V_m + V_f = 1$

Thus
$$\sigma_c = \sigma_f \cdot V_f + \sigma_m (1 - V_f) \quad (1)$$

If there is no slipping at the interface, then the strain ϵ in each of the components, is the same:

$$\epsilon_c = \epsilon_m = \epsilon_f$$

Now Young's modulus, $E = \sigma/\epsilon$

$\therefore E_{c1} = E_f \cdot V_f + E_m (1 - V_f) \quad (2)$

In the region of the second stage the fibre is extending elastically, while the matrix is extending plastically. If the fibre is in a high volume fraction and has a considerably higher elastic modulus than the matrix, E_{c2} is nearly equal to E_{c1} (E_{c1} & E_{c2} are the composite elastic moduli in the regions 1 and 2 respectively). The modulus of the composite will be the sum of the effective slopes on the stress-strain curves of the two phases multiplied by their volume positions:

$$E_{c2} = E_f \cdot V_f + (d\sigma_m/d\epsilon_m) \cdot (1 - V_f) \quad (3)$$

where $d\sigma_m/\sigma_{em}$ is the effective strain hardening coefficient of the matrix, which is normally much less than the modulus of the fibre and can be neglected. Therefore, the modulus of the elastic-plastic region of the stress-strain curve can be given as:

$$E_{c2} = E_f \cdot V_f$$

E_{c2} is nearly equal to E_{c1} (85% in 50 v/v aluminium-boron), it is not a truly elastic modulus because straining the composite into region II results in some permanent elongation.

In the third stage both fibre and matrix deform plastically. This deformation mode might be different from the deformation of the constituents alone with respect to necking and other plastic flow. In some ductile fibres, it has been found that the onset of necking has been delayed by the constraint of the matrix. This effect was pointed out by Pichler (1965)¹¹ in the silver-steel composite system and led to strengths higher than the summation of the strength of the constituents.

Stage IV in the stress-strain curve includes fracture of the high strength fibres, and the matrix transfers the load from broken fibre ends to unbroken segments and flows around the opening pores or cracks, normally fracture of the fibres causes failure of composite which terminates stage IV. If the matrix has sufficient ductility and the dynamic loads associated with multiple fibre fracture do not lead to catastrophic failure, deformation of the composite will continue up to a tensile strength of

$$\sigma_{cu} = \sigma_{mu} (1 - V_f) \quad (4)$$

where subscript u refers to ultimate values.

This case only happens when the volume fraction fibre is less than the minimum value. Provided a minimum volume fraction of fibres is exceeded the tensile strength of the composite is given by

$$\sigma_{cu} = \sigma_{fu} \cdot V_f + \sigma_m' (1 - V_f) \quad (5)$$

σ_m' is the stress on the matrix at a strain equal to the fibre strain at failure.¹²

The rule of mixtures (equation 5) is obeyed only if complete composite failure results when the fibre fails. This is the case when $\sigma_{cu} > \sigma_{mu} (1 - V_f)$

or

$$\sigma_{fu} \cdot V_f + \sigma_m' (1 - V_f) > \sigma_{mu} (1 - V_f)$$

$$V_f (\sigma_{fu} - \sigma_m' + \sigma_{mu}) > \sigma_{mu} - \sigma_m'$$

From which we define a minimum value of V_f , V_{min} , below which the rule of mixtures does not apply:

$$V_{min} = (\sigma_{mu} - \sigma_m') / (\sigma_{fu} - \sigma_m' + \sigma_{mu}) \quad (6)$$

Above this volume fraction the ultimate tensile strength of the composite rises. At some volume fraction above V_{min} the strength of the composite is equal to that of the matrix alone. Below this critical value, V_{crit} , no reinforcement occurs.

For reinforcement, by definition, the composite must be stronger than the matrix alone:

$$\sigma_{cu} > \sigma_{mu}$$

or

$$\sigma_{fu} \cdot V_f + \sigma_{m'} (1 - V_f) > \sigma_{mu}$$

Thus

$$V_{crit} = (\sigma_{mu} - \sigma_{m'}) / (\sigma_{fu} - \sigma_{m'}) \quad (7)$$

The strength of the composite can be plotted as a function of the fibre volume fraction, Figure 2:

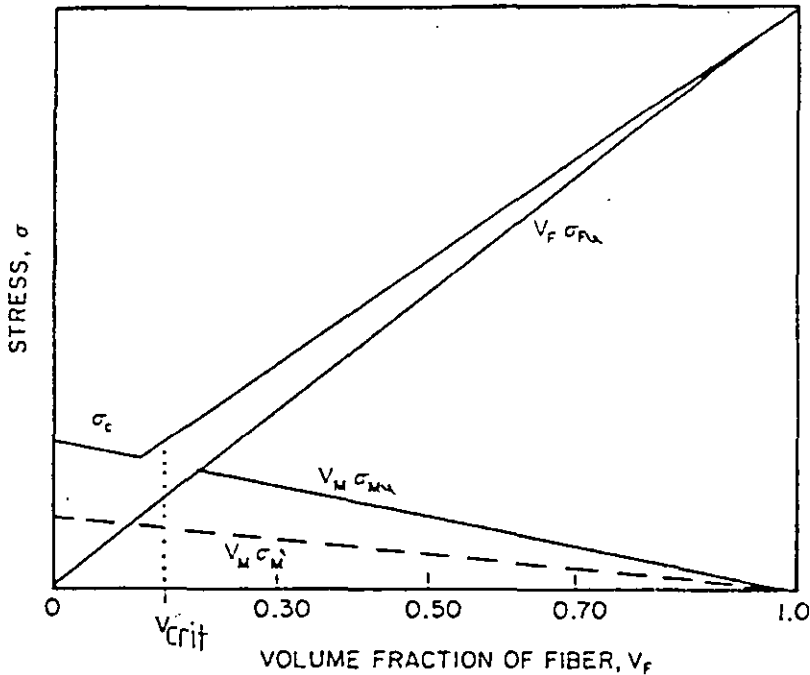


FIGURE 2: Rule-of-mixtures strength for a brittle, strong fibre with a ductile matrix (ref 12)

2.3.2 Discontinuous Fibres

The situation is more complicated when the reinforcement fibres are discontinuous, since the fibres in a composite are loaded up via interfacial shear stresses, the end portions of discontinuous fibres are under lower stresses than the central portion.

When a composite reinforced with uniaxially aligned fibre is stressed in a direction parallel to the fibres, the axial displacement in the fibre and matrix will be different due to the difference in elastic moduli, and shear stresses in the direction of the fibre axis are produced on planes parallel to this axis.

These shear stresses are the means by which tensile loads are transferred to (through the interface) and supported by the fibres.

From the balance of forces acting on a long, thin fibre impeded in stressed matrix in the z direction, Figure 3

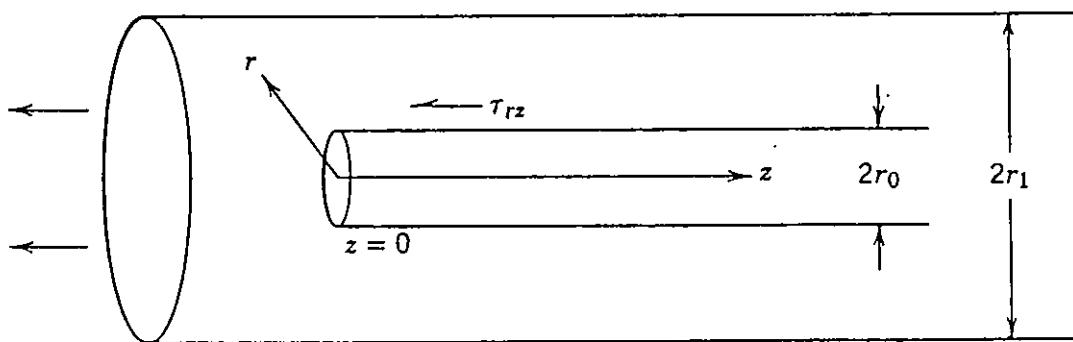


FIGURE 3: The distribution of stresses of a uniaxially loaded fibre in a matrix (ref 14)

$$dP = 2\pi r_0 \tau_{rz} dz \quad (8)$$

where P is the tensile load in the fibre of radius r_0 ,

τ_{rz} is the shear stress at the fibre-matrix interface and is a function of z .

Following Cox¹³, σ_{zz} is given approximately by:

$$\sigma_{zz} = E_f \cdot \epsilon \left[1 - \frac{\cosh \beta(z/2 - Z)}{\cosh \beta(l/2)} \right] \quad \text{for } 0 \leq z \leq l/2 \quad (9)$$

(both fibre and matrix are assumed to behave elastically).

where σ_{zz} is the tensile stress in the fibre, ϵ tensile strain in the composite, β is a function of the elastic constants of the fibre and the matrix, and of the fibre separation.

Equation (9) does not apply close to the fibre ends, where the actual shape of the fibre ends must be considered.

$E_f \cdot \epsilon$ is the stress in the fibre when subjected to a strain equal to that of the composite. From equation (9), σ_{zz} is less than $E_f \cdot \epsilon$, but approaches it when z approaches $l/2$ provided l is large.

From equations (8) and (9), we can find that the shear stress in the matrix at the fibre ends, τ_{\max} , is approximately equal to $\sigma_{f\max}$ (maximum stress in the fibre). If a fibre is appreciably strengthening a composite, $\sigma_{f\max}$ ($\sim E_f \cdot \epsilon$) for a long fibre is very large compared to the stress at which the matrix fails or yields plastically, so τ_{\max} is never attained. A matrix unable to flow plastically must fail. In the case of a metal matrix the shear stresses at the interface are relieved either by shear of the interface or by shear of the matrix, usually plastic flow occurs in the matrix and the interface does not fail at small strains.

Flow of the matrix means that τ_{rz} at $r = r_0$ in Equation (8) never rises above τ the flow stress in shear of the matrix. When the composite is subjected to a strain ϵ greater than the plastic yield strain of the matrix, the whole of the matrix is brought to its yield stress, and equation (9) becomes irrelevant.

By integrating equation (8) and substituting $P = \pi r_0^2 \sigma_f$, we have

$$\sigma_f = \frac{2\tau}{r_0} \cdot z \quad (10)$$

(σ_f is the stress in the fibre).

The strain in the fibre cannot exceed the strain in the composite ϵ , the fibres are loaded from both ends, and σ_f will build up to the value $E_f \cdot \epsilon$ at the fibre mid-portion provided the length a , Figure 4, exceeds

$$r_0 \left(\frac{E_f \cdot \epsilon}{2\tau} \right)$$

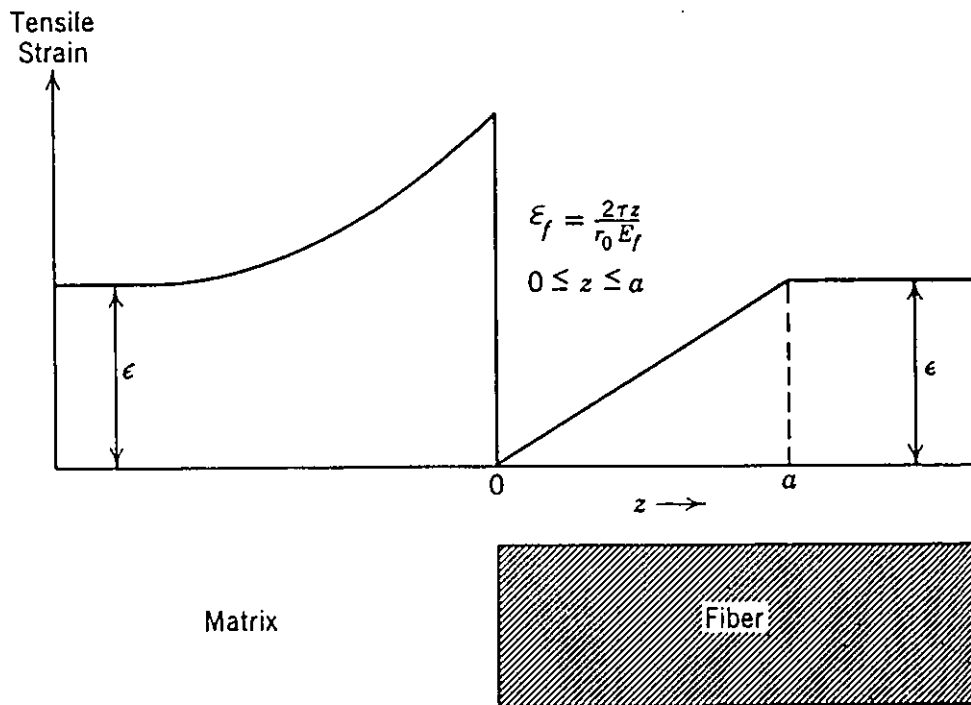


FIGURE 4: Distribution of tensile strain around a fibre end (Ref 14)

Figure 4 shows that the tensile strain in the matrix at the fibre ends is larger than in the composite as a whole, in the fibre it is less. The stress builds up linearly in the fibre and is elastic. The matrix flows round the ends of the fibre as well as parallel to it, the strain in the matrix is mainly plastic. It is possible to break a fibre by plastic flow of the matrix provided the stress in it builds up to the fracture stress $\sigma_{f.u}$.

If ℓ_c is the initial fibre length for this to occur, we have from equation (10)

$$\frac{\ell_c}{2} = \frac{r_0 \sigma_{f.u}}{2\tau} \quad \text{or} \quad \frac{\ell_c}{d} = \frac{\sigma_{f.u}}{2\tau} \quad (11)$$

ℓ_c is the critical length and ℓ_c/d the critical aspect ratio.

For a composite containing a large number of parallel discontinuous fibres dispersed in a ductile matrix, if the stress builds up linearly from the end of the fibre as shown in Figure 5, then the average stress in a fibre ($\bar{\sigma}$) over its length is:

$$\bar{\sigma} = \sigma_{f.u} \left(1 - \frac{\ell_c}{2\ell}\right) \quad (12)$$

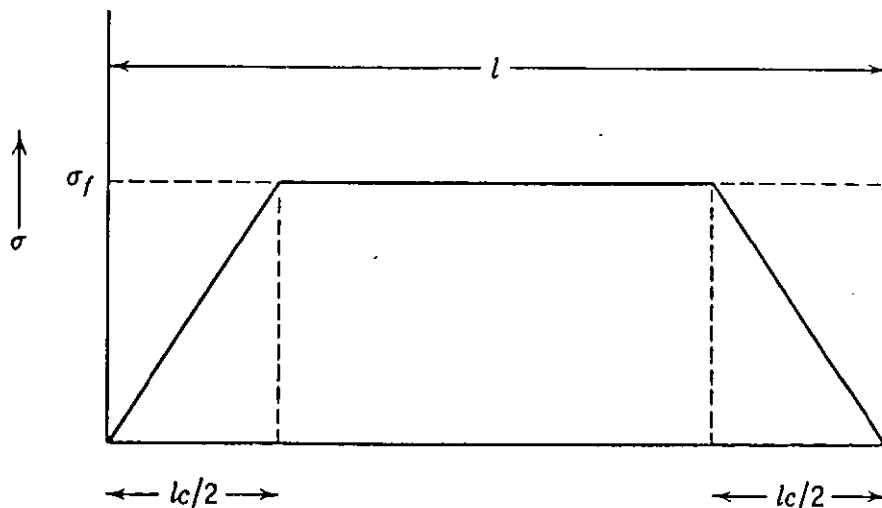


FIGURE 5: Expected variation of stress inside a fibre (ref 14)

Substituting in equation (5) we obtain the tensile strength of the composite

$$\sigma_{cu} = \sigma_{fu} \cdot V_f \left(1 - \frac{1}{2\alpha}\right) + \sigma_m' (1 - V_f) \quad (13)$$

where $\alpha = l/l_c$ and is a measure of the ratio of the actual fibre length to the critical length. From equations (5) and (13), we find that discontinuous fibres will always strengthen a composite less than continuous ones. However this will not be of importance if $\alpha = l/l_c$ can be made large. Figure 6 shows that 95% of the strength obtained with continuous fibres is reached with discontinuous ones, if l/l_c is equal to 10.

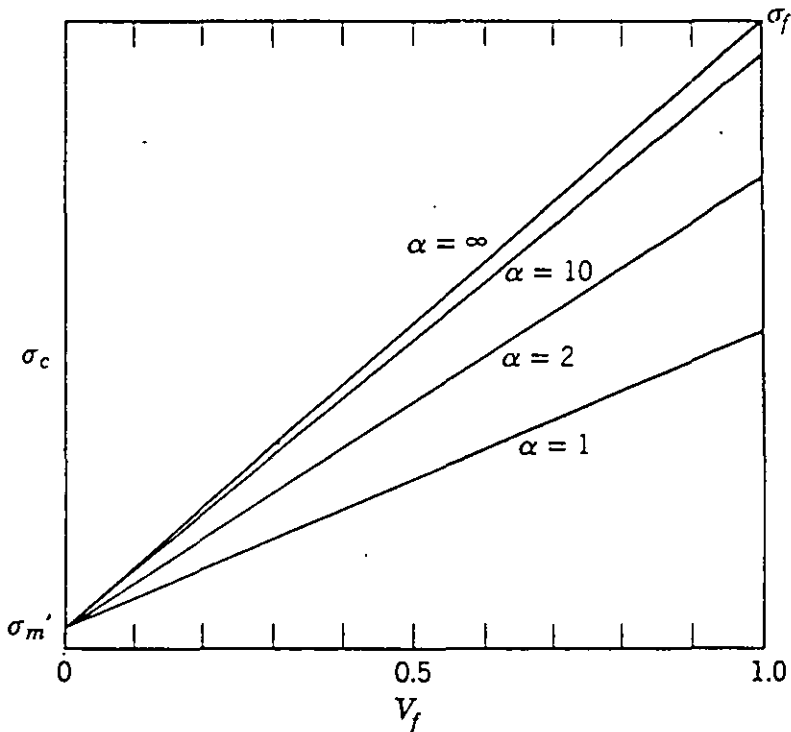


FIGURE 6: Theoretical variation of composite strength with volume fraction for discontinuous fibre, $\alpha = l/l_c$ (ref 14)

This analysis applies only when $l > l_c$ where the ultimate strength of the fibre is achieved. When $l < l_c$ the ultimate strength of the fibre is not achieved so that failure occurs when the ultimate stress of the matrix is reached, and the average stress in the fibre is:

$$\bar{\sigma}_f = \frac{\tau_f \cdot l}{2r_0}$$

and equation (5) is modified to

$$\sigma_{cu} = \frac{\tau_f \cdot l \cdot V_f}{2r_0} + \sigma_{mu} (1 - V_f) \quad (14)$$

where σ_{mu} is the ultimate stress of the matrix
 τ_f is the shear flow stress of the matrix.

In this case $l < l_c$ fibres tend to pull-out.

2.3.3 Fibre Orientation

Kelly and Davies¹⁰ have studied the effect of fibre orientation on a fibre reinforced metal with the metal matrix in the plastic state.

If the fibres are orientated at an angle θ to the applied stress σ , three possible modes of failure exist:

1. The matrix can flow parallel to the fibres until the fibres fail. By considering the planes on which the stresses act, the stress necessary to produce failure is given by:

$$\sigma_{f.u} = \sigma \cos^2 \theta \quad (15)$$

2. The matrix can fail in shear on a plane parallel to the fibres. The stress necessary to cause this failure is given by the equation:

$$\tau_{mu} = \sigma \sin\theta \cos\theta \quad (16)$$

The matrix however is usually constrained to some extent so that the value of shear stress (τ_{mu}) increases. The relation has been found to be:

$$\tau_u' = 1.5 \tau_{mu} \quad (17)$$

Using this increased value equation (16) becomes:

$$1.5 \tau_{mu} = \sigma \sin\theta \cos\theta \quad (18)$$

3. Alternatively failure could occur when the matrix fails by flowing transversely to the fibre. The stress that will cause this failure is given by:

$$\sigma_{f.u.p} = \sigma \sin^2\theta \quad (19)$$

where $\sigma_{f.u.p}$ is the ultimate strength of the fibre in plane strain.

This mode of failure is dependent on the inter-fibre spacing being sufficient so that no dispersion strengthening effect will occur.

$$\sigma_{f.u.p.} = 1.15 \sigma_{f.u} \quad (20)$$

($\sigma_{f.u}$ = ultimate strength in tension).

Substituting into equation (19)

$$1.15 \sigma_{f.u} = \sigma \sin^2 \theta \quad (21)$$

Figure 7 shows the variation of the fibre strength with orientation.

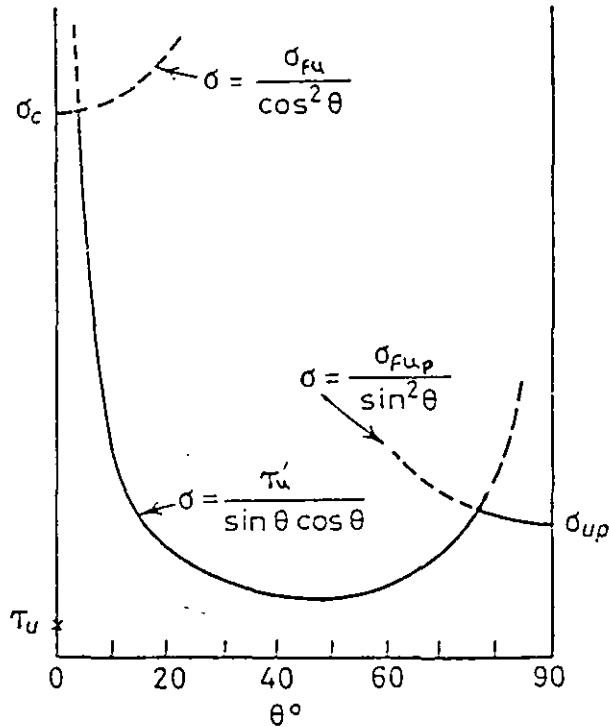


FIGURE 7: Variation of fibre strength with orientation (ref 10)

For very small angles of orientation the first failure mode is critical and the strength increases. At a certain value, called the critical angles, the second mode of failure becomes critical. A sudden loss in strength is seen to occur producing a minimum value at approximately 45 degrees. Toward the end of the orientation range the third mode of failure becomes critical. Thus it can be seen that for the majority of the range the important property is the shear

stress of the matrix, while for small angles of orientation it is the fibre strength, and for large angles of orientation it is the transverse stress.

2.3.4 Effect of Fibre Ends

The strength and failure behaviour of short fibre composites are complicated by the discontinuity of fibres and the interaction between the fibres and the matrix at the fibre ends. C.T. Sun¹⁵, using a finite element model, has studied the shear stress concentration near the fibre ends. This study showed a high shear stress concentration at the fibre end (Figure 8) which is dependent on the fibre end geometry. Sun's finding is confirmed by Pin and Sutcliff¹⁶

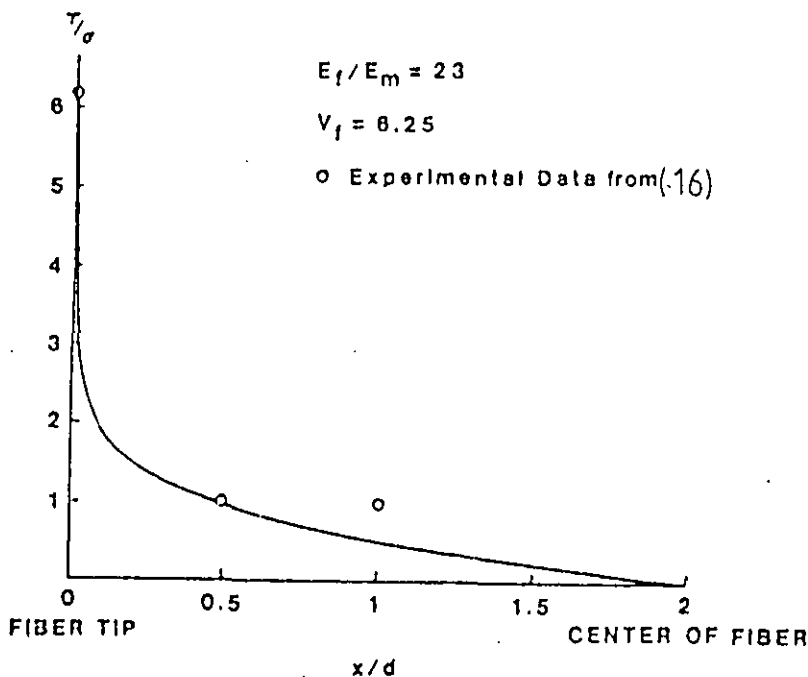


FIGURE 8: Shear stress concentration near fibre ends (ref 15)

whose experimental data (Figure 8) was obtained using a photoelasticity method.

Norio Sato¹⁷ suggested a fracture mechanism for short fibre composite in which fracture starts by interfacial cracks occurring at the fibre ends due to stress concentration.

Riley¹⁸, taking into consideration fibre length and stress distribution at fibre ends, obtained the following equation:

$$\sigma_{cu} = \frac{6/7}{1 + (5\ell_c/7\ell)} \sigma_{f.u} \cdot V_f + \sigma_m' (1 - V_f) \quad (22)$$

Fukuda and Chow¹⁹ used a probabilistic approach to the failure of fibres caused under the influence of the neighbouring fibre end, and they found:

$$\sigma_{cu} = \sigma_{fu} \cdot V_f \cdot F + \sigma_m' (1 - V_f) \quad (23)$$

where F is the reinforcement factor which is a function of the number of fibre ends in a defined critical zone.

Equations 22 and 23 should be compared with the modified rule of mixture for discontinuous fibre (equation 13):

$$\sigma_{cu} = \sigma_{fu} \cdot V_f (1 - \ell_c/2\ell) + \sigma_m' (1 - V_f) \quad (13)$$

In Figure 9, a comparison is made between the three previous predictions of the strength of a discontinuous fibre composite. The wide difference in the predicted values of composite strength is a reflection of the complexity and difficulty in simulating the actual composite.

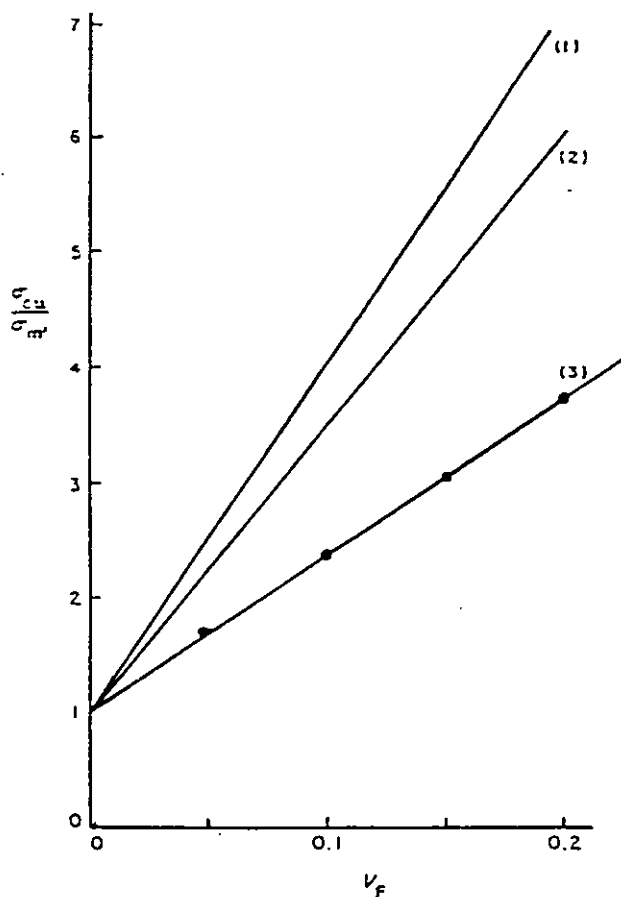


FIGURE 9: Strength of short fibre composites as a function of V_f with $l = 0.5$ mm.

1. Modified rule of mixtures (equation 13);
2. Riley's solution;
3. Fukuda's solution. (ref 19)

In the modified rule of mixtures (equation 13), only the fibre length was taken into consideration. Fukuda and Chou have derived their formula on the basis that fibres which end on the critical zone do not contribute to the strength of the composite (fibre length is a parameter which affects the probability of a fibre ending in the critical zone). Stress concentration at the fibre end was not considered, instead the effect of fibre ends on stress distribution in a neighbouring fibre was considered. The effect was on the average fibre stress and not the localized effect.

Riley considered both fibre length and stress concentration at fibre ends, but as other researchers made the assumption of constant equal axial strain between the fibre and the matrix material. This assumption is valid only for continuous fibre where the composite fails at fibre fracture, and for a short fibre composite with a high volume fraction of fibre²⁰.

Other classical assumptions had to be made all through the study of the strength of a short (discontinuous) fibre composite. These assumptions are:

- Fibres have equal length and strength
- There is no load transfer through fibre ends
- The effect of different fibres end geometries is ignored
- The effect of adjacent fibres to the stress distribution is ignored
- The only non-zero stress components are the axial stress in the fibre and the interfacial shear stress, and both axial and shear stress depend only on the axial coordinate of the fibre.

With all these assumptions it is questionable to what extent we can rely on these theoretical predictions of the strength of short fibre composite as a means to evaluate the quality of the actual composites. Although useful they should not be the only measure to assess a composite's quality.

2.3.5 Three-dimensional Randomly Oriented Discontinuous Fibre Composite

In this composite system, short fibres are objectively oriented in a random manner in the matrix material in order to achieve isotropic properties, unlike aligned fibre composites.

Theoretical analysis of this composite system is very limited and most available work arose through the analysis of the fibre misalignment effect on composite strength.

The rule of mixture is modified to^{21,22}:

$$\sigma_{cu} = \sigma_{fu} \cdot V_f \cdot F(l_c/l) \cdot C_o + \sigma_m' (1 - V_f) \quad (24)$$

where C_o is the orientation factor, which can be used to predict the strength of a randomly (3D) oriented fibre composite if the orientation factor is known for this case.

C_o can be estimated through theoretical analysis, but as the analysis is lengthy only the results are quoted here. Fukuda and Chou²³ have adopted the probabilistic approach to estimate the value of C_o and they found it to be:

$$C_o = 1/8$$

They obtained this value from their equation 52 ($C_o = f(B)$) at the limit of $\beta \rightarrow 0$, i.e. by discounting the critical zone (the basis of their analysis) or assuming that all fibres are bridging ones. This value of C_o should be compared with $C_o = 1/6$ obtained by Cox²⁴ and Christensen²⁵.

Christensen²⁵ has theoretically predicted the modulus of elasticity of a composite having fibres randomly oriented in three-dimensions:

$$E_{3D} = \frac{[E_{11} + (4\nu_1^2 + 8\nu_1 + 4)K_{23}][E_{11} + (4\nu_1^2 - 4\nu_1 + 1)K_{25}]}{3[2\sigma_{11} + (8\nu_1^2 + 12\nu_1 + 7)K_{23} + 6(\mu_{12} + \mu_{23})] + 2(\mu_{12} + \mu_{23})} \quad (25)$$

where μ_{12} and μ_{23} are the shear modulus of the composite in the 1-2 and

2-3 planes respectively.

E_{11} and ν_1 are the modulus and contraction ratio for uniaxial conditions
 K_{23} is the plane strain bulk modulus of the composite.

The moduli involved in equation (25) can be calculated from equations (8-12) in reference 25 if the properties of both fibre and matrix are known.

The value of E_{3D} given in equation (25) can be reasonably well estimated by the form²⁵:

$$E_{3D} = \frac{V_f}{6} \cdot E_f + [1 + (1 + \nu_m)V_f]E_m \quad (26)$$

for $V_f < 0.2$. ν_m is the Poisson's ratio for the matrix.

No experimental result is available for the 3D composite system and no comparison can be made with Christensen's prediction, but his prediction of E_{2D} seems to agree reasonably well with the experimental results of Lee²⁶.

Cox's²⁴ prediction of E_{3D} takes no account of matrix properties

$$E_{3D} = \frac{1}{6} E_f \cdot V_f \quad (27)$$

2.4 COMPATIBILITY OF COMPOSITE CONSTITUENTS

Composite materials by their nature include two or more dissimilar phases. These two phases have to be compatible with each other both physically and chemically if a successful coupling of the constituent is to take place. With metal matrix composites the physical compatibility problems of reinforcing a metal matrix with filament are often associated with the material's properties relating dilation to stress or thermal changes. The chemical compatibility problems relate mainly to interfacial bonding, interfacial chemical reactions, and environmental chemical reactions during composite fabrication and service.

The physical compatibility requirements dictate that the matrix should have sufficient ductility and strength in order to transfer the imposed loads to the reinforcing members evenly and without great discontinuities. In addition, local stresses in the matrix due to flow or possibly fibre ends should not cause high local stress concentration. For many applications, the mechanical properties of the matrix should include high strength and ductility and compliance^{27,28}. This requirement is more important when the reinforcement is short fibre. A very significant physical property relationship between the reinforcement and matrix is the thermal coefficient of expansion. Since the matrix is normally of higher expansion coefficient, it will be stressed in tension upon cooling from the normally high fabrication temperature. It is important that the disparity between thermal expansion coefficient should not result in the risk of high residual stresses (thermally induced) or the possibility of debonding during high temperature service.

Chemical compatibility is a more complex problem especially where there is a desire to form a strongly bonded interface, in order to allow efficient stress transfer and maintain continuity during heating-cooling cycles, and yet at the same time to prevent a destructive reaction both at fabrication and service temperatures. The first requirement implies the need for a chemical reaction²⁹, while the second requirement involves the prevention of a chemical reaction. Therefore

the ideal situation is one in which the reinforcement and matrix only react or are allowed to react to form a strong enough bond at fabrication but do not react at the operation (service) temperature. Alternatively a continuing reaction at the operating temperature could be accepted if the rate of reaction was sufficiently slow to give an adequate service life.

2.5 BONDING AND INTERFACE STABILITY

2.5.1 Bonding

The production of a good bond between the fibre and the matrix is the most important and also most difficult problem associated with the fabrication of composite materials. Good bonding should be achieved without any detrimental chemical attack or reaction at the constituent interfaces.

Good bonding is necessary for the transfer of load which is the principal objective of the reinforcement of a weak matrix by the high modulus high strength fibres. Good bonds may be promoted by:

- a) mutual interfacial diffusion restricted to the formation of a solid solution
- b) a superficial non-detrimental chemical reaction
- c) perfect interfacial contact between the components, which excludes any existing contamination layer at the interface.

These favourable bonding parameters can be promoted either in the liquid phase or in the solid phase.

I. *Liquid phase bonding:*

This is realised when the matrix is liquid during fabrication and wets the fibres. As bonding can only be realised if the components are brought into "intimate contact", the matrix (liquid) has to wet the fibres.

Wetting, however, requires either a certain degree of physical or chemical affinity. This affinity requirement is both difficult to promote and to control. It is most likely to start working when there is at least a partial solubility or when a detrimental chemical reaction is initiated. Wetting also depends on the mutual physical affinity between the components and this depends upon the ratio of their respective surface energy values.

Wetting properties can be improved by different means which modify the existing equilibrium between the initial surface tension forces by:

- a) modification of the chemical composition of the surface of the solid e.g. surface treatment of the fibres, such as cleaning, etching or coating.
- b) modification of the chemical composition of the liquid matrix e.g. addition of wetting agents
- c) modification of the wetting operation temperature and of the working atmosphere.

II. *Solid State Bonding (Diffusion Bonding)*

Diffusion is necessary to promote bonding and it should be restricted as it may lead to the formation of brittle phases at the interface. Diffusion is promoted by the application of high pressure and simultaneous heating (hot-pressing).

2.5.2 Interface Stability

I. *Chemical Stability*

The chemical stability can be estimated from reactions between bulk phases as well as from thermodynamic and kinetic data. In general both metals and ceramics react to varying degrees with each other.

Reported data on titanium-silicon carbide³⁰⁻³¹; nickel, cobalt and silver-silicon nitride³²; nickel-sapphire³³ and aluminium-sapphire³⁴; and nickel-silicon carbide³⁵ - indicate that rapid and severe fibre degradation occurs if extensive reactions occur between the matrix and fibres.

Investigating interfacial stability after exposure of composites to elevated temperatures can indicate their temperature limitations. Although alumina fibres are thermodynamically stable with respect to nickel, if nickel oxide is formed with diffusion of oxygen into the nickel, nickel oxide will react with alumina³⁶. To promote wetting and exhibit interfacial reaction with the matrix, fibres have been coated with both metal and ceramics. Any improved behaviour depends on the coating not being dissolved and the maximum time for dissolution (by diffusion).

II. *Mechanical Stability*

Mechanical stability of the interface is particularly important in fibre reinforced composites since the interface must transfer the applied load from the matrix to the fibres.

For efficient load transfer the interfacial shear strength (τ), should be:

$$\tau \geq \frac{d}{2l} \cdot \sigma_f$$

Fibres usually have an aspect ratio (l/d) from 100-1000, so that the interfacial strength need only be about 0.5% of the fibre strength (σ_f).

Although most engineering metals have shear strengths which exceed this, residual stresses from fabrication may cause flow or fracture at the interface. For example, the residual interfacial stress in a 2024 aluminium alloy-boron composite was found from X-ray line broadening to exceed the tensile yield strength of a control specimen of the matrix³⁷.

Plastic deformation in a ductile metal matrix can accommodate large interfacial stresses and strain. However, when the matrix cannot deform plastically, the interfacial shear strength should only be great enough to fully load the fibres to their breaking strength, so that the strain energy released when the fibre breaks can be absorbed by debonding at the fibre matrix interface³⁸. For large shear strength, the strain energy is released through crack propagation to adjacent fibres causing catastrophic failure of the composite.

The response of short fibre reinforced composites to applied loads is dependent on the strength and deformability of the interfacial zone as well as stress concentration at the interface. A weakly bonded interface may delaminate under applied stress and act as a crack.

At elevated temperature, the matrix strength will decrease and thus the fibre length required for efficient load transfer will increase. Mechanical gripping of the fibre by the matrix will be reduced at elevated temperature and cannot be relied on in this case.

2.6 FABRICATION METHODS

Many methods have been used in fabricating fibre-reinforced metals. Some of these will be briefly reviewed.

1. *Powder metallurgy techniques:*

This technique employs whiskers or short fibres. These are mixed with the matrix powder and then pressed to consolidate the matrix. Pressing could be followed by sintering to improve the matrix density. A major problem when using powder metallurgy is porosity and fibre breakage³⁹⁻⁴⁰.

2. *Vacuum infiltration of the fibres by molten metal:*

This technique has been a favourite method for the preparation of small specimens or to infiltrate a fibre preform with molten metals such as: aluminium; magnesium; silver; copper and alloy matrices. Volume contents of fibres as high as 80% have been reported⁴¹.

This technique is more suited to matrices of low melting temperature such as aluminium and magnesium. In addition to vacuum, external pressure may be used to facilitate infiltration. External pressure at the surface of a melt could be enough for the melt to infiltrate the fibre provided there is adequate venting.

3. Co-extrusion

In this method continuous wire or filament is drawn through a pressurised bath of the matrix metal and then through an extrusion die.

The temperatures employed can be much lower than with some other methods, and this reduces the possibility of a reaction between the fibre and the matrix. Mechanical difficulties with cooling have limited the use of this technique.

A similar technique is used to incorporate continuous fibres in a matrix by feeding the fibre through a pot of molten metal. The thickness of metal retained on the fibre can be regulated by the temperature of the bath and the speed at which the fibre is passed through the bath. Exposure time is critical to fibre degradation and, for example, boron fibres should not be exposed to aluminium for more than 30 sec in order to prevent loss of properties⁴².

4. *Deposition of matrix:*

Many techniques have been used to deposit a matrix metal onto fibres and whiskers.

In the plasma spray deposition method, a layer of fibres is laid up on a rotating mandrel and the matrix is plasma spray deposited on to the fibres. A second layer of fibres is put on, and the operations are repeated until the desired thickness and number of layers are attained. The composite is then hot pressed to eliminate porosity.

Vapour deposition has been employed for coating whiskers with the matrix metal. Electrodeposition provides an excellent means of applying matrix material to continuous fibres without the use of high temperatures. This produces a composite with very little degradation of fibre properties in comparison with some other methods. Excellent properties for a variety of fibres (B, SiC and W) in a nickel matrix have been reported^{43,44}.

5. Rolling

Hot or cold rolling can be employed to consolidate coated continuous fibres (processed by some other method like extrusion), or to introduce continuous fibres in matrix metal strips. However, this method is not suitable for brittle fibres which tend to break under the processing pressure.

6. *Hot pressing (diffusion bonding) method:*

In the hot pressing method a combination of heat, pressure, and plastic deformation is employed to produce fibre-reinforced composites. Alternate layers of matrix sheets and properly spaced continuous fibres or wires are hot pressed at a temperature in the range of 450-550°C to obtain the diffusion bond (matrix to matrix and matrix to fibres).

2.7 SQUEEZE CASTING

2.7.1 Introduction

Squeeze casting is the term used to describe the press-working of liquid metal into finished shapes. Solidification takes place under high pressure. Consequently, melt feed from hot spots into incipient shrinkage pores is achieved. The high applied pressure also keeps entrapped gases in solution and promotes intimate contact between casting and tooling for rapid heat extraction which results in a fine microstructure. No runners and gates are needed in squeeze casting and parts can be made to near net shape with a minimum of materials and energy utilization.

Russian literature credits D.K. Chernove with the envisioning of the concept of squeeze casting in 1878⁴⁵. However, it was not until 1937 that the first squeeze casting experiments were conducted for the production of brass and bronze cylinders. By 1965, Plyatskii⁴⁶ reported that the process had found application in large batch production at more than 150 plants. Several plants were producing over 200 different types of squeeze cast components using cast iron, steel, and various non-ferrous alloys.

Plyatskii's textbook on squeeze casting was responsible for providing the direction that future research would follow. It outlined process advantages and limitations, industrial applications, equipment and

tooling requirements for squeeze casting and generated the impetus for squeeze casting outside the Soviet Union.

Eight years of research at Toyota Motor Company (Japan) culminated in the introduction, in 1979, of squeeze cast aluminium alloy wheels into their production line for passenger cars⁴⁷. Wheels for mechanised combat vehicles were squeeze cast at GKN (UK)⁴⁸. The vehicle has 24 wheels and it is estimated that a 500 kg weight saving on each vehicle has been made by squeeze casting the wheels rather than forging them. Each wheel weighs 19 kg and solidifies in just 35s under a pressure of 600 bar. No subsequent machining is required except the drilling of bolt holes. In the USA, development work by Gould Inc showed squeeze casting to be a promising process for heavy-duty aluminium pistons⁴⁹. For diesel engines Wellworthy Ltd, an AEPLC company, in the UK, has also announced the successful production of squeeze cast diesel engine pistons for the commercial market⁵⁰.

2.7.2 The Process

Although squeeze casting is considered as a single production operation, four steps are involved (Figure 10). They are^{47,51}:

1. A measured quantity of molten metal is poured into an open, pre-heated metallic die cavity located in the bed of a metallic press.
2. Pressure is applied to the surface of the molten metal by lowering the upper die (punch) and closing the die.
3. The pressure is maintained until solidification is complete.
4. The upper die (punch) returns to its original position and the casting is ejected.

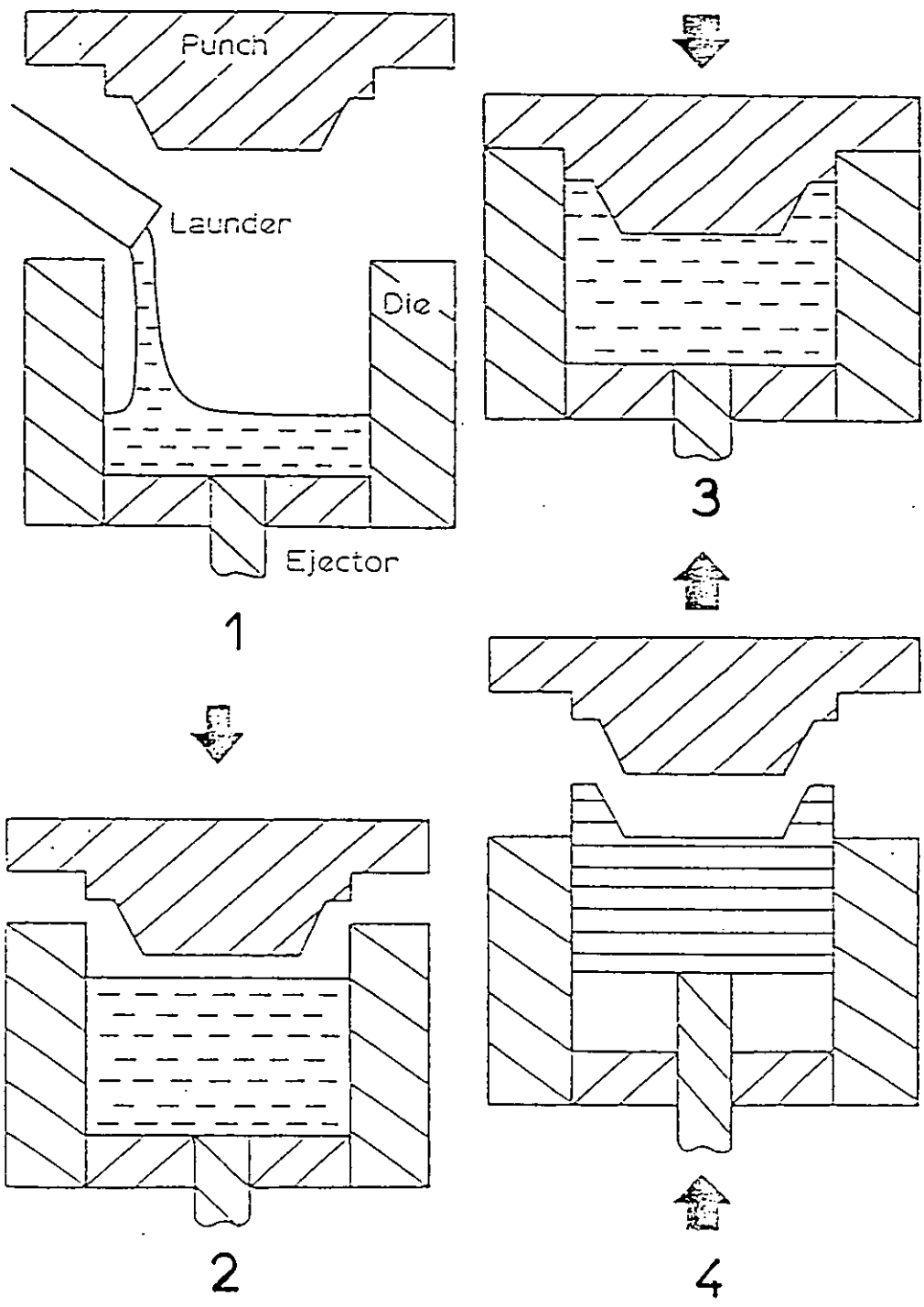


FIGURE 10: Steps in the manufacture of squeeze casting:

1. Molten metal poured into die
2. Punch activated
3. Pressure applied to molten metal
4. Casting ejected

(ref 51)

2.7.3 Advantages of Squeeze Casting

Squeeze casting may offer several advantages over forging and casting methods of production⁵¹⁻⁵³.

1. In the absence of a running and feeding system, a high metal yield is achieved.
2. An excellent surface finish and good dimensional reproducibility is possible, and the need for possible machining is minimised.
3. Squeeze casting may result in significantly improved mechanical properties^{47,54-56}.
4. Castings are heat treatable (compared with pressure die casting).
5. Complete elimination of shrinkage and gas porosity is possible.
6. Capability for producing a wide range of product sizes and section thicknesses⁵⁶.
7. Amenable to the production of a wide range of ferrous and non-ferrous alloys.
8. The ability to form complex shapes in a single operation at extremely low load (compared with forging loads) and at high production rates (compared with gravity die casting).
9. Fine grain size and metallurgical structure.
10. Isotropic mechanical properties are obtained under controlled production conditions.

2.7.4 Process Parameters

To produce successful squeeze cast components a number of process parameters need to be controlled.

1. *Metal casting temperature:*

The temperature at which the molten metal is poured into the die cavity is extremely critical from the standpoints of both casting quality and die life. Too low a casting temperature causes inadequate fluidity and results in incomplete die fill as well as cold laps on the casting surfaces. Too high a casting temperature, on the other hand, can cause extrusion of liquid metal through the tooling interfaces and can also result in shrinkage porosity in thick sections of the casting. The die life is also adversely affected by high pouring temperature. The ideal pouring temperature depends on the liquidus temperature, freezing range and die configuration. Narrow freezing range alloys tend to form solid layers almost immediately they contact the die wall and, therefore, the superheat is usually higher for these alloys. For aluminium alloys, the casting temperature is usually 10-100°C above the liquidus temperature⁴⁷ with the upper limit applicable to alloys with narrow freezing range. In the case of copper-based alloys and steels, the superheat required is usually 30-150°C since these alloys freeze more rapidly in contact with the metal die.

2. *Die temperature:*

Die temperature is maintained between 200 and 300°C. Lower temperature can lead to thermal fatigue failure in the die and cold laps on the surfaces of the casting. Very high die temperatures (above 400°C) can cause hot spots and shrinkage pores in the casting. Ferrous alloys have a greater tendency for welding to the surface of an overheated die.

3. *Temperature of pressure application:*

Some workers^{57,58} suggest that pressure should be applied when the metal is near the "zero fluidity temperature". This is interpreted as being reached when continuous solid phase skeletons have formed in a two phase alloy, and the metal loses its fluid flow properties. It is usually midway between the liquidus and solidus of the alloy.

However, according to others^{52,56} the metal should be liquid when the pressure is applied for squeeze casting to be fully effective. Pressure is best applied at a temperature near the alloy liquidus which would result in undercooling as a result of the increase of the melting point at pressures higher than one atmosphere⁵⁹. Undercooling will result in grain refinement which is proportional to the degree of undercooling, and a true squeeze casting consists of fine equiaxed grains as a result of correct pressurisation applied at the appropriate time.

Control of melt temperature is achieved by controlling the delay time between pouring and pressure application.

4. *Pressure level:*

A minimum pressure of 70 to 105 MN/m² is required in order to eliminate shrinkage and gas porosity for most ferrous and non-ferrous metals⁴⁷. However, the geometry of the casting frequently dictates the use of higher pressures for die filling and porosity control.

Porosity elimination is achieved by a "burst-feeding" liquid or semi-liquid metal through a network of solid skeletons and by keeping dissolved gases in solution. Raising the pressure level above the minimum consistent with the production of sound castings has been found to provide grain refinement and higher mechanical properties^{52,54,55}.

5. *Melt quality and quantity:*

Since the metal is poured directly into the die cavity it is important that dross and other suspended impurities are removed before pouring. Degassing is not usually necessary^{54,60} in this process.

Metering precise quantities of molten metal into the die cavity is essential, as this determines the casting dimension measured from the plane of contact of the punch.

2.7.5 Structure and Properties of Squeeze Castings

Studies by Epanchinstev⁶¹ on Al-Si, Cu, Pb and Fe-C alloy systems showed that pressurization widens the α -phase field for Al-Si alloys, and that squeeze casting could thus be used to produce single phase castings at an unusually high level of silicon. He demonstrated that when the melt is pressurized at the liquidus temperature, the application of pressure raises the liquidus temperature. This induces supercooling of the solidifying melt and grain refinement to the extent dictated by the pressure level and degree of supercooling. Epanchinstev reported a two fold increase in tensile strength, elongation, hardness, and impact strength, over gravity cast values, when pressures of 150 to 300 MN/m² were applied to a Cu-20 wt% Pb alloy during solidification.

Chatterjee and Das⁵⁵ observed refinement of the eutectic structure for Al-Si eutectic alloy, with smaller aluminium-rich dendrites and a higher volume fraction of primary aluminium phase. They reported a 50% increase in strength and elongation for squeeze casting over gravity casting.

McGuire⁴⁹ showed significant gain in fatigue strength (40%) squeeze cast E332-T5 Al alloy over gravity casting. Also the microstructural refinement appears to hold up even during exposure to elevated temperature (200°C).

Williams and Fisher⁵⁶ reported the mechanical properties of a wide range of casting and forging type aluminium alloys. Squeeze castings were found to have tensile properties which were superior to those of chill castings and equivalent to those of forging. Fatigue strength was improved as well.

2.8 THE CURRENT STATUS OF METALLIC-MATRIX COMPOSITES

2.8.1 Wettability of Ceramics by Liquid Metals

Wetting of certain interesting non-metallic fibres, such as carbon, silicon carbide, alumina, zirconia etc. has been more extensively studied as their incorporation in metal matrix depends entirely upon their wetting behaviour. Wetting of the ceramic fibres by the matrix, followed by interfacial bonding, is essential to the fabrication of sound composites because the interface is critically important, since it is the region through which the matrix transfers its load to the fibres.

Metals generally do not wet ceramics. A number of studies on the wetting behaviour of the Al/Al₂O₃ system have been reported⁶²⁻⁶⁸. The results of these investigations for contact angle as a function of temperature, despite some inconsistencies, indicate that a temperature well above the melting point of aluminium would be necessary to induce a wetting condition (> 900°C). Similar results on the wetting behaviour of the Al/SiC system have been reported⁶⁹⁻⁷¹, where the contact angle was 150°, 50°, 34° at temperatures of 900, 1000, 1100°C respectively. Calow⁵⁰ has reported the non-wettability of the Al/C and Cu/C systems, Al/C has a contact angle of 125° at 1000°C.

Two techniques have been developed to induce wetting in these systems (metals/ceramics). These involve coating of the fibres with wettable material, usually metals, and the addition of specific elements (wetting agents) to the molten matrix, and will be discussed separately.

I. *Coating of the reinforcement material:*

Coating is a widely used technique to induce wetting with the molten matrix by changing the chemical composition of the reinforcement surface.

Shrabian et al⁷² successfully used nickel-coated Al_2O_3 , SiC, SiO_2 , and C particles to fabricate aluminium composites. Nichrome and duplex coating of Ti-Ni have been found to promote wetting and bond formation between aluminium and alumina^{73,74}. A sputtered coating of Ni(Ti), Ni(Cr) and 1020 carbon steel on alumina was found to provide the desired wetting by the liquid aluminium^{75,76}.

This simple device of adjusting the surface properties of the ceramics by coating was not wholly successful. Although composites could be prepared, the coatings gave rise to some problems which are:

- coating adds extra cost to the already expensive reinforcement, while what is needed is a reduction of composite cost
- coatings could be gradually stripped from the reinforcement by the action of the molten matrix, causing the system to revert to a non-wetting one. Nickel coating on carbon and silicon carbide fibre was stripped off by liquid aluminium and caused an embrittling effect on the aluminium matrix by the formation of NiAl_3 ⁷⁷.
- coating adhesion to the reinforcement surface could be poor and debonding occurs at the reinforcement-coating interface⁵⁷ (nickel coated carbon fibre)
- some metalising techniques cause deterioration of the mechanical properties of fibres, as is the case when carbon fibre is coated with nickel or tungsten utilising the carbonyl route⁵⁸. Electrolytic deposition does not give rise to this fibre strength deterioration but in some cases the use of this method could be unsatisfactory due to limits imposed by throwing power.*

* Throwing power is the ability of an electroplating solution to deposit a metal coating of even thickness on shaped cathode surfaces.

II. *Modification of the chemical composition of the molten metal:*

Pure metals exhibit a very high surface tension which can be reduced by alloying. This approach is believed to be more attractive from the standpoint of cost and ease of composite fabrication. Imich⁷⁹ has described a method of preparing metallic matrix composites containing metallic and non-metallic material using wetting agents to induce wettability. These agents include metalloids having an atomic number higher than 13 (except halogens) for example, S, Se, Te, Si, alkaline-earth metals, including Li and Mg, or compounds other than halides of these elements. Imich has given 16 examples of successful incorporation of inorganic, non-metallic, solid substances (other than a halide) in liquid metals (such as zinc, steel, aluminium, and magnesium) alloyed with wetting agents, agitation was used for dispersion of the solid phase (reinforcement).

Champion⁸⁰ used lithium as a wetting agent to enhance the wetting of alumina fibre by liquid aluminium using a vacuum infiltration technique. Alumina fibre was successfully introduced to a molten Al-Mg alloy⁸¹, magnesium seems to be more effective when freshly added⁸². Wettability of carbon fibre by molten copper is improved when the melt is alloyed with Cr or V⁸³.

It can be concluded that the wetting of a ceramic reinforcement by liquid metals can be enhanced following either route (coating or wetting agent), although the use of a wetting agent is more attractive.

2.8.2 Composite Systems and their Properties

The availability of high strength ceramic fibres and the proven concept of composite strengthening has challenged metallurgists and material scientists to develop metal-matrix composites reinforced with those high strength materials. Consequently, large amounts of money and effort have been expended in developing fibre (and whisker) reinforced metal

composites for possible use at both ambient and elevated temperatures. For ease of review and discussion, metal composite systems will be subdivided according to their matrix material, unless otherwise stated, the reinforcement is continuous aligned fibre.

I. *Reinforced super-alloy:*

Since the invention of the gas-turbine engine attempts have been made to develop materials for turbine blades and vanes. This is because the operating efficiency of the engine is governed by its working temperature, which in turn is limited by the hot strength of the blade. Blades do not have to withstand high stresses but must accept moderate stresses for a long time. A thousand hours under a stress of 140 MN/m^2 at a working temperature of 1000°C is a commonly quoted value for conventional heavy alloys (nickel and cobalt base alloys) with a specific gravity of about 9 g/cm^3 . Since the rotating blades are largely stressed by their own mass, the requirement becomes a modest specific stress of about 15 MN/m^2 . Reducing the weight of blades also reduces the load on the disc to which they are attached, which may in turn be made lighter. The work carried out by Dean⁸⁴ on composites with a large percentage of tungsten wire in cast nickel base alloys showed excessive interaction between nickel and tungsten when hot pressed, but interaction was minimised (reaction zone $1 \mu\text{m}$ thick) by vacuum infiltration. Subsequent exposure at 1100°C for 100 hours produced a $5 \mu\text{m}$ reaction layer, increasing to $25 \mu\text{m}$ after 1100 hours. Nevertheless, with a 40% volume percent, the tungsten wire increased the 100 hour rupture strength at 1100°C by about 90 MN/m^2 . Because of the choice of tungsten, however, the composite was made denser by some 50%, which would raise the stress requirement by 50% as well. Regarded as a model for the use of less dense fibre, the reinforcement is impressive but other mechanical changes were also observed. Below 1100°C the strength of the composite was always less than that of the matrix, and below 900°C the yield stress was less than that of the matrix. This was attributed to internal tensile stress set up in the matrix by differential shrinkage on cooling from the fabrication temperature. The worst case was at room temperature when the

alloy matrix yielded at 700 MN/m^2 but the composite yielded at only 310 MN/m^2 .

Composites have been prepared by electroplating nickel onto wound filament of either carbon, silicon carbide, or boron, with volume percent up to 50% there has been little difficulty in developing tensile strengths well above 0.7 GN/m^2 ⁸⁵. However, sulphur and phosphorous, inadvertently introduced during plating, can cause premature interaction between the fibre and matrix and tests at 600°C - 900°C have been disappointing, possibly for this reason. In pure nickel, whiskers of silicon carbide and nitride have appeared stable at these temperatures, but are difficult to pack to large volume fractions.

In the deposition of a nickel matrix onto aligned fibre and whisker by the deposition of nickel carbonyl, some entrapped gas (carbon monoxide) was present which impaired the bond between nickel and alumina. However, this could be removed by heating to 1100°C in a vacuum for 22 hours and the composite densified by hot pressing at 1100 - 1300°C under a pressure of 3.5 - 42 MN/m^2 ⁸⁶. The resultant composite had a strengthening efficiency of 40-75% at room temperature in consequence of the mechanical bond generated during cooling. This bond was much reduced at high temperature and the strengthening efficiency was less than 10% at 1100°C . When a chemical bond was generated during fabrication, the bond was disrupted, even by a single thermal cycle⁸⁶, due to the disparity between the coefficients of thermal expansion.

In both the high and medium temperature ranges, it appears that further efforts are still needed to reinforce super alloys, stability of the interface (chemical and mechanical) being the major problem areas.

II. Reinforced titanium:

The very high cost of titanium determined that its main usage would be in chemical plants and in the aerospace industry, where it now tends to be used in areas which are hot, highly stressed, or subjected to impact, where aluminium would be unsuitable. Titanium also comprises some 25% of the weight of certain gas turbine engines currently in service. It withstands temperatures up to 400-500°C in the later stages of the compressor. Thus there is a good case for attempting to improve it by reinforcement.

Much composite research has been done with the alloy of composition Ti-6% Al-4%V, which has a tensile strength of 0.9 GN/m², falling to about 0.56 GN/m² at 530°C. At this temperature, a useful strength increase of 0.17 GN/m² was noted by Jech et al⁸⁷, when 20% molybdenum wire was incorporated by hot pressure. This demonstrated the feasibility of reinforcement, but density was also increased (density of molybdenum is 10.5 g/cm³).

Compatibility studies⁸⁸ showed that titanium reacts in the solid state at high temperature with available fibres, but the silicon carbide composites have a useful life of up to 500 hours at 600°C, and alumina whiskers, might last appreciably longer. Fabrication therefore was based on the minimum temperature and time, by hot pressing aligned fibres between layers of alloy foil. A typical cycle would involve 15 minutes at 850°C and 100 kg/cm².

Results for composites containing up to 30% volume percent have been reported for aligned fibres of silicon carbide⁸⁹, SiC coated boron^{89,90} and alumina⁹¹ in the Ti-6% Al-4%V alloy. Generally there was little change in tensile strength relative to the matrix alloy at room temperature, data varying from 10% loss to 20% gain. Density was slightly reduced and modulus increased by up to 50%. Transverse strength fell to 200-400 MN/m², suggesting poor bonding. At elevated temperature tensile strength was retained and showed a 40% advantage over the unreinforced material at 470°C. However, the useful life of the composite at

high temperature was limited due to a reaction between the matrix and the reinforcement. Significant amounts of titanium carbide and silicide were found to form at the silicon carbide-matrix interface⁹². These compounds degrade the composite's mechanical properties as stress-intensifying microcracks formed in the reaction layer at low strains⁹³⁻⁹⁵.

Titanium aluminides, produced by the reaction of the matrix alloy with aluminium coated SiC fibres, form a diffusion barrier which improves the useful life of the composite⁹⁶.

III. *Light alloy composites:*

The reinforcement of light alloys has attracted more interest than that of other metals. Since they are light, they contribute less dead weight than other matrix metals. They are not particularly strong and therefore can be readily strengthened by reinforcement. In early composite work⁹⁷, by Rolls-Royce on the silica fibre-pure aluminium system, the fibres were passed through a feeder head of molten aluminium which coated them with an even, adhering film. The fibres were hot-pressed with the composite's strength optimized by controlling the pressing cycle (one hour at 450°C under a pressure of 750 kg/cm²). Subsequent heating above 400°C degraded the fibre strength. Composites containing 50% v/v fibre had a tensile strength of 0.8 GN/m² which fell down to 0.5 GN/m² at 400°C. Transverse and off axis properties were poor (70 MN/m²). Moreover, since silica fibre has a modulus equal to that for aluminium, when the metal yielded the modulus was halved. High-modulus boron fibre was subsequently used. After plasma-spraying the fibre with aluminium, the composite was produced by hot pressing⁹⁸. The boron fibre had been coated with silicon carbide to prevent interaction. This treatment gave a higher composite tensile strength of 1.1-1.2 GN/m², a modulus of 220 GN/m² at room temperature, and a transverse strength of 0.1-0.14 GN/m², for a composite containing 50% v/v fibre. In this case, complete fan units were made and tested on an existing gas turbine (JT6D).

The high stiffness of the blade also permitted the elimination of supports, used in titanium construction, and a 40% reduction in weight was found to be feasible.

Workers at the Toyota Motor Corporation in Japan have employed alumina fibre FP (invented by Du Pont Company scientists in the USA) to reinforce connecting-rods for an experimental high-performance engine⁹⁹. It is claimed that replacement of traditional forged steel connecting rods by fibre-reinforced aluminium parts, some 35% lighter in weight, may lead to increased fuel efficiency, faster engine response, and lower engine vibration. It is also suggested that additional weight saving may be possible if the technology was adopted for other key reciprocating components. Toyota and Art Metal (a Japanese piston manufacturer) are developing alumina fibre reinforcement bands for diesel engine pistons to replace the cast iron insert for the top ring¹⁰⁰. The band is in fact extended up to the piston crown. Toyota claims improved durability at high temperatures, abrasion resistance and improved cooling. Certainly, the fact that the ceramic is carried in aluminium will result in good heat dissipation.

Several methods of producing pistons with ceramic fibre reinforcement have been patented¹⁰¹⁻¹⁰⁵. Although they are different in detail such as reinforcement shape and location, they rely in principle on infiltrating a fibre preform (reinforcement) with liquid metal under pressure.

Work at Du Pont de Nemours and Co, Canada¹⁰⁶ on the reinforcement of aluminium and magnesium with their alumina FP fibre showed some encouraging results. Using the vacuum infiltration technique several matrix metals such as : aluminium, magnesium, lead, copper and zinc were reinforced with fibre FP. It is claimed that high quality composites were achieved. Magnesium and its alloys wet the fibre in use, whereas aluminium, lead, copper and zinc do not, additions of small amounts of active metals such as lithium, calcium or magnesium were used to promote wetting. Lithium concentrations in excess of 3.5-4% in an aluminium

matrix were shown to significantly reduce these composites' tensile strength as a result of severe chemical attack of the fibre. From tests conducted on fibre extracted from the matrix it was established that the presence of this level of lithium had reduced the strength of the fibres themselves. At lithium concentration 3.3 wt%, contact for 10 minutes between the fibre and the molten alloy at 700°C did not affect the composite's tensile strength. Composites of Al-2.0-2.4 wt% Li containing 30-60 v/v FP fibre had axial tensile strengths of 386-655 MN/m² compared with 159 MN/m² for the matrix alloy. The value of the transverse strength of a composite containing 30% v/v fibre was similar to the value of tensile strength of the matrix alloy. However, for a composite containing 60% v/v fibre the value of transverse strength was 241 MN/m² which indicates the strength of the bond between the fibre and the matrix. Axial and Transverse moduli of 262 and 165 GN/m² were recorded at 60% volume percent fibre. Axial tensile strength was shown to decrease less than 5% for temperatures up to 316°C, even though the strength of the matrix decreased by 80% at this temperature. A composite containing 55% volume percent fibre demonstrates a constant linear thermal expansion coefficient of $7.2 \times 10^{-6} \text{ (}^\circ\text{C)}^{-1}$ over a temperature range of 20-400°C.

Similar attractive properties have been demonstrated for FP/Mg composites¹⁰⁷. Axial tensile strengths and moduli of 552 MN/m² and 200 GN/m² respectively were achieved for a 50% volume percent fibre composite. The transverse tensile strength of 131 MN/m² obtained indicates that a good fibre/matrix bonding was achieved in the as-cast composite. Mechanical properties of both Al and Mg composites are in good agreement with those predicted by the rule of mixtures.

Aluminium composites reinforced with Nicalon^{(R)*} fibre were produced by the liquid metal pressing method¹⁰⁸. The tensile strength of these composites was shown to obey the rule of mixtures up to 40% volume

* Nicalon^(R) is a trade name for SiC fibre developed by S. Yajima at Nippon Carbon Co Ltd (NCK) Japan.

percent fibre, at higher fibre content no further reinforcement was observed. This was explained by fibre misalignment and contact between fibres at high fibre content. A composite of SiC/Al-6061 produced a tensile strength and modulus of 780 MN/m² and 98 GN/m² respectively for 35% v/v fibre. The transverse tensile strength was only 60 MN/m². A composite of SiC/Al-1100 had similar properties (UTS 800 MN/m² at 30% v/v fibre).

Al-1100 matrix reinforced with chopped SiC fibre has a tensile strength of 270 MN/m². The tensile strengths of composites with continuous fibre stay nearly constant at temperatures up to 400°C. However at 500°C, the tensile strength drops suddenly. Fibres extracted from the composite tested at 500°C retain their original strength which indicates that the sudden drop of composite strength at the temperature was not a result of the deterioration in fibre strength. It was found that the weak fibre/matrix bond at 500°C resulted in debonding and fibre pull-out and this was responsible for the strength decrease.

The tensile strength of SiC/Al alloy at a fibre content of 30% v/v (800 MN/m²) was higher than those observed with alumina FP/Al-Li of Du Pont at fibre content 60% v/v (655 MN/m²). This can be simply explained by considering the fact that SiC fibres have a tensile strength of 2450 MN/m²¹⁰⁸ compared with 1380 MN/m² for alumina FP¹⁰⁷. The weaker transverse strength of SiC/Al compared with FP/Al is possibly an indication of a weak SiC fibre/matrix bond due to a short time of fibre contact with the melt. In contrast, alumina FP were allowed to be in contact with the molten matrix for 3-5 minutes which apparently produced a strong fibre/matrix bond without fibre strength deterioration.

Lloyd¹⁰⁹ has employed the hot pressure technique to prepare composites of a superplastic alloy (Alcan-8050, Al-5 wt% Ca-5 wt% Zn) reinforced with a variety of fibres and wires such as: boron fibre and stainless steel, chromel, tungsten, and eutectoid steel wires, Hot pressing was

carried out in air at 500-510°C for 30 minutes at pressures of up to 70 MN/m². Substantial improvements in composites tensile strengths were observed for all reinforcements. The best results were obtained with boron fibres which have the highest tensile strength. Composites containing 25% volume percent boron fibres have a tensile strength in the order of 840 MN/m² compared with 170 MN/m² for the matrix alloy. The clever selection of the matrix alloy to suit the fabrication process was probably behind the success in preparing good quality composites.

In a patent (1950 granted 1957) by Imich⁷⁹, a process was described for the fabrication of metallic-matrix composites reinforced by metallic or non-metallic substances to include oxides and carbides. According to this process a wetting agent is used to modify the wetting characteristic of the matrix alloys. The reinforcement is incorporated and dispersed in an agitated liquid or pasty metal. Wetting agents are elements having an atomic number higher than 13 (except halogens) for example, S, Se, Te, Si, Li, Ca, Mg and Cu, or compounds (other than halides) of these elements.

Attempts by Mehrabian⁹⁸ (1974) to incorporate particles of SiC, Al₂O₃, and glass in an agitated liquid Al-5% Si-2% Fe alloy was not successful. However, particles were successfully incorporated in an agitated slurry of the Al-alloy (according to Imich Si and Fe are wetting agents) and later fibres were incorporated in a slurry of Al-Mg and Al-Cu alloys^{110,111} but fibre breakage was observed.

Rohatgi¹¹² (1981) successfully incorporated alumina, illite, and silicon carbide particles in an agitated, fully-liquid Al-11.8 wt% Si. Pre-treatment of the particles was claimed to be necessary to promote wetting. Particles were heated in air for 3 hours at 900°C. Later Mehrabian⁸¹ succeeded in incorporating discontinuous alumina fibre (grade FP) in an agitated, fully-liquid Al-Mg alloy. To increase the fibre concentration and to align the fibres in two directions Mehrabian used a special die where liquid metal was squeezed out through a ceramic filter. Although

this method may increase the fibre concentration it is doubtful whether the concentration would be uniform because a higher concentration of fibre would be expected adjacent to the ceramic filter. Further, to achieve the alignment of fibre claimed it would be necessary to remove a much larger volume of liquid than was the case in the work reported. However, the liquid metal infiltration method is a simpler process for fabricating composites with a high concentration of aligned fibre.

Das and Chatterjee were successful in dispersing silicon carbide whiskers in fully liquid aluminium alloy (Al-4.5 wt% Cu)⁵². A mixture of SiC whiskers and aluminium powder was pressed into small briquettes which were then degassed in vacuum at a temperature of 450°C. The briquettes were then immersed in the liquid metal for not less than 25 minutes during which time the wetted whiskers were suspended in the melt. The liquid composite was then squeeze cast, using conditions determined in previous investigations by the author^{54,55}. The whiskers were randomly oriented in the matrix which resulted in isotropic properties for the composite.

Squeeze casting provided a stronger matrix which was further reinforced by the whiskers. Squeeze casting the matrix alloy at a pressure of 206 MN/m² produced a tensile strength of 185 MN/m², and this was raised to 280 MN/m² by incorporating only 0.5% volume percent of whiskers. This should be compared with a tensile strength of 110 MN/m² for the matrix alloy cast at atmospheric pressure. The strengthening is far more than can be expected from the whisker volume percent according to the rule of mixtures. The strengthening mechanism of whiskers appears to be different from that for fibres⁵². Several publications have appeared after the work by Das describing a method of fabrication for fibre reinforced metals by squeeze casting^{78,113-117}. In these methods a pre-heated continuous fibre preform (except for work in reference 98, where loose chopped fibres were used) was placed in a hot metallic die where the fibre preform was infiltrated by liquid metal under pressure.

Examining the work by Fukunaga¹¹³⁻¹¹⁶, it is obvious that processing conditions were selected and optimized to ensure the adequate infiltration of the fibre by the melt, rather than to achieve squeeze cast structure or properties. A die with runner system on a die casting machine was used as well to produce "squeeze cast composites"¹¹⁴. The same argument is true concerning the work by G. David⁷⁸ and Nakata¹¹⁷. David "squeeze cast" a wide-freezing range (113°C) tin alloy using a very high superheat temperature ($156 \pm 15^\circ\text{C}$). Nakata "squeeze cast" Al and its alloys (Al-4.5 Cu, Al-11.6 Si, Al-4.8 Mg) using conditions, such as: casting temperature (800°C), applied pressure (49 MN/m²), and die temperature (300°C). However, it is well known that squeeze casting conditions should be selected for each metal or alloy so that the desired structure and properties are obtained. These workers made no attempt to achieve the structure and properties expected in squeeze casting, instead an attempt was made to realise full infiltration of the fibre by liquid metals. The process is probably more accurately described as pressure infiltration rather than squeeze casting, reserving the term (squeeze casting) to describe a casting process by which distinctive structures and properties are obtained. However, a tensile strength and modulus of 500 MN/m² and 115 GN/m² respectively was observed by Nakata for SiC fibre/aluminium matrix composite compared with the matrix strength of 120 MN/m². The strength of the tin alloy used by David was doubled when reinforced with a 40% volume percent addition of chopped fibre aligned in two directions.

The fatigue data for metal-matrix composite is not extensive, although some useful micromechanical studies have been carried out. When assessing the data it is important to relate the test to the application. Forsyth et al¹¹⁸ hot-rolled small proportions of steel wires (< 14%) into aluminium alloy sheet and found that the fatigue limit strength on small, rotating bending specimens was not improved. At higher stresses, the composite survived longer than the matrix alloy and this was related to a ten-fold reduction in the rate of crack propagation. Moreover, the most effective angle for the wires was 45° to the crack, not 90°. The wires were relatively coarse (0.2 mm) and poorly adhering. While studying the fatigue of silicon-fibre reinforced aluminium, tested in plain bending, Baker¹¹⁹ noted that endurance tests at low stresses

revealed progressive disintegration of the matrix throughout, but that at higher stresses failure was by propagation of large cracks through both fibre and matrix.

Mordike et al¹²⁰ have concluded from their studies that glass fibre increases the fatigue resistance of aluminium. The S-N curve is tilted towards higher stresses - crack initiation would seem relatively easy but crack propagation is often arrested by a glass fibre. Only in the case of the fine fibres is a significant displacement of the fatigue limit observed.

CHAPTER III.

COMPOSITE PRODUCTION

CHAPTER 3
COMPOSITE PRODUCTION

3.1 THE DESIGN OF COMPOSITE SYSTEMS

The objective of this study was to produce and evaluate a composite system of isotropic and improved mechanical properties (such as specific strength and modulus, proof stress, etc) in relation to the matrix alloy. The composite was to be suitable for service at room and moderately high temperatures (350°C).

It is logical as a first step to design a composite system to possess the desired properties. This involves the selection of the most appropriate individual components for the system. The components must exist in harmony with each other without degradation of their desired properties, both at fabrication and under service conditions. The production method and conditions should be taken into consideration at this stage. Fibres probably have the best shape for reinforcement because their function in the composite will be mainly as load carriers. Aluminium alloys are ideal matrices because of their low density and compatibility with most available fibre materials.

In order to achieve isotropic properties a matrix of isotropic properties needs to be reinforced in all directions (random). Random reinforcement dictates the use of short fibres.

There is no readily available technique to produce composites reinforced with randomly oriented fibres.

The powder metallurgy technique results in excessive fibre breakage, the electrodeposition technique is limited by its throwing power and other techniques are more suited for fabricating composites reinforced with aligned fibres or wires.

The general approach was to establish a simple and cost effective technique which could be adopted by industry to produce reinforced components of different size and shape. To minimise costs, uncoated short fibres were to be used with elements considered as wetting agents present in the normal composition of the alloy matrix.

In the previous chapter the effects of squeeze casting, in respect of improvements in tensile strength and ductility and grain structure refinement, were described. The matrix of an alloy reinforced by short fibres plays a much greater part in the load transfer to the fibre than does the matrix when reinforced with continuous fibres. Consequently, in a short fibre reinforced matrix, it would be necessary for the matrix to possess a high tensile strength and ductility. The ductility being necessary for both load transfer and reduction in stress concentration. The improvements in tensile strength and ductility provided by squeeze casting would therefore be beneficial to composite production.

3.1.1 Selection of the Reinforcement Fibres

Nicalon^(R), chopped silicon carbide fibre, supplied by Nippon Carbon Co Limited (Japan), and 'Saffil' alumina fibre grade RF, supplied by ICI Limited (UK) were chosen as reinforcement fibres for their high tensile strength and modulus, thermal stability at high temperature, and compatibility with aluminium alloys.

The typical properties of Nicalon^(R) silicon carbide and 'Saffil' RF alumina fibres are listed in Tables 1 and 2 respectively.

TABLE 1: Typical Properties of Nicalon^(R) Silicon Carbide Fibres

Filament diameter	10-15 μm
Filament length	3 mm
Cross-section	Round
Filament per yarn	500
Density	2.55 g/cm^3
Tensile strength	250-300 kg/mm^2
Tensile modulus	18-20 $\times 10^3 \text{ kg/mm}^2$ 176 GPa
Maximum permissible temperature	1250 $^{\circ}\text{C}$
Coefficient of thermal expansion	3.1 $\times 10^{-6}/^{\circ}\text{C}$ (parallel to fibres)

TABLE 2: Typical Properties of 'Saffil' Alumina Fibres - RF Grade

Mean fibre diameter	3 μm
Mean fibre length	0.5 mm
Cross-section	Round
Density	3.3 g/cm^3
Tensile strength	2000 MPa (200 kg/mm^2)
Tensile modulus	300 GPa (30 $\times 10^3 \text{ kg/mm}^2$)
Maximum vs temperature	1600 $^{\circ}\text{C}$
Crystal phase	Mainly delta alumina

3.1.2 Selection of the Matrix Alloys

An aluminium alloy containing 4.5% Cu was selected as the matrix material. The choice of this alloy was primarily for two reasons: first, copper improves the wetting characteristics of silicon carbide with molten aluminium^{79, 121}, second, the alloy has a high ductility which is useful in redistributing stress and arresting the leading edge of the propagating crack during plastic deformation. This alloy has the same

composition (Al-Cu 4.5) as LM11 (BS 1490:1970) and 2L92. The alloy was prepared from electrolytically pure copper and commercially pure aluminium (LM0). It was later found that this alloy did not provide an adequate bonding with alumina fibre and LM5 (Al-3.5 to 5% Mg) was then selected as a matrix alloy to be reinforced with the alumina fibre. This alloy has high ductility and magnesium is a strong wetting agent^{79,52,121}.

The certified chemical composition of the alloys is given in Tables 3 and 4.

TABLE 3: The Chemical Composition of LMO used for Preparation of the Matrix Alloy Al-4.5 Cu

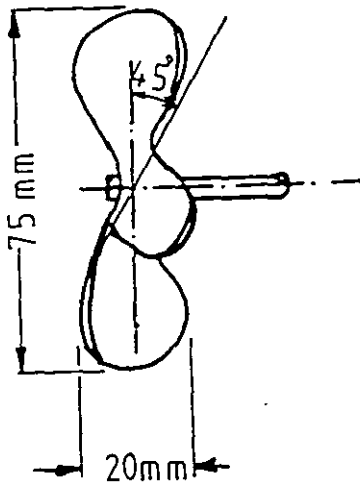
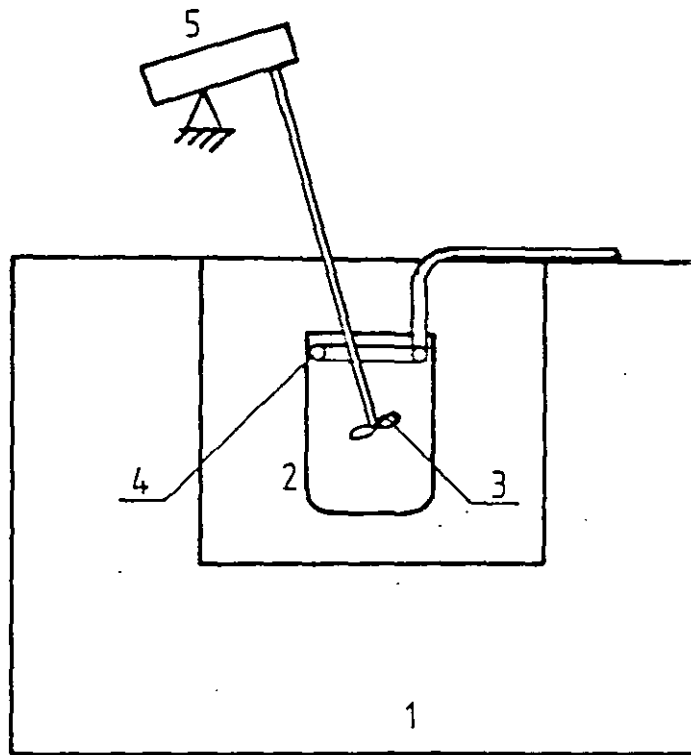
Cu	Mg	Si	Fe	Mn	Ni	Zn	Pb	Sn	Ti
<.01	<.01	0.04	0.12	<.01	<.01	0.02	<.01	<.01	<.01

TABLE 4: The Chemical Composition of the LM5 Matrix Alloy

Cu	Mg	Si	Fe	Mn	Ni	Zn	Pb	Sn	Ti
.01	3.75	.02	.27	.47	.01	.02	<.01	<.01	.10

3.2 EXPLORATORY ATTEMPT TO PRODUCE COMPOSITES

The arrangement shown in Figure 11 was used in the first attempts to produce a composite of Al-4.5 Cu/SiC and Al₂O₃ fibres. It consists of a crucible (Mullite grade J/A) placed inside a resistance wound furnace, and a triple blade impeller slightly immersed below the melt and driven by a variable speed motor. Stainless steel was used as a material for the



3

FIGURE 11: Vortex Equipment

1. Furnace; 2. Crucible; 3. Impeller;
4. Ring tube; 5. Drive motor

impeller which was coated with a refractory to minimise its dissolution in the melt. The rotational speed of the impeller was first adjusted to form a deep vortex cone in the molten alloy. To minimise oxidation of the melt, a continuous flow of oxygen-free, dry nitrogen was maintained through a ring shaped tube placed in the inside upper part of the crucible. Nitrogen bubbles were used for melt degassing before fibre introduction. Several attempts to incorporate the as-received fibres in the molten alloy (Al-4.5 Cu), which was kept at temperatures ranging from 700-850°C, were unsuccessful. SiC fibres were only partially accepted in the melt, over 80% of the fibres were rejected. Rejection of fibres is most likely to be a direct result of poor wetting by the melt, even at temperatures as high as 850°C.

3.2.1 Difficulties Met and Solved in the Production of Composites

I: *Fibre Wetting:*

It was observed that very few silicon carbide fibres were accepted in the melt whilst the full rejection of alumina fibres was an indication of the absence of any wetting between the fibres and the melt. The use of a high melt temperature (up to 850°C) to promote fibre wetting was not successful.

It was believed that one or more of the following: surface contamination; adsorbed gases; or a passive film on the surface of the fibres were possible causes for the absence of wetting. A surface analysis facility was not available to confirm any of these assumptions. However, exposure of the fibres' surface to heat might result in the burn off of contamination, energize the atoms of adsorbed gases and free them, and break down any passive film. On this basis a group of experiments was conducted in which fibres (SiC and Al₂O₃) were heated in air for 3 hours at temperatures of 300-1000°C, at 100°C intervals up to 800°C and 50°C intervals between 800°C and 1000°C. The heat treated fibres were then introduced into a degassed melt, held at 850°C, using the technique described earlier. It was established that only those fibres heated

at 900°C or higher were fully wetted, at 850°C fibres were partly rejected, an indication of poor wetting. As a next step, fibres were heated in air at 900°C for periods of time up to 3 hours, at 30 minute intervals, to establish the minimum time of heat treatment which would provide full wetting of the fibres by the melt, all other conditions remaining unchanged. It was concluded that the heat treatment of fibres at 900°C for not less than 2 hours was necessary to achieve full acceptance of the fibres by the melt and this technique was adopted.

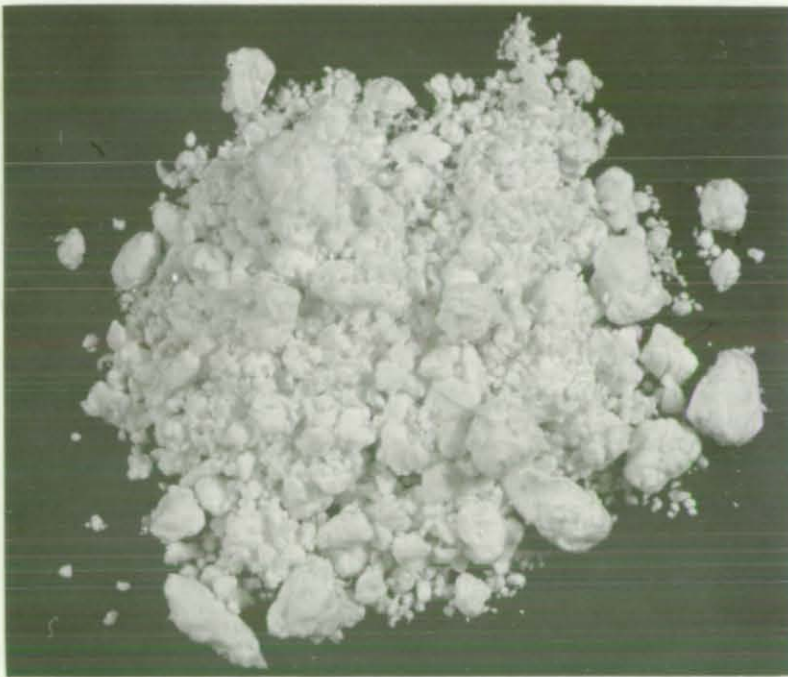
II: *Fibre Separation and Dispersion:*

Although the fibres, when heat treated as described, were wetted, not all of them were well dispersed in the melt. Clumps of fibres were present in the squeeze cast composite. Poor dispersion of fibres reduce the reinforcement efficiency of the fibres and cannot be tolerated. The as-received fibre was of matted form, as can be seen in Figure 12. A strong vortex in the melt could not separate the fibres, in fact it caused the fibres to agglomerate and form small balls of fibres leaving only the already loose fibre well dispersed. It was realised that the fibres must be well separated before introducing them into the melt if an adequate dispersion of fibres is to be achieved. It was possible to manually separate silicon carbide fibres using a soft brush. However, it was not possible to separate the smaller alumina fibre manually.

A higher percentage of silicon carbide fibres were well dispersed when they were manually separated, then heat treated in air at 900°C for 2 hours, and introduced to a degassed melt of Al-4.5 Cu held at 800°C using the vortex technique. It was observed that the separated fibres tend to agglomerate into clusters as a result of even slight handling. These clusters remain unbroken in the melt and the resulting casting. The tendency of fibres to agglomerate is a result of mechanical interlock and the presence of static charge, in the case of silicon carbide fibre.



(a)



(b)

FIGURE 12: As-received Fibre

- a) Nicalon^(R) silicon carbide fibre
- b) 'Saffil' alumina fibre-RF grade

At this stage, it was obvious that there was a need for the fibre to remain separated when they come into contact with the melt. To overcome the limitations of inadequate manual separation, which was both time consuming and impracticable, a mechanical method was required and this is described in Section 3.3.1.

III: *Melt Oxidation:*

The provision of nitrogen gas cover through the ring shaped tube above the melt (Figure 11) did not provide adequate protection from oxidation. The protective oxide film at the melt surface was continuously broken by the action of the vortex and fresh alloy exposed and oxidized due to the inefficient nitrogen cover.

The approach to solve this problem was to provide continuous nitrogen flow in to a well sealed furnace in which the melt was held, the nitrogen flow rate being adjusted to maintain a positive pressure inside the furnace.

IV: *Propeller Material and Design:*

The refractory coating on the metallic propeller was easily eroded away by the action of the vortex and the presence of abrasive fibre. This was accelerated by cracks observed in the coating due to the difference in the thermal expansion coefficient of the coating and the propeller material (stainless steel).

Powder released from the coating consistently caused fibre rejection, because it was attracted to the fibre surface and acted as a barrier between the fibre and the melt. An uncoated propeller could not be used because it was rapidly dissolved in the melt causing an uncontrollable change in the melt chemistry. Graphite was later used as the material for the propeller because it is not wet by aluminium, details are provided in 3.3.2.

The shaft to which the propeller is attached, was joined to the drive motor by a close fit joint and secured by a grub screw. This joint could not provide adequate alignment between the two shafts, misalignment was enlarged over the length between the motor and the propeller (453.5 mm), and brought the latter out of balance at high rotational speed. This problem was solved by the elimination of the joint and the design of the propeller for improved efficiency which allowed the use of a lower rotational speed whilst still creating a strong enough vortex, details are provided in Section 3.3.2.

3.3 DESIGN AND MANUFACTURE OF EQUIPMENT

3.3.1 Fibre Separation Device

Three design options were considered and tried. They were:

I: *Venturi Effect:*

A device consisting of a venturi tube was designed and fabricated (Figure 13). The dimensions of the venturi tube (mainly diameters) were selected so that a reasonable gas (nitrogen) flow (10 litres/min) would create a pressure lower than one atmosphere in the reduced section area (region A, Figure 13). Fibres placed in the container (B) which is mounted on the top of the venturi tube would be drawn into the gas flow by the effect of differential pressure, and directed onto the top of the melt.

On trial, the device was frequently blocked by bridging fibres (SiC and Al_2O_3). Increasing the gas flow rate was not an adequate solution, because clusters of fibre were forced through the tube, and the separated fibres were carried out of the crucible.

This design was ruled out.

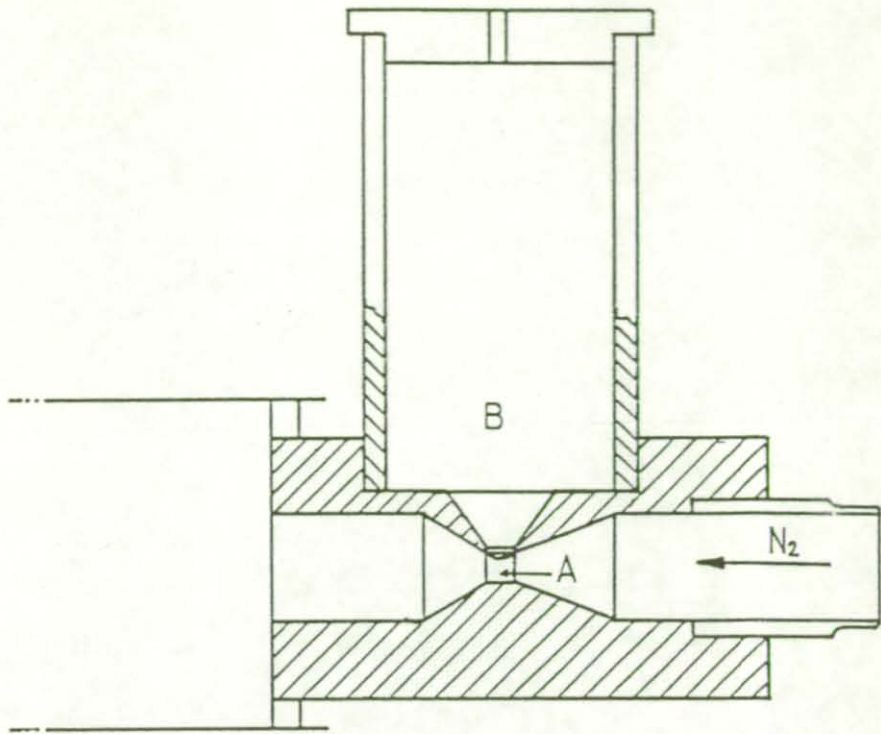


FIGURE 13: Venturi Device for Separation of Fibre

II: *Vibrator (vibrating hopper):*

In theory, a particle placed on a surface vibrating in the Y direction (Figure 14) and inclined to the horizontal at an angle θ , will travel down (X direction) at velocity $V = x.f$, f is the frequency of vibration. This is analysed as follows:

Let a,b represent the final positions of the surface vibrating at frequency f and amplitude A , a particle P at position (1) will be carried up to (2), the particle at (2) will travel down vertically by gravity, when the surface descends from a to b at accelerations higher than gravity. The particle will meet the moving up surface at (3) to be carried up to (4) and so on, the resultant movement of the particle in the X direction is x for each cycle, so

$$V = x.f$$

$$x = y \tan \theta$$

y is a function of θ , A and f .

According to this analysis, the velocity at which a particle will travel down the slope is a function of the vibration frequency and amplitude, in addition to the angle θ .

It was assumed that the gentle impact of vibration would separate the as-received fibres by breaking down the fibre clumps. Separated fibre, according to the analysis, could be fed and directed to the agitated melt in order to fabricate the composite desired.

On the basis of this analysis, a device was designed and fabricated, Figure 15, consisting mainly of a circular tray made of wrought aluminium for minimum weight. The cavity of the tray was parted by a wire screen designed so that only separated fibre would go through when the

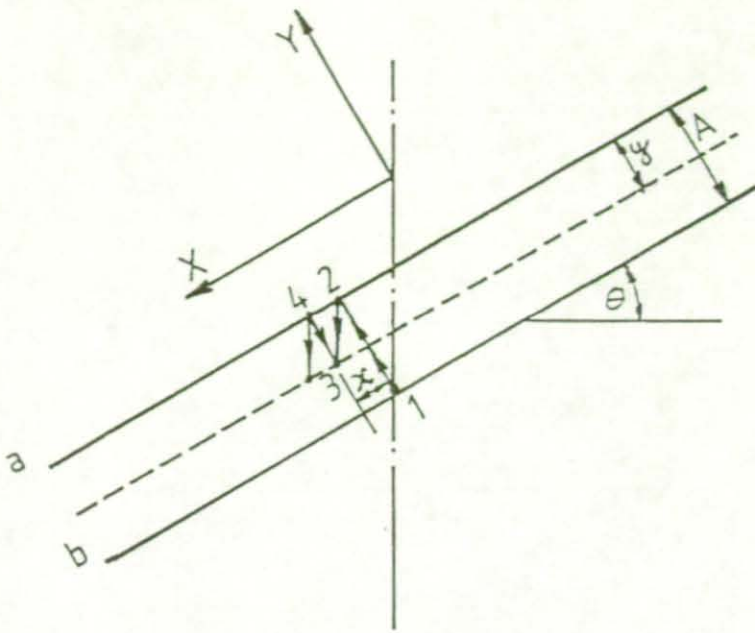


FIGURE 14: Theory of Vibrator



FIGURE 15: Vibrator Arrangement for Separation of Fibre

as-received fibre was placed in the tray cavity behind the screen. The tray was attached to a vibrator with the facilities to control vibration frequency and amplitude and the tilt angle (θ). A special attachment was provided to receive separated fibre leaving the tray and direct them to the top of an agitated melt, held in a furnace as described in Section 3.2.

The factors which influenced the feed rate of separated fibres (f , A and θ) were adjusted for maximum feed rate and separation of fibres (SiC and Al_2O_3). During trials the following were observed:

A: *Silicon carbide fibre:*

The as-received fibre was first heat treated in air for 2 hours at $900^{\circ}C$ to promote wetting. The pre-treated fibres were then placed in the tray cavity of the vibrator device described and vibration frequency and amplitude were adjusted in combination with the tilt angle for maximum rate of fibre separation and feed.

It was observed that a high rate of fibre feed could be obtained. However, fibre separation was slow and only partial. The fibre separation rate did not exceed 2g/min and only 70 per cent of the fibres were fully separated. Although it was possible to introduce and disperse the silicon carbide fibres within the melt using this technique, it was not considered a completely satisfactory technique to use.

B: *Alumina fibre:*

The same technique was used to separate and feed the pretreated alumina fibre but a much lower percentage of alumina fibre was fully separated ($\approx 15\%$), probably due to a stronger interlock between the alumina fibres. This technique was therefore ruled out for use with alumina fibres.

III: *Mechanical Separation of Fibres:*

A device similar to those used in the textile industry to comb wool was designed and a model was fabricated, Figure 16.

The device basically consisted of a flat wire brush fixed on a block of wood together with a segmental roll on which another wire brush was fixed. The two brushes were engaged to form the fibre separation zone. The wires on the flat brush which were not functioning in the separation zone were sealed off to ease fibre movement toward the separation zone.

The segmental roll is driven by a four-link mechanism, this was designed so that continuous rotational movement of the drive link (link a in Figure 16) will be converted to a rocking movement of the segmental roll. The rocking angle was chosen to be 120° , a larger segment angle, 240° , was chosen to seal off the top of the device frame, so that unseparated fibre could not be carried over through that area. A transparent material (perspex) was chosen as the structural material to enable the fibre separation operation to be observed. A section of the wire brush used is shown in Figure 17, it is the sort of brush used for file card. The wire density was reduced so that a suitable spacing between the wires was obtained (3 mm). A smaller spacing could result in excessive fibre breakage (SiC fibre length 3 mm). Softer plastic brushes could not be used, because a build up of static charge on the silicon carbide fibres would create difficulties in keeping them separated.

When the segmental roll advances it draws the fibre placed on the flat wire to the separation zone. Separated fibres are released when the roll retracts and can be directed to the melt for fabrication of the composite.

During trials silicon carbide fibres were well separated at a satisfactory rate using this model device. However, the separation of alumina fibres was not satisfactory as some fibres were not well separated.

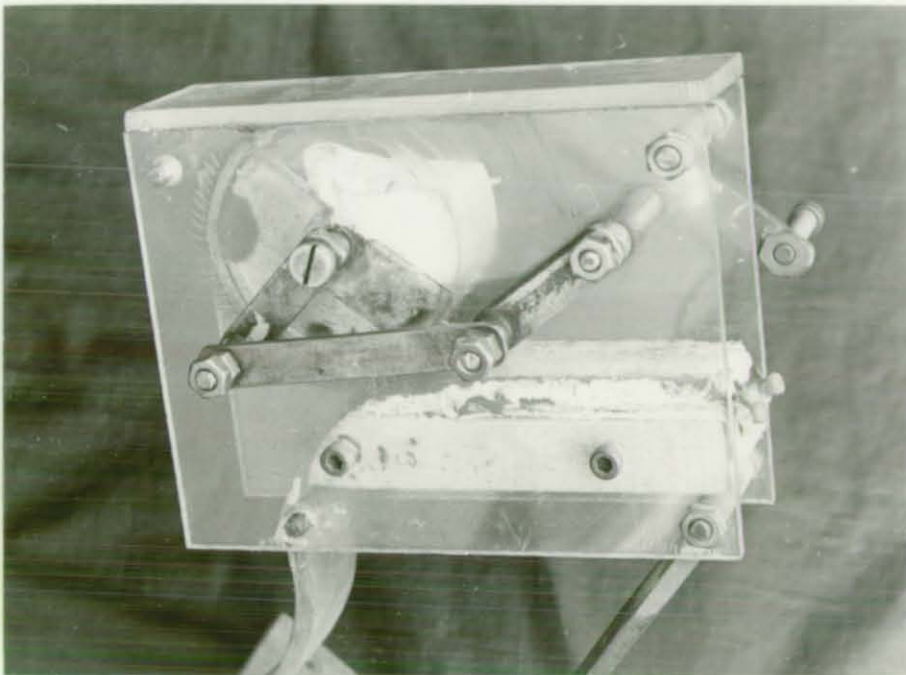
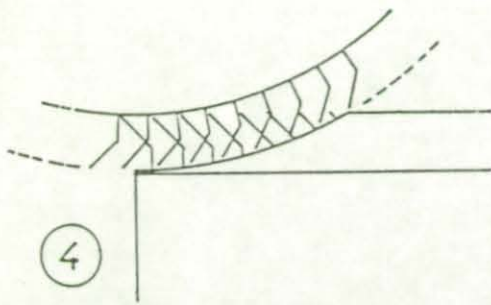
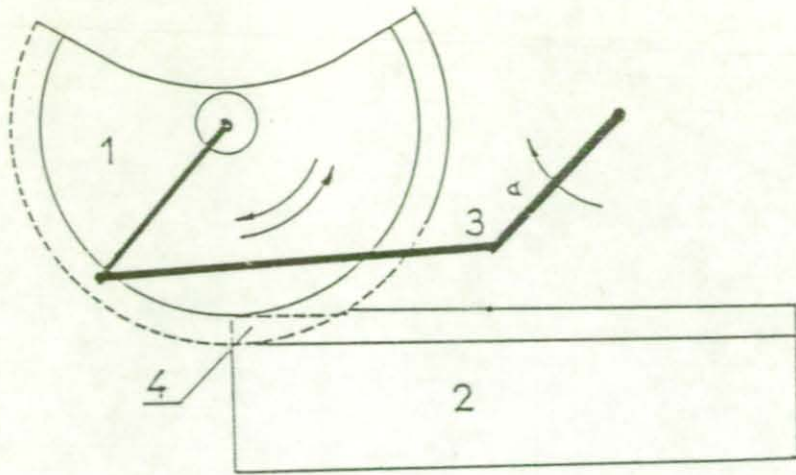


FIGURE 16: Initial Design of the Device for Mechanical Separation of Fibre

1. Segmental wire brush; 2. Stationary wire brush;
2. Four-link mechanism; 4. Separation zone

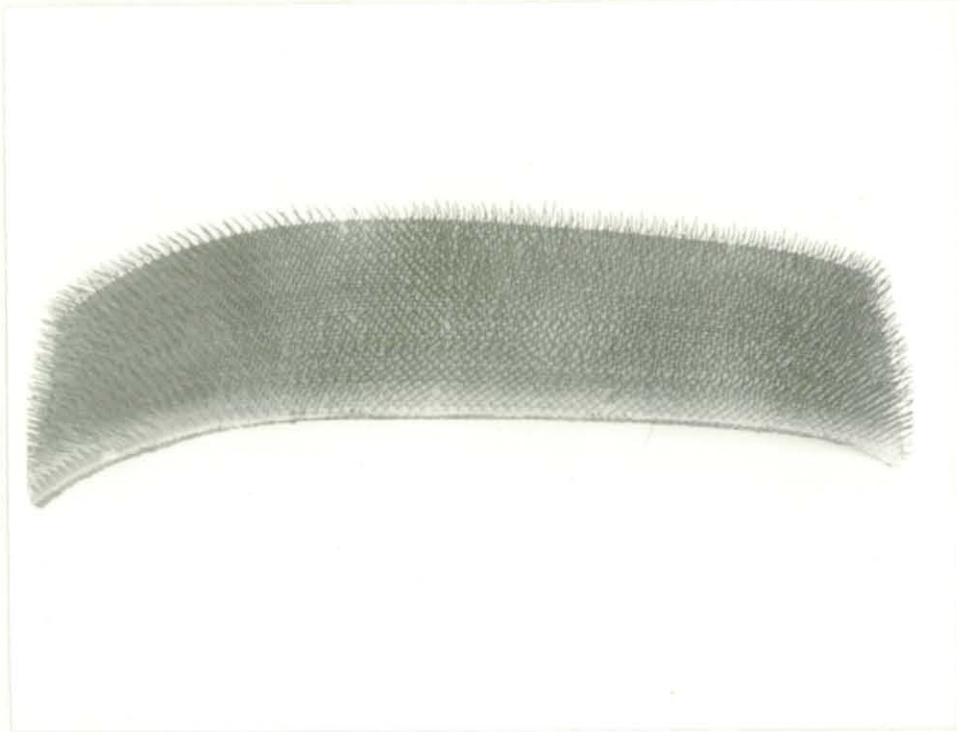


FIGURE 17: Section of the Wire Brush

From the experience gained it appeared that it would be difficult to break the strong mechanical interlock of the as-received alumina fibre during a single separation operation without damaging them. This problem was solved, as detailed in Section 3.5, by dividing the separation of alumina fibres into two stages. In the first stage, the clumps of fibre are broken down by dispersing them in an agitated alcohol-water solution. After filtering and drying the fibres were well prepared for the final stage of separation by the mechanical method used for silicon carbide fibre.

Although the device described was successfully used to separate silicon carbide fibre, and as a second stage separation for alumina fibre, the following shortcomings were observed:

1. Because the fixed wire brush is tilted to facilitate fibre feed to the separation zone by gravity, this feed method was not satisfactory because it was occasionally necessary to manually intervene and move the fibres close to the separation zone. On other occasions, too much fibre was gravity fed in, and made separation more difficult. In addition this caused undesirable fibre breakage at separation.
2. Some separated fibres tend to accumulate next to the separation zone.

Final Design:

The general approach to the fibre separation method was acceptable. However, modifications were considered necessary in order to eliminate the shortcomings and improve the efficiency of separation.

A modified design of the fibre separation device was developed and is shown in Figure 18. The device consists of a moving belt made of a wire brush, a specimen of which is shown in Figure 17. The belt moves on two knurled rolls made of medium carbon steel. Provision was made

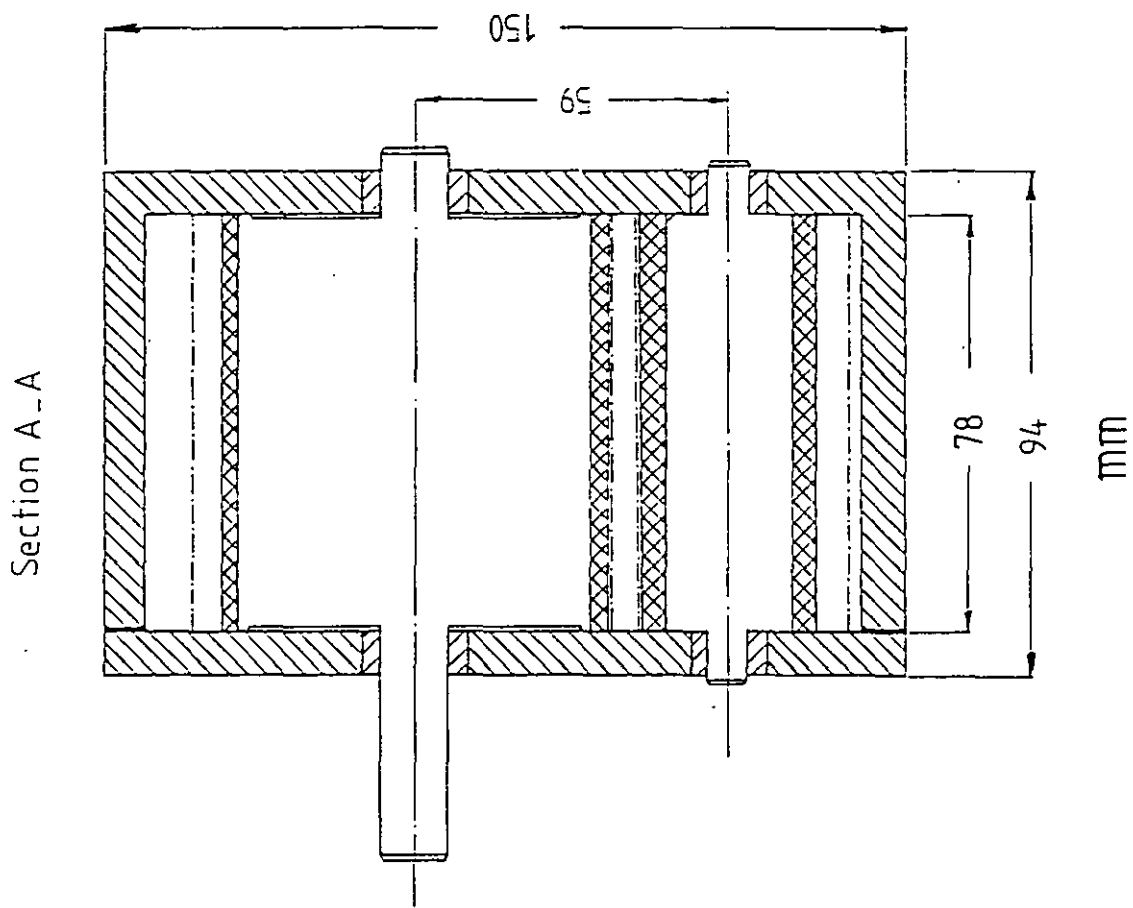
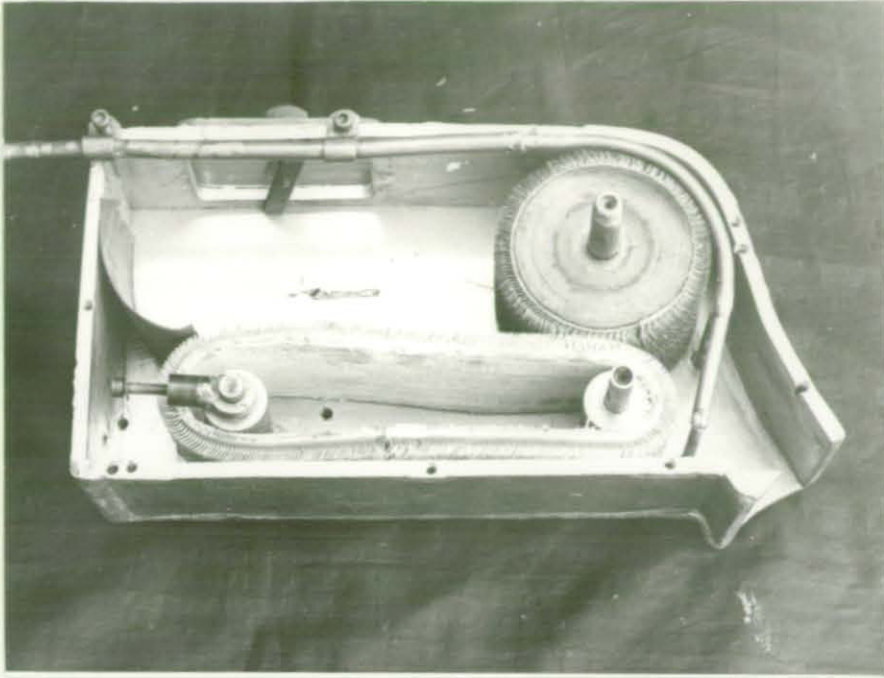


FIGURE 18: Fibre Separation Device (final design)

to adjust the belt tension. A wire brush roll is engaged with the wire brush belt to form the fibre separation zone, both moving in the direction indicated (Figure 18) and with a speed ratio of 3:1, the moving belt being the slower.

The speed ratio was disregarded whenever it was necessary to adjust the movement speed of the belt, which controls the rate of fibre feed into the separation zone. Both the wire brush, roll and belt are manually driven. The roll and belt are located in relation to each other so that clearance in the radial direction in the separation zone is kept to minimum (< 0.1 mm), to prevent unseparated fibres passing through in the axial direction. The brush wires of the roll pass through the spacing between the wires of the belt. Two nitrogen nozzles are located in relation to the roll and belt to detach fibre carried over by the wires, after passing through the separation zone, and direct them down into the melt through a chute (not shown). The nitrogen nozzles also provide a continuous cover of nitrogen above the melt and thus prevent excessive oxidation of aluminium.

The whole mechanism is enclosed inside a frame made of aluminium sheet which incorporates an access covered with a removable lid of a transparent material (perspex). The access is used for loading the fibres to be separated and to observe the rate of fibre feed to the separation zone so that adjustment of the movement of the belt can be made if necessary. An inside view of the device is shown in Figure 19a, which shows the components and the structure of the device, Figure 19b shows the external appearance. During trials, silicon carbide fibres were well separated and directed into the melt at a controllable rate. The device was also satisfactory as a second stage to separate alumina fibres after pretreatment in an alcohol-water solution (this will be detailed in Section 3.5). The design was adopted and used as a part of the arrangement for producing composites reinforced with fibres (SiC and Al_2O_3).



(a)



(b)

FIGURE 19: Fibre Separation Device

3.3.2 Stirring Propeller and its Shaft

In the primary set up described in 3.2, difficulties concerning the stirring propeller and its shaft were experienced as discussed in 3.2.1-IV. These difficulties were:

1. The refractory coating used to prevent dissolution of the propeller material (stainless steel or carbon steel) in the molten aluminium was eroded away, leaving the propeller material exposed to the melt and releasing powder which consistently caused rejection of the fibres.
2. The close-fit joint between the drive motor and propeller shafts did not provide adequate alignment between the two shafts, which brought the propeller out of balance at high rotational speeds.

These difficulties were overcome by choosing anode type graphite as the material for the propeller and by the elimination of the joint. Graphite was chosen because it is not wet or dissolved by the molten aluminium. Furthermore the propeller could be designed and shaped to provide higher efficiency, so that a strong enough vortex could be created in the melt at a lower rotational speed to minimise the balance problem. The length of the propeller shaft could not be reduced because the minimum length was already used.

A triple blade marine design propeller was designed for maximum propeller downwash, for the dimensions, and reduced drag which would result in improved efficiency of the propeller. The dimensions and configuration of the propeller are shown in Figure 20.

A blank of graphite was first turned down to a dimension close to the external dimension of the propeller and then a $\frac{1}{2}$ " BSF internal thread was cut into the blank propeller boss. The blank was then screwed onto the propeller shaft and turned down to the final external dimension. By following this procedure good balance of the finished propeller was



FIGURE 20: Graphite Propeller

Diameter	75 mm
Propeller-blade angle	45°
Propeller-blade width	43 mm (maximum at the blade tip)
Diameter of the propeller's shaft	13.35 mm
Ends with	½" BSF thread

obtained. The final configuration of the blades and hub were carefully hand machined.

The drive motor and propeller shafts were replaced by a one piece shaft which avoided any joints. At one end the shaft is fixed to two ball-bearings in the drive motor, at the other end the stirring propeller is fixed by a $\frac{1}{2}$ " BSF thread. The shaft diameter and overall length are 13.35 and 488.5 mm respectively.

3.3.3 Modification of the Squeeze Casting Die and Punch

In earlier work on squeeze cast aluminium-silicon alloys containing graphite, at Loughborough University, the squeeze casting die illustrated in Figure 21 was used by P R Gibson¹²².

Certain modifications were carried out jointly with P R Gibson to the squeeze casting die and punch.

Figure 21 shows that the simple punch allowed no means for extraction of the casting after solidification. Extraction was facilitated by a bolt screwed to the punch which intruded into the molten metal during squeeze casting. After the casting had solidified, it was unscrewed. This method was considered impracticable and since the press used is a single action one, no provision could be made for an ejector pin. Therefore a new punch was manufactured to incorporate a dovetail as shown in Figures 22 and 23. A shoulder was also incorporated to prevent the punch from moving too far, and interfering with the die taper. The punch was manufactured from H13 die steel, hardened and tempered in accordance with the material supplier's instructions. An insert was placed in the cavity of the die (Figure 22) to reduce the unnecessary (for this work) extra length of the casting and consequently the aspect ratio.

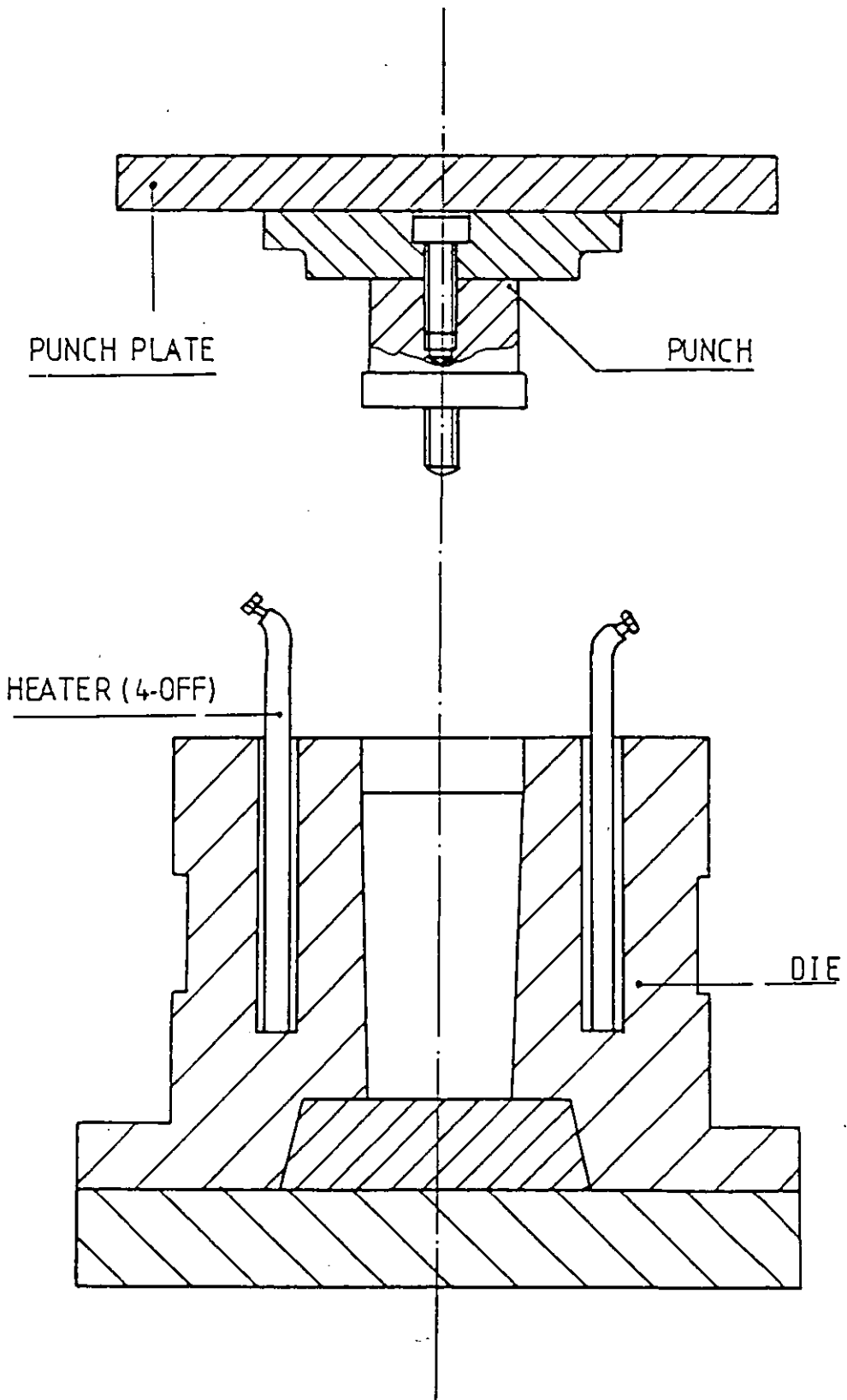


FIGURE 21: Squeeze Casting Die (before modification)

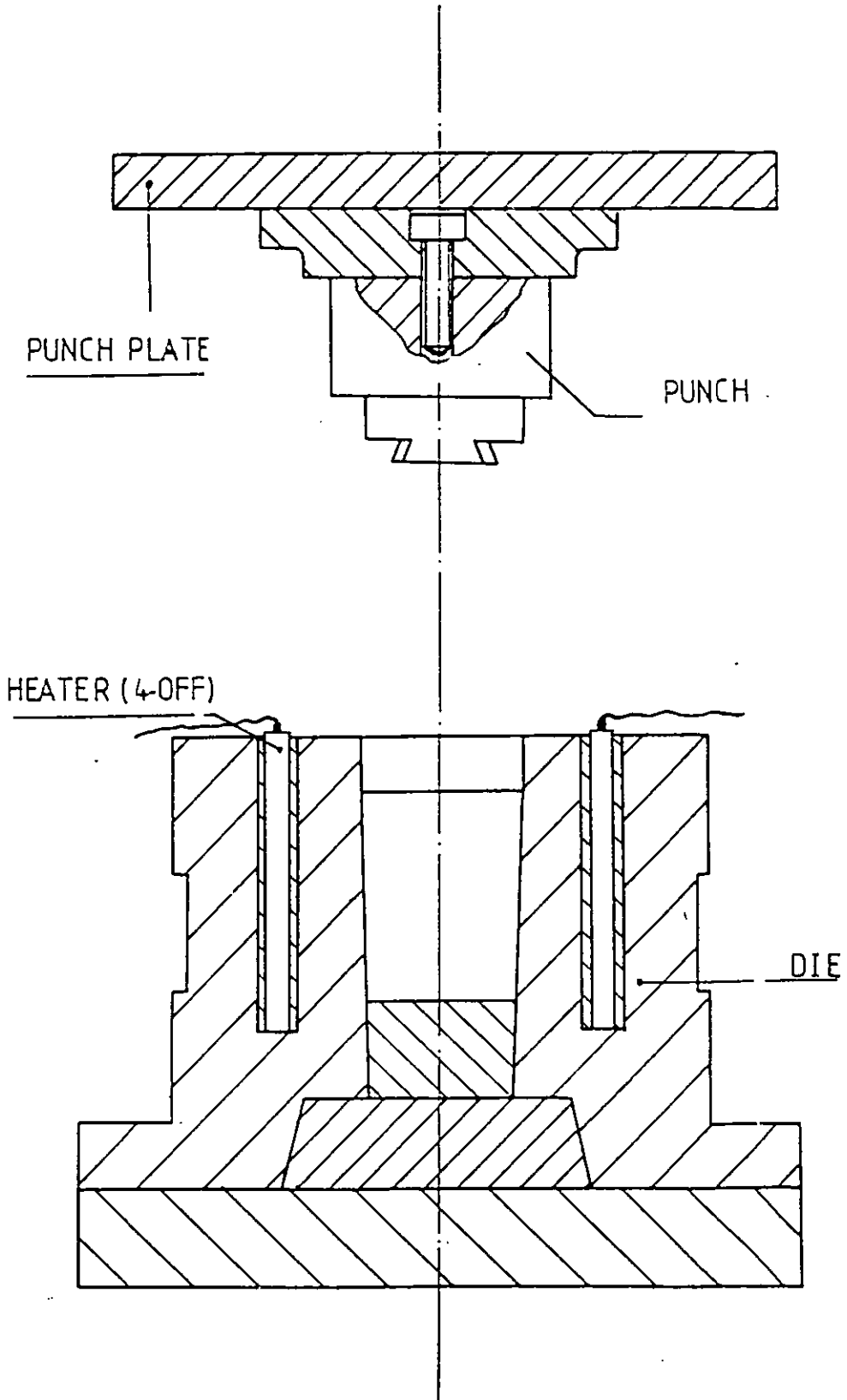


FIGURE 22: Squeeze Casting Die (after modification)



FIGURE 23: Modified Punch

3.4 EXPERIMENTAL SET-UP FOR THE PRODUCTION OF SQUEEZE CAST COMPO-SITES

The equipment used for the production of squeeze cast composites consisted mainly of two parts:

1. Set-up for the production of liquid composites
2. Set-up for squeeze casting the liquid composites.

3.4.1 The Set-Up Used for the Production of Liquid Composites

Certain difficulties met at the exploratory stages led to the development of the final set-up described here (Figures 24 and 25), which is mainly an assembly of components designed and fabricated as described in Section 3.3. These consisted of:

1. A Morgan electrical resistance crucible furnace with 0-1000°C Eurotherm contact breaker type controller.
2. A Mullite (grade J/A) crucible, inside diameter 95 mm and depth 200 mm.
3. A Fisons 1.5/1T 5851/14H variable speed stirring motor.
4. A triple blade graphite propeller (Figure 20).
5. A framework for attachment of the stirring motor to the furnace (Figure 25). This allows easy adjustment of the position of the propeller (driven by the motor) in relation to the crucible. The motor is fixed onto the attachment by a cam type lock.
6. A device for fibre separation (Figures 18 and 19).
7. A chute to aid the direction of fibres leaving the separation device into the melt. This is cemented to the furnace lid.

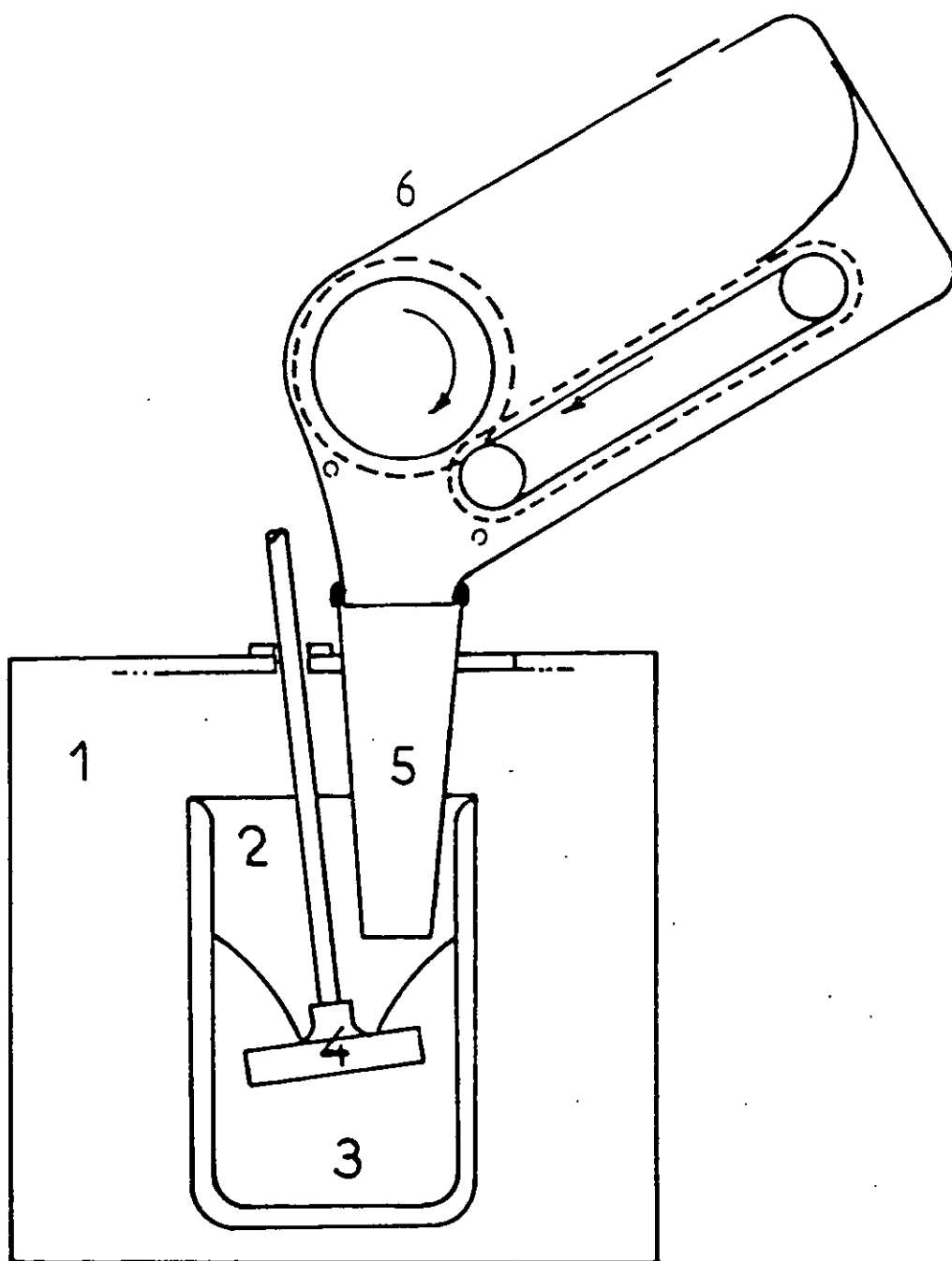
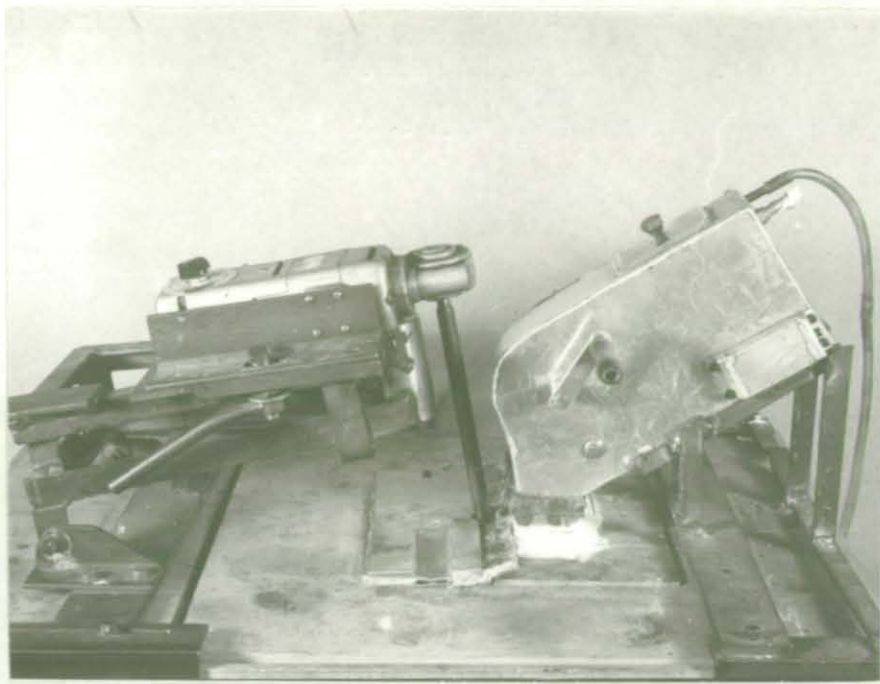
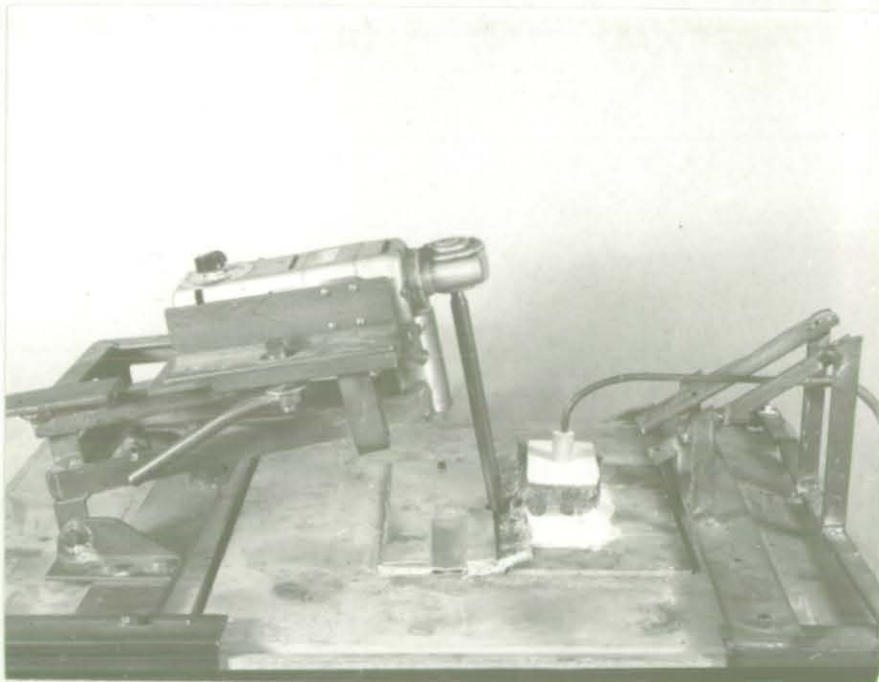


FIGURE 24: Arrangement (schematic) for Introducing Fibre into Molten Alloy

1. Resistance furnace
2. Crucible
3. Liquid metal + fibre
4. Graphite stirrer
5. Chute
6. Fibre separation device



(a)



(b)

FIGURE 25: Arrangement for Introducing Fibre into Molten Alloy

The furnace is covered by a two-piece lid, to facilitate easy assembly or withdrawal of various components. Areas of interface between various components (lids and furnace, shaft and lids, and fibre separation device and chute) are well sealed using a refractory cloth to minimise nitrogen gas leakage. A positive pressure of dry, oxygen-free nitrogen was maintained inside the furnace to minimise oxidation of the molten aluminium. Nitrogen was fed into the furnace through the fibre separation device or external tube after the withdrawal of the separation device, when fibre separation and introduction into the melt had finished (Figure 25b).

3.4.2 Squeeze Casting Equipment

The modified die and punch shown in Figure 26 (and illustrated in Figure 22) were employed to squeeze cast the matrix alloys and the composite produced. This enabled the production of squeeze castings in an ingot shape (Figure 26). This casting enabled all the samples which were required for mechanical tests to be produced in the sizes and shapes required.

Die heating was carried out by four equispaced 500W cartridge heaters (manufactured by Cole Equipment Ltd) in conjunction with a Eurotherm temperature controller and chromel-alumel thermocouple. This allowed accurate control of the die temperature in the range between ambient temperature and 400°C.

The die and punch are fitted to a 50 tons single action plastics press (Turner).

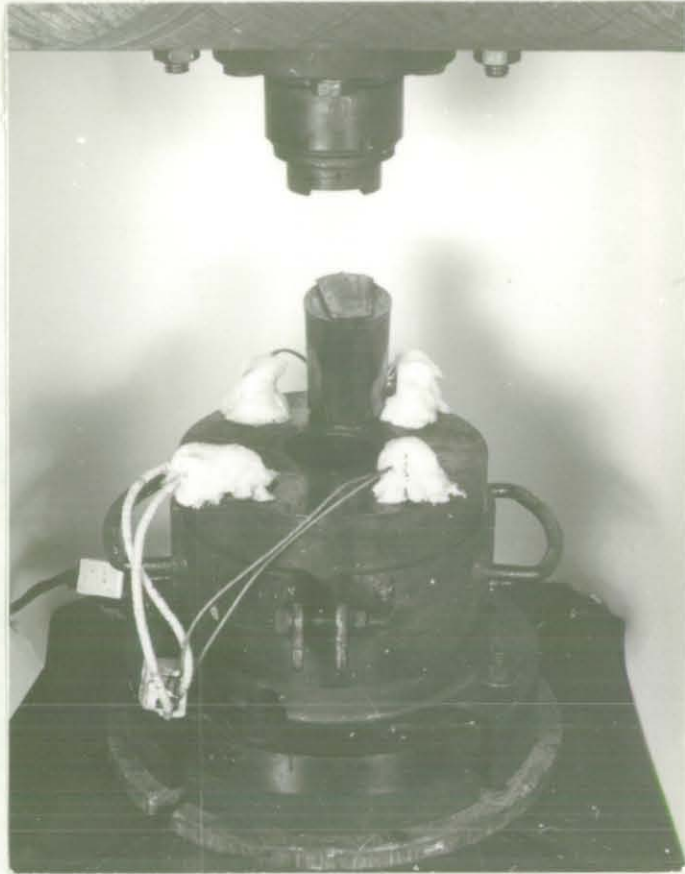


FIGURE 26: Squeeze Casting Die and Punch

3.5 METHODS OF COMPOSITE PRODUCTION

Production of composites can be divided into three steps:

1. Preparation of the composite constituents (fibres and matrix).
2. Preparation of a liquid composite.
3. Squeeze casting the liquid composite produced.

3.5.1 Preparation of Matrix Materials and Fibres

I: *Preparation of the Matrix Alloys:*

Two aluminium alloys were used as a matrix material to be reinforced with short fibres (see 3.1.2), Al-4.5% Cu, and Al-3.75% Mg. The Al-Cu alloy was first reinforced with silicon carbide or alumina fibres, later only the Al-Mg alloy was reinforced with alumina fibre. The alloy Al-3.75% Mg was purchased in small ingots and ready for use (see 3.1.2 and Table 4). The Al-4.5% Cu alloy was produced by melting the required quantity of LMO (commercially pure aluminium, see 3.1.2, Table 3). A predetermined quantity of electrolytically pure copper was then added to produce a final composition of 4.5% by weight of copper in aluminium. The melt temperature was maintained between 725-775°C until all the copper was fully dissolved. Nitrogen degassing was carried out for five minutes to remove dissolved hydrogen and oxidation was minimised by ensuring that the melt surface was not disturbed. The melt surface was then skimmed off and the alloy cast into steel ingot moulds which produced ingots of 0.3-0.5 kg. The alloy was produced in quantities of 8-10 kg.

II: *Preparation of Fibres:*

Two kinds of fibres were used, silicon carbide and alumina fibre. The reasons for selection and the specifications of these fibres are given in 3.1.1 and Tables 1 and 2 respectively.

a) *Preparation of Nicalon^(R) silicon carbide fibre:*

These fibres were heated in an oven for 2 hours at a temperature of 900°C, in circulated air. The treated silicon carbide fibres were then ready to be separated and dispersed in the melt. The necessity for this pretreatment and the conditions employed is discussed in 3.2.1-I.

b) *Preparation of 'Saffil' alumina fibres - grade RF:*

Two methods of pretreatment of the alumina fibres were used:

1. In this method preparation of the alumina fibre consisted of two stages: primary separation and heat treatment. In the first stage, the fibres were partially separated by breaking down the existing clumps of fibre, this was carried out using the set-up shown in Figure 27. As-received fibre were dispersed in a mechanically stirred solution of alcohol-water (10-15% v/v alcohol) for 5 minutes. Alcohol improved the wetting of the alumina fibre by water enabling the solution to flow into the pores of the fibre cluster and displacing the gas phase making fibre separation easier. After the fibres had been well dispersed in the solution, the stirrer was retracted and the fibres filtered through a Buchner funnel under reduced pressure. This procedure was repeated three times using deionised water, instead of the solution mentioned, in order to wash off the fibres. The filtered fibres have a disc shaped mass. This mass was thoroughly dried in an oven at a temperature of 160-175°C. The use of temperatures in this range was critical, drying at lower temperatures in the region of 100°C produced a compact mass of fibre. At a temperature in the recommended range the sudden evaporation of moisture forced the fibres apart producing a fluffy mass of fibres.

In the second stage the fibres were heat treated in circulated air for 2 hours at 900°C. This treatment was identical to that used for silicon carbide fibres.

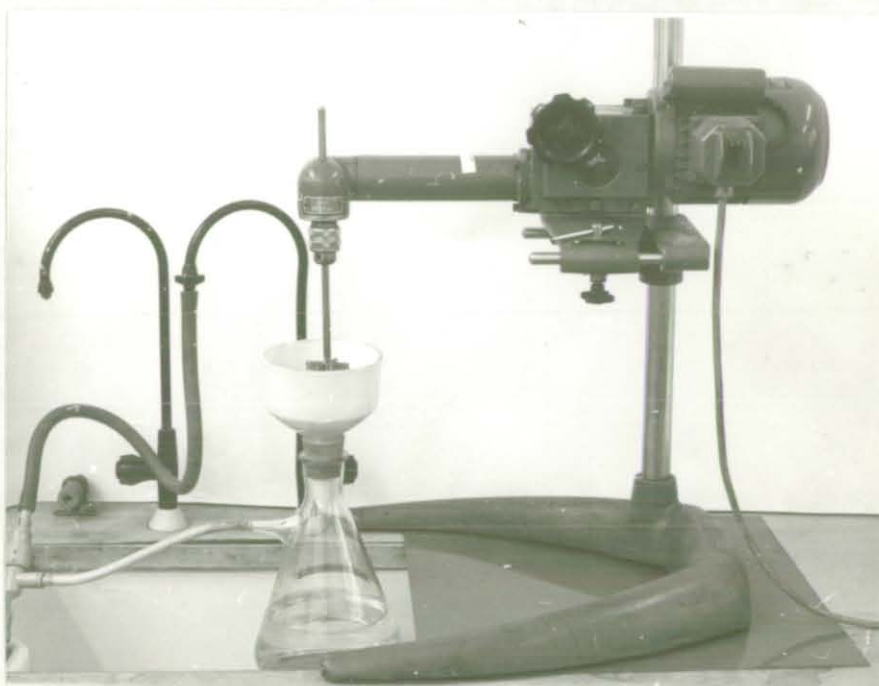


FIGURE 27: Arrangement for First Stage Separation of Alumina Fibre

2. It was found at a later stage that the heat treatment of silicon carbide fibre affects their strength (this will be detailed later). However, it was not possible to examine the effect of similar heat treatments on the much smaller alumina fibre. As a precaution, attempts were made to replace the heat treatment of alumina fibre by some other method of cleaning the surface of the fibres to enhance their wettability with the molten matrix alloy.

It was found that the following treatment was satisfactory in providing a clean surface on the fibre as well as a primary separation stage. The set-up described in the first method of preparation of alumina fibres was used (Figure 27). Fibres were dispersed and pickled for five minutes in a stirred hydrochloric acid diluted in deionised water (15% v/v hydrochloric acid), the fibres were then filtered. Following this, the fibres were washed off three times by dispersing them in deionised water followed by filtering. The resulting mass of fibre was then dried out at 160-175°C. This procedure produced a fluffy mass of clean alumina fibres.

Pickled alumina fibres were well wetted by water and it was not necessary to use an alcohol-water solution.

It was visually recognisable that alumina fibres treated by either method were cleaner when compared with the as-received fibres, as indicated by their whiter colour. This suggests that the treatment resulted in the removal of some kind of contamination from the fibre surface.

Note:

Attempts to replace the heat treatment of silicon carbide fibres failed. A treatment similar to that for alumina (by pickling in a diluted hydrochloric acid), resulted in the formation of fibre agglomerates especially

at the washing stages, even when gentle air agitation was employed (Figure 28). The fibre agglomerates were strongly interlocked and it was not possible to separate these fibres without damaging them.

3.5.2 Preparation of Liquid Composites

The set-up shown in Figure 25 and illustrated in Figure 24 was used to separate and disperse pre-treated fibres of silicon carbide or alumina in the molten matrix alloy (Al-Cu or Al-Mg). The procedure was as follows:

- A charge (0.75-0.8 kg) of the matrix alloy (LM5 or Al-4.5 Cu) was melted in the electric furnace
- The melt was degassed by bubbling dry, oxygen-free nitrogen through for 3-4 minutes. Degassing was carried out at a temperature between 700-730°C
- The melt was then held at the temperature for fibre dispersion (melt temperature varied and is reported for each group of castings in the following section - 3.6)
- The melt surface was then skimmed off
- Both the drive motor (to which the propeller is attached) and the fibre separation device were assembled onto the furnace and a nitrogen gas flow of 5-6 litres/minute immediately provided through the fibre separation device
- A predetermined quantity of pretreated fibre (silicon carbide or alumina) was loaded into the fibre separation device
- A deep vortex was then created in the melt using the graphite propeller

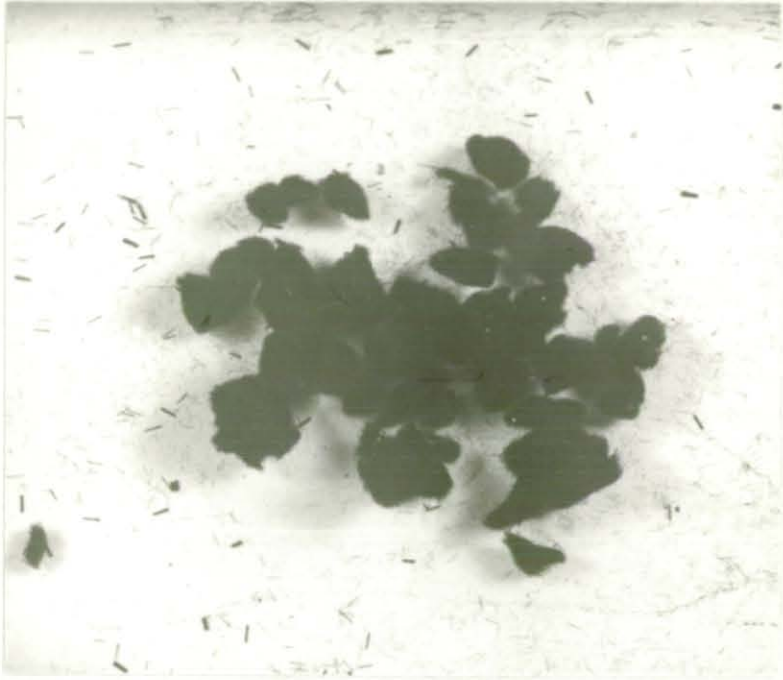


FIGURE 28: Silicon Carbide Fibre Treated in Alcohol-Water Solution

- Fibres were then fed to the separation zone (inside the separation device, see 3.3.1-III), by advancing the moving belt, and separated and introduced to the melt by rotating the wire brush roll. The two nitrogen nozzles helped to detach the fibres carried over by the wires and direct all the separated fibres down into the melt through the chute.
- Separated fibre was drawn by the vortex and dispersed in the melt
- After the predetermined quantity of fibres had been introduced and dispersed in the melt the fibre separation device was then retracted. Nitrogen flow was then provided through an alternative source (Figure 25b).

3.5.3. Squeeze Casting the Liquid Composite

The squeeze casting die was heated up to 110°C, and a thin layer of water-based, colloidal graphite parting agent applied to the cavity of the die and the punch. The die temperature was then raised to 250°C.

The liquid composite was cooled to the squeeze casting temperature, poured into the die cavity and squeeze cast. The conditions for squeeze casting were:

- | | |
|--|---|
| - Die temperature | 250°C |
| - Squeeze pressure | 140 MN/m ² |
| - Time delay before pressure application | 5 seconds |
| - Pressure duration | 60-90 seconds |
| - Pouring temperature | Superheat: 40°C for composites
with a Al-4.5Cu matrix
50°C for composites
with a LM5 matrix. |
| - Parting agent | DAG 2582 - supplied by Acheson
Colloids Company. |

The casting parameters were determined from the literature, including previous work by Chatterjee⁴¹, as well as some preliminary investigations on squeeze casting of the matrix alloys used. This will be detailed in the following section. The squeeze cast ingot was then extracted and prepared for the planned examinations and tests.

3.6 GROUPS OF CASTINGS PRODUCED

Using the methods and equipment described earlier, several groups of castings were produced:

GROUP I: Squeeze Cast Matrix Alloys (Al-4.5 Cu, and Al-3.75 Mg):

The matrix has more influence on the tensile properties of a short fibre composite than it has on a continuous fibre composite. A matrix of high strength and ductility is therefore desirable. An equiaxed matrix structure is essential in order to obtain isotropic properties when the matrix is reinforced with randomly oriented fibres.

The objectives of these experiments were to ensure that equiaxed matrix structures were obtained and that the optimum squeeze casting condition (pressure) for higher strength and ductility were determined.

Both matrices were squeeze cast at various pressures between 70 and 180 MN/m², which corresponds to a press load of 15 ton and 40 ton. Outside this range the press did not function properly (a press load test is detailed in Appendix I). The matrix alloy Al-4.5 Cu has a freezing range of 79°C* (liquidus at 647°C and solidus at 568°C) and it was squeeze cast at 40°C superheat. The alloy Al-3.75 Mg (LM5) has a freezing range of 62°C* (liquidus at 642°C and solidus at 580°C) and it was squeeze cast at 50°C superheat. The time delay before pressure

* Data of solidification was obtained from published phase diagrams. Due to the presence of impurities in the used alloys, the values of data are approximate.

application was 5 seconds for both alloys. Colloidal graphite was used as a die dressing, and nitrogen gas was used for degassing the melts before squeeze casting.

GROUP II: Sand and Gravity Die Cast Matrix Alloys

The objective of these experiments was to compare the tensile properties of sand and gravity die cast matrices (Al-4.5 Cu, and Al-3.75 Mg) with those obtained by squeeze casting.

Both alloys were sand cast in green sand mould to produce a casting with the same shape and dimensions of the squeeze casting. A large feeder head was provided (feeder mass = 1.5 the mass of the ingot). The melt was degassed with nitrogen gas and cast at 700°C.

Gravity die casting was carried out using the squeeze casting die. Provision was made for a large feeder head using a sleeve of insulating material placed on the top of the die cavity. The feeder head had a mass ratio similar to that used for sand casting. The die was heated up to 250°C and dressed using colloidal graphite. Melts of both alloys were gravity cast at 700°C after degassing with nitrogen gas.

GROUP III: Squeeze Cast Al-4.5 Cu Reinforced with Silicon Carbide or Alumina Fibre (heat-treated)

The objectives of these experiments were to produce composites of Al-4.5 Cu alloy reinforced with either silicon carbide or alumina fibre, as well as to evaluate the structural quality and the tensile properties of the heat treated composites at room temperature.

Composites were produced using the technique described in Section 3.5. Alumina fibres were given an initial treatment in alcohol-water solution and then heat treated (see 3.5, 1.II.1). Fibres (SiC and Al₂O₃) were introduced and dispersed in the melt which was held at 800°C. Squeeze cast composites containing the following volume percentage of fibres (SiC or Al₂O₃), 0, 2, 4, 6, 8 and 10 were produced.

It was not possible to incorporate higher percentages of fibres in the matrix because the liquid composite became too viscous to pour. In addition, the risk of fibre breakage increases when stirring a viscous composite. The composites produced were solution treated at 545°C for 2 hours, quenched in hot water (80-90°C) and then precipitation hardened for 6 hours at 180°C.

Heat treatment conditions were experimentally determined (see Section 3.7).

GROUP IV: Squeeze Cast Composites of Al-4.5 Cu/SiC and Al-3.75 Mg/Al₂O₃
(as-cast)

Poor dispersion and bonding between the alumina fibres and the Al-Cu matrix was observed in the previous group of composites (III). For this reason the aluminium alloy LM5 (Al-3.75 Mg) was used as a matrix alloy to be reinforced with alumina fibre (see 3.1.2).

Poor properties of the heat treated composites in group III, could be a result of the low ductility of the heat-treated matrix. In this group of castings, composites were not heat treated.

Fibres were introduced to melts held at a temperature of 760°C for the matrix alloy Al-4.5 Cu, and 730-740°C for the matrix alloy LM5. Higher temperatures (800°C for the group II castings) were found to be unnecessary. In addition, higher temperatures caused some reaction problems in the case of the LM5 alloy (see 3.8.2).

Alumina fibres were pretreated as described in 3.5.1-II.b.2. by pickling them in diluted hydrochloric acid without the need for heat treatment.

The other fabrication conditions and the production techniques were as described in Section 3.5.

A group of squeeze cast composites of Al-4.5 Cu/SiC, and Al-3.75 Mg/ Al_2O_3 were produced with fibre contents up to 10 percent volume.

The main objective was to evaluate the tensile properties at room temperature, as well as to examine their structural integrity.

GROUP V: Squeeze-Cast Composites with Controlled Contact Time Between the Fibres (SiC and Al_2O_3) and the Melt (Al-Cu and Al-Mg)

Some tensile properties of composites in Group IV, such as proof stress, were substantially improved. Other properties such as modulus of elasticity did not improve in the case of Al-Mg/ Al_2O_3 composite, and improved only with up to 6% v/v SiC fibre in the case of Al-Cu/SiC fibre composite. Ultimate tensile strength did not improve in either case.

Considering the sound structural quality of these composites, it was the uncontrolled reaction between the fibres and the melts which was thought to be responsible for the generally unsatisfactory results obtained (despite the encouraging improvement in some properties). The reaction between the fibres and the molten matrices must be controlled so that a strong bonded interface is developed without deterioration of the fibre's strength, and optimum reinforcement is obtained. This is best judged by the tensile strength of the resulting composite. The extent of reaction between the fibre and the melt is dependent on their chemistry, the melt temperature, the atmosphere, and the time of contact. Keeping all factors, other than time of contact constant, a group of squeeze cast composites of both Al-4.5 Cu/SiC and Al-3.75 Mg/ Al_2O_3 containing a fixed volume percent of fibre (4%) was produced.

Although the planned time of contact was: 0, 5, 10, 20 and 30 minutes, a period of time was necessary to introduce and disperse the fibres into the melt, as well as to cool down the liquid composite to the squeeze casting temperature. The actual average* time of contact was: 6.5, 11.5,

* Half the sum of times of contact of the first and last fibre introduced to the melt.

15.5, 26.5, and 36.5 minutes in the case of alumina fibre and the alloy Al-3.75 Mg (held at 740°C). The average time of contact between silicon carbide fibre and the molten Al-4.5 Cu alloy, which was held at 760°C, was: 8, 13, 18, 28.5 and 39 minutes.

Pretreatment of alumina fibre was as for previous groups and described in 3.5.1-II.b.2 by pickling in hydrochloric acid.

VI: Squeeze-Cast Composites Under Controlled Time of Contact

It was found from the previous group of composite castings that a contact time of 18 minutes between silicon carbide fibre and a melt of Al-4.5 Cu alloy held at 760°C; and a contact time of 15.5 minutes between alumina fibre and a melt of Al-3.75 Mg held at 740°C; produced composites with maximum tensile strength. At these conditions a group of squeeze cast composites of Al-4.5 Cu/SiC and Al-3.75 Mg/Al₂O₃ was produced. The fibre content was up to 10% v/v for both composite systems.

Specimens from these composites were tensile tested at room temperature, the main objective being to assess the tensile properties of composites so produced.

VII: Final Squeeze Cast Composites (Al-4.5 Cu/SiC and Al-3.75 Mg/Al₂O₃) Under Controlled Time of Contact

It was concluded from the results obtained for the previous group of squeeze cast composites (Group VI), that the desired tensile properties (for both composite systems) had been reached under the production conditions. The final evaluation of both composite systems could therefore be carried out, which was the objective of this final group of castings.

3.7 HEAT TREATMENT OF THE SQUEEZE CAST Al-4.5 Cu ALLOY

Although the Al-4.5 Cu alloy is equivalent in composition to LM11 and 2L92, squeeze casting was expected to produce some alteration of the alloy microstructure^{55,61} which would affect its heat treatment conditions, mainly in terms of time needed.

An attempt was made to establish the heat treatment conditions for the squeeze cast Al-4.5 Cu alloy. Specimens of the dimensions 15 x 15 x 25 mm, were solution treated (in groups) at 545°C for 2, 4 and 6 hours and then quenched in hot water (80-90°C). A precipitation hardening treatment was carried out for each group for 2, 4 and 6 hours at 180°C. The temperatures for heat treatment were established from the Al-Cu phase diagram. The effectiveness of heat treatment was assessed by the resulting hardness of the specimens.

3.8 OBSERVATIONS ON COMPOSITE PRODUCTION

3.8.1 Fibre Rejection

In addition to the fibre rejection problem encountered by the existence of powder released from the stirrer's refractory coating in the early exploratory work, fibres were rejected from the melt as a result of the presence of any powdery materials, such as graphite powder released when a stirring propeller made of the type of graphite used in spark erosion machine electrodes was used. Fine graphite powder was attracted to the fibres' surface which acted as a barrier and prevented wetting. This problem was experienced with both fibres (SiC and Al₂O₃), however alumina fibre seems to be more tolerant of the presence of powdery materials.

The graphite used (anode type) has a large grain structure and at working conditions releases comparatively larger particles of graphite (> 0.2 mm) which did not cause any rejection problem with the fibres.

3.8.2 Reaction of the LM5 Alloy with Atmosphere

It was observed at an early stage that the alloy LM5 (Al-3.75 Mg) developed some reaction products at the melt surface when held at a temperature 760°C under a nitrogen cover. The reaction product was cauliflower-like in appearance and covered with a white compound of non-metallic appearance (Figure 29). The reaction product started to accumulate rapidly at the melt surface and at the crucible periphery (Mullite grade J/A) after a certain time (~ 15 minutes at 760°C). The reaction rate then appeared to slow down. A melt held in a graphite crucible under the same conditions developed reaction products (at the melt surface) different in appearance (Figure 29) and in a reduced quantity. A normal protective oxide film was developed at the melt surface when the nitrogen cover was replaced by air introduced at the same rate as nitrogen (6 litres/min) and the melt was held in a Mullite crucible.

Three samples of the reaction products mentioned above were analysed using the Energy Dispersive Spectroscopy and Wavelength Dispersive Analysis Techniques. Analysis was carried out by A.E. Developments Limited, and a report was provided which is enclosed in Appendix II. This will be discussed in Chapter 6. However, it was observed that the reaction was time dependent and started after holding the melt for a certain time, which in turn was dependent on temperature. At 780°C the reaction product started to appear after only 5-7 minutes compared with 15 minutes at 760°C , whereas at 740°C the reaction product slowly developed after 40 minutes.

It was possible therefore to produce the LM5 matrix composite providing the melt temperature was maintained below 740°C (730 - 740°C) and the processing time did not exceed the time needed for the reaction to develop.

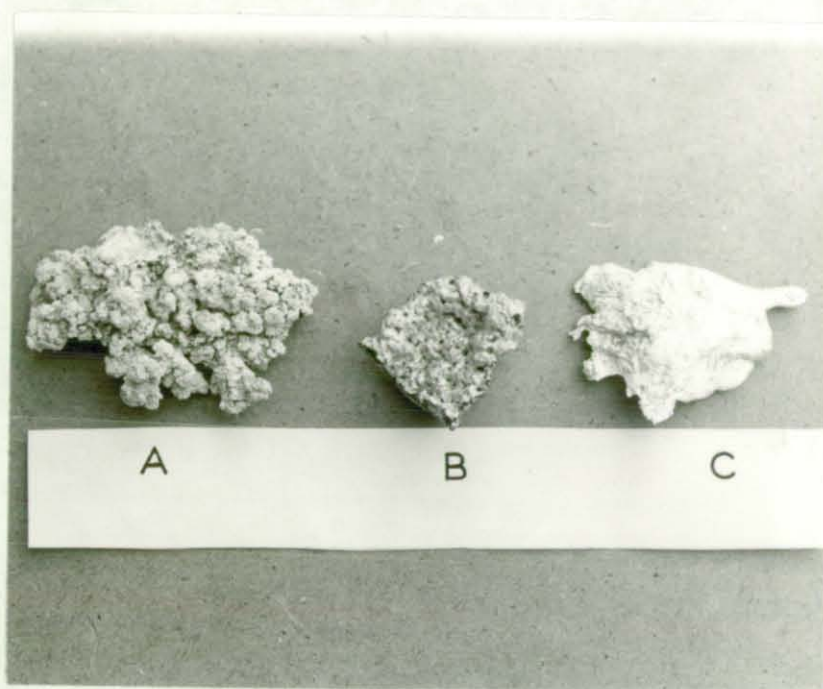


FIGURE 29 : Reaction Product of a Melt of Al-3.7 mg at the Following Conditions:

- a) Melt was held in a mullite crucible under a nitrogen cover
- b) Melt was held in a graphite crucible under a nitrogen cover
- c) Melt was held in a mullite crucible, air was introduced at the same rate as nitrogen

CHAPTER IV

COMPOSITE EVALUATION

CHAPTER 4
COMPOSITE EVALUATION

4.1 PREVIEW

Composites are combinations of at least two phases. In order to achieve a composite of sound quality, it is essential to start with components possessing the desired properties and to ensure that these properties are retained when the components are combined together. The capability of the production technique used, to provide these requirements, will be a part of the evaluation process, which includes the following:

1. Examination for fibre damage as a result of processing such as fibre breakage and surface damage.
2. Examination of the structural quality of the squeeze cast matrix alloys.
3. The room temperature tensile properties of squeeze cast matrix alloys at various casting pressures. Tensile properties include: ultimate tensile strength, offset proof strength, elongation and reduction in area.
4. Room temperature tensile properties of sand and gravity cast matrix alloys (for the purpose of comparison).
5. Examination of the soundness of squeeze cast composites.
6. Fibre distribution and orientation in the matrix alloys.
7. Assessment of the heat treatment conditions for the matrix alloy Al-4.5 Cu.

8. Room temperature tensile properties of both composite systems.
9. Assessment of the isotropic tensile properties of the composite systems.
10. High temperature tensile properties of the composite systems.
11. The effect of thermal cycling on room temperature tensile properties of both composite systems.
12. Fatigue life of the composites compared to those of the matrix alloys.
13. Examination of the tensile and fatigue fractures.
14. Examination of the fibre-matrix interface.
15. The effect of fibre on machining tool wear.

4.2 EXPERIMENTAL PROCEDURE AND TECHNIQUES

4.2.1 Fibre Damage

Fibre breakage:

The as-received silicon carbide and alumina fibres are on the average 3 mm and 0.5 mm in length respectively. Fibres were examined for possible breakage during processing. The following samples of both fibres were examined for length:

- as-received fibres (SiC and Al₂O₃)
- as-received and separated fibres using the fibre separation device (no pre-treatment)
- pre-treated and separated fibres (pre-treatment of both SiC and Al₂O₃ fibre is described in 3.5.1-II.a and 3.5.1-II.b.2 respectively)
- fibre extracted from composite by dissolving away the matrix in a solution of HCl:HF (depassivator):H₂O (30:0.5-1:70, v/v).

Fibre length was measured using a Vickers Photoplan optical microscope with eyepiece micrometer (a glassdisc with a scale of 100 divisions placed in the image plane of the eyepiece). The magnification of the object image is determined by the objective, the tube lens, and the eyepiece of the microscope, whereas the magnification of the eyepiece micrometer depends solely on the eyepiece. The size of the object examined must therefore be determined by calibration of the length of the object in μm or mm which is projected by a given objective on a division of the eyepiece micrometer. This value is called the micrometer value. It is different with each objective eyepiece combination for a certain tube lens.

A glass plate, with scale, $1\text{ mm} = 100$ divisions (stage micrometer) was used for calibration, the objective/eyepiece combination used was 5X/10X. It was found that 75 divisions on the eyepiece micrometer corresponded to 1 mm (100 divisions) on the stage micrometer.

Examination for fibre breakage as a result of mechanical separation of fibres was repeated whenever the separation device was maintained or its condition was in doubt.

Surface damage of fibres:

The following samples were examined for surface damage and defects:

- as-received fibres (SiC and Al_2O_3)
- pre-treated fibres (as in 3.5.1-I and B-2)
- pre-treated and separated fibres
- fibre extracted from composite (as in 4.2.1).

Scanning electron microscopy (Cambridge 'Stereoscan') was used for surface examination. The high magnification and great depth of field made possible the direct examination of the small fibre surfaces.

4.2.2 Metallographic Examination

Metallographic examinations were carried out to assess the structural quality of squeeze cast, sand cast, gravity cast matrix alloys (Al-4.5 Cu and Al-3.75 Mg), and the squeeze cast composites (Al-4.5 Cu/SiC, Al-3.75 Mg/Al₂O₃).

Structural quality was evaluated by examining the grain size and freedom from defects such as porosity and inclusions. Additionally, the structural quality of the composite was evaluated by observing fibre distribution and orientation.

Specimens for the purpose of macrostructural examination were produced by cutting vertical and horizontal sections from castings. Observations on the fibre distribution and orientation in the matrix alloy were made on similarly cut specimens. However for the majority of examinations, specimens were cut from different locations in the casting at planes parallel and perpendicular to the direction of the squeeze casting punch movement.

Observation of fibre distribution and orientation became a standard quality control procedure, which was carried out on samples of castings from all composite castings. Naked eye examination for visible defects such as voids and porosity were carried out for all castings when they were sectioned in preparation for machining of different test specimens.

Metallographic specimens were prepared by grinding (Buehler hand grinder or Metaserv rotary grinder) with successive grades of wet silicon carbide papers up to P600 grit, specimens were then rough polished with a nylon cloth and 6 μm diamond pastes and fine polished with 1 μm diamond paste and a metron cloth (on a Metaserv polisher). Grinding through 600 grit paper provided a flat matrix surface, however, the matrix adjacent to fibre (hard phase) was eroded away on polishing leaving fibre projected above the plane of the matrix. This was avoided by

applying a minimal pressure during polishing, and grinding with silicon carbide paper up to 1200 grit which reduced the polishing needed.

The following etchants were used for macrostructural examination:

- Macro etchant for the alloy Al-4.5 Cu
 - 5 ml HF
 - 20 ml HCl
 - 20 ml HNO₃
 - 60 ml H₂O
 - Duration of etching 10-30 seconds
 - Specimens were then cleaned with solution of 50% HNO₃.

- Macro etchant for the alloy Al-3.75 Mg
 - 15g of cupric chloride (CuCl₂)
 - 100 ml H₂O
 - Duration of etching 5-15 seconds.

4.2.3 Electron Probe Microanalysis

Electron beam microanalysis method was used to study the chemistry of the interface between the fibre and the matrix alloy in both composite systems. Analysis was carried out on specimens of composite with fibre exposed to the melt for different periods of time (castings group V), specimens of composite in casting, group VI, and specimens of as-cast and heat-treated Al-4.5 Cu matrix/SiC fibre composite (castings group III). It is desirable to study the variation in thickness of the reaction zone (if any) with time of exposure of fibre to the melt, however this may not be possible using this technique because of the small dimensions of both fibre and the reaction zone. A Cambridge Microscan 5 was used in this study.

4.2.4 Hardness Testing

Hardness testing to evaluate the heat treatment conditions of the alloy Al-4.5 Cu (see Section 3.7) was carried out using a Vickers Pyramid Hardness Testing Machine (Vickers-Armstrong). Hardness testing was used to measure hardness differences of specimens subjected to different heat treatment conditions. An average of minimum of three measurements was taken from each specimen.

4.2.5 Thermal Cycling

There is a considerable mismatch of thermal expansion coefficients between the Al-matrices (Al-Cu and Al-Mg) and the fibres (SiC and Al_2O_3)*. During thermal cycling, stresses and strains would develop due to the thermal mismatch between the two phases. Stresses are likely to concentrate at the interface, which might result in failure of the interface if the stresses developed are high enough.

Specimens of both composite systems (Al-Cu/SiC, and Al-Mg/ Al_2O_3) containing various amounts of fibres up to 10% v/v were thermally cycled between room temperature and 350°C. Specimens were taken from castings group VII. The specimens were heated in a furnace for 25 minutes and then quenched in air. A chromel/alumel thermocouple was inserted in the centre of a dummy specimen and was connected to a chart recorder in order to monitor the temperature of the specimens during cycling. A thermal cycle is shown in Figure 30.

Specimens, after thermal cycling, were machined and tested at room temperature (tensile).

* The specified thermal expansion coefficients of SiC fibre and Al-3.75 Mg is $3.1 \times 10^{-6}/^{\circ}C$ and $2.3 \times 10^{-6}/^{\circ}C$ respectively, $6 \times 10^{-6}/^{\circ}C$ (85) for Al_2O_3 fibre, and expected to be around $23 \times 10^{-6}/^{\circ}C$ for the matrix alloy Al-4.5 Cu

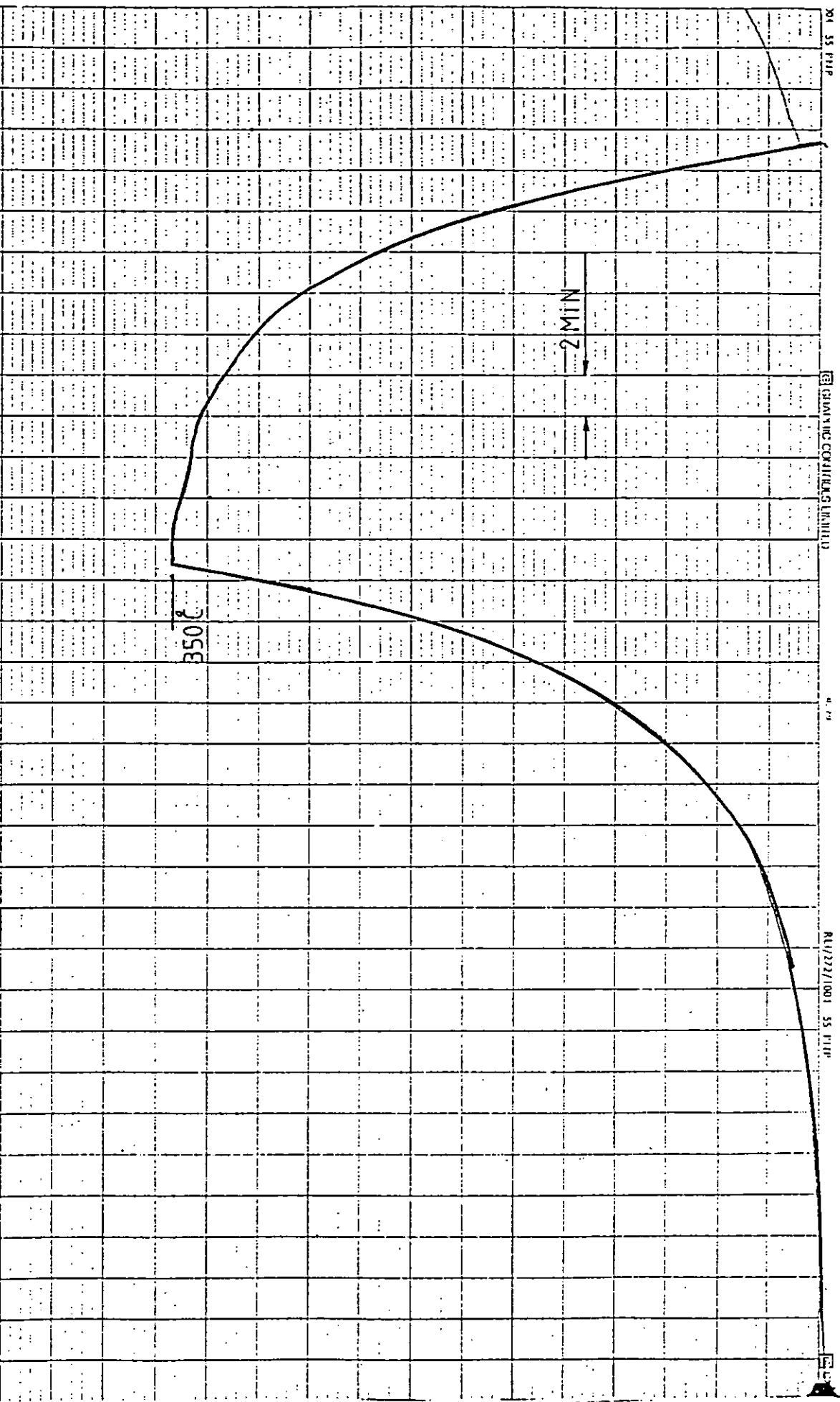


FIGURE 30: Thermal Cycle

4.2.6 Room Temperature Tensile Test

Tensile tests at room temperature were carried out for specimens of the following castings:

- squeeze castings of both matrix alloys (Al-4.5 Cu and Al-3.75 Mg), squeeze casting was carried out at various pressures (castings group I)
- sand and gravity castings of both matrix alloys
- squeeze cast composites (castings groups III-VII)
- squeeze cast composites to assess their expected isotropic tensile properties. Specimens included fibre-free castings (control). Specimens were taken from casting groups IV and VI
- squeeze cast composites subjected to thermal cycling as described in 4.2.5.

All tensile tests were carried out using Hounsfield No 18 tensile specimens*, except for castings in group III, where Hounsfield No 16 tensile specimens* were used. The dimensions of the casting ingot dictated the use of the smaller tensile specimens No 14* for the tensile tests were carried out to assess whether the tensile properties of the castings showed any anisotropy.

* Hounsfield tensile specimens have the following dimensions at ratio $L_0/D_0 = 3.54$

<u>Specimen No</u>	<u>Gauge Length (mm)</u> L_0	<u>Diameter (mm)</u> D_0
14	22.7	6.4 - 6.426
16	32.1	9.05- 9.09
18	45.4	12.8 -12.85

The approximate locations of the test specimens in the casting ingots are shown in Figure 31.

On machining, specimens of composites, particularly those with high content of fibre, had rough surfaces with some scratches, this was a result of the presence of fibre. Specimens were smoothed down using successive grades of silicon carbide papers up to 600 grit.

Tensile tests were carried out using a Mayes ESH250 tensile test machine with load cell and strain rate control. The machine is also provided with facilities which enable the use of a displacement transducer (D5.100 AG supplied by R.D.C. Electronics Limited) to sensitively and accurately measure elongation in the specimens, which made accurate measurement of the elastic modulus possible. Separate load vs extension graphs at extended scale were obtained for the calculation of the value of the elastic modulus, 0.1 mm extension or 5 kN. Load was represented by 10" on a recording chart.

Hounsfield gauges were used for the measurement of percentage elongation and reduction in area.

Specimens were tested for: ultimate tensile strength (engineering), 0.1 offset proof stress, modulus of elasticity, percentage elongation, and percentage reduction in area. All tests were carried out at strain rate $1.835 \times 10^{-4} \text{ s}^{-1}$. Average values were taken from a minimum of three test specimens taken from more than one casting.

4.2.7 High Temperature Tensile Test

Composite castings in group VII were tensile tested at temperatures 20, 150, 200, 250 and 300°C. Test conditions, except for temperature, were as for tests conducted at room temperature.

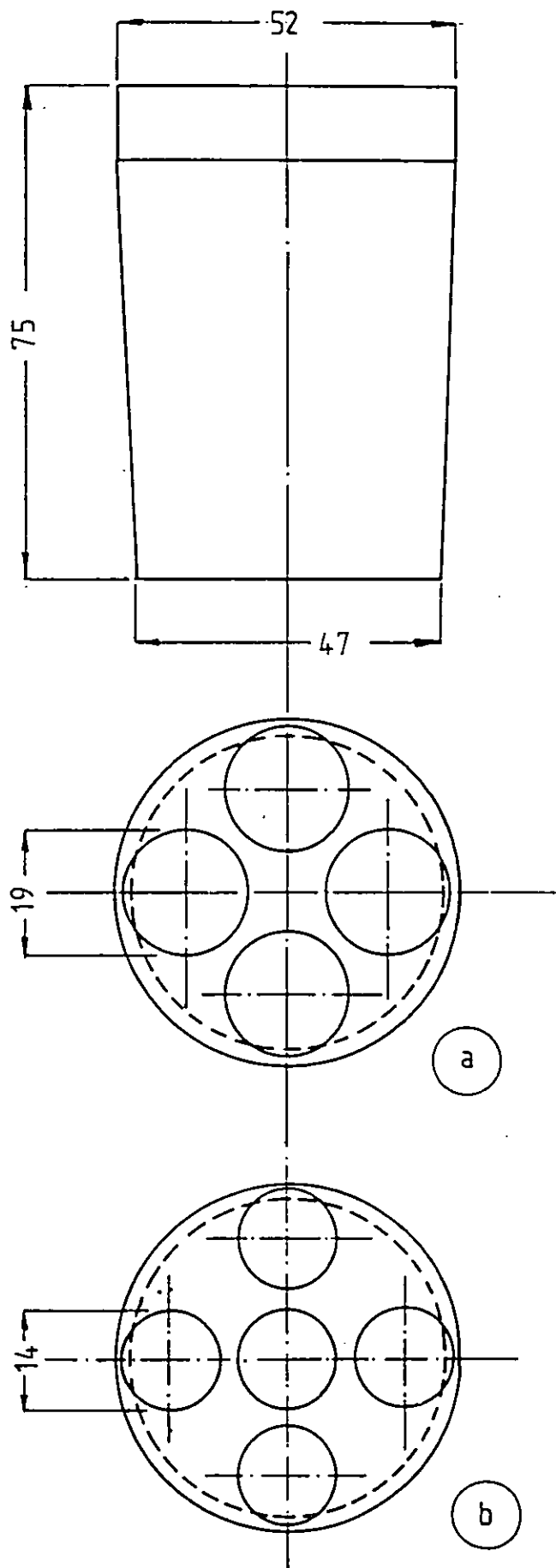


FIGURE 31: The Approximate Location of the Hounsfield Tensile Specimens in the Ingot Casting

/Continued

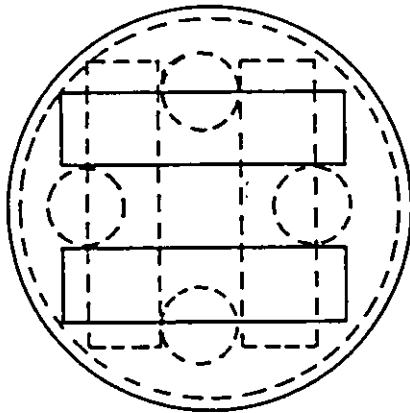
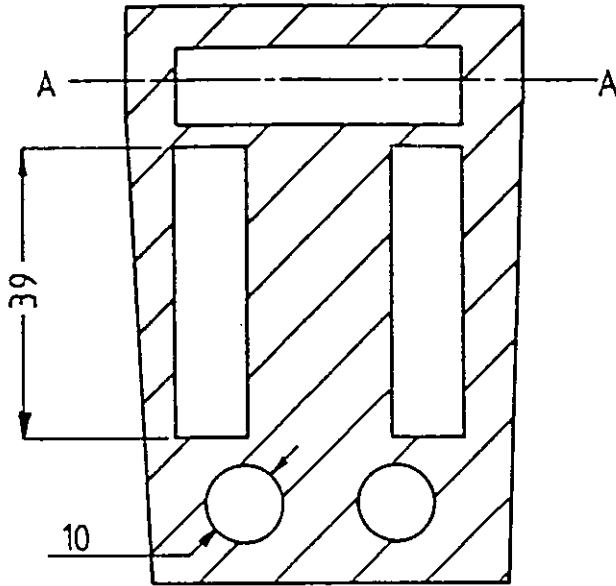


FIGURE 3k: continued

- a. Hounsfield tensile specimen No 18
- b. Hounsfield tensile specimen No 16
- c. Hounsfield tensile specimen No 14

Test specimens were vertically enclosed in a three-zone resistance wound furnace with temperature control, and power input control for each zone. The temperature of the specimens was found to be always lower than the control set temperature, in addition, there was a temperature gradient over the length of the specimens. For this reason, temperature setting and power input to each furnace zone were adjusted by trial and error to achieve a specified and uniform temperature over the volume of the test specimens. This was carried out using a dummy specimen into which three chromel/alumel thermocouples were inserted at three locations across the axial direction of the specimens, in the radial direction, temperature gradient was less than 2°C over the radius of the specimen at 200°C . The thermocouples were connected to a calibrated chart recorder.

A close control of the temperature of the specimen was possible, however, there was always some temperature gradient over the length of the specimen because of heat conduction to the frame of the test machine through the chucks. Temperature gradient was within acceptable limits, $2-4^{\circ}\text{C}$ at 150°C , $4-7^{\circ}\text{C}$ at 250°C and $5-8^{\circ}\text{C}$ at 300°C which is less than 3% of the test temperature.

When the correct adjustment to the temperature control was made and the desired test temperature was consistently reached in the dummy specimen at acceptable temperature gradient over its length, the dummy specimen was removed and cooled down to room temperature. Then it was put back into the furnace, and the time needed to reach the test temperature was recorded. This was repeated three times and the average time was taken. This procedure was repeated for each test temperature.

Actual test specimens were left in the furnace of the test machine for 10 minutes at test temperature.

4.2.8 Fatigue Testing

Specimens of squeeze cast composites, both Al-Cu/Sic and Al-Mg/Al₂O₃, as well as sand and gravity cast matrix alloys, Al-Cu and Al-Mg, were tested for fatigue life. Composite specimens were taken from castings group VII. Fatigue testing was carried out using a Wöhler-type (rotating bending) machine manufactured by GTG Engineering Ltd, Loughborough.

The recommended test specimen No K70B (Figure 32) was used, the test specimens have a section modulus, Z, equal to $\frac{\pi d^3}{32} = \frac{1}{184} m^3$, d = diameter of the specimen which is $3.81 \times 10^{-3} m$.

The manufacturers of the machine recommend a reverse bending stress (F) of 0.5 x UTS to be used for fatigue testing. The reverse bending stress F, is obtained from the formula

$$F(MN/m^2) = \frac{M(Nm)}{Z(m^3)}$$

where M is the bending moment which can be set to the wanted value (up to 6.8 Nm) on the machine.

A reverse bending stress of 95 MN/m² was selected, this corresponds to M set at 0.561 Nm.

The machine rotating speed was 2850 rpm which allowed 1.71×10^5 stress reversals per hour.

Specimens for fatigue testing were carefully machined and finished. Care was taken to minimise work hardening of the specimens surface on machining, as well as to ensure freedom from surface scratches in particular transverse scratches. The following procedure was followed:

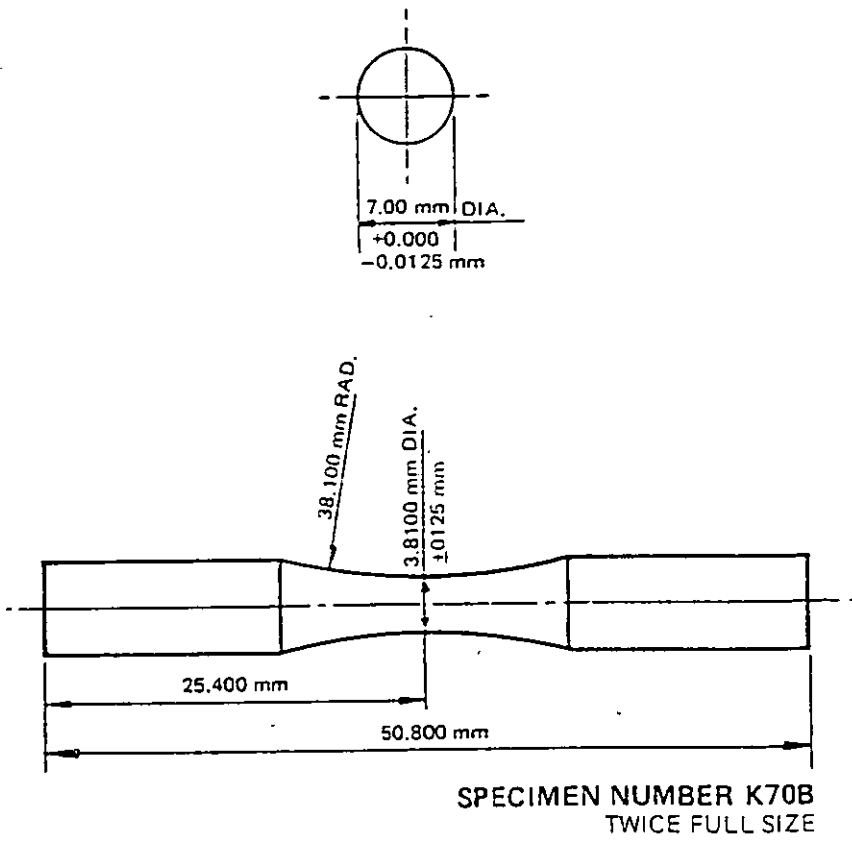


FIGURE 32: Fatigue Test Specimen

- specimens were machined to 0.127 mm oversize in diameter
- two cuts 0.025 mm deep in turning
- one cut 0.0127 mm deep in turning to finished size
- specimens were then transversely polished with 240 grit emery cloth in the lathe
- longitudinally polished with 600 grit followed by 1200 grit by hand
- final polish with a fine metal polish (Brasso metal polish).

Four specimens were taken of each composite or alloy casting, and an average was taken of time to failure. The fatigue life was then expressed in terms of number of reversals to failure.

4.2.9 Fractured Surfaces Examinations

The fracture surfaces of the specimens which were fractured by destructive tests (tensile and fatigue tests) both at room and high temperatures were examined using a Cambridge 'Stereoscan' scanning electron microscope. The great depth of field made possible the direct examination of the irregular topography of composite fracture surfaces from various angles. No preparation of the fracture surfaces was necessary. The main objective of these examinations was to observe the mechanism of composite fracture and the behaviour of the interface between fibre and matrix.

Examinations were carried out on representative specimens taken from each squeeze cast composite group.

4.2.10 Tool Wear Test

On sectioning of the composite cast ingots in preparation for machining of specimens for various tests, excessive tool wear was observed.

A bandsaw with a high speed steel blade was initially used for sectioning of the cast ingots. Although this tool was satisfactory when sectioning fibre-free casting ingots, the presence of fibre in composite castings greatly reduced the efficiency and the useful life of the tool due to rapid wear. At high fibre content the useful life of the tool was very limited which made the use of this tool impracticable. Later a special abrasive cut-off wheel (Buehler-10-4250) was used for sectioning the cast ingots. With squeeze casting it is possible to achieve a good surface finish and dimensional accuracy which makes the need for machining limited to the working surfaces. For this reason, machinability is not a major problem with squeeze cast components. However the awareness of the observed difficulty in machining a squeeze cast composite is important. With this in view a quantitative study on tool wear was carried out. The main objective of this study was to quantitatively examine the effect of the presence of fibres in the matrix on tool wear. The recommended procedure and conditions for tool-life tests by BS 5623:1979 and ISO 3685:1977 were followed as far as possible.

The limited amount of available test materials (composites) and the expense of silicon carbon fibre made it necessary to economise on material for the test. For this reason, testing was carried out while machining (turning) specimens for tensile tests. Specimens were taken from composite castings group VII.

Machining conditions were:

- cutting tool round, 4.76 mm in diameter, sintered tungsten carbide tool
rake angle 7° , clearance angle 8°
corner radius $\frac{1}{2} D = 2.38$ mm.
- average cutting speed 32 m/min
- feed rate 0.05 mm/min
- depth of cut 1.14 mm

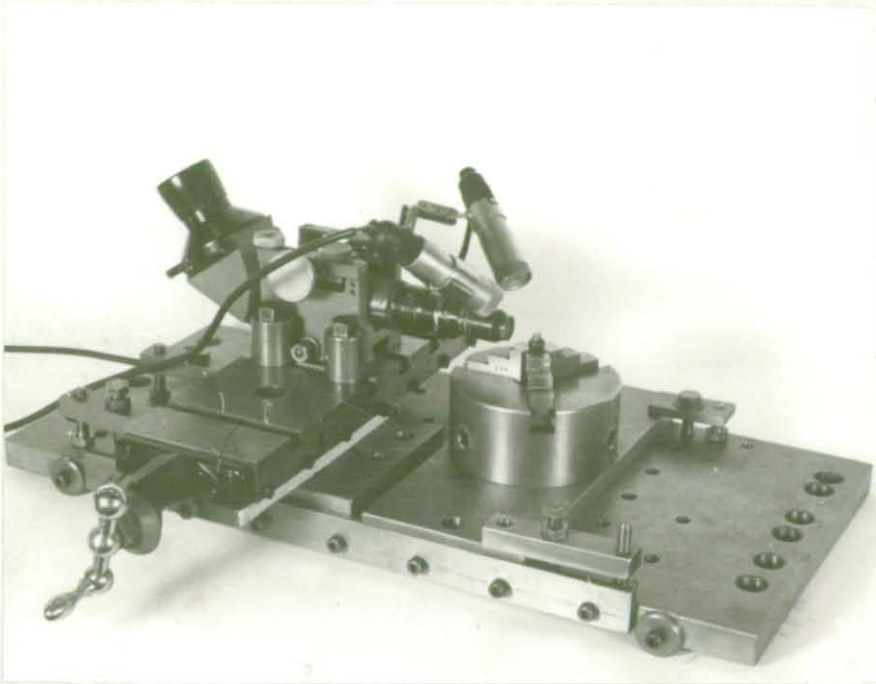


FIGURE 33: Arrangement for Measuring Wear on Cutting Tool

were compared with tensile strength values for the similarly tested as-received fibre. Although the heat treatment temperature of 900°C is well below the specified permissible service temperature of 1250°C for these fibres, the tensile strength values of the heat treated fibre were consistently lower than those for the as-received fibre. In a previous examination (4.2.1) of the surface of both the heat treated and the as-received fibre using a SEM, no surface defect as a result of heat treatment was observed.

In order to detect the causes of the reduction of the fibre tensile strength on heat treatment the following tests were carried out.

4.3.1 The Effect of Heat Treatment Conditions on the Tensile Strength of the Nicalon^(R) Silicon Carbon Fibre

Fibre of SiC were usually placed into a preheated muffle furnace for heat treatment, and kept at the temperature (900°C) for 2 hours after which fibre was taken out for further processing in preparation for fabrication of composite. Treated fibre when tested for tensile strength showed reduced tensile strength. Thermal shock at introduction of the cold fibre into the preheated furnace or at the withdrawal of the hot fibre to the relatively cool atmosphere was initially thought to be a possible cause of the reduction in tensile strength of the fibre on heat treatment. Another possible cause could be the exposure to atmosphere (air) at the temperature of heat treatment. For this reason, in addition to samples of the as-received fibre and fibre heat treated as usual (900°C for 2 hours in air), samples of fibre heat treated at the following conditions were tested for tensile strength. Fibres were heated in air unless otherwise stated.

1. Fibres were placed in the preheated furnace (900°C) and left at the temperature for 2 and 3 hours after which fibres were taken out.

2. Fibres were placed in the cool furnace and heated up to 900°C. Fibres were left at this temperature for 3 hours. The furnace was then switched off and left to cool down to room temperature. Heating up time was 2.5 hours and cooling down time was 4.5 hours.
3. As in 2 but heat treatment temperature was 800°C.
4. As in 2 but fibres were heated in vacuum of 5×10^{-5} torr. The smaller heat capacity of the furnace which was used for heat treatment in vacuum affected the heating up and cooling down times which were 1.5 and 2 hours respectively.
5. Fibres were placed in the preheated furnace (900°C) and left for 3 hours, the furnace was then switched off and fibres were left to cool down to room temperature inside the furnace.
6. Fibres were placed in the cool furnace then heated up to 900°C and left for 3 hours. Fibre was then taken out and placed on a cool block of copper for quick quench.

Silicon carbide fibres were 3 mm long which make them unsuitable for tensile tests, however it was possible to find some longer fibres (3-4 cm) which were tensile tested after being subjected to one of the heat treatment cycles described earlier.

Fibres were tensile tested using the set-up shown in Figure 34. The ends of a single fibre were fastened with glue to the ends of a fine string (Figure 35). One end of the string was hooked to a burette stand, while the other end was hooked to a plastic beaker through a three-point string hanging arrangement. The gauge length of the tested fibre was 15 mm. Loading was carried out by gradually dripping water in the plastic beaker using a graduated pipette. At load close to the estimated load of failure water was dripped at a slower rate and very close to the water level in the beaker to minimise impact. Load at failure was the sum of the weight of the wet beaker including the strings

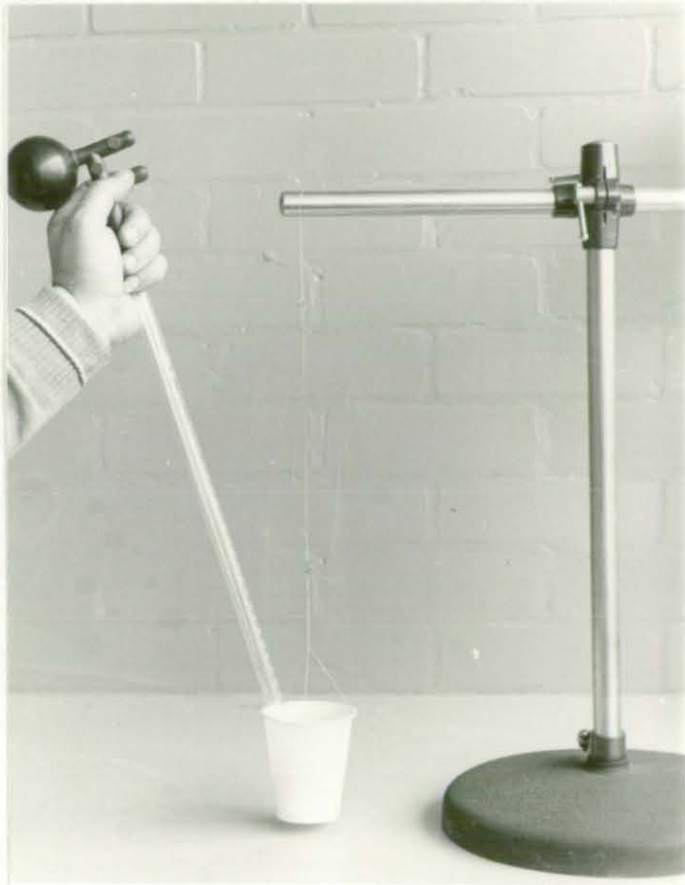


FIGURE 34: Set-up for Testing Fibre (Tensile)

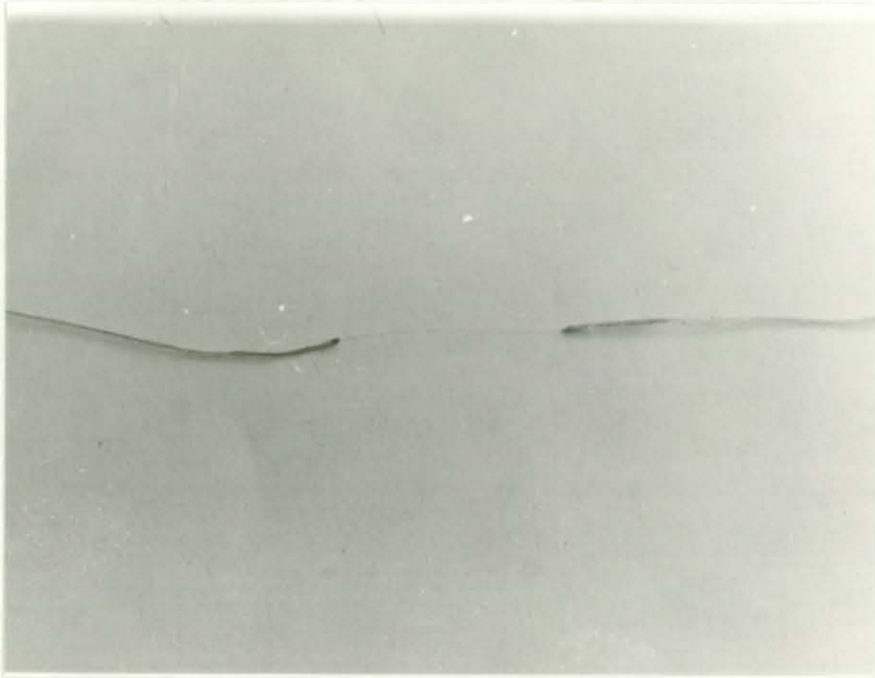


FIGURE 35: A Fibre (Middle) in Preparation for Tensile Test

below the fibre and the weight of the water which was dripped into the beaker. The graduations on the pipette enabled the direct reading of the volume of water consumed to $\sim 0.1 \text{ cm}^3$. Density of water was considered to be 1 g/cm^3 .

Initial tests were carried out by loading a bundle of fibre which was grabbed by a small chuck with rubber lining. Results from these tests were inaccurate because it was not possible to uniformly load the individual fibre in the bundle and to achieve a concentric loading. Concentric loading of a single fibre was also not possible using chucks. However fastening the ends of the fibre to the centre of a fine string using a flexible glue resulted in concentric and gentle loading of the fibre.

The diameter of fibre was measured using a Sigma Comparator in a constant temperature room. The flat tip of the apparatus was left to rest against a highly finished gauge block. Then the scale reading was zeroed. The fibre was then placed between the apparatus tip and the block diameter of the fibre was directly read on the scale, divisions on the scale were down to $0.5 \mu\text{m}$. Using the described technique, samples of SiC fibres were tested for tensile strength. Readings were only taken from tests where fibre was fractured in the middle. A minimum of 15 readings was taken for each sample of fibre.

4.3.2 Differential Thermal Analysis (DTA)

The chemical analysis of the Nicalon^(R) silicon carbide fibre shows that these fibres contain appreciable amounts of carbon and oxygen. Assuming that the oxygen is present in the fibre as SiO_2 , the molar ratio of compounds in the SiC fibre is $\text{SiC}:\text{C}:\text{SiO}_2 = 1:0.59:0.46$ ¹²³. Although the pure β -SiC is expected to be thermally stable at temperatures in the region of 900°C , the impure Nicalon silicon carbide might behave differently. In order to detect if there is any physical or chemical alteration in the fibre material on heating, a DTA study was carried out using a Linseis apparatus with microvolt recorder, Figure 36.

In the DTA, the temperature of the sample is compared with the temperature of an inert substance (of similar thermal properties) at the same temperature level, so that only the difference will be recorded (against time), this difference in temperature indicates the occurrence of either endothermic or exothermic reaction in the sample.

In this investigation a pure β -SiC powder was used as inert reference material, which was put into a very thin platinum cylinder, in which the thermocouple is centered (Pt-Pt/Rh), a powdered sample of Nicalon^(R) silicon carbide fibre of equal weight (0.65g) to the reference material was put into the other cylinder. A heating speed of 5°C/minutes was used, the differential thermocouple of Pt-Pt/Rh was set at 0.05 mV for high sensitivity. The test was run twice from room temperature up to 950°C and 1400°C.

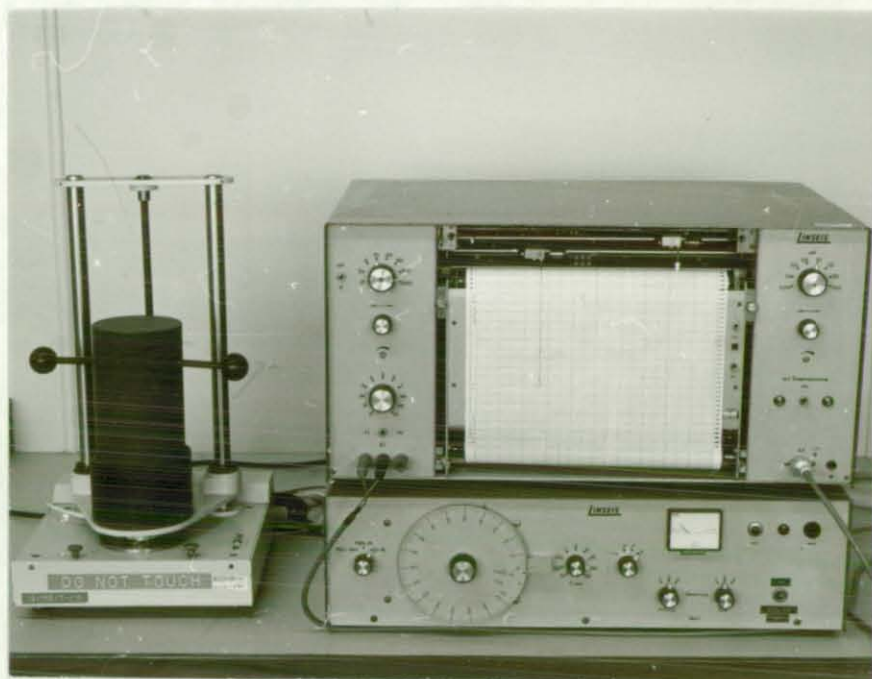


FIGURE 36: Linseis Apparatus (DTA)

CHAPTER V

RESULTS AND OBSERVATIONS

CHAPTER 5

RESULTS AND OBSERVATIONS

5.1 MACROSTRUCTURE

Squeeze casting produced a fine equiaxed grain structure within the castings of both Al-4.5 Cu and Al-3.75 Mg matrix alloys. Figures 37 and 38 show the macrostructure of the squeeze cast Al-4.5 Cu and Al-3.75 Mg matrix alloy respectively in comparison with the macrostructure of the same alloys sand and gravity die cast. Similarly, squeeze cast composites (of both matrices) had a fine equiaxed grain structure.

Squeeze castings were consistently free from porosity, whereas some gas porosity was observed in the sand and gravity die cast matrix alloys. Unless care was taken to free the molten matrix alloys from oxide and other foreign substances before casting, some inclusions were observed in the squeeze castings.

5.2 ROOM TEMPERATURE TENSILE PROPERTIES OF THE CAST Al-4.5 Cu AND Al-3.75 Mg MATRIX ALLOYS

The room temperature tensile properties of the Al-4.5 Cu and Al-3.75 Mg matrix alloys squeeze cast at various pressures, are presented in Figures 39 and 40 respectively. Gravity die castings were considered to be the same as squeeze castings produced under atmospheric pressure (0.1 MN m^{-2}). The tensile properties of the sand castings were included for comparison. Experimental results are shown in Table A3.1 for the Al-4.5 Cu matrix alloy and in Table A3.2 for the Al-3.75 Mg matrix alloy (Appendix III).

For both alloys, squeeze castings exhibited improved tensile strengths when compared to those cast under atmospheric pressure (gravity die and sand castings). The strength of the alloys increases with the increase in pressure, the rate of increase being reduced at higher pressures. The percentage elongation and reduction in area values also increase with increase in strength.

5.3 HEAT TREATMENT OF THE SQUEEZE CAST Al-4.5 Cu MATRIX ALLOY

The heat treatment conditions of the squeeze cast Al-4.5 Cu matrix alloy were assessed by determining the Vickers hardness number values of the treated specimens. Heat treatment consisted of solution treatment at 545°C for 2, 4 and 6 hours and precipitation treatment, for the same specimens, at 180°C for 2, 4 and 6 hours.

Experimental results are shown in Table 5. Solution treatment for more than 2 hours did not result in further measurable increase in hardness.

5.4 EXAMINATION OF THE FIBRE SURFACES

Scanning electron microscope examination of the surfaces of the SiC fibre revealed the following:

- The presence of some surface defects and contaminations in the as-received SiC fibre (Figure 41);
- An absence of surface contaminations in the heat treated fibre (Figure 42a);
- No surface damage of fibre, as a result of the mechanical separation and heat treatment, was observed;
- Fibre extracted from composite had a rough surface compared with the as-received fibre (Figure 42b). Fibre (SiC) exposed (24 hours) to the acid solution, which was used to dissolve the matrix, had a smooth surface similar to that of the as-received fibre.

Examination (SEM) of the Al₂O₃ fibre surfaces revealed the absence of any evidence of surface damage as a result of fibre treatment in diluted hydrochloric acid or mechanical separation (Figure 43a). No surface contamination was observed using the SEM technique. However, fibres (Al₂O₃) were whiter in colour when treated in hydrochloric acid solution

and were more readily wetted and dispersed in the alcohol-water solution used for the first stage separation of Al_2O_3 fibre. Extracted Al_2O_3 fibre has a rough surface (Figure 43b). The acid solution which was used to dissolve the matrix, has no effect on the surface appearance of fibre when exposed to that solution for 24 hours.

5.5 FIBRE BREAKAGE

Fibres (SiC and Al_2O_3) were checked for breakage at the different processing stages. This was carried out by measuring the length of fibre after each processing stage as described in Section 4.2.1. Length distribution of SiC and Al_2O_3 is listed in Tables 6 and 7 respectively. Although an effort was made to achieve accurate and representative sampling of fibres, the tendency for shorter fibres to segregate and settle down has limited the accuracy of sampling. In addition, fragments of a broken fibre could have been counted more than once. Samples of fibre extracted from the composite include fibre broken on cutting the composite specimens in preparation for dissolving the matrix alloy.

From visual estimation and results in Tables 6 and 7, and keeping in mind the foregoing comments, fibre breakage was estimated to be less than 5% at the final processing stage. The fibre separation device has to be well maintained and accurately assembled, in particular the condition of the wire brushes and their positioning in relation to each other, otherwise a high rate of fibre breakage may result.

5.6 FIBRE DISTRIBUTION AND ORIENTATION

5.6.1 Microscopic Examination

Microscopic examination of the polished composite specimens of both systems (Al-Cu/SiC and $\text{Al-Mg/Al}_2\text{O}_3$ composites) indicated that fibres were uniformly distributed and randomly oriented (3D) in the matrix alloys. Examples of the nature of fibre distribution and orientation are presented in Figures 44, 45 and Figures A4-1 and A4-2 (Appendix 4)

for the Al-Cu/SiC composite and in Figures 46, 47 and Figure A4.3 (Appendix 4) for the Al-Mg/Al₂O₃ composite. It was observed that most of the SiC fibres tend to be associated with a Cu-rich phase, possibly Cu Al₂, see Figure 48.

Alumina fibres were poorly dispersed in the Al-4.5 Cu matrix (casting group III) possibly due to poor wetting, see Figure A4.4.

5.6.2 Tensile Properties of the Composite Parallel and Perpendicular to the Punch Movement

Tensile tests on composite specimens, cut from planes parallel and perpendicular to the direction of the punch movement were carried out to confirm isotropic properties, as a supplement to the microscopic examination of fibre orientation in the matrix alloys. Provided that the matrix alloy has isotropic tensile properties, a random orientation of fibre (in three dimensions) would be expected to result in isotropic tensile properties in the composite as a whole. Because both transverse and longitudinal specimens had to be prepared from the same ingot for proper comparison, the specimen size used for tests had to be smaller (Hounsfield No 14) for this test. The gauge length of this specimen was too small to accommodate the available displacement transducer and it was not possible to measure the values of the elastic modulus in these tests. Room temperature tensile properties of the Al-4.5 Cu matrix/SiC fibre composite, in two directions, are shown in Table 8 for specimens taken from castings group IV and in Table 9 for specimens from casting group VI. Similar results for the Al-3.75 Mg matrix/Al₂O₃ fibre composite (castings group VI) are shown in Table 10. Results indicate that fibre free castings (control) of both matrix alloys, have no directional properties. The results in Tables 9 and 10 indicate that composites (of both systems) are slightly stronger in the direction perpendicular to the punch movement. The difference in strength is insignificant and composites can be considered to be of isotropic tensile properties. This is another indication of random orientation of fibre in three dimensions.

5.7 ELECTRON PROBE MICROANALYSIS

Electron probe microanalysis (EPMA) indicated the existence of a thin Cu-rich layer around the SiC fibre in the as-cast Al-Cu/SiC composite, whereas an even distribution of Cu at the fibre/matrix interface (as well as in the matrix) was indicated for the heat treated composite. In neither case (Al-Cu/SiC and Al-Mg/Al₂O₃ composites) was there evidence of any change in the distribution or concentration of elements at the fibre/matrix interface as a result of variation in time of contact between the fibre and the molten matrix. Typical EPMA analysis output charts are shown in the following figures:

- Figure 49: SiC fibre-Al-Cu matrix, contact time 18 minutes (as-cast)
- Figure 50: SiC fibre-Al-Cu matrix, contact time 39 minutes (as-cast)
- Figure 51: SiC fibre-Al-Cu matrix, fully heat treated, contact time 18 minutes
- Figure 52: Al₂O₃ fibre-Al-Mg matrix, contact time 15.5 minutes (as-cast)

It was not possible to make any accurate measurement of either the chemistry or the thickness of the reaction zone because of its relatively small dimension.

5.8 TENSILE PROPERTIES OF THE SQUEEZE CAST COMPOSITES

Composites tested in tension, can be grouped under three sections:

- SECTION I: initial groups of squeeze cast composites, where the time of contact between the fibre and the molten matrix was not controlled (casting groups III and IV).
- SECTION II: squeeze cast composites (casting group V) where the objective was to establish the time of contact between the fibre and the molten matrix which would result in optimum tensile properties (composites contain 4% v/v fibre).

SECTION III: squeeze cast composites with controlled time of contact between the fibre and the molten matrix according to the findings of the results of tests (tensile) carried out on casting group V.

SECTION I:

This includes two groups of squeeze cast composites, heat treated (casting group III) and as-cast (casting group IV):

Group III: Composites of Al-4.5 Cu matrix reinforced with either SiC or Al₂O₃ fibre. The composites were fully heat treated and tested (tensile) at room temperature. Tensile properties are shown in Table 11. The results indicate a reduction in the values of tensile properties as a result of the addition of fibre, the reduction increasing with the increase in the volume percent of fibre in the matrix.

Group IV: Composites of Al-4.5 Cu matrix reinforced with SiC fibre and Al-3.75 Mg matrix reinforced with Al₂O₃ fibre. The tensile properties of the Al-4.5 Cu/SiC composite (as-cast) are shown in Figures 53 and 54, and in Table A3.3 (Appendix 3). Tensile properties are plotted against the fibre volume (%) present in the composite. With the increase in the fibre content UTS values slightly decreased, while the values of 0.1% PS were substantially increased. Values of the elastic modulus were significantly increased with up to 6% v/v fibre. At higher volume content of fibre there was no further (measurable) increase. Both percentage elongation and reduction in area decreased with the increase in the fibre volume percent. The tensile properties (room temperature) of the Al-3.75 Mg/Al₂O₃ composites are shown in Figures 55, 56 and in Table A3.4 (Appendix 3). Results show a similar trend to those of the Al-Cu/SiC composite with the exception of the elastic modulus where there was no measurable improvement.

SECTION II:

The tensile properties of both composite systems (Al-Cu/SiC and Al-Mg/Al₂O₃) are plotted against the time of contact between the fibre and the molten matrix. Results are shown in Figure 57 (and Table A3.5) for the Al-4.5 Cu/SiC composite and in Figure 58 (and Table A3.6) for the Al-3.75 Mg/Al₂O₃ composite. Time of contact had a similar effect on the tensile properties of both composite systems. In the case of Al-Cu/SiC, UTS and elastic modulus showed maximum values at approximately 18 and 25 minutes respectively. The 0.1% PS values increased with an increase in the time of contact. The rate of increase is reduced at longer time of contact. Both percentage elongation and reduction in area values decreased with the increase in time of contact.

Results for Al-Mg/Al₂O₃ composite showed similar trends to those of Al-Cu/SiC. UTS and elastic modulus had maximum values at approximately 15.5 and 19 minutes respectively.

SECTION III:

The contact time between the fibre and the molten matrix for squeeze castings in groups VI and VII was controlled according to the findings of the tensile test results of composites in group V. Composites contain up to 10% v/v fibre. Composites (Al-Cu/SiC and Al-Mg/Al₂O₃) of group VI, as-cast and thermally cycled, were tested (tensile) at room temperature, while composites of group VII were tested (tensile) at both room and elevated temperatures.

Group VI: The room temperature tensile properties of the squeeze-cast composites of group VI (as-cast) are shown in Figures 59 and Table A3.7 for the Al-4.5 Cu/SiC composites and in Figure 60 and Table A3.8 for the Al-3.75 Mg/Al₂O₃ composite. For both composite systems the results indicated a moderate increase in the values of UTS as a result of the presence of fibre (up to 10% v/v).

A substantial increase in the values of 0.1% PS and the elastic modulus were obtained but there was a reduction in the values of percentage elongation and reduction in area (Tables A3.7 and A3.8). The composite with 10% v/v SiC fibre has 0.1% PS and elastic modulus values of 185 MPa and 82 GPa respectively compared with values of 107 MPa and 71 GPa respectively for the fibre-free squeeze castings (control).

The tensile properties (room temperature) of the thermally cycled Al-Cu/SiC and Al-Mg/Al₂O₃ composites (casting group VI), Tables 12 and 13 respectively, indicate a slight reduction in the values of UTS for composites with 8 or 10% v/v fibre as a result of the thermal cycling treatment. Reduction in the UTS values occurred after 5 cycles, further cycling (up to 20 cycles) showed no further effect. Other tensile properties were not affected by cycling.

Group VII: Results of the tensile test (at room and high temperature) of composites in group VII are shown in Figures 61 (UTS), 62 (0.1% PS), 63 (elastic modulus) and in Table A3.9 for the Al-4.5 Cu/SiC composite, and in Figures 64 (UTS), 65 (0.1% PS), 66 (elastic modulus) and Table A3.10 for the Al-3.75 Mg/Al₂O₃ composite. Tensile properties are plotted against the volume content of fibre for each test temperature. Tensile properties at room temperature, for both composite systems, are in agreement with those for composites in group VI.

Strengthening efficiency (UTS composite/UTS control) is slightly improved at 200°C and maintained up to 300°C in the case of Al-Mg/Al₂O₃ composite. A more pronounced increase in strengthening efficiency is shown at 200°C in the case of the Al-Cu/SiC composite. However, this improvement was not maintained at higher temperatures.

The improvement in the values of 0.1% PS and elastic modulus (as a result of the addition of fibre) is maintained up to 300°C, with the exception of 0.1% PS of the Al-Cu/SiC composite where it was decreased at 250 and 300°C. Both composite systems, at 250°C, still have 0.1% PS and elastic modulus values similar to those for the matrix alloys at room temperature.

5.9 FATIGUE LIFE

Results of the fatigue tests (rotating bend), Table 14, indicate that specimens of the squeeze cast matrix alloys (Al-4.5 Cu and Al-3.75 Mg) have a longer fatigue life compared with those for specimens of sand and gravity cast matrix alloys. Fatigue life is further improved as a result of the addition of fibre. Fatigue life increased with the increase in the volume content of fibre in both composite systems.

5.10 FRACTURE OF COMPOSITES

5.10.1 Tensile Fracture

I. *Effect of contact time between the fibre and the molten matrix alloy (casting group V) on fibre bonding and integrity.*

Figures 67, 68 and 69 show some features of the tensile fracture of the Al-Cu/SiC and Al-Mg/Al₂O₃ composites respectively, when examined with a scanning electron microscope. Fibres (SiC and Al₂O₃) were allowed to be in contact with the respective molten matrix alloy for different periods of time. During the study of fracture surfaces the following observations were made:

- Fibres of SiC exposed to the melt for ~18 minutes were well bonded to the matrix with no noticeable fibre deterioration (Figure 67b), whereas shorter contact time resulted in poor bonding of the fibres to the matrix (Figure 67a). A longer time of contact caused fibre deterioration (Figure 68).

- contact time has a similar effect on alumina fibres with the optimum contact time, found to be ~ 15.5 minutes, resulting in adequate bonding without fibre deterioration. Poor bonding was observed at shorter times of contact and deterioration of fibres at longer times of contact, see Figure 69.

II. *Fracture of composite, with controlled time of contact between fibre and the molten matrix (casting groups VI and VII), at different test temperatures.*

Figures 70-72 and 73-74 show typical examples of fractured Al-Cu/SiC and Al-Mg/Al₂O₃ composites (respectively) at different test temperatures. Figure 75 shows the typical fracture characteristics of squeeze cast Al-4.5 Cu matrix alloy at room temperature and 300°C. During the course of this investigation the following observations were made:

- Fracture at room temperature of the squeeze cast matrix alloys (Al-Cu and Al-Mg), took place by separation along a plane at ~ 45 degrees to the tensile stress axis, whereas at test temperatures higher than 200°C, fractures were characterised by typical 'cup-and-cone' fracture
- Composites tested at room temperature fractured by separation normal to the tensile stress, 'cup-and-cone' fracture was observed for composites with a low volume content of fibre (2-4%) at test temperatures of 250 and 300°C.
- No fibre pull-out was observed at test temperatures up to 300°C (for both composite systems).
- Fracture of SiC fibre, positioned at about 90 degrees to the stress axis, was characterised by splitting of fibre. Splitting of fibre is probably aided by surface defects (Figure 71b) or pre-fracture in the fibre under stress (Figure 71a). Very few split fractures (of fibre) were observed in the case of alumina fibre composites.

- Non-isotropic flow of the matrix material was observed in the close vicinity of the fibres (SiC and Al_2O_3).
- Study of the fractured surfaces indicates the presence of a state of complex stresses near the fibres.

III: *Fracture of composites with no control on time of contact between the fibre and the molten matrix alloys (initial group of castings III and IV).*

This includes two groups:

1. Fracture of composites of group IV (Al-Cu/SiC and Al-Mg/ Al_2O_3). Observations on fracture of this group of composites were identical to those for composites in groups VI and VII (5-10-1-II) with the following exceptions:
 - some SiC fibre deterioration was observed in composites containing relatively high volume fraction fibre (8 and 10%), see Figure 76
 - pull-out of alumina fibre, positioned at near 90 degrees to the tensile stress axis, was observed indicating inadequate bonding of fibre. No pull-out of the fibres aligned nearly parallel to the tensile axis was observed (Figure 77).
2. Heat treated composites (group III).
 In this group the Al-4.5 Cu matrix was reinforced by either SiC or Al_2O_3 fibres. Composites were solution and precipitation treated.
 Fracture of composites reinforced with alumina fibre indicate inadequate bonding of fibre and poor distribution, see Figure 78. Clustering of fibres was also observed in the composite system during examination for fibre distribution (Figure A4.4). The following observations were made on the fracture of composites (heat treated) reinforced with SiC fibre, Figure 79:

- no fibre pullout
- in comparison with the fracture of the as-cast composites, there was little flow of the matrix material in the close vicinity of the fibres
- in some cases, decohesion of the interface of the fractured fibre was observed. However it is not clear whether failure of the interface took place before or after fracture of the fibre
- some fibre deterioration was observed in composites containing 10% v/v fibre.

5.10.2 Fatigue Fracture

Figure 80 shows fatigue fracture of specimens of gravity die cast (a) squeeze cast matrix (b) and squeeze cast Al-Cu/SiC composites (c). Figures 81 and 82 show some features of the fatigue fractures of composites of Al-Cu/SiC and Al-Mg/Al₂O₃. The following observations were made for both composite systems:

- squeeze castings, fibre-free and composites, had a smoother fracture surface compared with those for sand and gravity die castings
- no interface failure was observed, fibres in the fracture plane, were fractured
- the site of fatigue crack initiation was not detected
- in some cases fatigue crack arrest by fibres was observed, see Figure 81a
- occasionally fatigue crack redirection by a fibre was observed rather than by failure of the interface, Figure 82a. This was accompanied by flow of the matrix material.

5.11 TOOL WEAR

In this test no significant crater wear was observed. Flank wear contributed most to the end of the useful tool life and was taken as the tool wear criterion.

Results are shown in Table 15. Figures 83 and 84 show the effect of the volume content of fibre on flank wear for Al-Cu/SiC and Al-Mg/Al₂O₃ composites respectively. The average width of the flank wear land (VB_B), at a constant volume of removed material (60 cc), is plotted against the volume content of fibre in the composites.

The results show a significant increase in flank wear as a consequence of the presence of fibre. Wear rate increased with the increase in fibre content. Silicon carbide fibre has more effect on tool wear than alumina fibre.

5.12 THERMAL STABILITY OF NICALON^(R) SILICON CARBIDE FIBRE

5.12.1 Tensile Strength (Room Temperature) of Fibre Subjected to Different Heating Cycles

Results of the tensile test are shown in Table 16. Results indicate the following:

- The measured average tensile strength of the as-received fibre is well in agreement with the specified 250-300 kg/mm² (see 3.1.1, Table 1), which is an indication of the adequacy of the technique used for testing (tensile)
- Fibre tensile strength decreases with an increase in diameter
- The tensile strength of fibres exhibits some scatter, as is usual for brittle solids. This has been reported by Anderson et al¹²⁴ and Yajima et al¹²⁵

- The tensile strength of fibre was reduced as a result of heating (within test conditions). This was observed in all heating cycles (Table 16)
- Reduction in fibre strength is dependent on heating time, cycles 1 and 2
- fibre heated in air and in vacuum were similarly affected, cycles 3 and 5
- no significant effect of rapid cooling or heating up and heating temperature (800°C and 900°C) was observed within the test conditions.

5.12.2 Differential Thermal Analysis (DTA)

DTA tests on the as-received Nicalon^(R) silicon carbide fibre, Figure 85, showed two exothermic reactions at 300°C and 1025°C (peak) respectively, and an endothermic reaction at 1275°C (peak).

TABLE 5: Vickers hardness number values of the squeeze cast Al-4.5 Cu alloy subjected to different heat treatment conditions
(Values in brackets represent the average)

Duration of Precipitation Treatment at 180°C (hrs)	Duration of Solution Treatment at 545°C (hrs)			
	0	2	4	6
0	56.6	81.6	83.4	83.4
		86	87	87
	54.2	88.9	86	91.7
		86	87	84
	54.9	87.8	87	83.4
		86	87.8	85
	55.2	87.8	87.8	86
		83.4	88.9	83.4
	55.8	86	83.4	87
	87	87	86	
	53.6	87	87	86
	55.5	87.8	88.9	83.4
	55.2	86	83.4	86
	(55.3)	(86.2)	(86.5)	(85.5)
2		109	106	105
		107	107	107
		106	109	106
		107	106	107
		(107.75)	(107)	(106.25)
4		123	120	120
		121	120	123
		120	121	121
		121	120	123
		(121.25)	(120.25)	(121.75)
6		128	127	127
		127	126	127
		125	125	126
		129	128	127
		(127.25)	(126.5)	(126.75)

TABLE 6: Length distribution of silicon carbide fibres subjected to different processing treatments

Fibre Length mm %	<1	$\geq 1 < 2$	$\geq 2 \leq 3$	>3
As received	2	3	95	0
As received and separated	5	3	92	0
Pre-treated and separated	4	5	91	0
Extracted from a composite	6	7	87	0

TABLE 7: Length distribution of alumina fibre subjected to different processing treatments

Fibre Length mm %	<0.2	$\geq 0.2 < 0.35$	$\geq 0.35 \leq 0.5$	>0.5
As received	7	31	60	2
Pre-treated and mechanically separated	10	24	66	0
Extracted from a composite	14	27	56	3

TABLE 8: Room temperature tensile properties of the Al-4.5 Cu/SiC fibre composite, in directions parallel and perpendicular to the punch movement. Castings group IV.

(Values in brackets represent the average)

Volume % Fibre	UTS MPa	0.1% PS MPa	Elastic Modulus GPs	Elongation %	Reduction in Area %	Remarks
0 //	185	108		17	15	
	182	106		18	16	
	186	107		15	13	
	183	103		14	12	
	(184)	(106)		(16)	(14)	
⊥	185	107		17	15	
	182	105		14	13	
	186	108		16	14	
	179	108		13	11	
	(183)	(107)		(15)	(13)	
4 //	179	138		6	5	
	183	143		7	6	
	181	140		8	7	
	177	139		5	3.5	
	(180)	(140)		(6.5)	(5.4)	
⊥	178	144		6	5	
	182	148		4	4	
	180	146		5	4.5	
	176	143		4	3.5	
	(179)	(145.5)		(4.75)	(4.25)	
8 //	178	166		7	6	
	176	163		6.5	6	
	180	167		5	4.5	
	175	164		4.5	3.5	
	(177.25)	(165)		(5.75)	(5)	

Continued...

TABLE 8: continued

Volume % Fibre	UTS MPa	0.1% PS MPa	Elastic Modulus GPa	Elongation %	Reduction in Area %	Remarks
↓	177	167		5	4	
	175	165		4	3.5	
	181	170		6	4.5	
	179	169		5	4	
	(178)	(167.75)		(5)	(4)	

TABLE 9: Room temperature tensile properties of the Al-4.5 Cu/SiC fibre composite, in directions parallel and perpendicular to the punch movement. Castings group VI
(Values in brackets represent the average)

Volume % Fibre	UTS MPa	0.1% PS MPa	Elastic Modulus GPa	Elongation %	Reduction in Area %	Remarks
0 // ⊥	185	111		17	16	
	182	112		15	15	
	181	106		16	14	
	184	102		16	15.5	
	(184)	(108)		(16)	(15)	
	183	105		17	16.5	
	185	108		16	16	
	181	106		15.5	14.5	
179	105		16	16.5		
(182)	(106)		(16.4)	(16.9)		
6 // ⊥	190	157		6	5	
	188	155		5.5	4.5	
	187	154		5	4	
	191	154		4.5	4	
	(189)	(155)		(5.25)	(4.4)	
	193	162		4.5	3.5	
	189	159		5	4	
	194	161		4	3.5	
192	158		3.5	3		
(192)	(160)		(4.25)	(3.5)		
8 // ⊥	162	136		2	1.5	Inclusion
	195	171		4.5	3.5	
	193	170		4	3	
	194	168		4	3	
	(194)	(169.6)		(4.1)	(3.16)	
	199	176		4.5	3.5	
	196	173		4	3	
	195	172		4	3	
198	175		3.5	2.5		
(197)	(174)		(4)	(3)		

/Continued...

TABLE 9: Continued

Volume % Fibre	UTS MPa	0.1% PS MPa	Elastic Modulus GPa	Elongation %	Reduction in Area %	Remarks
10 //	199	184		3	2.5	
	197	182		2.5	2	
	200	184		2.5	2	
	196	182		2	2	
	(198)	(183)		(2.5)	(2.1)	
⊥	205	190		2.5	2	
	204	189		2.5	2	
	201	187		2	1.5	
	202	186		2	1.5	
	(203)	(188)		(2.25)	(1.75)	

TABLE 10: Room temperature tensile properties of the Al-3.75 Mg/Al₂O₃ fibre composite in directions parallel and perpendicular to the punch movement. Castings group VI.
(Values in brackets represent the average).

Volume % Fibre	UTS MPa	0.1% PS MPa	Elastic Modulus GPa	Elongation %	Reduction in Area %	Remarks
0 // ⊥	235	148		17	16	
	231	145		16.5	16	
	234	146		16	15.5	
	232	145		15.5	15	
	(233)	(146)		(16.25)	(15.6)	
	233	145		17	6	
	231	144		16	15.5	
	228	142		17.5	16.5	
232	145		16	16		
(231)	(144)		(16.6)	(16)		
4 // ⊥	237	165		13	12	
	234	162		12.5	11.5	
	234	164		11.5	11	
	235	162		11	10.5	
	(235)	(163)		(12)	(11.25)	
	236	168		12	11	
	235	169		11	11.5	
	232	166		10.5	10	
233	165		10.5	9.5		
(234)	(167)		(11)	(10.5)		
6 // ⊥	242	176		10	9	
	241	175		9	8.5	
	239	174		8.5	7.5	
	238	175		8.5	7.5	
	(240)	(175)		(9)	(8.12)	
	244	180		8.5	7.5	
	245	181		7.5	7	
	239	178		8	7.5	
244	177		8	7.5		
(243)	(179)		(8)	(7.4)		

/Continued...

TABLE 10: continued

Volume % Fibre	UTS MPa	0.1% PS MPa	Elastic Modulus GPa	Elongation %	Reduction in Area %	Remarks
8 //	244	182		6.5	6	
	241	180		6	5.5	
	243	183		6.5	5	
	240	179		5.5	4.5	
	(242)	(181)		(6.1)	(5.25)	
⊥	243	184		6	5.5	Inclusion
	245	185		6.5	5	
	231	172		3.5	3.5	
	244	186		5.5	4.5	
	(244)	(185)		(6)	(5)	
10 //	245	189		4	3.5	
	243	187		3.5	3	
	244	188		4	3	
	240	184		3.5	3	
	(243)	(187)		(3.75)	(3.12)	
⊥	247	194		3.5	3	
	243	191		3.5	2.5	
	244	190		3	2.5	
	246	193		4	3	
	(245)	(192)		(3.5)	(2.75)	

TABLE 11: Room temperature tensile properties of the heat treated, squeeze cast Al-4.5 Cu matrix composite, reinforced with either SiC or Al₂O₃ fibre. Casting group III.

Volume % Fibre	UTS MPa	0.1% PS MPa	Elastic Modulus GPa	Elongation %	Reduction in Area %	Remarks
0	334 333 335	219 217 218	70.6 70.8 72	5 5 4.5	4 4 4	
SiC fibre 2	332 334 331	218 217 216	70.4 79 71	4 3.5 4	3 3 4	
4	296 294 295	210 206 208	70.1 77 70	4 3.5 4	3.5 3 3.5	
6	277 273 275	196 197 198	66.5 66.9 67	3 2.5 3	2.5 2 3	
8	251 248 250	194 190 193	65 64 66	2 1 2	1 0.5 1	
10	216 215 217	180 179 181	49 51 46	0.5 0.5 1	- - 0.5	
Al ₂ O ₃ fibre 2	281 279 280	219 215 217	71.1 70.5 71.8	4 3.5 4.5	4 3 4	
4	270 269 272	209 206 211	67 65 68	3 3.5 4	2.5 3 4	

/Continued...

TABLE 11: continued

Volume % Fibre	UTS MPa	0.1% PS MPa	Elastic Modulus GPa	Elongation %	Reduction in Area %	Remarks
6	308	219	62	3.5	3	
	304	218	61	3.5	3	
	307	222	63	4	4	
8	281	216	70.5	4	3	
	280	215	70.1	3.5	3	
	283	217	71	4	3.5	
10	301	219	69.5	3	2.5	
	307	217	68.7	3	2.5	
	305	221	70.5	3.5	3	

TABLE 12: Room temperature tensile properties of the squeeze cast Al-4.5 Cu/SiC composite subjected to thermal cycling between 20°C and 350°C. Casting group VI
(Values in brackets represent the average)

Volume % Fibre	UTS MPa	0.1% PS MPa	Elastic Modulus GPa	Elongation %	Reduction in Area %	Remarks
0 before cycling*	(183)	(107.5)	(70.7)	(17)	(14)	
5 cycles	182 180 181 (181)	107 105 106 (106)	70.8 70.5 71.7 (71)	16.5 16 15.5 (16)	16 15.5 14.5 (15.3)	
10 cycles	185 186 181 (184)	106 106 103 (105)	71 70.4 70.4 (70.6)	71 16.5 17.5 (17)	16.5 15.5 16 (16)	
20 cycles	185 184 180 (183)	108 107 106 (107)	70.7 70.9 70.8 (70.8)	15.5 15 14.5 (15)	15 14.5 13.5 (14.3)	
6 before cycling*	(190.5)	(156.5)	(77.5)	(5)	(4)	
5 cycles	189 186 186 (187)	157 154 154 (155)	79 78 77.1 (78)	5 4.5 5.5 (5)	4 3.5 4 (3.8)	
10 cycles	187 185 186 (186)	157 156 155 (156)	77.8 77.1 77.6 (77.5)	6 5.5 5 (5.5)	5.5 5 4.5 (5)	
20 cycles	189 188 187 (188)	157 154 154 (155)	77.6 77.1 79 (77.9)	6 5.5 5 (5.5)	5.5 5 4.5 (5)	

/Continued...

TABLE 12: continued

Volume % Fibre	UTS MPa	0.1% PS MPa	Elastic Modulus GPa	Elongation %	Reduction in Area %	Remarks
8 before cycling*	(195.7)	(170)	(79.7)	(4)	(3)	
5 cycles	189 186 186 (187)	170 168 169 (169)	78.5 77.9 77.7 (78)	4.5 4 3.5 (4)	4 3.5 2.5 (3.5)	
10 cycles	190 187 187 (188)	173 170 170 (171)	78 77.5 77 (77.5)	5 4.5 4 (4.5)	4.5 4 3.5 (4)	
20 cycles	190 186 188 (188)	172 170 171 (171)	77.7 78 77 (77.5)	5 4.5 4.5 (4.6)	4 3.5 4 (3.8)	
10 before cycling*	(197.7)	(184.5)	(82)	(3)	(2.5)	
5 cycles	191 193 192 (192)	186 185 184 (185)	82 81 81.5 (81.5)	3.5 3.5 2.5 (3.1)	3 2.5 2 (2.5)	
10 cycles	196 191 195 (194)	186 182 184 (184)	83 82 81. (82.1)	2.5 3 2.5 (2.6)	2 2.5 2 (2.1)	
20 cycles	193 192 188 (191)	188 187 183 (186)	83 82.1 80.9 (82)	2.5 2.5 2.5 (2.5)	2 2 1.5 (1.8)	

* Quoted average values are those presented in Figure 58 and Table A3.7 for the same groups of castings.

TABLE 13: Room temperature tensile properties of the squeeze cast Al-3.75 Mg/Al₂O₃ fibre composite subjected to thermal cycling between 20°C and 350°C. Casting group VI.
(Values in brackets present the average)

Volume % Fibre	UTS MPa	0.1% PS MPa	Elastic Modulus GPa	Elongation %	Reduction in Area %	Remarks
0 before cycling*	(230)	(146)	(70.9)	(17)	(16)	
5 cycles	235 233 234 (234)	146 145 141 (144)	71 70 70.5 (70.5)	18 17.5 18.5 (18)	17 16 16.5 (16.5)	
10 cycles	233 234 229 (232)	147 146 142 (145)	71.1 70.4 70.3 (70.6)	17.5 16.5 17 (17)	16.5 16 16.5 (16.3)	
20 cycles	231 232 236 (233)	147 141 141 (143)	71 70.5 70.9 (70.8)	16.5 17 16 (16.5)	15 16 15 (15.3)	
6 before cycling*	(242)	(177)	(74)	(8)	(7)	
5 cycles	241 238 238 (239)	177 173 175 (175)	74 73 73.5 (73.5)	8 7 7.5 (7.5)	7.5 6.5 6 (6.5)	
10 cycles	242 238 240 (240)	180 175 176 (177)	75 74 74.5 (74.5)	8 8.5 7.5 (8)	7 7.5 7 (7.1)	
20 cycles	243 241 239 (241)	176 175 171 (174)	74.1 73 73.5 (73.5)	9 8.5 8 (8.5)	8 8 7.5 (7.8)	

/Continued...

TABLE 13: continued

Volume % Fibre	UTS MPa	0.1% PS MPa	Elastic Modulus GPa	Elongation %	Reduction in Area %	Remarks
8 before cycling*	(240)	(180)	(75.4)	(6)	(5.5)	
5 cycles	239 236 236 (237)	180 177 177 (178)	76 75.5 75 (75.5)	7.5 7 7.5 (7.3)	7 6.5 6.5 (6.6)	
10 cycles	238 235 235 (236)	181 180 177 (179)	76 75 75.8 (75.6)	7 6 6.5 (6.5)	6 5.5 5.5 (5.6)	
20 cycles	241 239 237 (239)	179 176 177 (177.3)	75 75.5 74.5 (75)	7.5 7 7.5 (7.3)	7 6.5 7 (6.8)	
10 before cycling*	(243)	(186)	(76)	(4)	(3.7)	
5 cycles	237 236 239 (238)	186 185 181 (184)	76 75 75.5 (75.5)	5 4.5 5.5 (5)	4.5 4 4 (4.16)	
10 cycles	237 234 234 (235)	186 181 182 (183)	75.6 75 75.3 (75.3)	6 5.5 5.5 (5.6)	5 4.5 4.5 (4.6)	
20 cycles	240 235 236 (237)	189 187 185 (187)	76.5 75.9 75.5 (75.9)	4.5 5 4 (4.5)	4 4.5 3 (3.8)	

* Quoted average values are those presented in Figure 59 and Table A3.8 for the same group of castings.

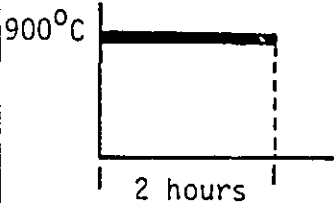
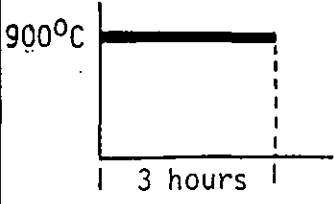
TABLE 14: Fatigue Life

Percent Fibre v/v	Duration to failure (HRS) Test No					Av	Fatigue Life (Reversals $\times 10^5$)
	1	2	3	4	5		
	<u>Al-4.5 Cu/SiC Composite</u>						
(Sand cast) 0	2.4	1.4	1.9	2.6	1.2	1.9	3.25
(Gravity die cast) 0	3.25	2.1	3.2	1.9	2.3	2.55	4.36
(Squeeze cast) 0	3.65	3.15	2.6	4.01	3.2	3.32	5.68
2	4.45	3.2	1.9	4.6	3.92	3.23	5.52
4	4.8	3.7	4.9	3.9	3.2	4.1	7.01
6	4.81	3.4	6.2	5.7	2.3	4.48	7.66
8	6.4	5.1	4.3	3.15	5.6	4.91	8.4
10	7.2	3.7	5.6	4.5	6.92	5.58	9.55
	<u>Al-3.75 Mg/Al₂O₃ Composite</u>						
(Sand cast) 0	3.1	4.8	3.9	1.9		3.42	5.86
(Gravity die cast) 0	4.6	3.2	5.4	2.3		3.87	6.63
(Squeeze cast) 0	2.1	4.9	6.5	3.1		4.15	7.1
2	1.9	6.3	4.5	3.6		4.07	6.97
4	3.8	5.9	4.6	3.5		4.45	7.61
6	6.7	3.16	5.7	4.8		5.09	8.70
8	5.35	2.9	6.9	7.1		5.56	9.51
10	3.45	6.65	7.34	6.31		5.94	10.15

TABLE 15: Effect of fibre volume percent on the tool wear (flank wear) Al-Cu/Sic and Al-Mg/Al₂O₃ composites

Percent Fibre v/v	Flank Wear VB _B (mm)							
	Volume of removed material cc							
	Al-4.5 Cu/Sic				Al-3.76 Mg/Al ₂ O ₃			
	20	40	60		20	40	60	80
0	0.025	0.05	0.076	0	0	0.006	0.008	
2	0.089	0.127	0.178	0.038	0.051	0.083	0.101	
4	0.114	0.185	0.279	0.051	0.076	0.114	0.127	
6	0.203	0.254	0.330	0.051	0.108	0.127		
8	0.279	0.343	0.406	0.064	0.102	0.147		
10	0.305	0.419	0.452	0.101	0.127	0.153		

TABLE 16: Tensile Strength (room temperature) of SiC fibre subjected to different heating cycles

Heat Treatment Cycle	Test No.	Load gm	Diameter μm	UTS kg/mm^2
As-received	1	18.3	10.92	195
	2	46.7	15.24	256
	3	22.1	10.16	272.5
	4	21.3	10.16	262
	5	28.9	10.63	325
	6	44.7	12.7	352
	7	26	10.16	320
	8	46.3	15.24	254
	9	40.7	15.24	223
	10	46.7	15.24	256
	11	35.6	12.7	281
	12	21.1	10.5	244
	13	25.8	11	272
	14	39	12.7	306
	15	34.6	12.5	282
Average UTS				273 (2680 MPa)
Cycle 1 	1	23.6	11	248
	2	27.74	15.75	152
	3	22.65	12.5	184
	4	20.34	14.5	123
	5	19.9	10	254
	6	21.8	12.7	172
	7	19.7	14.75	115
	8	24.5	15.24	134
	9	21.8	10.5	252
	10	26.7	14.5	162
	11	20.2	11	213
	12	23.5	12.5	192
	13	21.1	10.16	260
	14	16.9	11.5	163
	15	240	12.5	196
	16	25.5	17	156
Average UTS				184 (1825 MPa)
Cycle 2 	1	20.8	15.25	114
	2	18.3	12.7	144
	3	16.8	12.7	133
	4	24.3	13.9	160
	5	20.3	10.16	250
	6	29.3	16.51	137
	7	23.5	15.24	128
	8	16	12.2	136

/Continued...

TABLE 16: continued

Heat Treatment Cycle	Test No	Load gm	Diameter μm	UTS kg/mm^2
Cycle 2 (contd)	9	18.2	15.24	100
	10	13.4	12.7	105
	11	12.3	10.16	151
	12	23.1	14.7	136
	13	18.5	11.7	172
	14	13.7	10.16	169
	15	23.3	14.2	147
	16	17.5	12.7	138
	17	26.9	16.5	126
		Average UTS		144 (1411 MPa)
Cycle 3	1	19.5	10.16	240
	2	22	12.7	173
	3	14.6	10.16	180
	4	20.5	15.24	112
	5	21.3	19.5	71
	6	12.1	12.7	95
	7	19.7	11.94	176
	8	19.3	12.7	152
	9	16.5	12.7	130
	10	23.1	12.7	182
	11	22.3	14.2	140
	12	25	13.7	170
	13	19.6	11.7	162
	14	13.6	10	173
	15	18.9	11.7	176
	16	19.6	14	127
		Average UTS		155 (1520 MPa)
Cycle 4	1	23.3	17	103
	2	19.7	10	251
	3	14.9	11.5	144
	4	24.5	12.5	200
	5	21.1	10.5	244
	6	25.8	11	272
	7	21.9	15.25	120
	8	20.5	11	216
	9	29.6	14.5	179
	10	28.7	14.75	168

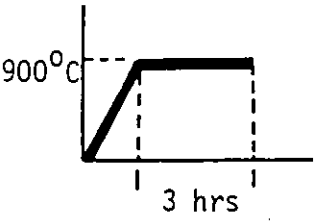
/Continued...

TABLE 16: continued

Heat Treatment Cycle	Test No	Load gm	Diameter μm	UTS kg/mm^2	
Cycle 4 (contd)	11	35.5	18	140	
	12	18.2	15	103	
	13	24.1	15	136	
	14	36.8	18	145	
	15	20.7	14	135	
	16	25.3	15	143	
	17	20.7	11.7	192	
	18	25.1	12.5	204	
	Average UTS				172
					(1687 MPa)
Cycle 5 (in vacuum)	1	20.4	17.78	82.5	
	2	23.4	17.27	100	
	3	10.8	11.43	106	
	4	15.4	12.32	130	
	5	13.9	9.9	181	
	6	20.1	14.48	122	
	7	12.7	10.16	156	
	8	17.5	13.08	130	
	9	15.6	12.7	124	
	10	14.9	10.16	183	
	11	20.2	12.7	160	
	12	28.9	15.75	149	
	13	19.4	11.7	180	
	14	15.3	11.5	147	
	15	26.8	15	152	
Average UTS				140	
				(1375 MPa)	
Cycle 6	1	53	20.32	163	
	2	23.8	14.73	140	
	3	21.1	12.7	166	
	4	44.4	17.57	183	
	5	19.4	15.24	106	
	6	25.3	16.5	120	
	7	15.7	10.16	193	
	8	16.3	10.16	201	
	9	22.1	12.5	180	
	10	14.9	11	156	
	11	18.2	14.5	110	
	12	24.6	15	139	
	13	15.6	12.3	131	
	14	13.5	10.16	166	
	15	21.2	14.48	129	
Average UTS				152	
				(1493 MPa)	

/Continued..

TABLE 16: continued

Heat Treatment Cycle	Test No	Load gm	Diameter μm	UTS kg/mm^2
Cycle 7 	1	18.7	15.2	103
	2	15.3	12.7	121
	3	19.6	14.7	115
	4	17.6	14.2	111
	5	19.5	12.7	153
	6	10.5	10.16	129
	7	12.8	10.16	158
	8	15.7	12.7	124
	9	24.1	14.73	141
	10	21.9	12.5	178
	11	20.6	15.24	113
	12	13.6	11	143
	13	15.7	12.3	132
	14	13.1	10.5	151
	15	16.9	12.5	138
	16	18.1	15	102
		Average UTS		132 (1295 MPa)

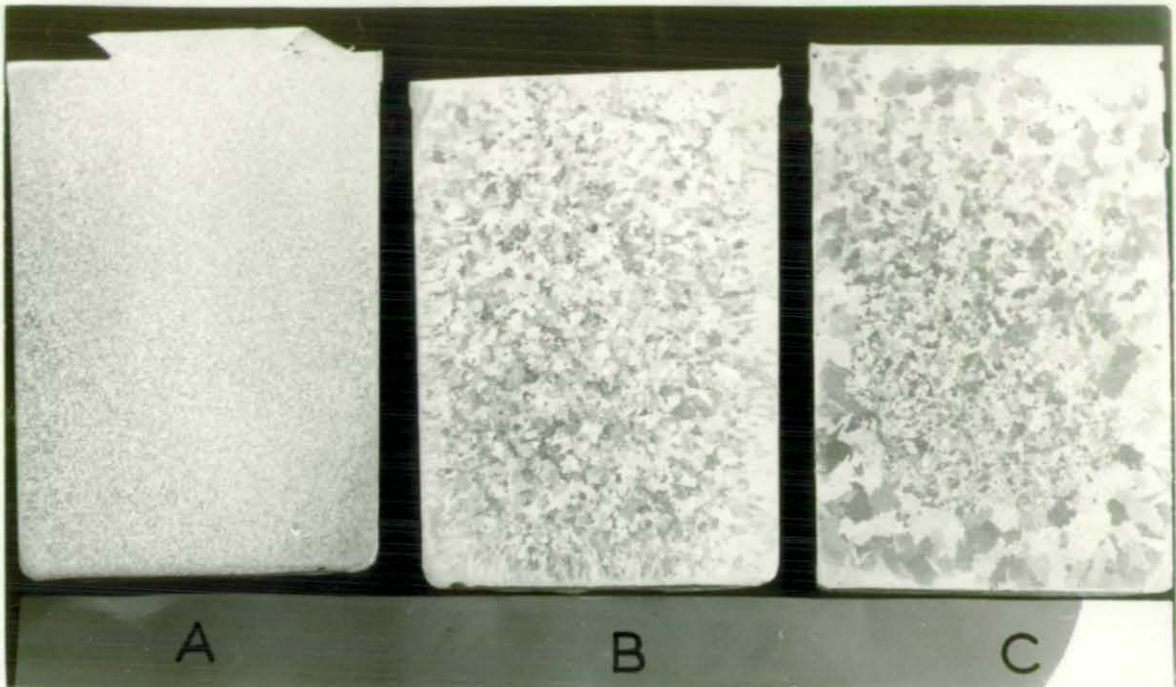


FIGURE 37: Macrostructure of the cast Al-4.5 Cu matrix alloy. Die temperature 250°C , casting temperature 700°C (sand and gravity die cast), and 687°C (squeeze cast).
 A. squeeze cast (squeeze pressure 140 MPa)
 B. gravity die cast,
 C. sand cast.

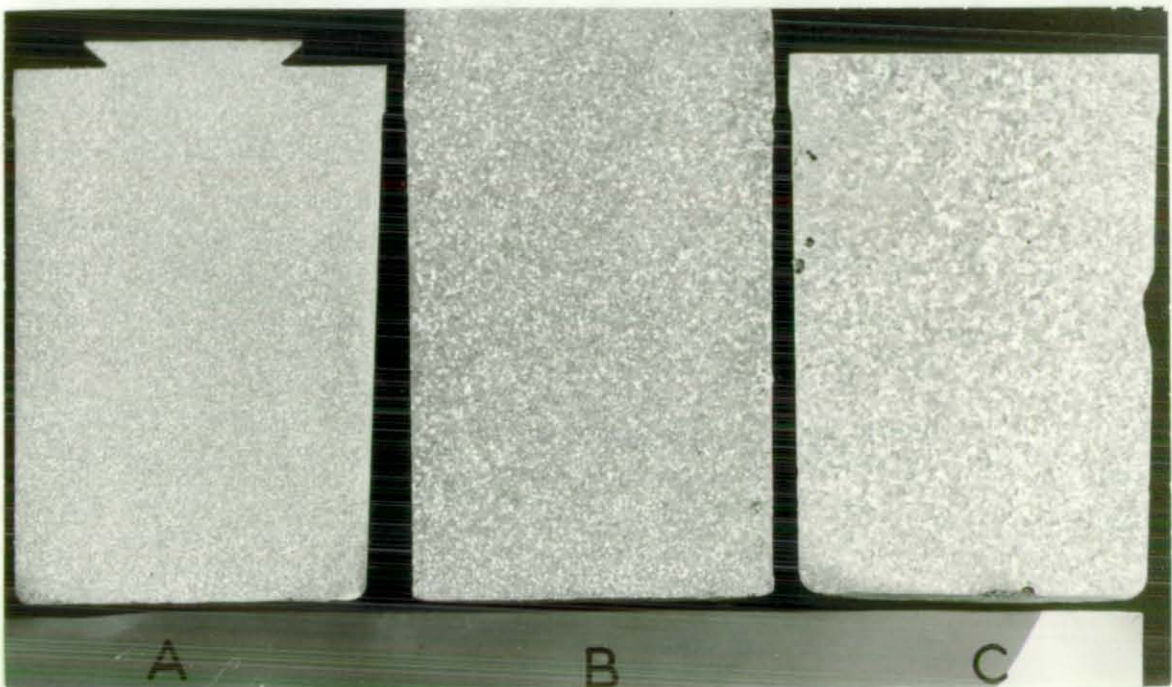


FIGURE 38: Macrostructure of the cast Al-3.75 Mg matrix alloy. Die temperature 250°C , casting temperature 700°C (sand and gravity die cast), and 692°C (squeeze cast).
 A. squeeze cast (140 MPa)
 B. gravity die cast
 C. sand cast.

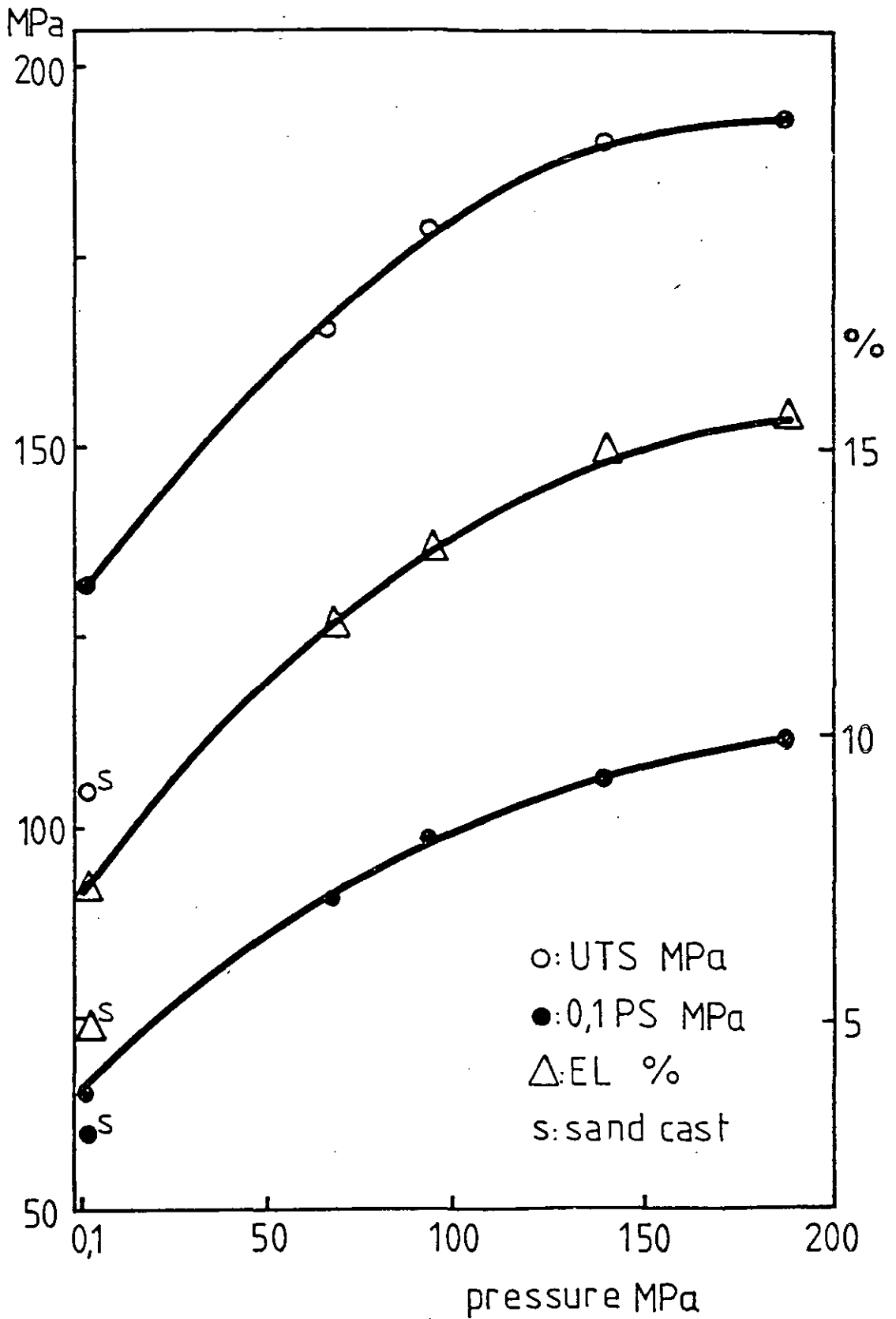


FIGURE 39: Effect of solidification pressure on the tensile properties of the Al-4.5 Cu alloy

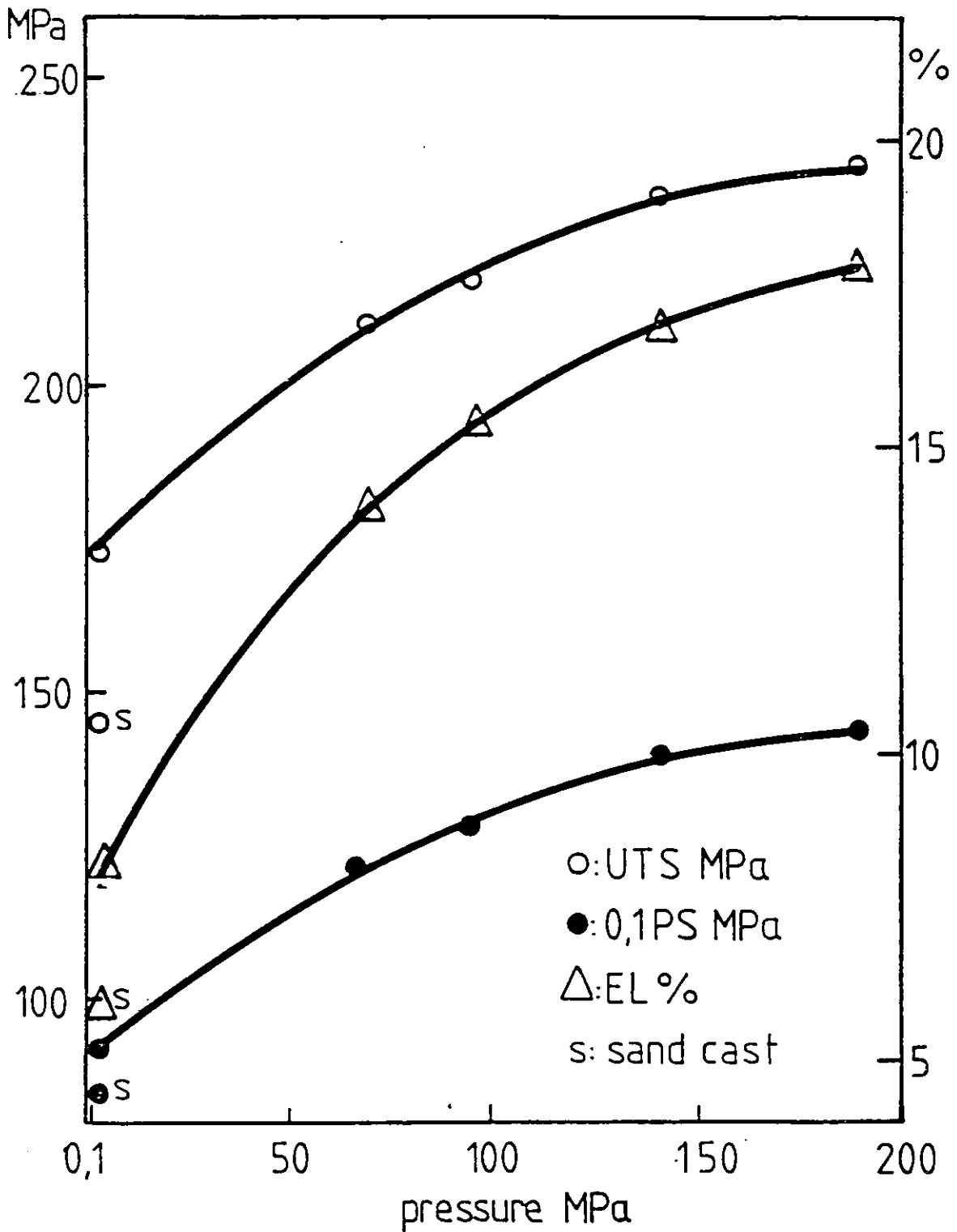
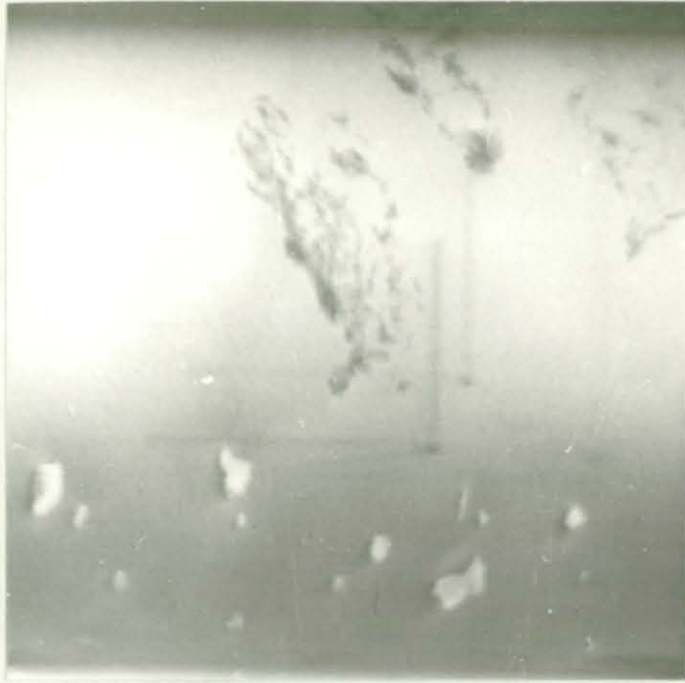


FIGURE 40: Effect of solification pressure on the tensile properties of the Al-3.75 Mg alloy (LM5)

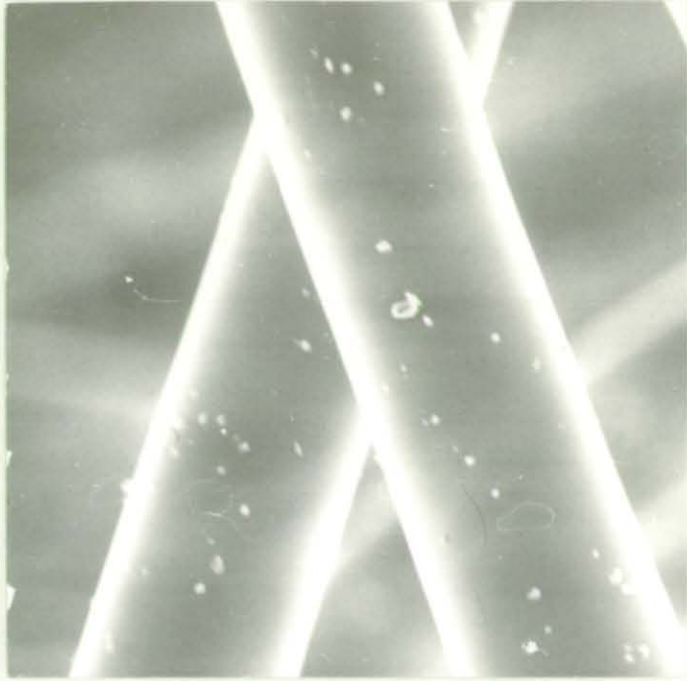


a) X9500



b) X1700

FIGURE 41: SEM photomicrographs of the as-received SiC fibre

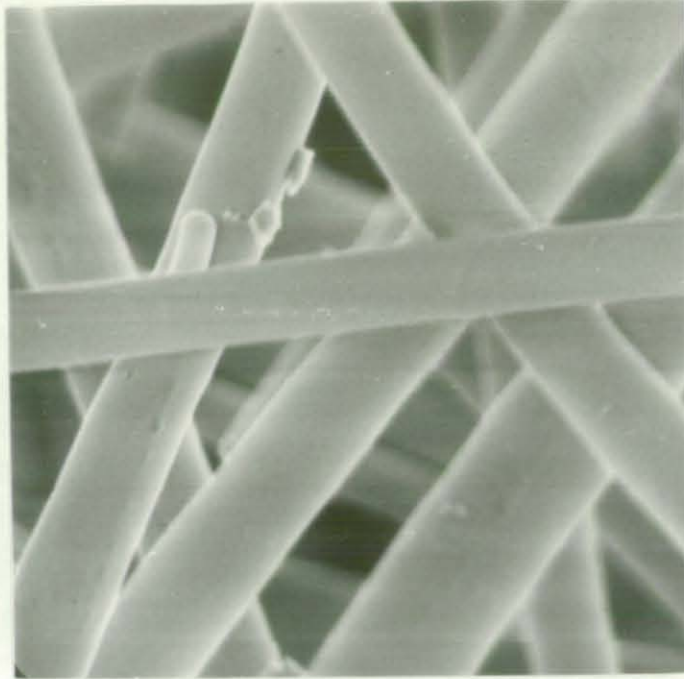


a) X1.8K

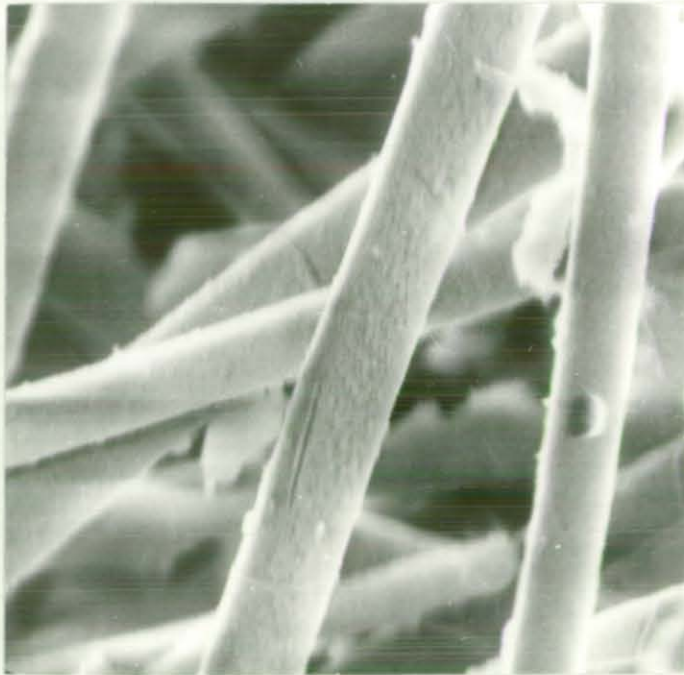


b) X1.6K

FIGURE 42: SEM photomicrographs of SiC fibre
a) Heat treated
b) Extracted from composite



a) X 4.5K



b) X5K

FIGURE 43: SEM photomicrographs of Al₂O₃ fibre

- a) pre-treated and mechanically separated fibre
- b) extracted from composite.

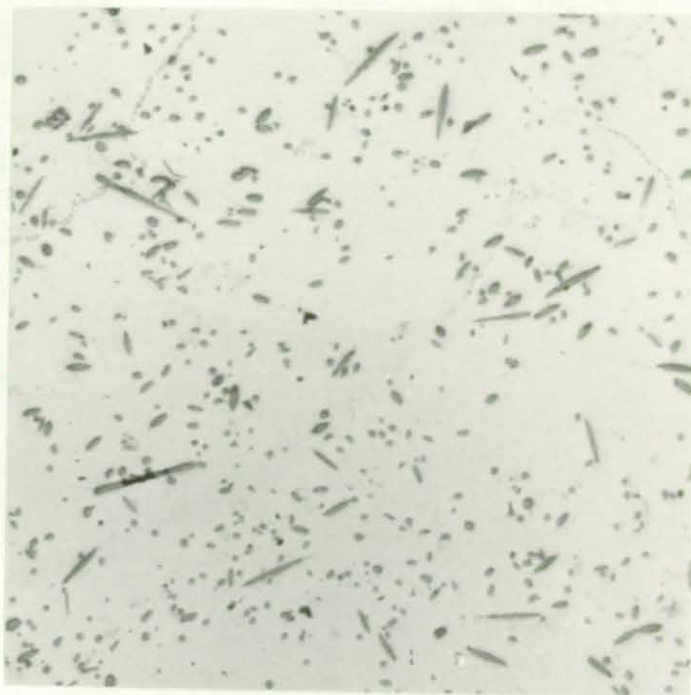


FIGURE 44: Fibre distribution and orientation (Al-Cu/SiC) silicon carbide fibre at two perpendicular planes 8% v/v fibre X70

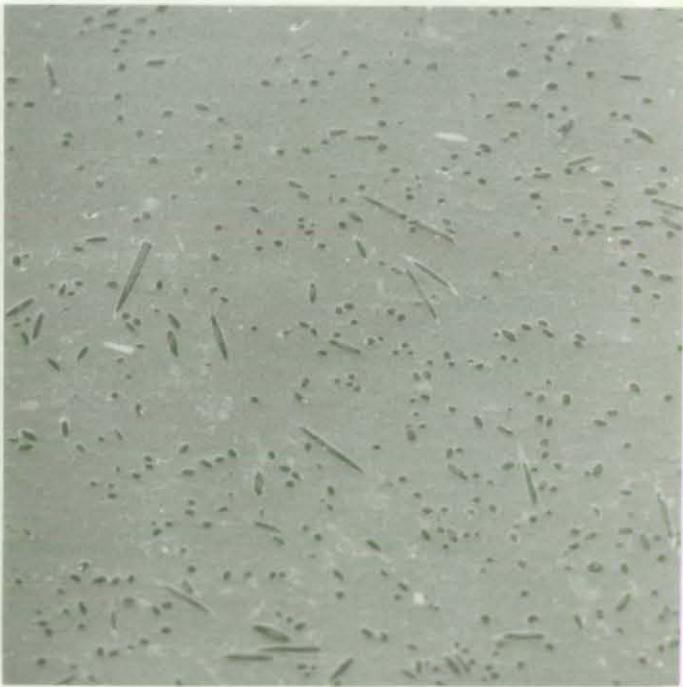
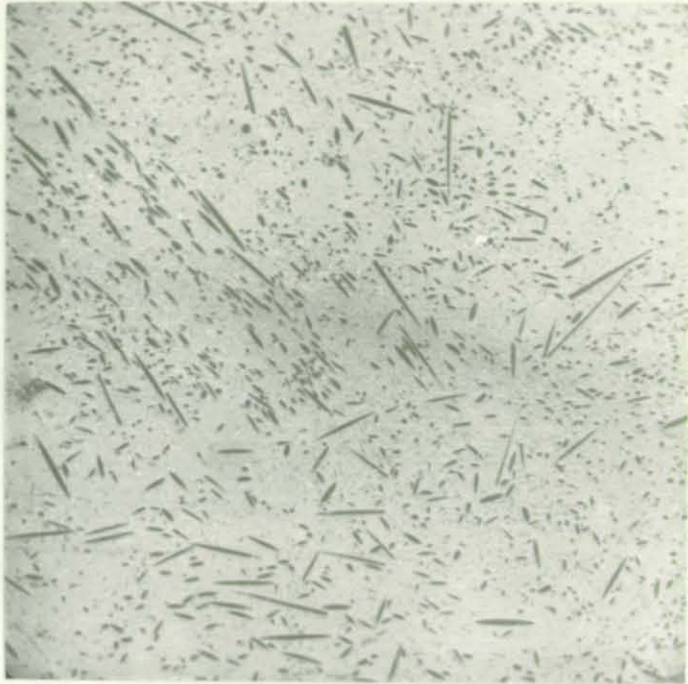


FIGURE 45: Fibre distribution and orientation
(Al-4.5 Cu/SiC composite)

- | | |
|----------------------------------|-----|
| a) 10% v/v silicon carbide fibre | X50 |
| b) 8% v/v silicon carbide fibre | X75 |

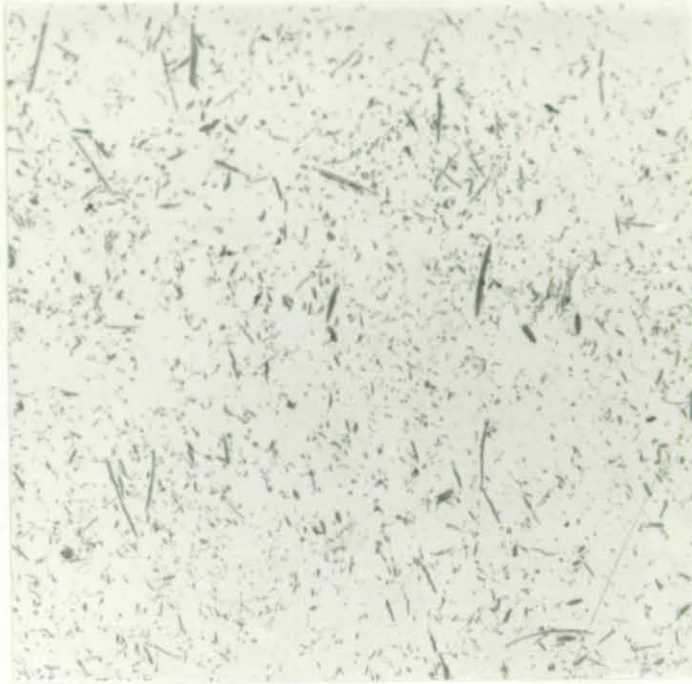
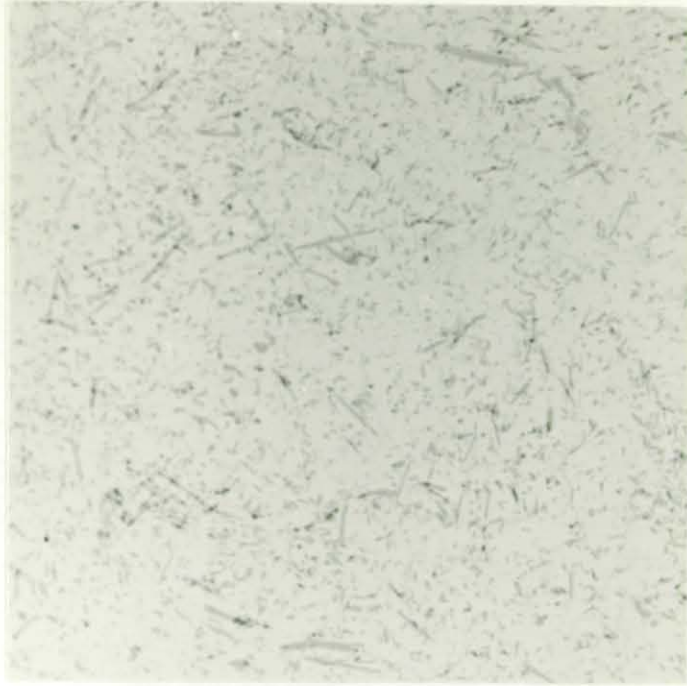


FIGURE 46: Fibre distribution and orientation
(Al-3.75 Mg/Al₂O₃ composite)
Alumina fibre at two perpendicular planes
8% v/v fibre, X100



(a)



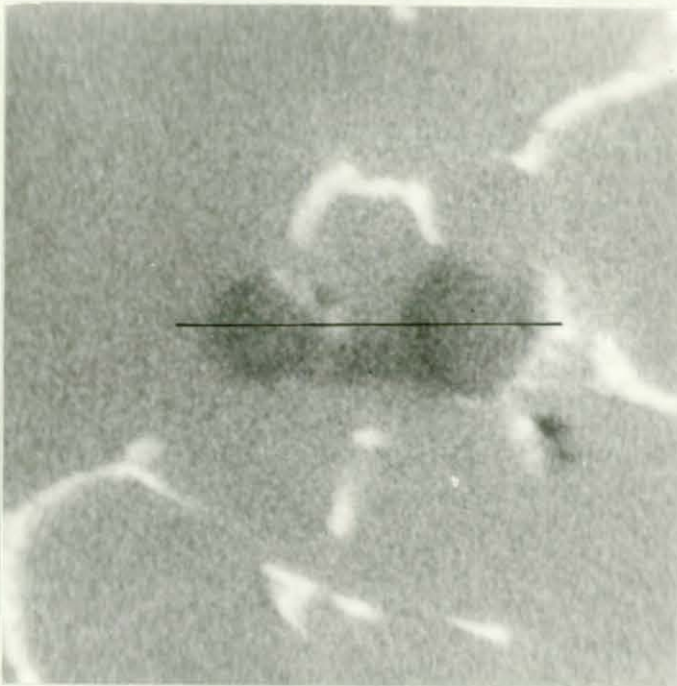
(b)

FIGURE 47: Fibre distribution and orientation (Al-3.75 Mg/Al₂O₃ composite)

- a) 10% v/v alumina fibre X100
b) 8% v/v alumina fibre X100



FIGURE 48: Silicon carbide fibre associated with a Cu-rich phase.
(Scattered electron image X1K)



X 1K

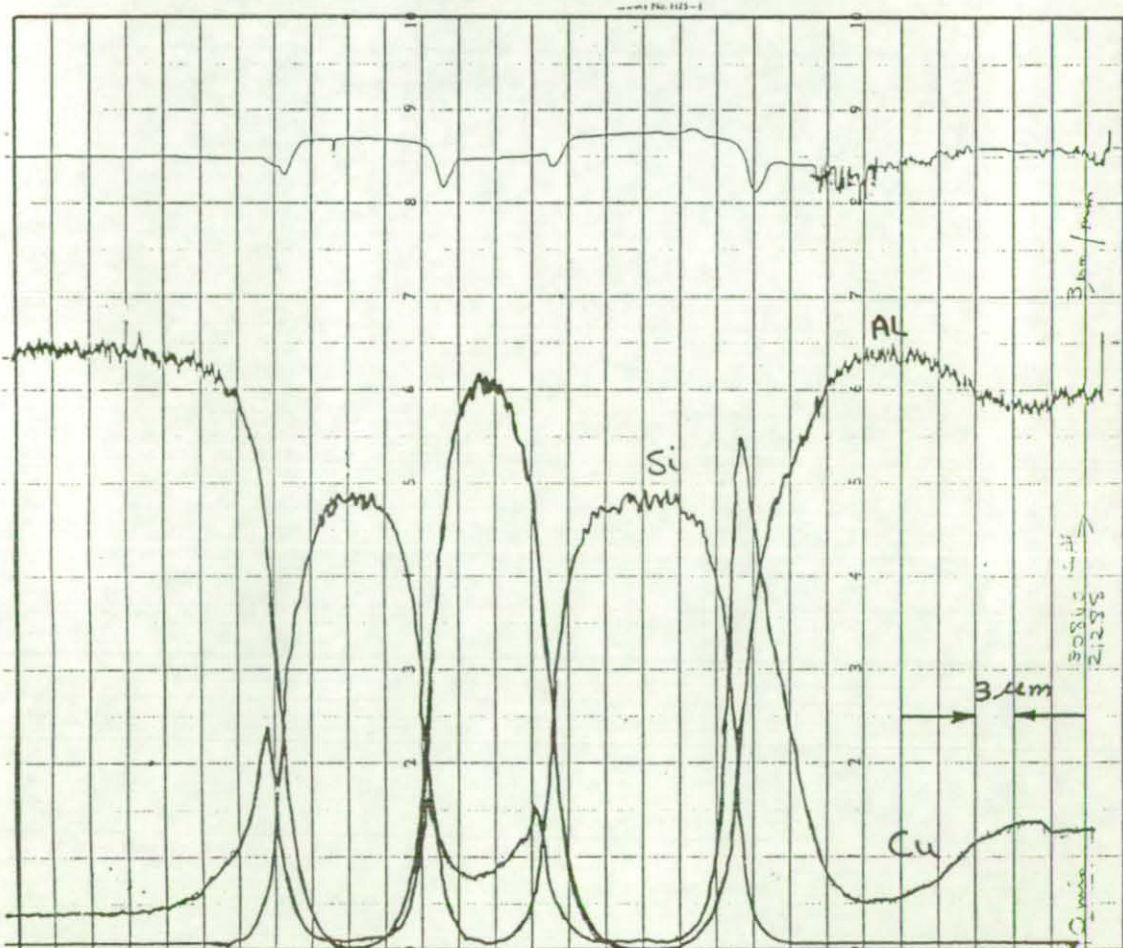


FIGURE 49: Scattered electron image and corresponding EPMA line scanning pattern for Al-4.5 Cu/SiC composite. Fibre/melt time of contact 18 minutes (as-cast)

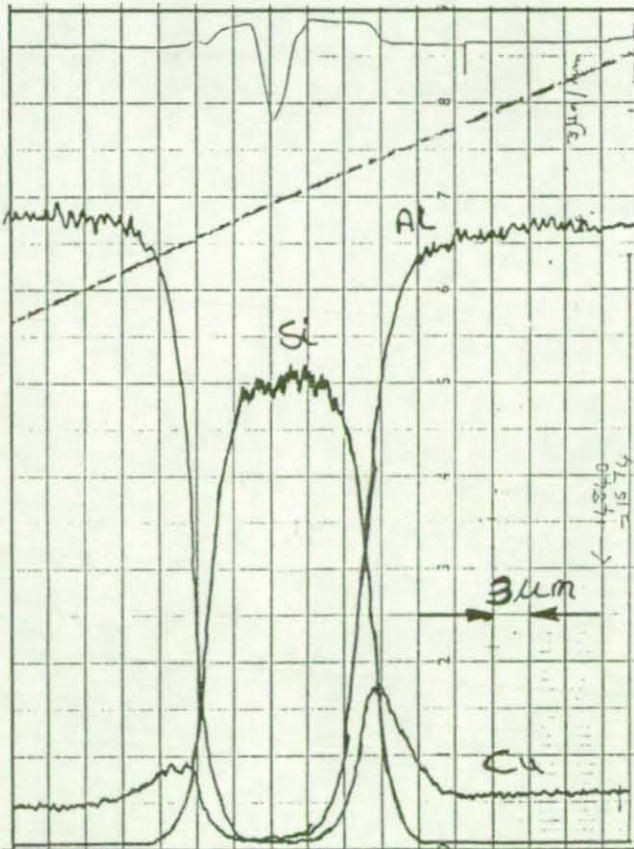
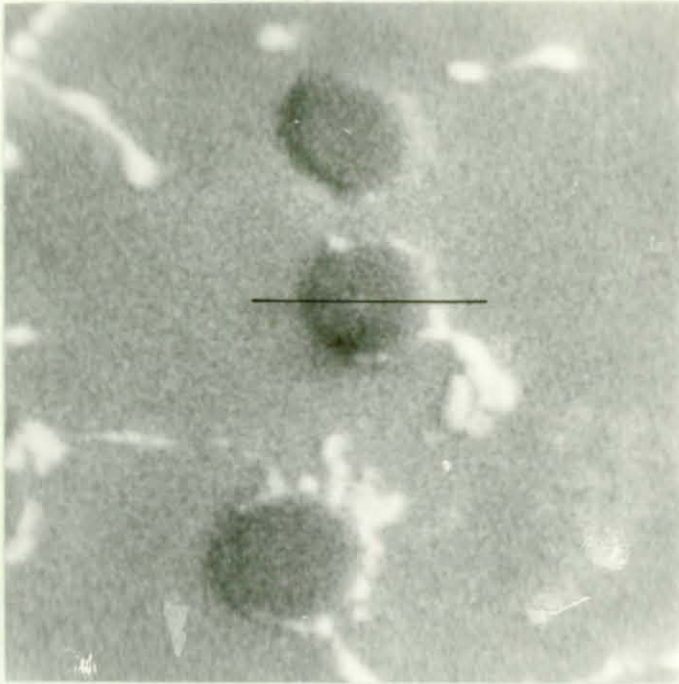


FIGURE 50: Scattered electron image and corresponding EPMA line scanning pattern for Al-4.5 Cu/SiC composite. Fibre/melt time of contact 39 minutes (as-cast)

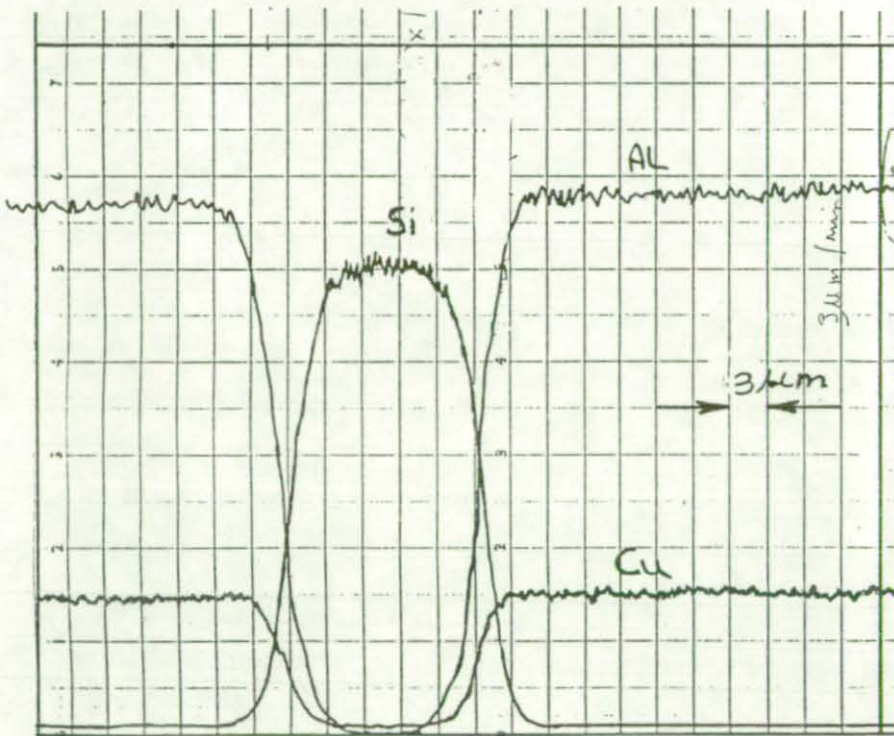
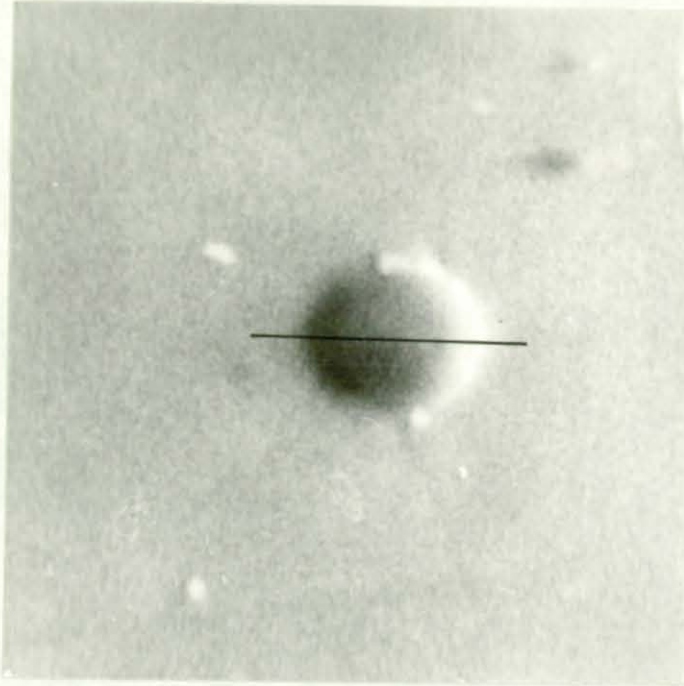


FIGURE 51: Scattered electron image and corresponding EPMA line scanning pattern for Al-4.5 Cu/SiC composite. Fully heat treated (contact time 18 minutes)

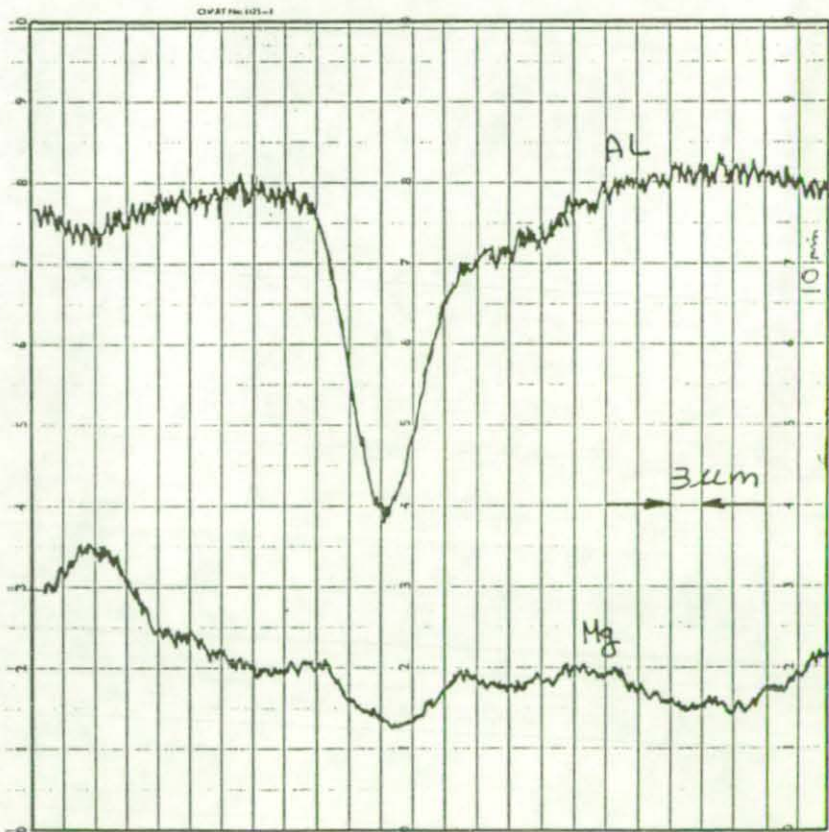
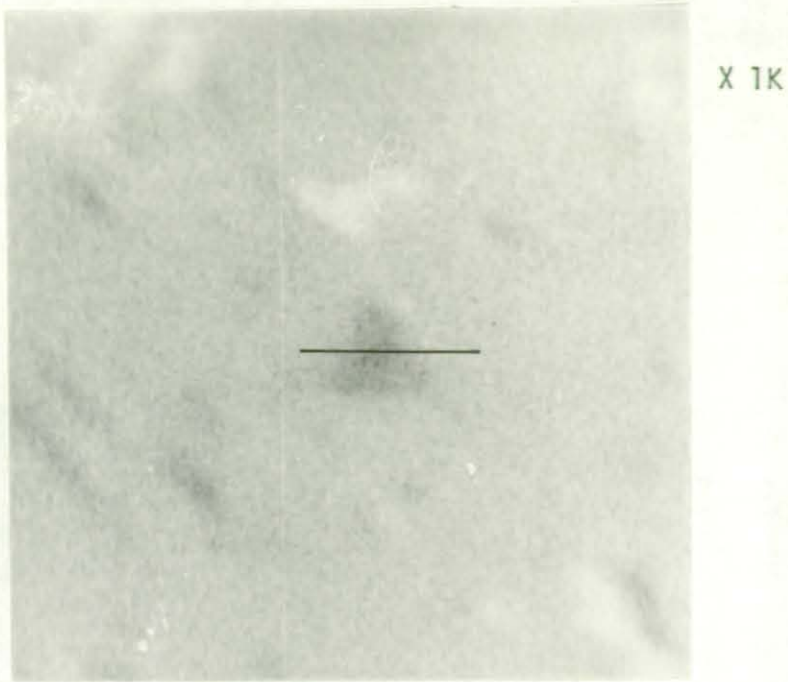


FIGURE 52: Scattered electron image and corresponding EPMA line scanning pattern for Al-3.75 Mg/Al₂O₃ composite. Fibre/melt time of contact 15.5 minutes (as-cast)

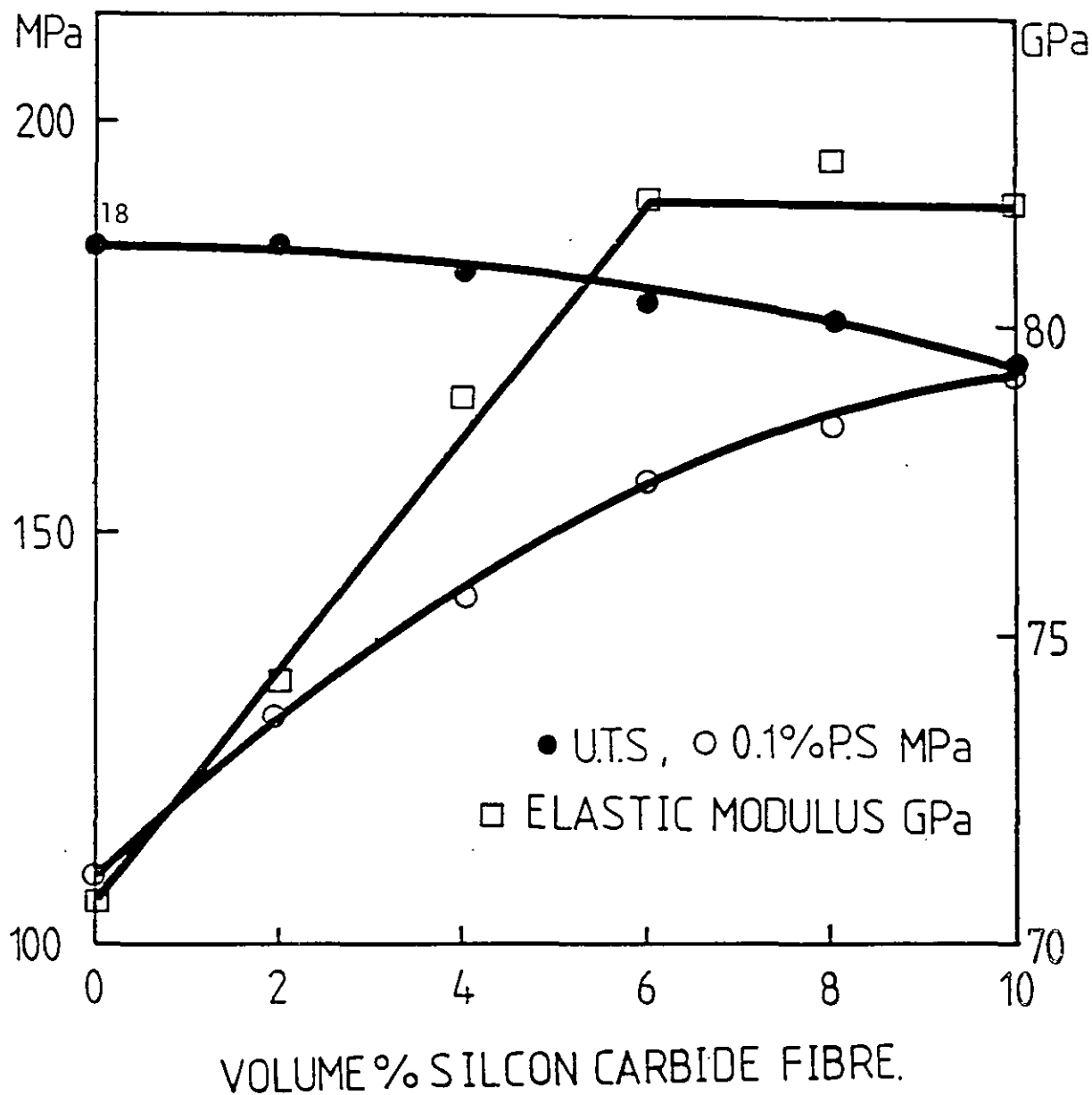


FIGURE 53: Room temperature tensile properties of the squeeze cast Al-4.5 Cu/SiC composite
Casting group IV

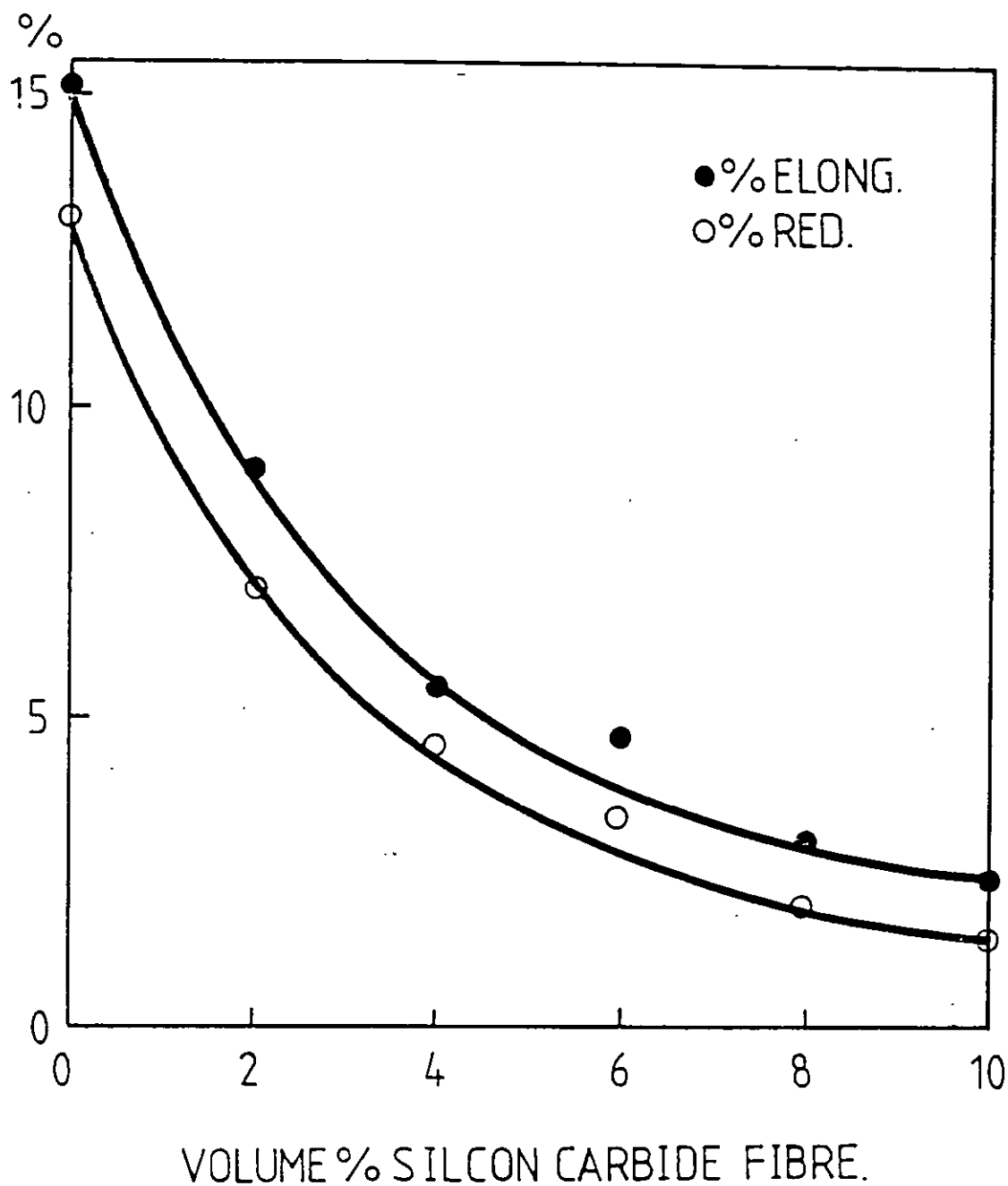


FIGURE 54: Percentage elongation and reduction in area of squeeze cast Al-4.5 Cu/SiC composites

Casting group IV

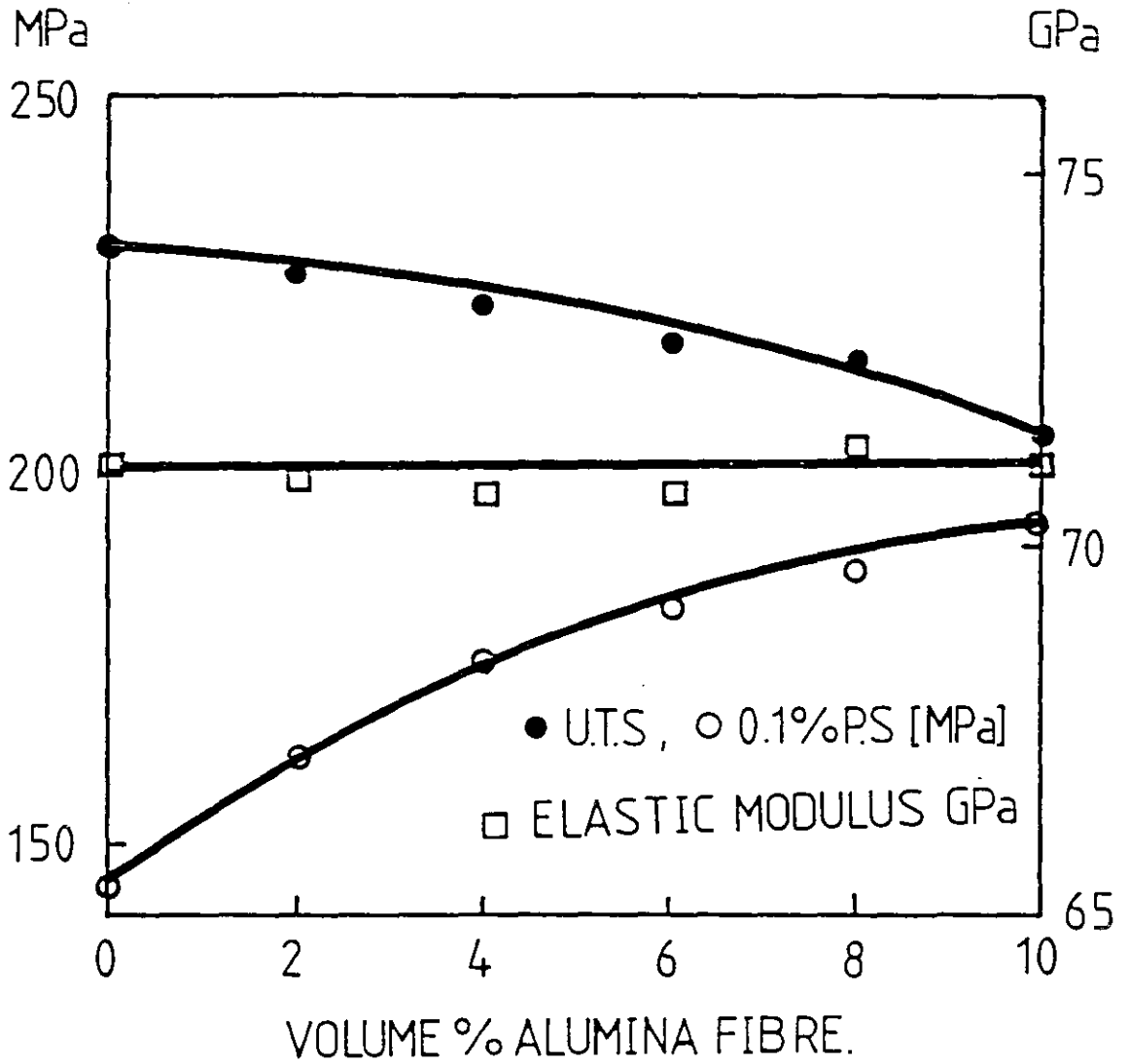


FIGURE 55: Room temperature tensile properties of the squeeze cast Al-3.75 Mg/Al₂O₃ composites. Casting group IV.

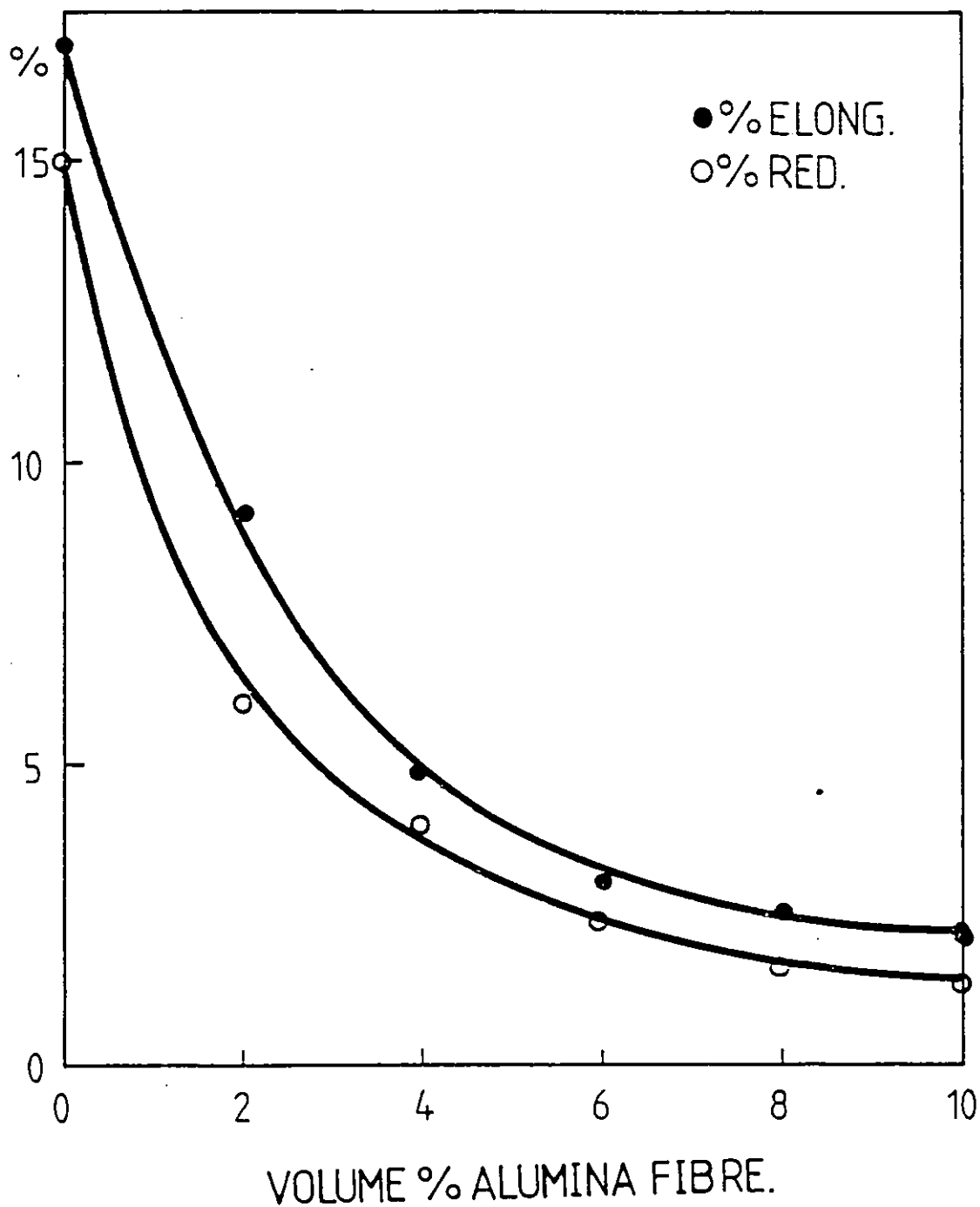


FIGURE 56: Percentage elongation and reduction in area of squeeze cast Al-3.75 Mg/Al₂O₃ composites

Castings group IV

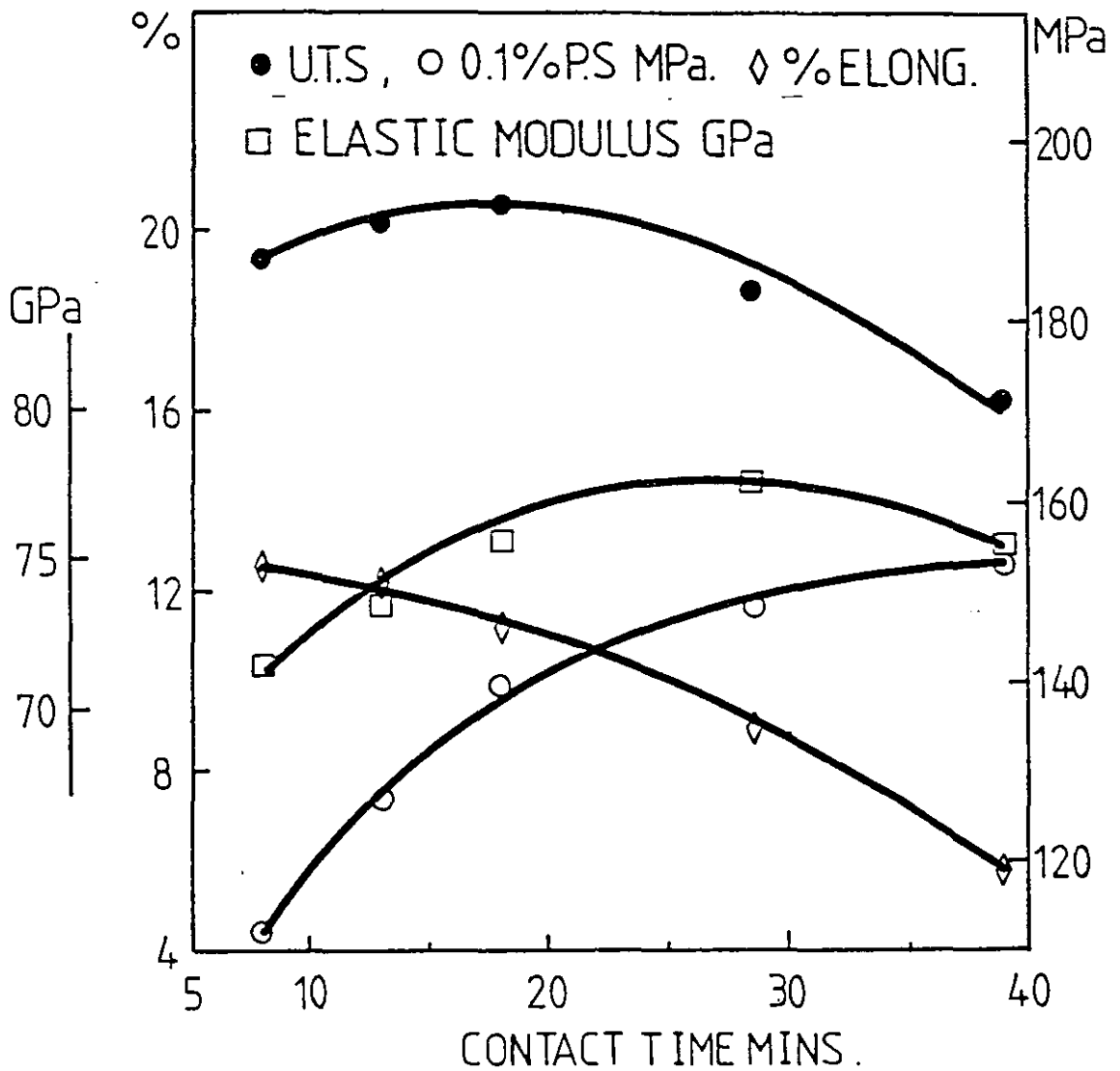


FIGURE 57: Effect of contact time between silicon carbide fibre and the molten (760°C) Al-4.5 Cu matrix alloy on the room temperature tensile properties of squeeze cast composites containing 4 volume percent fibre Casting group V.

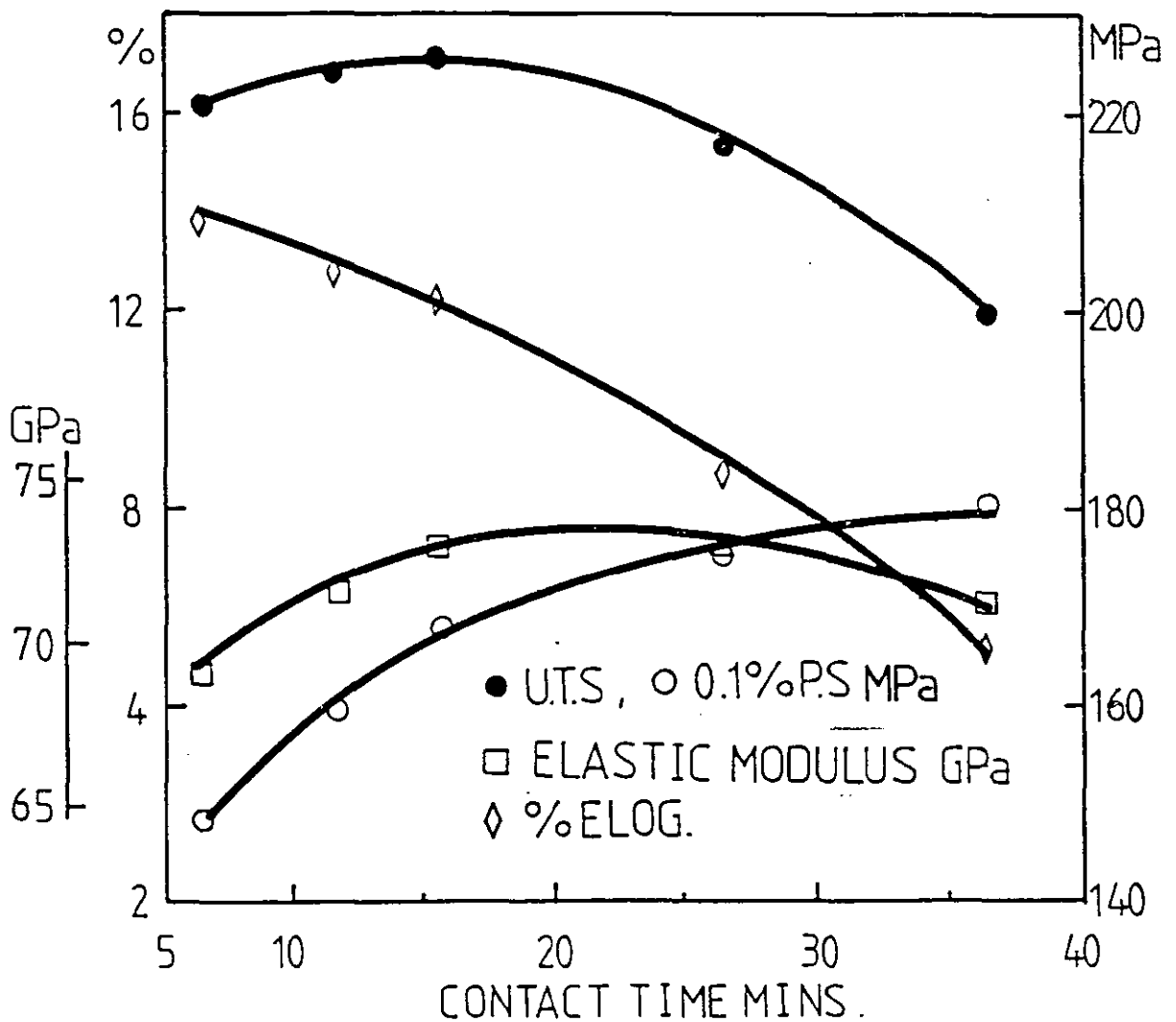


FIGURE 58: Effect of contact time between alumina fibre and the molten (735°C) Al-3.75 Mg matrix alloy on the room temperature tensile properties of squeeze cast composites containing 4 volume percent fibre. Casting group V.

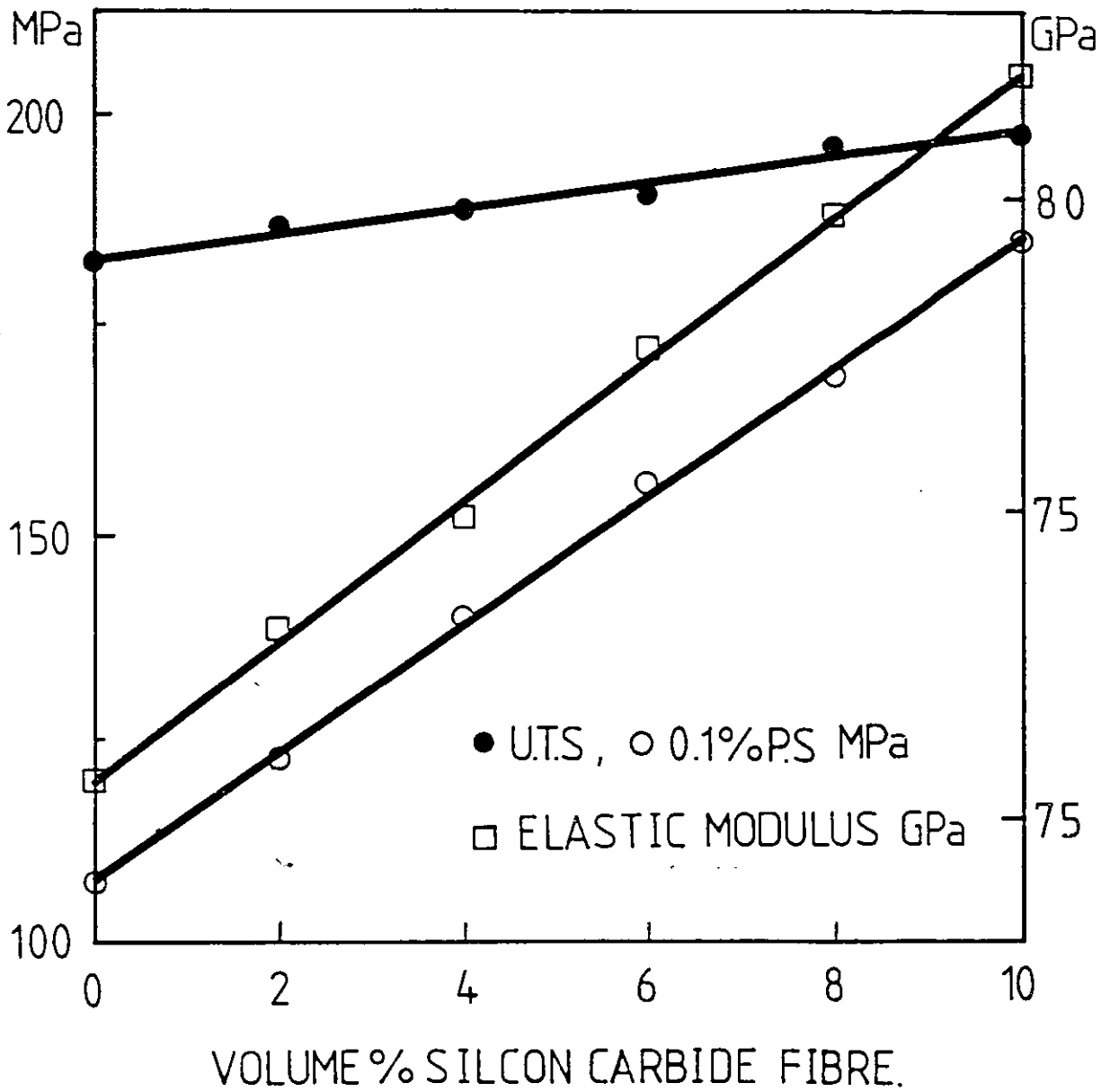


FIGURE 59: Room temperature tensile properties of the squeeze cast Al-4.5 Cu/Sic composites

Castings group VI.

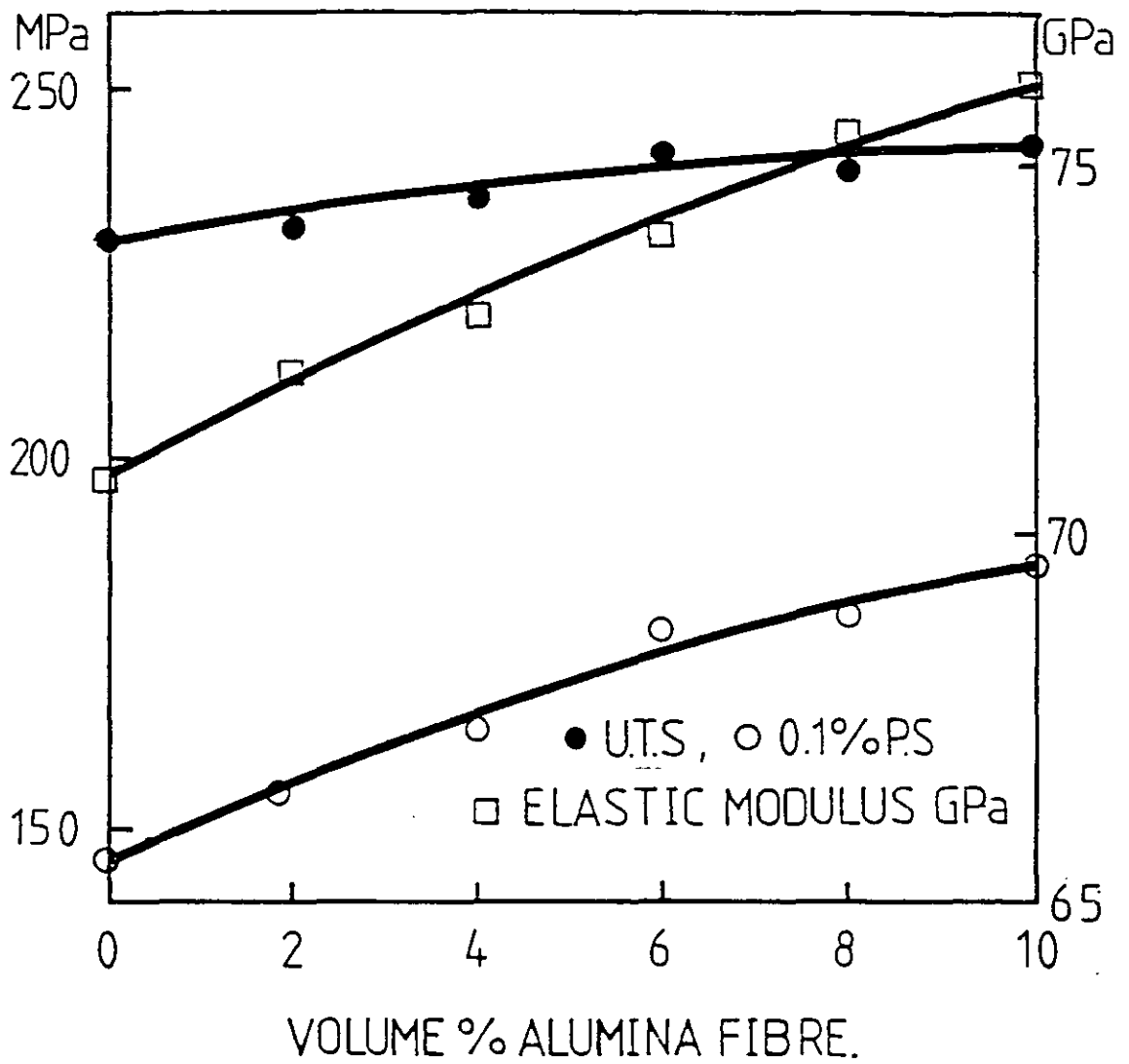


FIGURE 60: Room temperature tensile properties of the squeeze cast Al-3.75 Mg/Al₂O₃ composites
Castings group VI

U.T.S MPa.

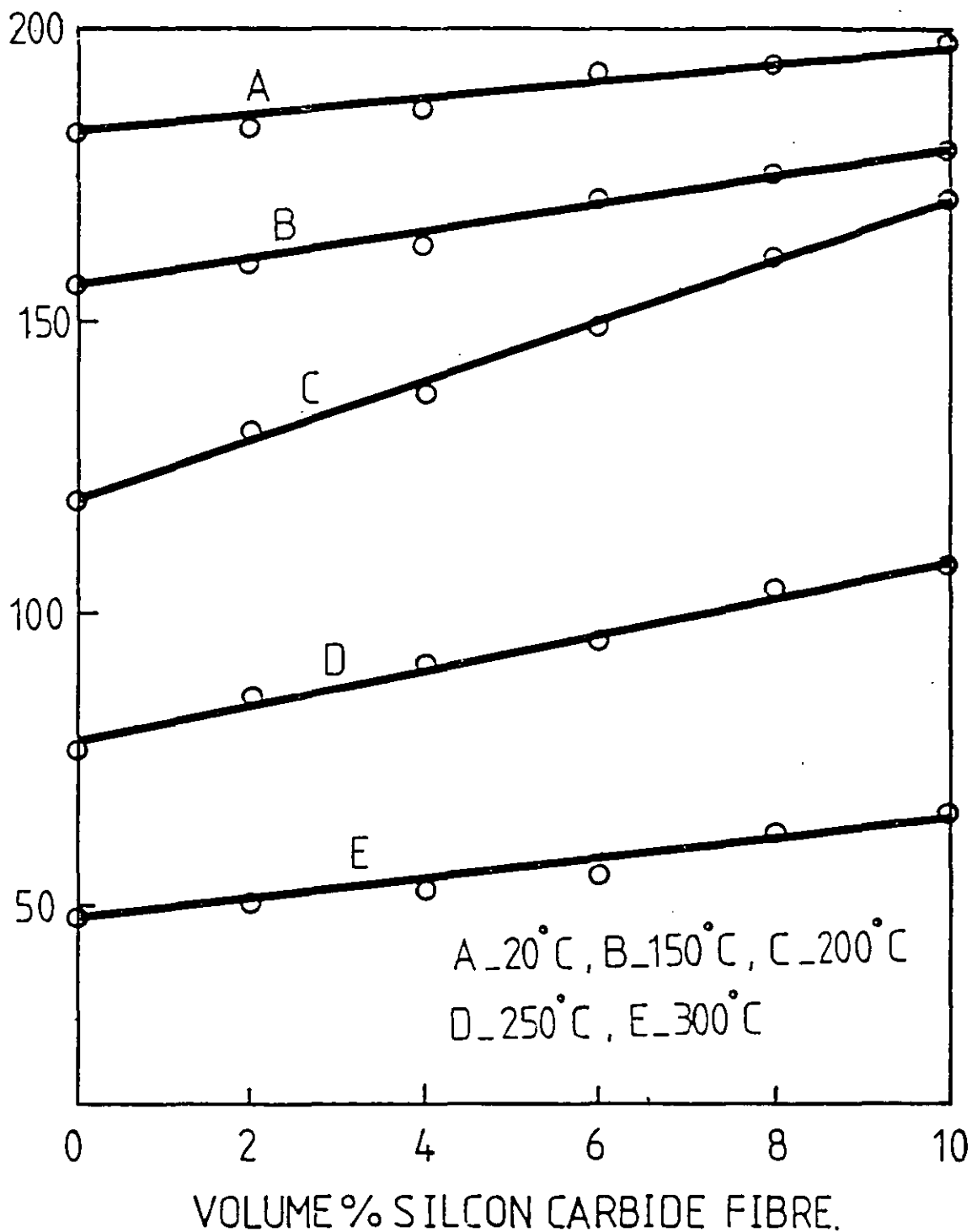


FIGURE 61: Effect of fibre percent volume on the UTS of squeeze cast Al-4.5 Cu/SiC composites at different temperatures. Casting group VII.

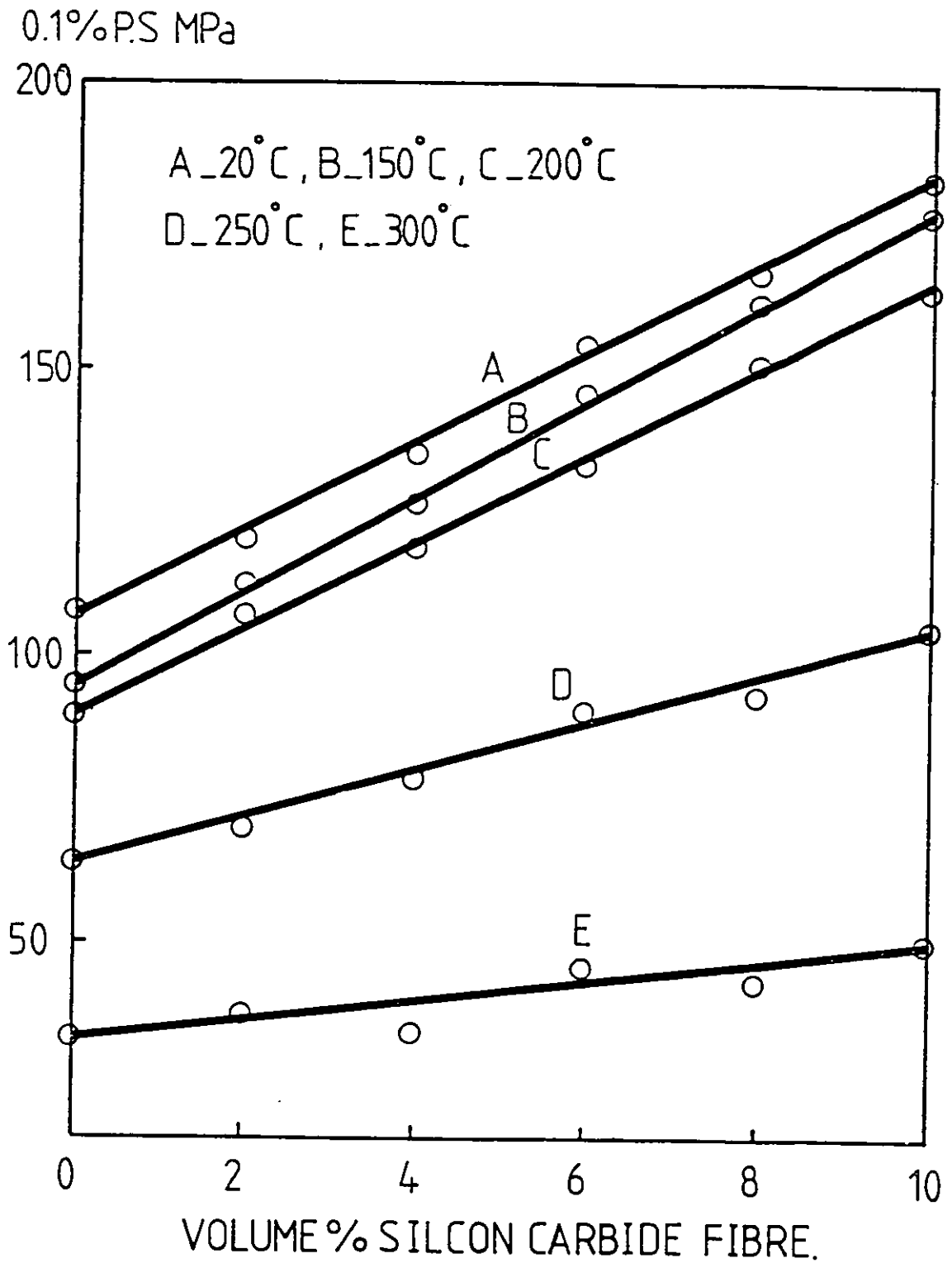


FIGURE 62: Effect of fibre volume percent on the 0.1% PS of squeeze cast Al-4.5 Cu/SiC composites at different temperatures. Casting group VII.

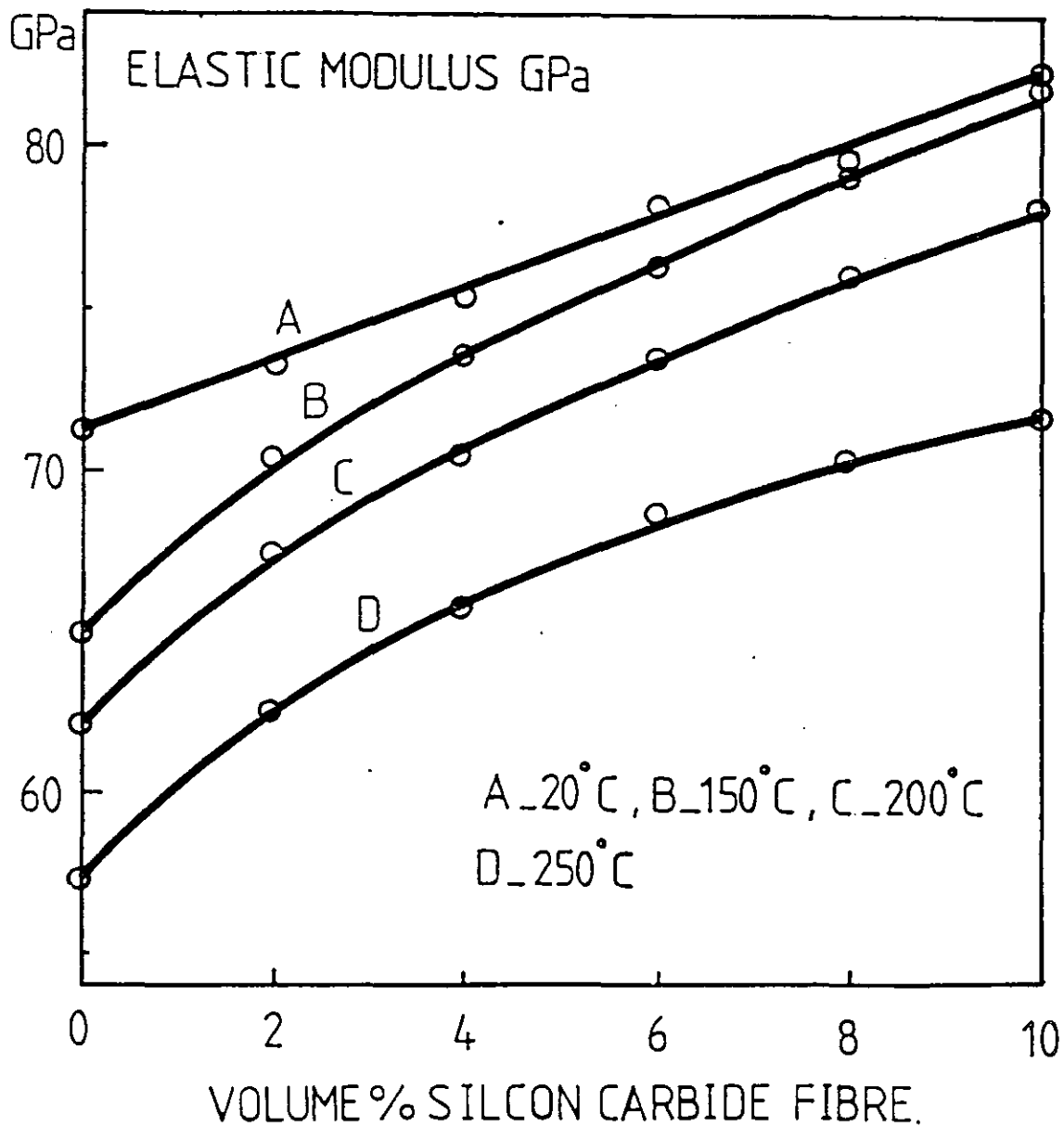


FIGURE 63: Effect of fibre volume percent on the elastic modulus of squeeze cast Al-4.5 Cu/SiC composites at different temperatures. Casting group VII.

U.T.S. MPa.

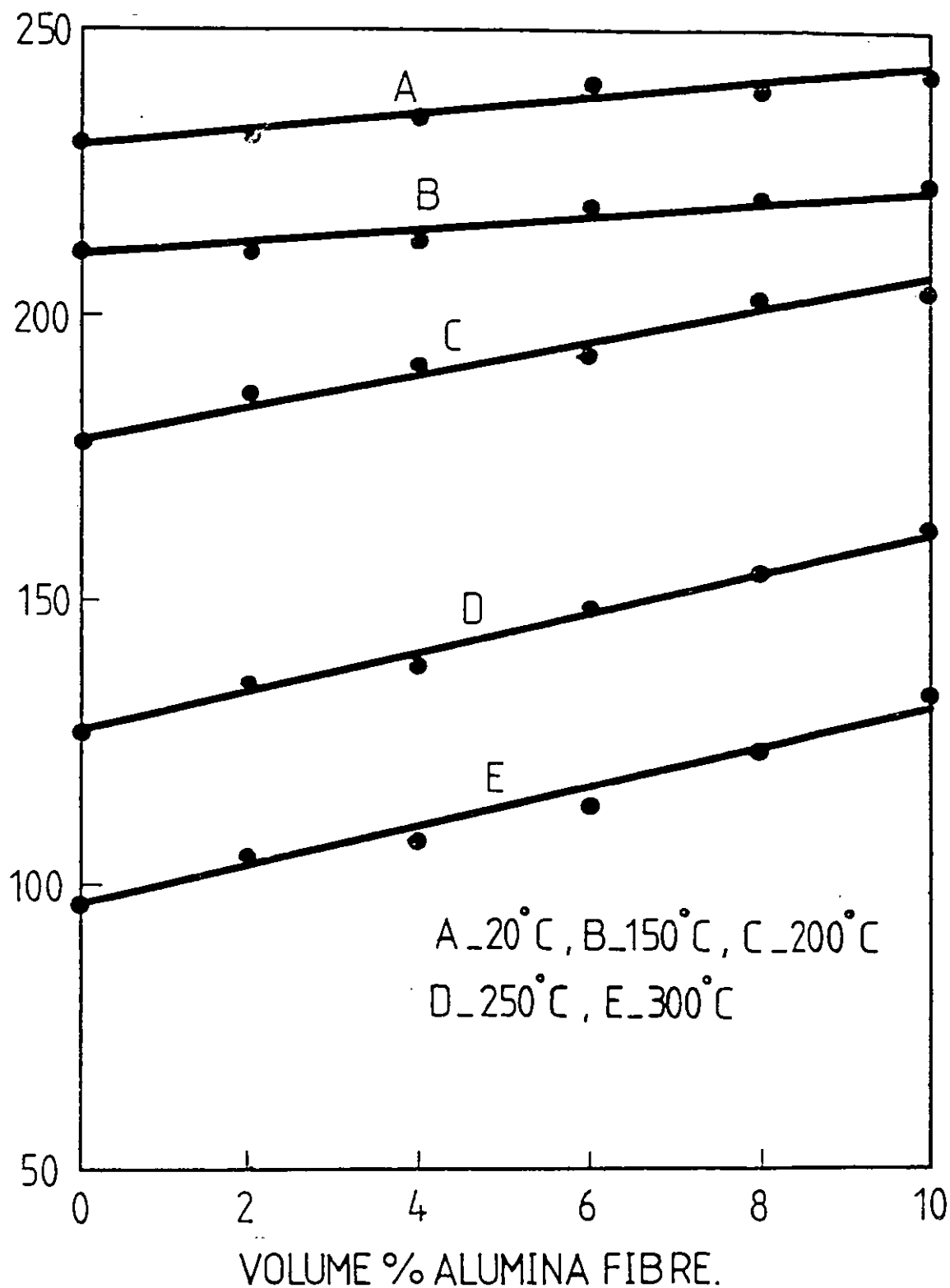


FIGURE 64: Effect of fibre volume percent on the UTS of squeeze cast Al-3.75 Mg/Al₂O₃ composites at different temperatures Casting group VII.

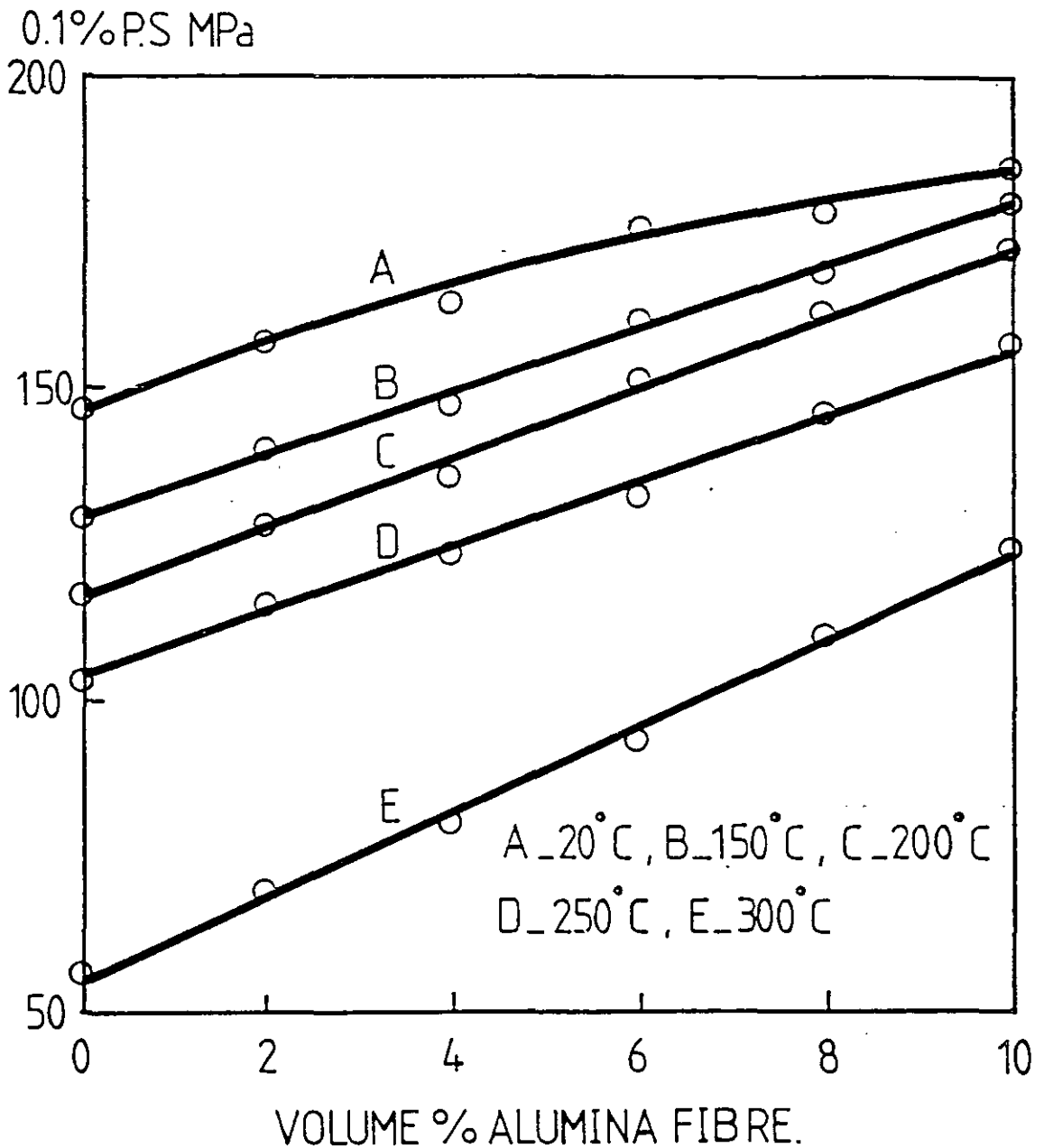


FIGURE 65: Effect of fibre volume percent on the 0.1% PS of squeeze cast Al-3.75 Mg/Al₂O₃ composites at different temperatures. Casting group VII.

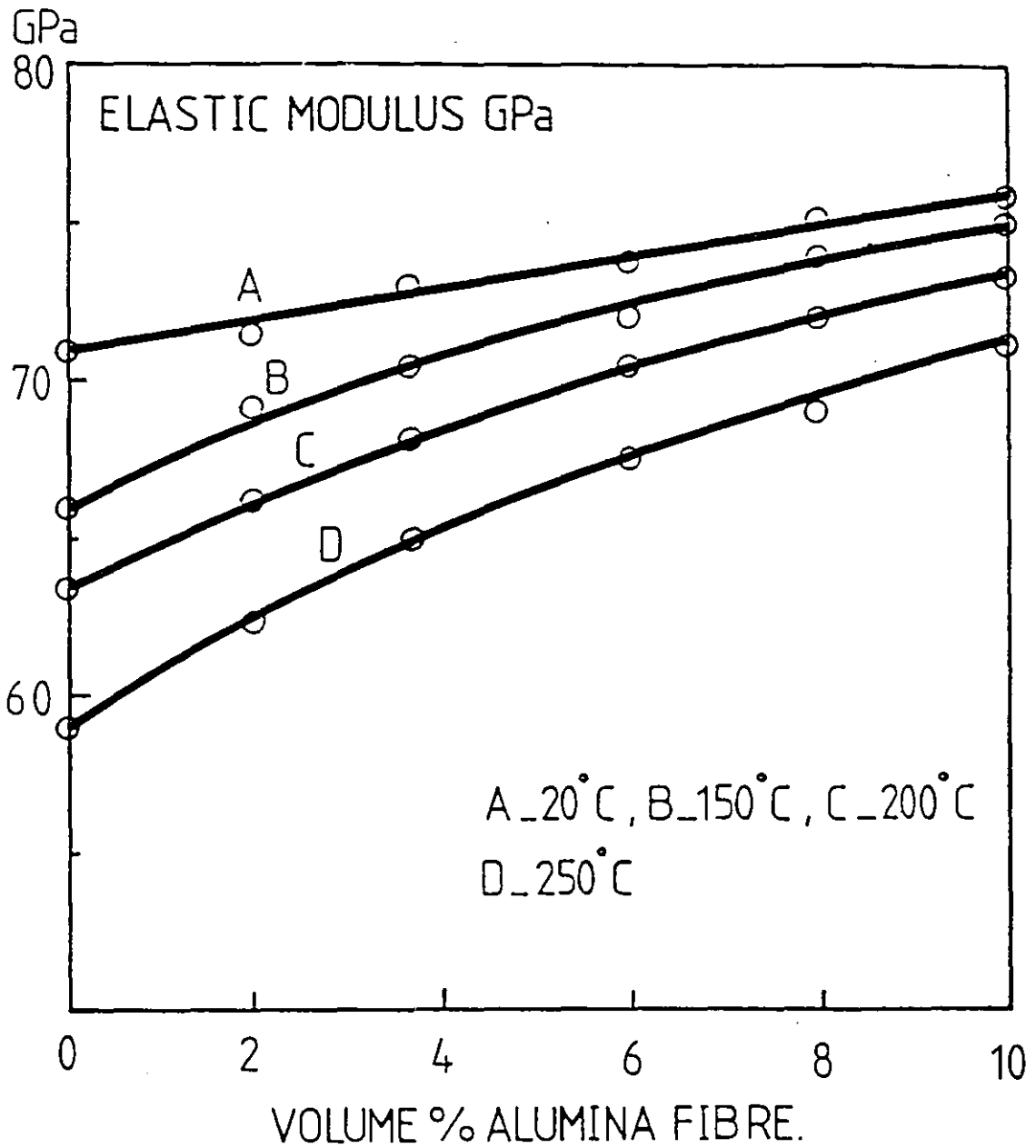


FIGURE 66: Effect of fibre volume percent on the elastic modulus of squeeze cast Al-3.75 Mg/Al₂O₃ composites at different temperatures. Casting group VII.



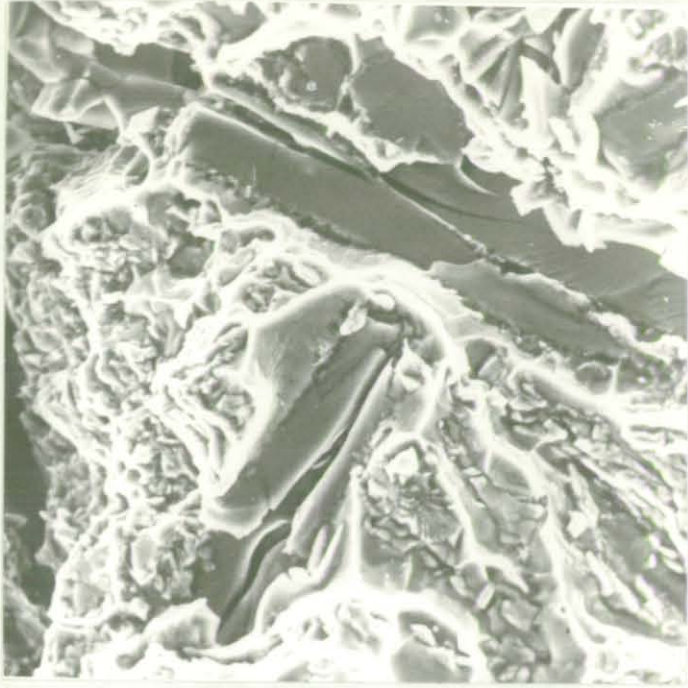
a) X400



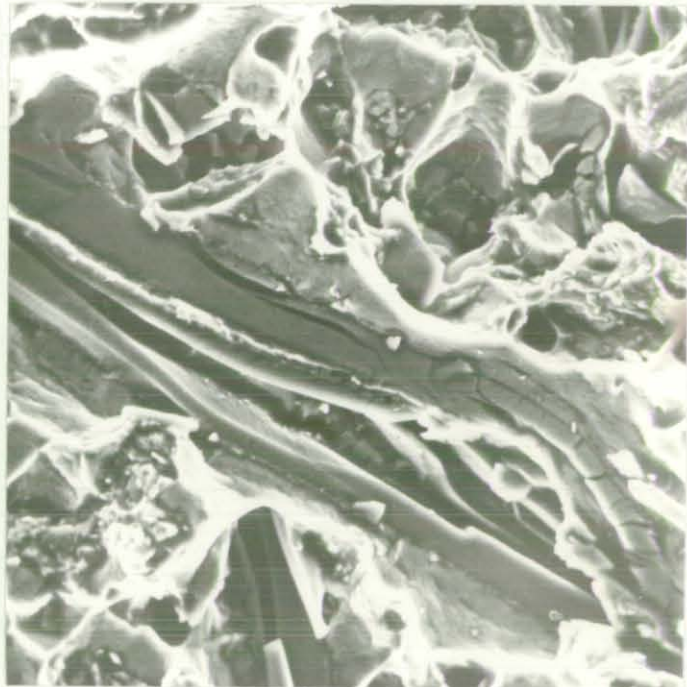
b) X800

FIGURE 67: Effect of the time of contact between SiC fibre and the molten (760°C) Al-4.5 Cu matrix alloy on fibre bonding and degradation

a) Poor bonding, 8 minutes; b) Adequate bonding, 18 minutes



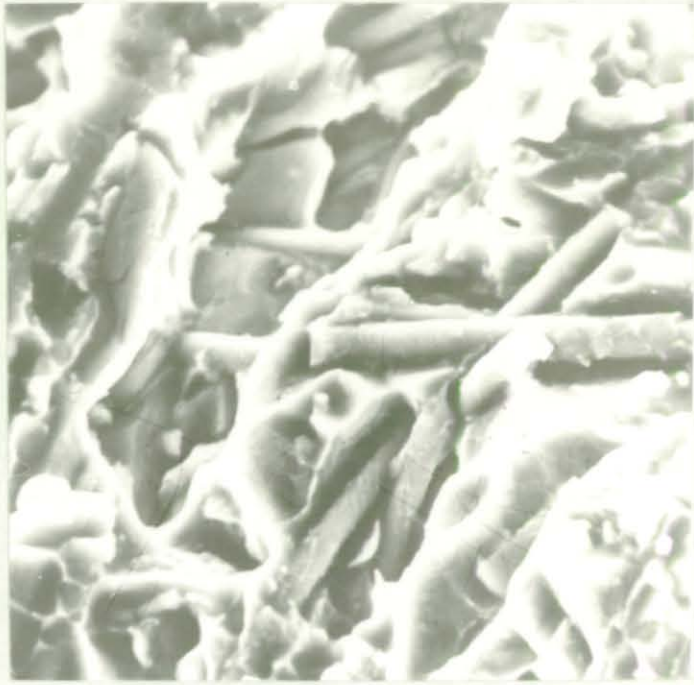
a) X800



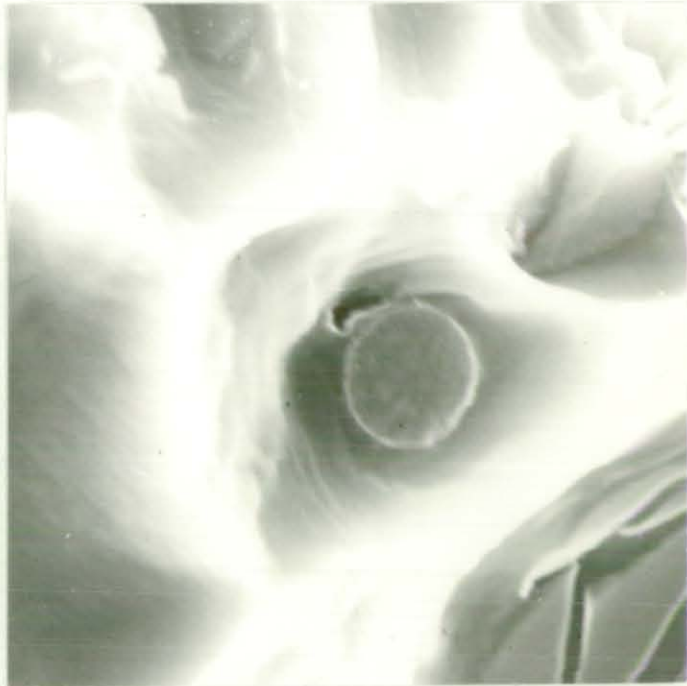
b) X800

FIGURE 68: Effect of the time of contact between SiC fibre and the molten (760°C) Al-4.5 Cu matrix alloy on fibre bonding and degradation

a) Fibre degradation 28.5 minutes; 6) Severe fibre degradation 30 minutes



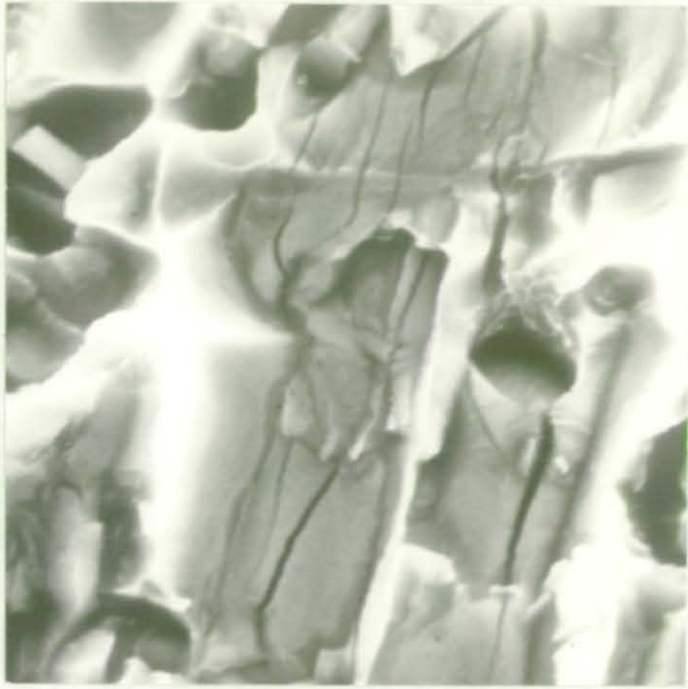
a) X2.4K



b) x11K

FIGURE 69

/Continued



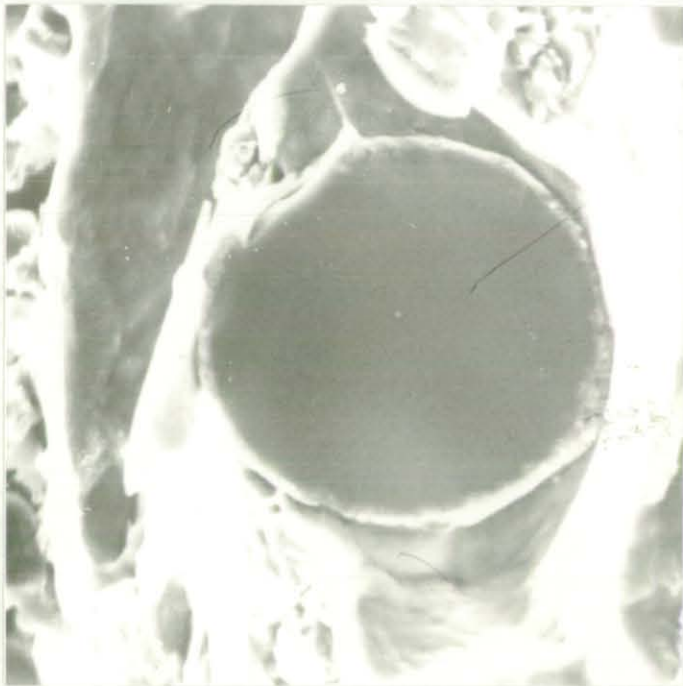
c) X4K

FIGURE 69: Effect of the time of contact between Al_2O_3 fibre and the molten (735°C) Al-3.75 Mg matrix alloy on fibre bonding and degradation

- a) Poor bonding, 6.5 minutes
- b) Adequate bond, 15.5 minutes
- c) Fibre degradation, 26.5 minutes

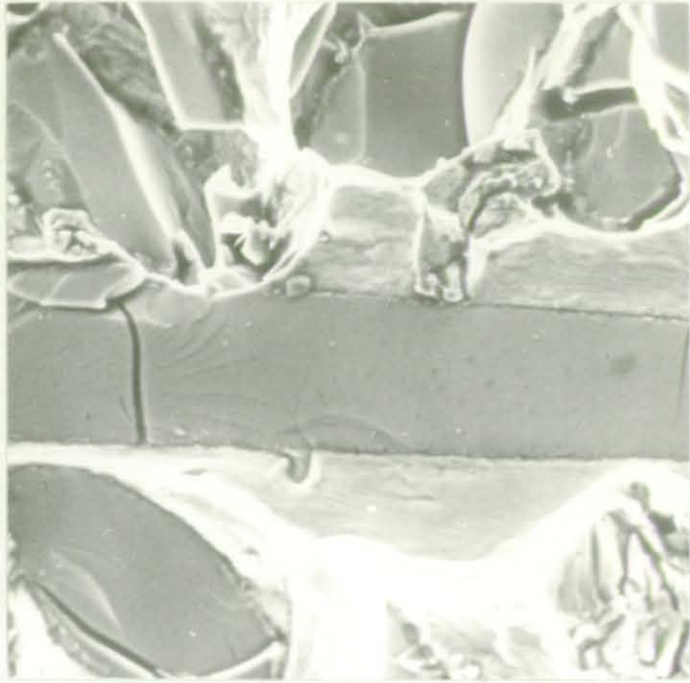


a) X140

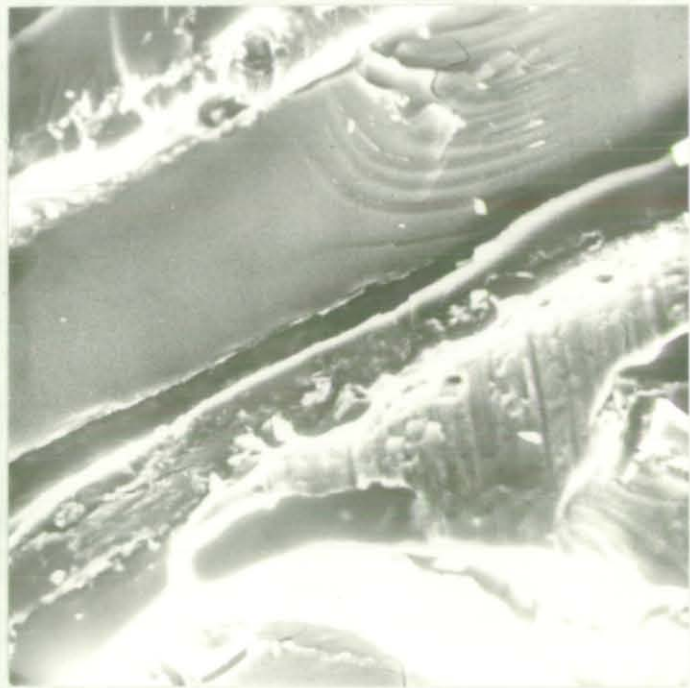


b) X3.5K

FIGURE 70: Fibre fracture in composite of Al-Cu/Sic (room temperature)
Casting group VII



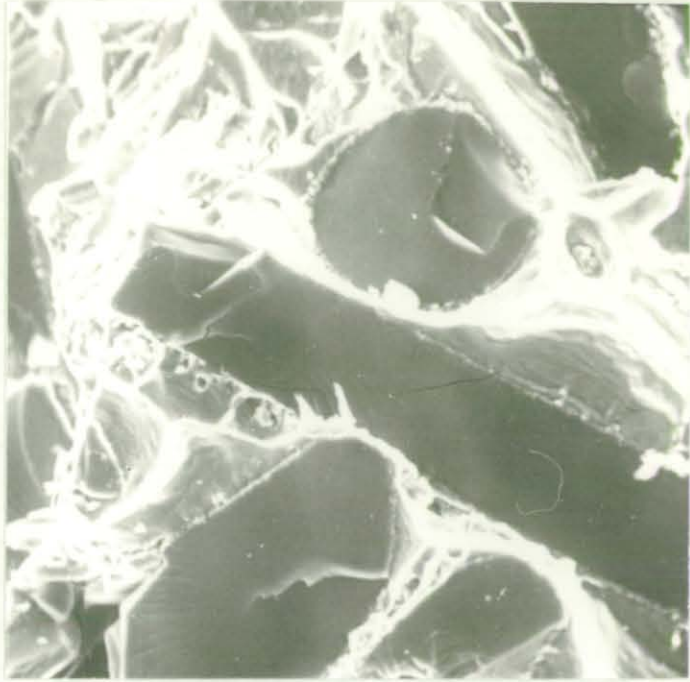
a) X700



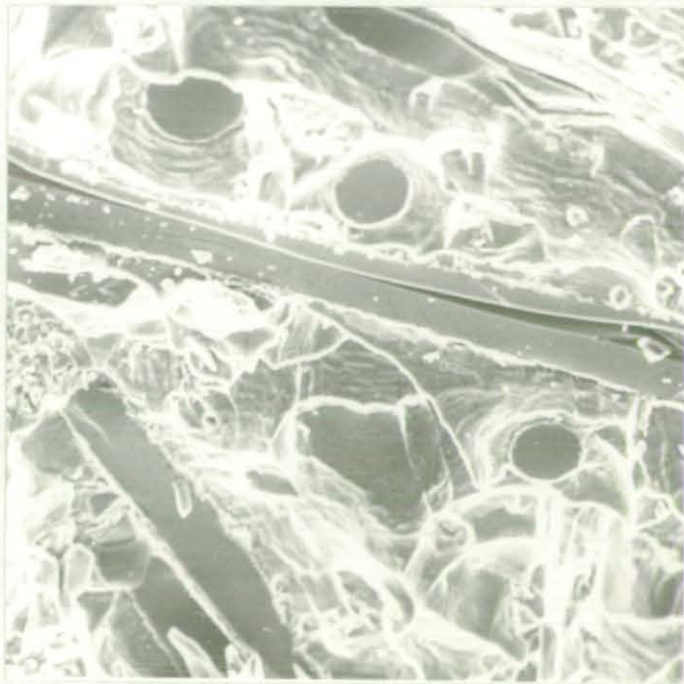
b) X2.4K

FIGURE 71: Fibre fracture in composite of Al-4.5 Cu/SiC

- a) 10% v/v SiC fibre, casting group VI
- b) 6% v/v SiC fibre, casting group IV



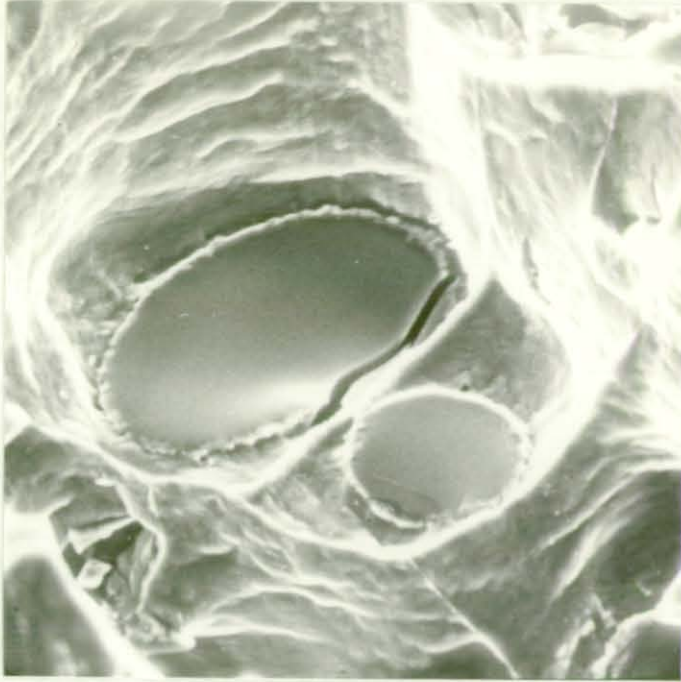
a) X1.3K



b) X700

FIGURE 72

/Continued



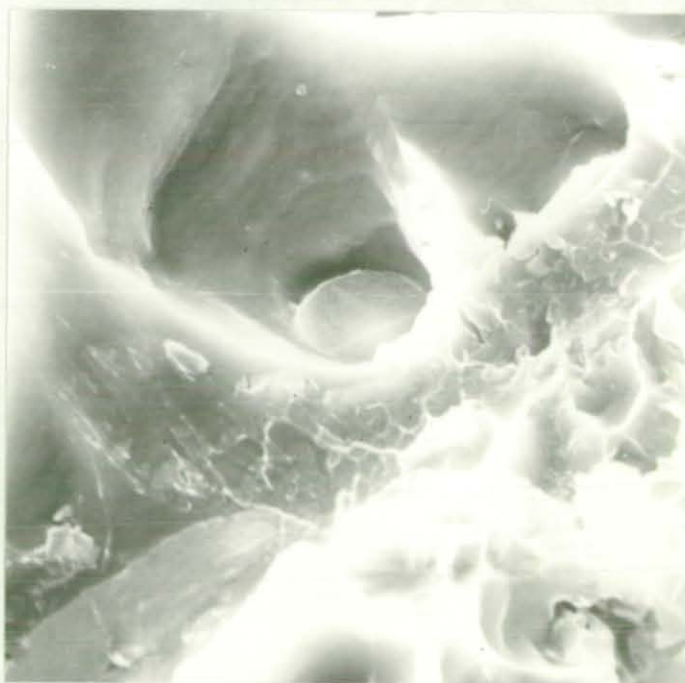
c) X2.2K

FIGURE 72: Fracture (tension) of the Al-Cu/SiC composite (squeeze cast) tested at high temperatures

- a) 10% v/v SiC fibre, fractured at 150°C
- b) 8% v/v SiC fibre, fractured at 200°C
- c) 6% v/v SiC fibre, fractured at 300°C



a) X10K

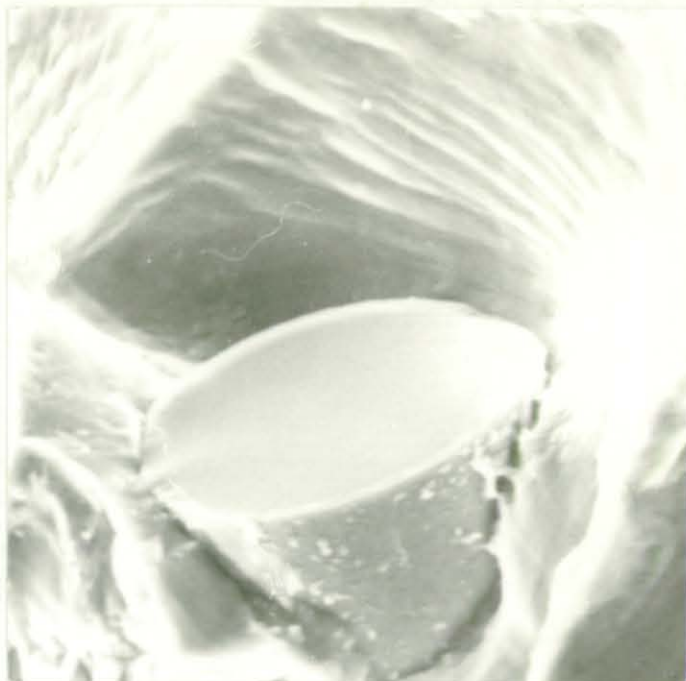


b) X5K

FIGURE 73: Fracture (tension) of Al-Mg/Al₂O₃ composite (room temperature)

a) 8% v/v alumina fibre, castings group VI

b) 10% v/v alumina fibre, castings group VII



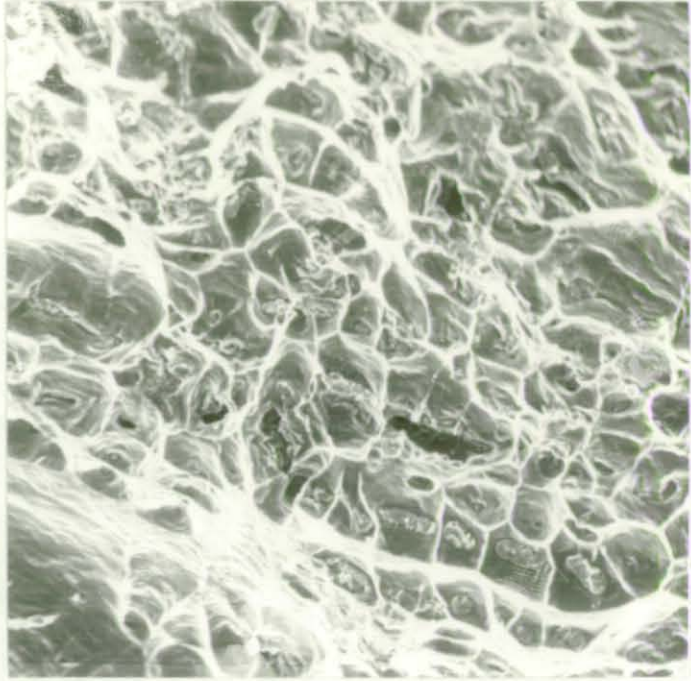
a) X4K



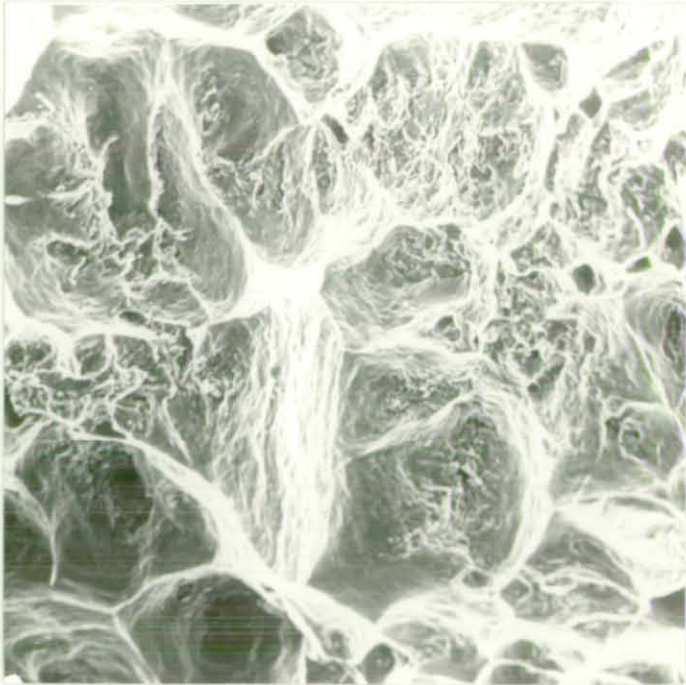
b) X1.6K

FIGURE 74: Fibre fracture (tension), Al-3.75 Mg/Al₂O₃ composite

- a) Fibre fracture and matrix flow marking, test temperature 250°C, fibre content 2% v/v
- b) Fibre fracture, test temperature 250°C, fibre content 10% v/v



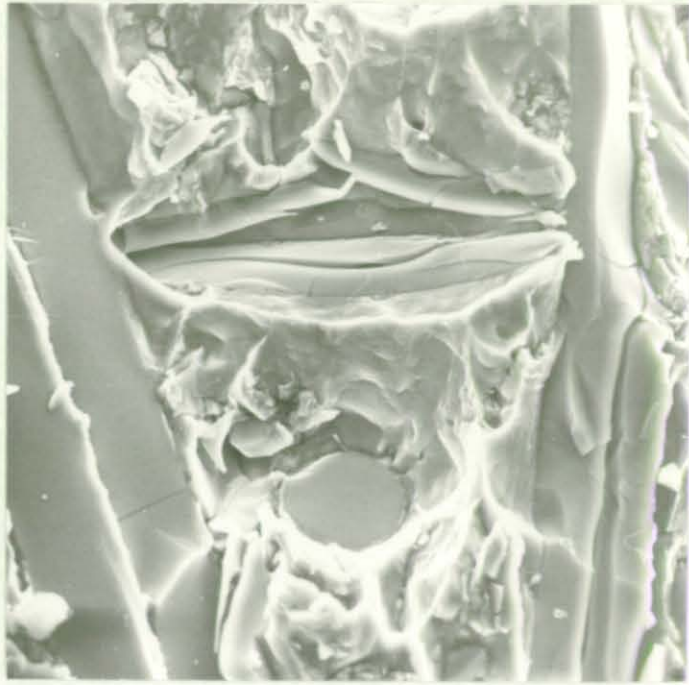
a) X600



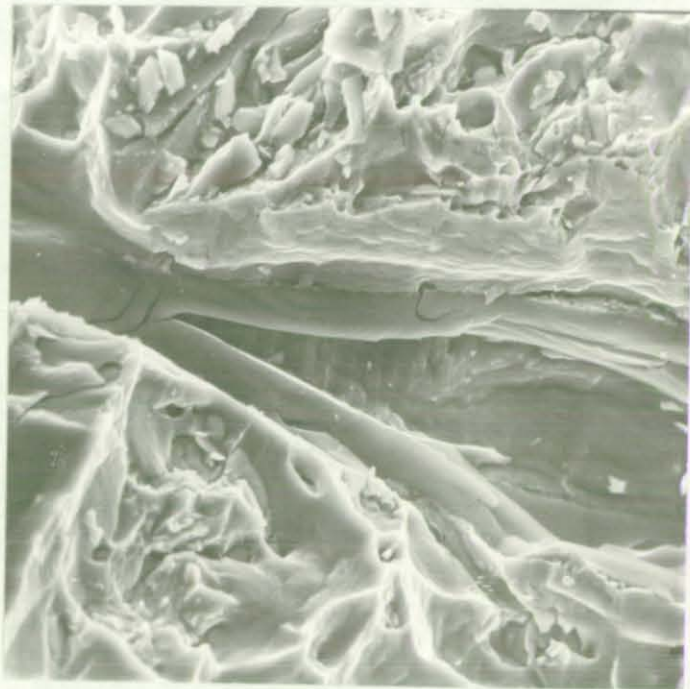
b) X600

FIGURE 75: Fracture (tension) of the squeeze cast Al-4.5 Cu matrix alloy (As-cast)

- a) Room temperature
- b) 300°C



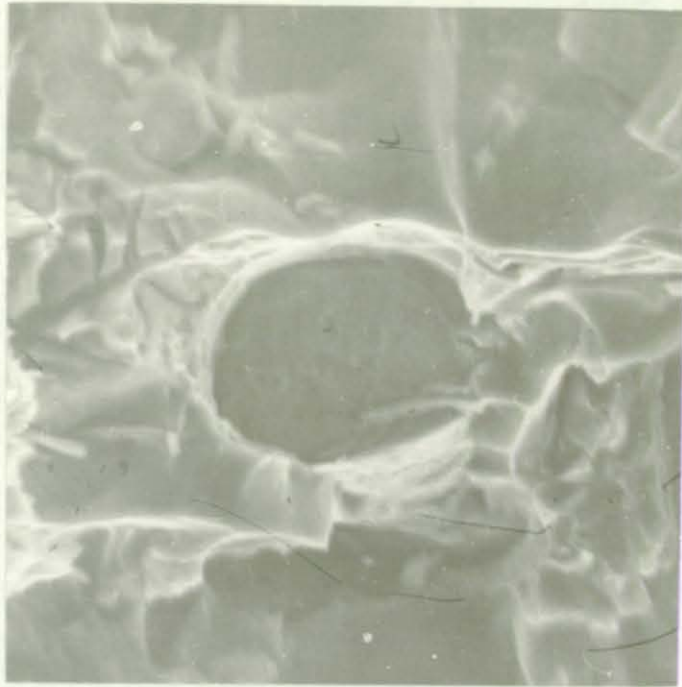
a) X1K



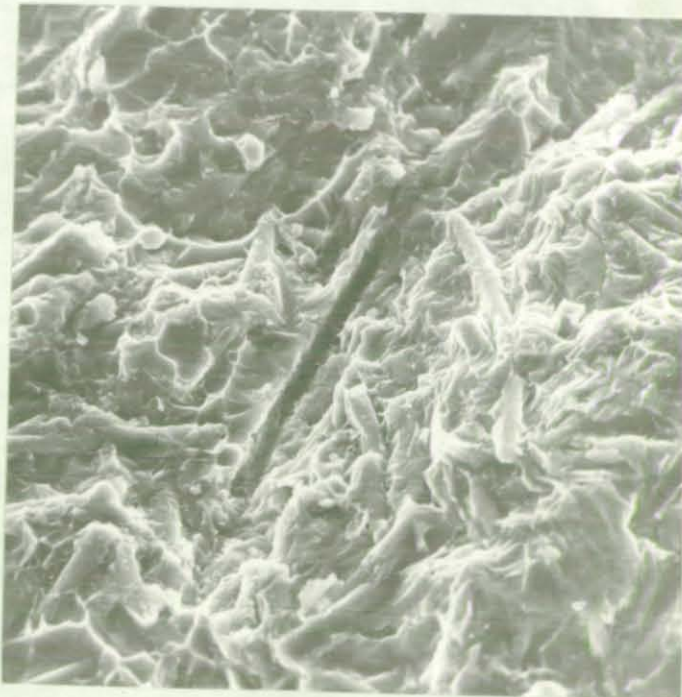
b) X900

FIGURE 76: SiC fibre degradation in Al-Cu/SiC composites of castings group IV at high fibre content

a) 8% v/v; b) 10% v/v



a) X4K



b) X1K

FIGURE 77: Fracture (tension) of Al-Mg/Al₂O₃ composite (room temperature) Castings group IV

- a) 4% v/v alumina fibre
- b) Poor bonding, 10% v/v alumina fibre

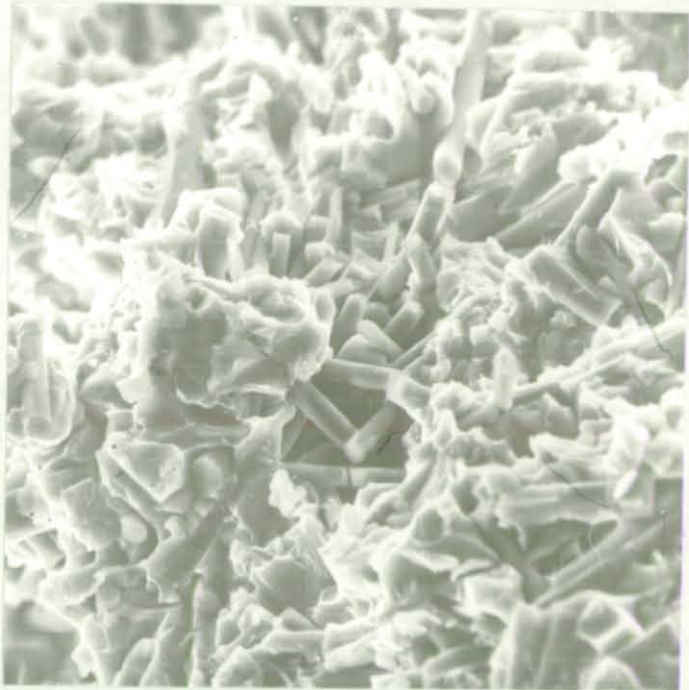
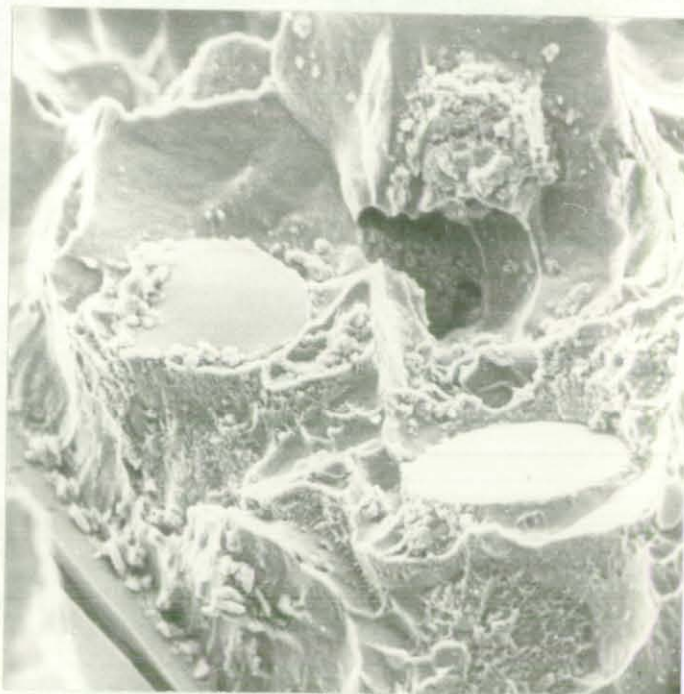


FIGURE 78: Inadequate bonding and distribution of Al₂O₃ fibre in Al-4.5 Cu matrix. Castings group III



a) X2K

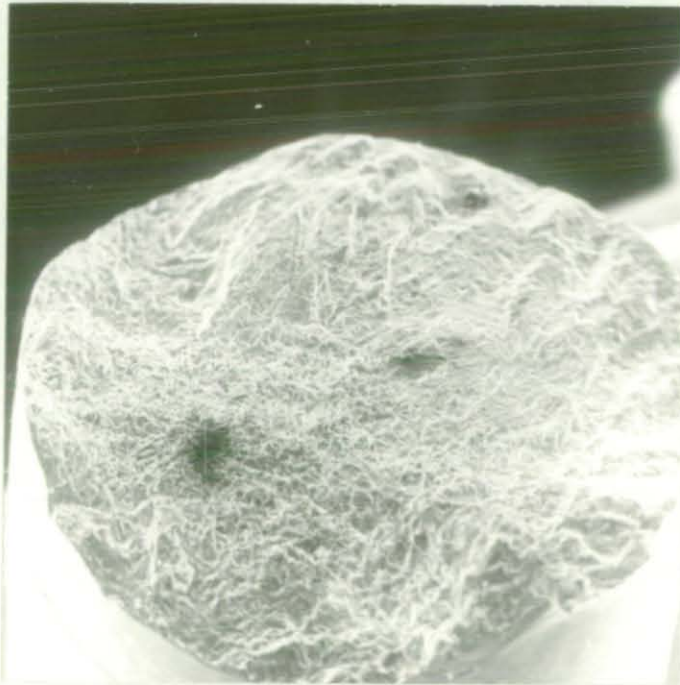


b) X2K

FIGURE 79: Fracture (tension) of the heat treated Al-4.5 Cu/SiC composite (Castings group III)



a) X26



b) X27

FIGURE 80

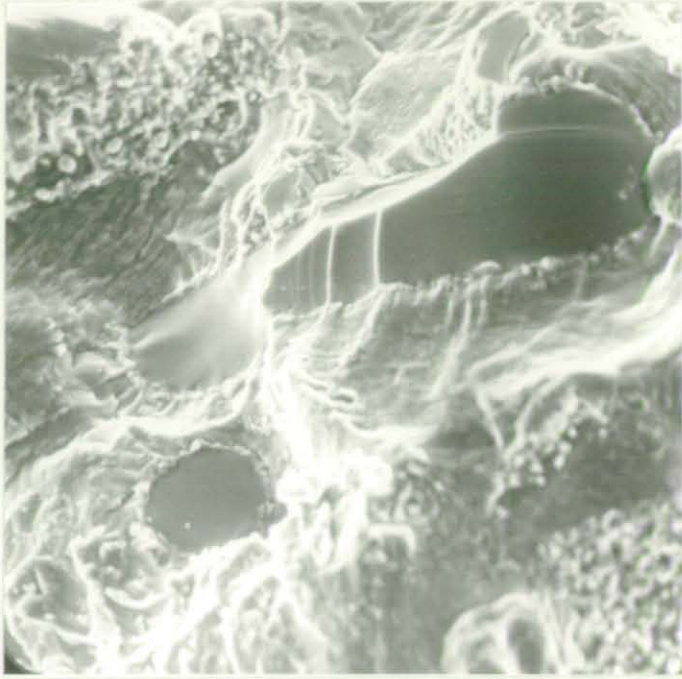
/Continued



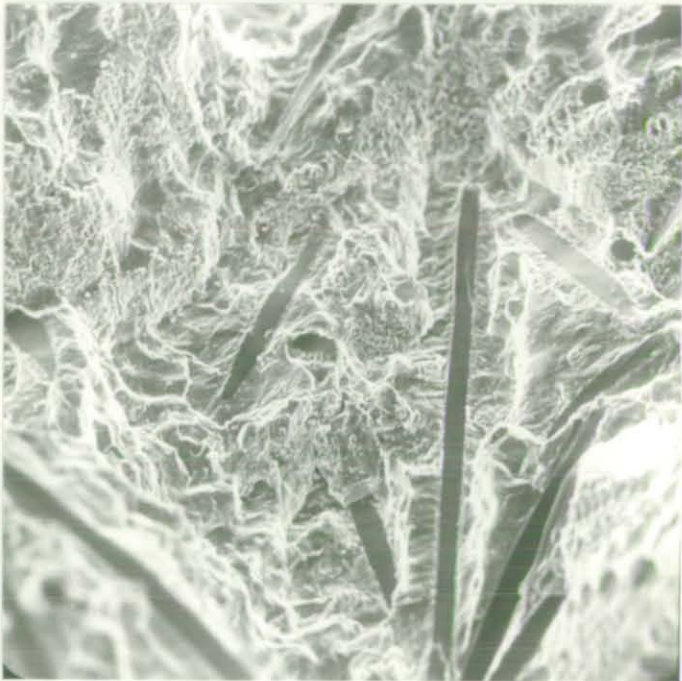
c) X26

FIGURE 80: Fatigue fracture surfaces:

- a) Gravity die cast Al-4.5 Cu matrix alloy
- b) Squeeze cast Al-4.5 Cu matrix alloy
- c) Squeeze cast Al-4.5 Cu/SiC composites,
fibre content 6% v/v



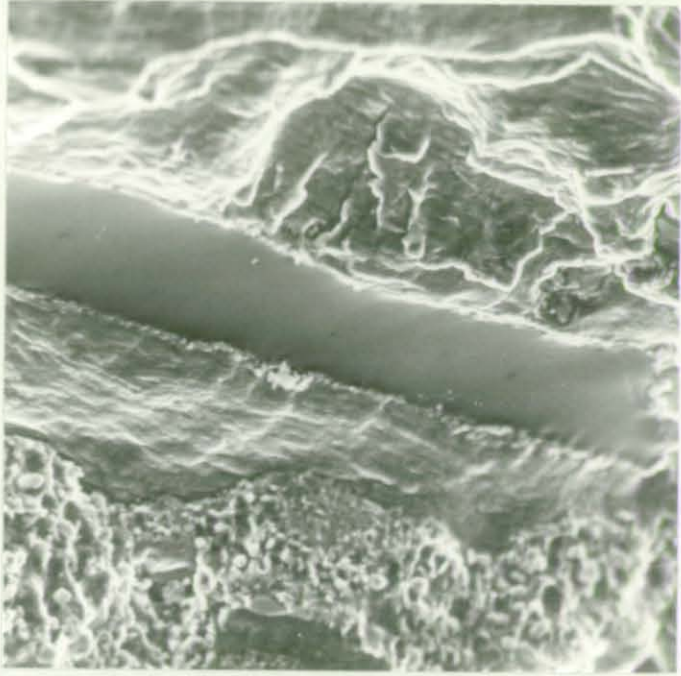
a) X1.4K



b) X280

FIGURE 81

/Continued



c) X1.4K

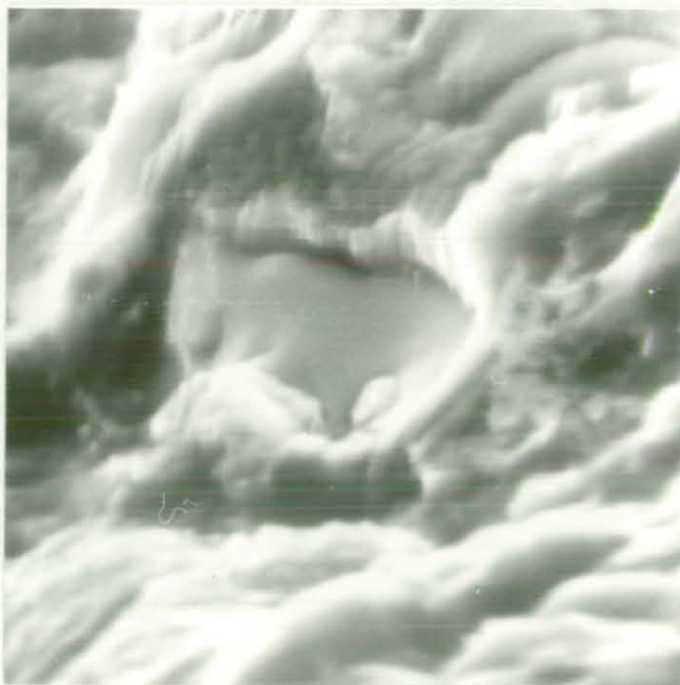
FIGURE 81: Fatigue fracture surfaces of Al-4.5 Cu/SiC composite

a) Crack arrested by a fibre, 8% v/v SiC fibre

b and c) Fractured SiC fibres



a) X6.5K



b) X12K

FIGURE 82: Fatigue fracture, Al-3.75 Mg/Al₂O₃ composite.

- a) Matrix flow around a fractured fibre
- b) Fractured fibre

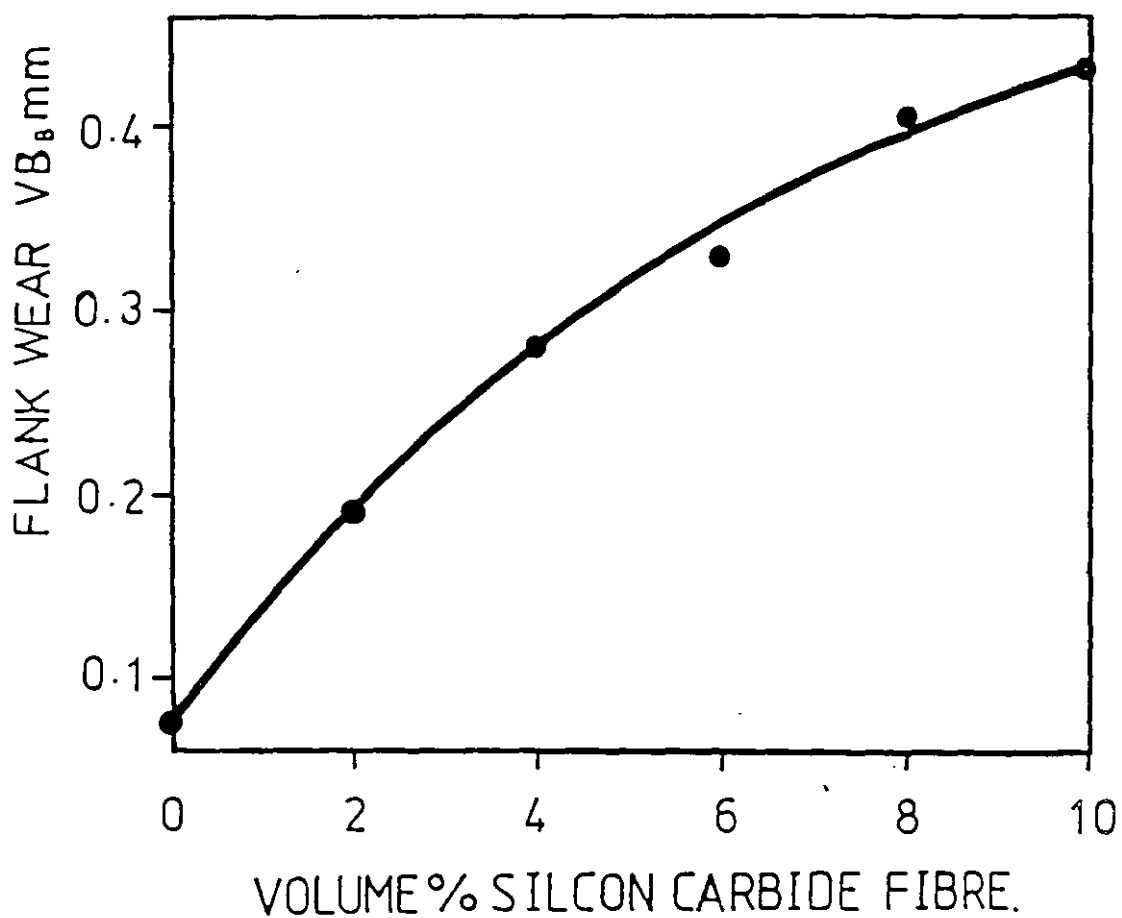


FIGURE 83: Effect of volume percent fibre on flank tool wear (Al-Cu/SiC composites). Casting group VII.

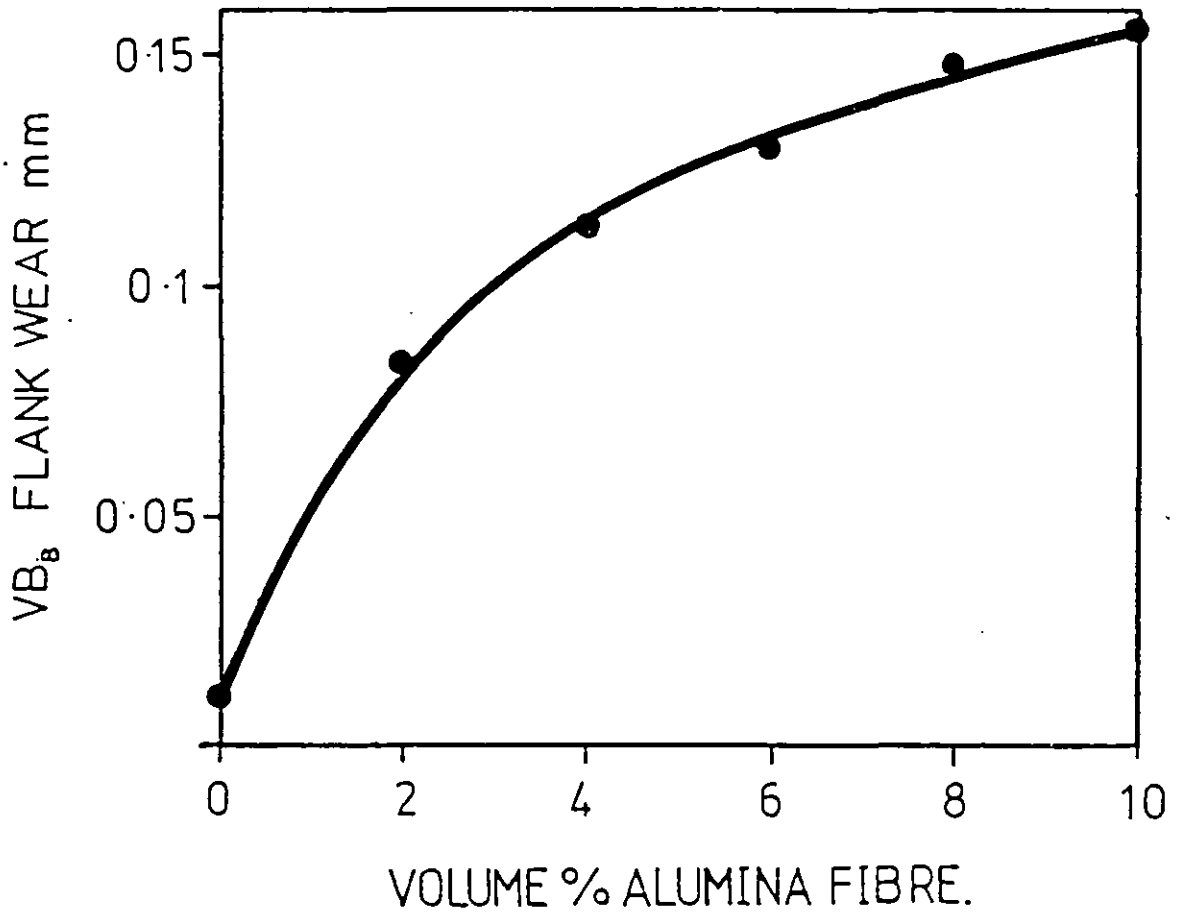


FIGURE 84: Effect of volume percent fibre on flank tool wear (Al-Mg/Al₂O₃ composites). Casting group VII.

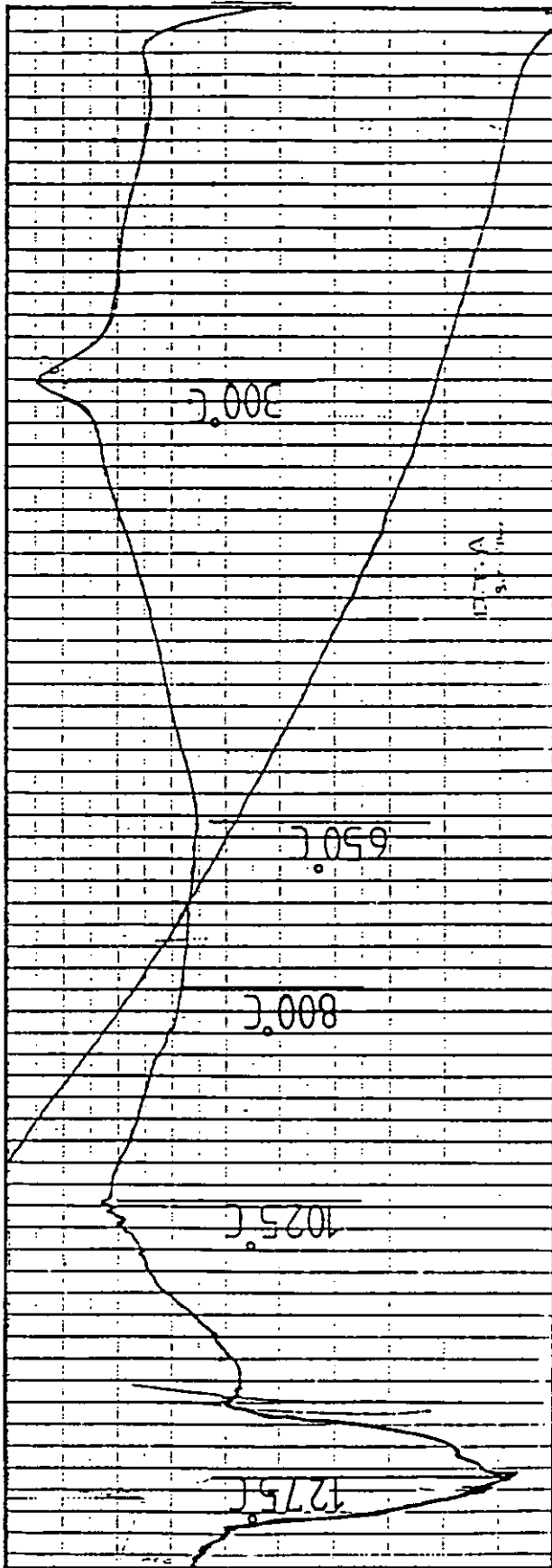


FIGURE 85: DTA Thermogram of Nicalon (R) Silicon Carbide Fibre

CHAPTER VI

DISCUSSION

CHAPTER 6DISCUSSION6.1 THE STRUCTURE AND PROPERTIES OF THE SQUEEZE CAST MATRIX ALLOYS
(Al-4.5 Cu and Al-3.75 Mg)

Squeeze casting produced pore-free fine equiaxed structures for both Al-4.5 Cu and Al-3.75 Mg matrix alloys (Figures 37 and 38). Their tensile properties were substantially higher than those produced by gravity die casting and sand casting (Figures 39, 40 and Tables A3.1 A3.2). Gravity die castings and sand castings also had larger grains and some gas porosity. The Al-4.5 Cu matrix alloy when squeeze cast under a pressure of 188 MPa had an increase of 50%, 58%, 121% and 128% in the values of UTS, 0.1 offset proof stress, percentage elongation, and percentage reduction in area respectively compared to the gravity die cast alloy (pressure 0.1 MPa). The Al-3.75 Mg matrix alloy when squeeze cast under the same pressure (188 MPa) had an increase of 38%, 57%, 131% and 138% in the values of UTS, 0.1 offset proof stress, percentage elongation and percentage reduction in area respectively compared to the gravity die cast alloy.

The grain refinement of squeeze castings is a result of two factors: rapid rate of heat extraction (cooling rate) and under-cooling. It is reported that Al-4.5 Cu alloy when poured at 700°C into a steel die (die temperature 200°C) showed a cooling rate of 5°C/S when solidified under atmospheric pressure compared to 140°C/S when solidified under 65 MPa pressure¹²⁶. Das and Chatterjee reported a similar effect of pressure on cooling rate⁵⁵. The rapid cooling is brought about by the intimate contact made between molten metal and the die surface. The applied pressure dispenses with the air gap which normally forms at the casting/die interface during the cooling of conventional die casting.

The phase equilibrium diagram depicts conditions of equilibrium (slow cooling rates) at atmospheric pressure. However, these are not the conditions encountered during squeeze casting. The application of pressure causes the melting point of most alloys to increase (Bi and Si being exceptions)¹²⁷. The majority of metals show a rise of 2-6°C for every 98 MPa of external pressure applied⁵⁹. Therefore, if the initial alloy temperature is near the liquidus line, as is the case with squeeze casting, when pressure is applied the liquidus line moves above the alloy temperature and under-cooling occurs¹²⁸.

Pressure applied during solidification, increases the solubility of gases in metal⁵⁴, so that more gas can be held in solution in the metal. Pressure can also affect gas bubble formation during solidification¹²⁹. Provided the pressure is high enough, total elimination of gas porosity is possible⁵⁴. Porosity caused by solidification shrinkage can also be eliminated by forced feeding of liquid metal into these voids. In squeeze casting, the shrinkage is fed from areas inside the casting itself and the feed metal has a shorter route to travel to those cavities making feeding more effective. Pressure may also result in the collapse of the solid, which is relatively weak near its melting point, to close the cavities, if already formed. The increased solubility of gases in the metal under pressure, the prevention of bubble formation, and the effective feed into shrinkage cavities, resulted in the observed sound structure of squeeze castings of both matrix alloys, whereas the same alloys when solidified under atmospheric pressure developed gas and shrinkage porosity. Total elimination of porosity was achieved at squeeze pressures in the range 70-188 MPa.

In addition to grain refinement and elimination of porosity, pressure applied on the liquid alloy is expected to change the relationship between the phases by altering the equilibrium temperature-composition relation, and is likely to affect the shape and distribution of the phases⁵⁴. Toshio et al¹³⁰ attributed the improvement in tensile strength of the squeeze cast Al-4.5 Cu alloy (in addition to grain refinement and

freedom from porosity) to the decrease of the intermetallic compound CuAl_2 and the disappearance of a Cu-rich layer around α -Al grain boundaries as a result of solidification under pressure. These combined effects of pressure might explain the substantial improvement in the tensile properties of both matrix alloys.

The isotropic tensile properties of the squeeze cast Al-Cu and Al-Mg alloys (Tables 9 and 10) is an expected result typical of equiaxed structures.

The reported tensile properties* (Figure 39) of the squeeze cast Al-4.5 Cu, within the range of squeeze pressure 70-138 MPa, are in agreement with reported tensile properties of the same alloy squeeze cast¹³¹. UTS values are in agreement with the findings of previous work by Das and Chatterjee⁵² (other properties were not reported). Williams and Fisher⁵⁶, reported tensile properties of the squeeze cast LM5 (Al-3.5 Mg) similar to those produced in squeeze casting of Al-3.75 Mg cast under pressure of 140 MPa, however, the exact composition of their alloy (LM5) and the squeeze casting conditions are not clear.

The improvement in tensile properties, of both matrix alloys, produced by squeeze casting, is significant when the alloys are to be reinforced with short fibre where the matrix alloy is more responsible for the load transfer between fibres than it is in a continuous fibre composite and it contributes more to the final strength of the composites. The high ductility of the squeeze cast matrix alloys is essential to: accommodate expansion differences between the two phases (matrix and fibre); transfer load to fibre; and reduce stress concentration.

Squeeze castings, of both matrix alloys, had improved fatigue life (Table 14) compared with those for sand and gravity die castings.

* Tensile properties include UTS, 0.1%PS and percentage elongation and reduction in area.

The fatigue life of the squeeze cast (140 MPa) Al-Cu matrix alloy is 75% and 30% higher than that for the sand and gravity die cast alloy. The increase in fatigue life of the squeeze cast Al-Mg alloy was lower (30% and 7 % respectively).

Fatigue properties are frequently correlated with tensile strength. Although these correlations are only approximations and hold only for the restricted condition of smooth, polished specimens which have been tested under zero mean stress at room temperature, they still indicate a relation between tensile strength and fatigue life. High ductility of squeeze casting is expected to make fatigue crack initiation and propagation more difficult. The absence of porosity, as a possible site for crack initiation, and microstructural refinement are also possible reasons for improved fatigue life of squeeze castings. Improvement of fatigue life of aluminium alloys by squeeze casting has been reported by several researchers^{45,56,132}, however, the mechanism by which squeeze casting improves fatigue life is not clear yet.

6.2 HEAT TREATMENT OF THE SQUEEZE CAST Al-4.5 Cu ALLOY

The experimental results (Table 5) indicate that solution treatment of the squeeze cast Al-4.5 Cu alloy at 545°C for 2 hours followed by precipitation treatment at 180°C for 6 hours produced maximum hardness. Solution treatment for longer than 2 hours did not produce any further increase in hardness.

The British Standard ('L' series) recommends solution treatment for 12-16 hours at 525-545°C for the gravity die cast equivalent 2L92 alloy (Al-4.5 Cu) followed by precipitation treatment for 12-14 hours at 120-170°C. The shorter time of solution treatment of the squeeze cast Al-4.5 Cu alloy, compared with those recommended for the gravity die cast equivalent alloy can be explained by the fact that due to rapid

solidification under pressure, a higher percentage of copper was kept in solution. In addition, with the refinement of structure, and less CuAl_2 precipitates¹³⁰, less copper needed to diffuse and for shorter distances. This might have resulted in the shorter time of solution treatment required.

The maximum hardness obtained of 127 VHN compared with 55 VHN for the as-cast specimens, could suggest that precipitation treatment, at the temperature, for 6 hours (consequent to solution treatment) produced hardness near the maximum hardness to be expected from such heat treatment. Nevertheless, it is still necessary to investigate the effect of longer precipitation treatment. The rapid solidification, induced by squeeze casting, is not expected to influence the time of precipitation treatment.

6.3 WETTING OF FIBRES

I. Al-Cu/SiC and Al-Mg/ Al_2O_3 systems:

It is believed that Cu improves the wetting characteristics of silicon carbide by molten aluminium^{79,118-121}. Similarly magnesium is a strong wetting agent and improves the wetting of alumina by molten aluminium^{79,82,121}. However, there was no adequate wetting between the as-received fibres (SiC and Al_2O_3) and the corresponding molten alloy even at temperatures up to 850°C. Poor wetting was indicated by partial rejection and poor dispersion of fibre. Surface contamination of fibre was believed to be responsible for the observed poor wetting. Wetting involves interaction forces on an atomic scale. Such interaction forces are quite short-range so that they do not develop until the atoms of the constituents approach within a few atoms diameter of each other. Contamination acts as a barrier and keeps atoms of constituents apart which impairs wetting.

SEM examinations of the SiC fibres indicated the presence of some foreign substances (contaminations) on the surface of the as-received fibre (Figure 41). These contaminations were not observed (SEM) on the surface of the heat treated (900°C for 2 hours, see 3.5.1.IIa) fibre (Figure 42a). Fibres (SiC) subjected to this treatment were fully accepted and dispersed in the molten Al-4.5 Cu alloy which is an indication of adequate wetting enhanced by the removal of surface contamination on heating. SiC fibre heated at lower temperatures, or for shorter times, were partially rejected indicating the necessity for heating fibres at not lower than 900°C for a minimum of 2 hours (3.2.1.I) to achieve their full acceptance.

Alumina fibre treated by either pickling in a diluted hydrochloric acid or heating at 900°C for 2 hours (3.5.1.IIb) were well wetted and accepted by the molten Al-3.75 Mg alloy. However, as a precaution only the first method (pickling) was used to produce composites of Al-Mg/Al₂O₃ because of the adverse effect of heat treatment on the strength of SiC fibre (5.12.1). Although no surface contamination of Al₂O₃ fibre was observed using the SEM technique, the whiter colour of these fibres observed after pickling indicated the removal of surface contamination which was not resolved by the SEM technique. Unlike the as-received fibres the pickled fibres were more easily wetted by water*. This is another indication of a change in the surface characteristics of these fibres when pickled in the acid solution.

In either case, no change in the crystal structure of fibre materials (SiC or Al₂O₃) was expected as a result of the pre-treatment (heating or pickling). Therefore, the improved wetting between the treated fibres and the corresponding molten alloy was possibly due to the observed removal of surface contamination.

* Alcohol-water solution was used to separate the as-received Al₂O₃ fibre as a first stage treatment (3.5.1.IIb.1), alcohol was found to improve the wetting of as-received fibre by water. Alcohol addition was not necessary when fibres were pickled in diluted hydrochloric acid.

From the foregoing discussion, it is evident that in both cases (Al-Cu/SiC and Al-Mg/Al₂O₃) fibres were well wetted and dispersed in the molten alloys provided they were pre-treated to free their surfaces from contamination. Therefore it is not necessary to use the more expensive coated fibre or employ^a special wetting agent. Commercial alloys of aluminium containing elements such as Cu and Mg provide adequate wetting for good interface bonds to be developed.

II. Al-Cu/Al₂O₃:

This composite system was only investigated in the early stages (casting group III). Provided that the fibres were heat treated (900°C for 2 hours, 3.5.1.IIb.1) only a small percentage of fibre was rejected (~95% acceptance), however fibres were not well separated (Figure A4.4). Possibly because the melt failed to flow into the pores of the fibre clusters to displace the gas phase and aid fibre dispersion.

In addition weak interface bonding was observed in this composite system (Figure 78). Similarly treated fibres were well wetted and dispersed in a melt of Al-Mg alloy (Figures 46,47). This could indicate that Mg is more effective than Cu to induce wetting of Al₂O₃ fibre by molten aluminium.

6.4 STRUCTURE OF THE SQUEEZE CAST COMPOSITES (Al-Cu/SiC AND Al-Mg/Al₂O₃)

Composites are structure sensitive materials, structural defects could significantly affect their properties. In general, defects could be related to either the matrix, the fibre or the interface. These will be discussed separately.

I. The Matrix

The squeeze cast composites (Al-Cu/SiC and Al-Mg/Al₂O₃) had a fine equiaxed structure similar to those observed for the squeeze cast matrix alloys (see 6.1). Equiaxed structures produced matrices of isotropic tensile properties (see Tables 8-10), which are essential to produce the observed isotropic tensile properties of the Al-Cu/SiC and Al-Mg/Al₂O₃ composites (see Tables 8-10).

Squeeze cast composites were free from porosity. Composites are more sensitive to porosity than other structural materials. Porosity can drastically lower the elastic modulus of the composites. Cohen et al¹³³ used the following formula to express the modulus E_v in terms of void content C_v :

$$E_v = E_0 (1 - C_v^{2/3})$$

at 10% v/v porosity, E_v would be 0.78 E_0 .

Some inclusions (oxide-like) were observed in the composite structures, particularly in those with an Al-Mg matrix. Although a protective cover of nitrogen was used during the production stages, total elimination of oxidation was not expected (this will be further discussed in 6.5). However, the level of inclusion contents was low, inclusions were only observed in a few fractured specimens. Specimens containing inclusions, revealed at fracture, were discarded.

II. The Fibre

Fibres, as reinforcement, were selected for their strength. Therefore it is essential that they retain their strength when combined with the matrix alloy. Surface damage and severe reaction with the matrix

during the production stages, would affect their strength. Surface examination (SEM) of the processed fibres (SiC and Al_2O_3) showed no surface damage, whereas the relatively rough surface of fibres subsequently extracted from composites (Figures 42 and 43) is an indication of a possible reaction between the fibres and the corresponding molten alloy during production. Chemical reaction was found to be necessary so that a strong interface bonding can be developed in order to allow efficient stress transfer to the fibres. However, this reaction must be controlled to prevent fibre deterioration. This will be discussed further in 6.6.

Fibre breakage was kept to a minimum during the processing stages. Fibre breakage was estimated to be less than 5% in total at the final processing stage. (See 5.5 and Tables 6 and 7). In order to achieve this low level of fibre breakage, as well as good separation of fibre, it is essential that the fibre separation device be well maintained and accurately assembled. Of particular importance is the condition of the wire brushes and their positioning in relation to each other. (See 3.3.1.III - final design).

The observed (microscopic) uniform distribution and random orientation (3D) of fibres is an essential requirement of sound composites of isotropic properties. (See Figures 44-47 and Figures A4.1-3). Random orientation of fibres (SiC and Al_2O_3) was confirmed by the observed 'isotropic' tensile properties of both composite systems (Al-Cu/SiC and Al-Mg/ Al_2O_3) when tested (tensile) in directions parallel and perpendicular to the punch movement, as shown in Tables 9 and 10. (Matrices are of isotropic tensile properties). Punch movements on squeeze casting, to compensate for metal shrinkage on solidification, possibly caused slight alignment of the fibres in the direction perpendicular to the punch movement, which resulted in composites being slightly stronger in that direction. However, the difference in strength is insignificant (Tables 9 and 10) and the composites can be considered to have isotropic tensile properties.

III. Interface

The most important and also the most difficult problem associated with the fabrication of composite materials, is the production of good interfacial bonding between the fibres and the matrix. It should be achieved however, without detrimental chemical attack or reaction at their interface.

The transfer of load, which is the main objective of the reinforcement of weak matrices by the high strength and high modulus fibre, depends first of all on good bonding. Without bonding, there is no transfer of load to the fibre and hence no reinforcement. Therefore a strong bond, preferably of a chemical nature, is necessary from the standpoint of maintaining the integrity and stability of the interface under the work environmental conditions. If only mechanical bonding is in existence at the interface, premature failure of the interfacial bonds is possible, particularly during use at elevated temperatures.

Pretreatment of fibres (SiC and Al_2O_3) provided good wetting between the fibres and the molten matrix alloys which resulted in the intimate interfacial contact between the two phases, observed throughout this investigation, with the exception of the very first castings of Al-Cu/ Al_2O_3 composite in which poor wetting was observed.

Providing that the fibres (SiC and Al_2O_3) were exposed to the respective molten matrix alloy for sufficient time*, at the temperature, strong interfacial bonds were developed as indicated by the fracture of the fibres and the absence of fibre pull-out even at test (tensile) temperatures up to 300°C as shown in Figures 70-74. Fibres, exposed to the melt for a shorter time exhibited weak bonding which resulted in fibre pull-out indicating the necessity for a stronger chemical bond

* ~18 minutes at 760°C for Al-4.5 Cu/SiC and ~15 minutes at 730-740°C for Al-3.75 Mg/ Al_2O_3 composite system. See 5.10.1.1.

and the inadequacy of mechanical bonding, particularly when fibres were positioned normal to the tensile load. Fibre deterioration resulted when fibres were exposed to the melt for a long time due to severe chemical attack, see Figures 67-69. Further discussion on this subject will follow in 6.6.

Strong interfacial bonding was also observed in the composites fractured by fatigue as shown in Figures 81 and 82. EPMA analysis (line scanning), of the Al-Cu/SiC interface, consistently indicated the presence of a thin Cu-rich layer around the SiC fibre in the as-cast Al-4.5 Cu/SiC composite, Figures 49 and 50. This layer was not resolved by the scattered electron image (Figures 49,50). In addition to the observed Cu-rich layer around the fibre, most fibres appeared to be associated with the typical α -Al/CuAl₂ eutectic phase which was a common feature of the structure of the Al-4.5 Cu matrix alloy, see Figure 48. Das and Chatterjee⁵², in earlier work, observed the tendency of SiC whiskers to be associated with the CuAl₂ phase at the grain boundaries, the whiskers seemed to migrate to the grain boundaries which were the last areas to solidify. However, the movement of the much larger fibres used in the present investigation would be restricted. G C Levi¹¹¹ reported that Cu-rich products caused by chemical reaction on the fibre matrix (Al-Cu/Al₂O₃) interface were observed around the fibre. Fukunaga et al¹³⁴ reported the presence of a Cu-rich layer of irregular form around SiC fibre (Al-4 Cu/SiC) which was of the Al-CuAl₂ eutectic composition when a bundle of pre-heated fibre (550°C) was infiltrated, under pressure (49 MPa), by a melt of Al-4 Cu alloy (700°C). They suggested a formation process of the eutectic phase around the fibre as shown in Figure 86, by which the α -Al phase crystallisation occurs on the fibre surface during infiltration of the molten metal into a fibre bundle, since the temperature of the fibre is lower than that of the molten metal. In the next stage, the solid phase grows under an increasing pressure and finally the liquid phase becomes of eutectic composition, a relative movement of the primary phase to the fibre takes place due to the solidification shrinkage, so that the liquid phase (eutectic) is

squeezed into the small gaps between the fibres and the solid phase. The combined effect of the pressure and solidification shrinkage produces a eutectic of an irregularly formed structure surrounding the fibres.

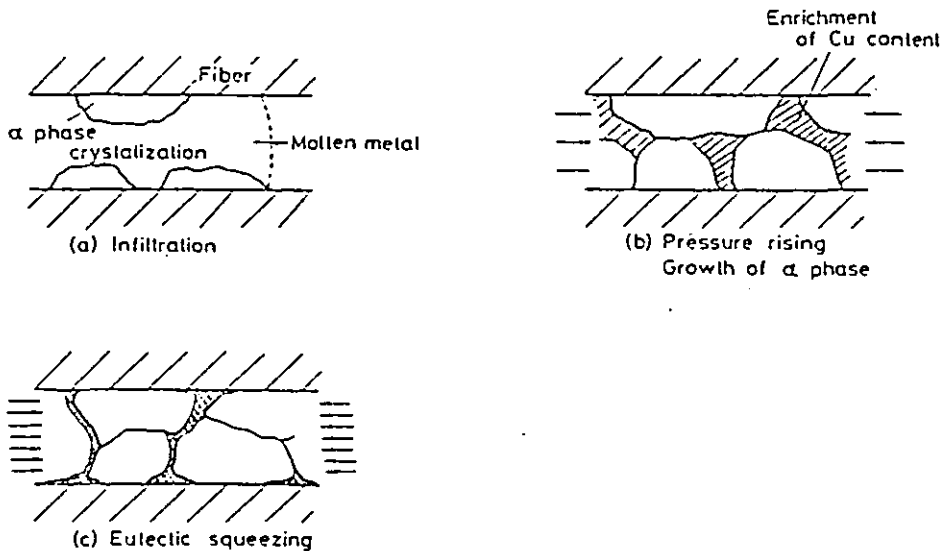


FIGURE 86: Formation model of eutectic by squeeze casting (ref 134)

The proposed formation model (Fukunaga) of eutectic around the fibre, might explain the formation of the eutectic phase at some fibre surfaces, using the authors' experimental conditions. However, if α -Al phase crystallisation occurs first on the surface of fibre, taking into account that α -Al is the main constituent of the alloy, it would be difficult to explain the presence of the thin Cu-rich layer at the entire surface of all fibres, without exception.

In this investigation, distinction was made between a thin layer of Cu-rich phase, which seemed to coat the entire surface of all fibres, and the α -Al/CuAl₂ eutectic which is present at the surface of most of the fibres as well as in the bulk of the matrix. The eutectic phase does not usually cover the whole surface of the fibres, see Figures 48-50.

The width of the observed Cu-rich thin layer surrounding the fibres was too small ($\sim <1 \mu\text{m}$) to be accurately analysed using the EPMA technique.

According to Warren and Andersson¹²¹, Cu at its melting point did not develop any reaction with silicon carbide even after 3 hours of contact. Therefore it is unlikely that the observed Cu-rich layer around the fibre was a product of reaction (chemical) between Cu and SiC. Fibre (SiC) in the melt, could act as heterogeneous nuclei. The essential properties of such nucleating particles are not well defined, however it is accepted that wetting and crystalline similarity are important requirements¹³⁵. Heterogeneous particles should be wetted, the smaller the contact angle, the greater the tendency of the liquid metal to wet the surface of the heterogeneous particle and the greater will be the potential of this particle to initiate crystallisation. A certain measure of crystalline similarity between the liquid metal and the heterogeneous particle is necessary for effective nucleation. The difference in the basic lattice unit size of the two crystal systems should not be more than 15% to 20% for the particles to act as heterogeneous nuclei¹³⁵.

SiC satisfies both these requirements* for acting as heterogeneous nuclei in the Al-Cu melt. However, if fibres were to initiate nucleation, α -Al would be expected to crystallise first at the fibre surfaces which is in contradiction with the observed presence of a Cu-rich layer at the fibre surfaces. Therefore Cu concentration at the fibre surfaces must have formed by another mechanism.

* SiC is wetted by the molten Al-4.5 Cu alloy. SiC, Al and Cu have a face-centred cubic lattice with lattice unit size of 4.36¹³⁶, 4.04¹³⁷ and 3.608 Å¹³⁷ respectively.

Although SiC (β) fibre and aluminium have a similar specific heat capacity of 52.54¹³⁶ (at 200°C) and 53.26¹³⁸ (at 100°C) J/kg.K respectively, SiC fibre has a thermal conductivity of 0.255 W/cm°C¹³⁶ (at 200°C) compared with 2.11 W/cm°C¹³⁶ (at 200°C) for aluminium. Therefore it is possible that during solidification, SiC fibres retain their heat longer and then dissipate heat to the cooler 'melt' during solidification, and in effect they create a local hot zone around them, so that solidification of the Cu-enriched* liquid (around the fibre) ends at the surface of fibre, which would be expected to result in the observed Cu-rich thin layer at the fibre surface. In fact, the formation of a hot zone around the fibre could be responsible for the fibre not acting as heterogeneous nuclei. According to the proposed mechanism, providing that an alloy is saturated with a solute, solute concentration around the fibres would be expected under similar experimental conditions. Fibres of significantly higher heat capacity, compared with that for the alloy (at the same temperature), would give rise to a similar effect. However, element concentration could form around the fibres by other mechanisms as well, such as a chemical reaction between the fibres and certain elements present in the molten alloy. The solute (or solute-rich region) concentrated around the fibres and formed by the proposed mechanism, should wet the fibre surface in order to achieve a strong interfacial bond.

The association of fibres with the α -Al/CuAl₂ eutectic (not the Cu-rich layer, see Figure 48) could be a result of liquid metal (eutectic) feed into solidification shrinkage around the fibre, when close enough, under pressure.

The brittle Al-Cu eutectic at the fibre surface is not expected to initiate cracks on loading because the fracture strain of the Al-Cu eutectic ($\sim 0.3\%$)¹³⁴ is higher than the fracture strain of the SiC fibres

* Cu-enriched due to normal solute rejection into the remaining liquid.

(ϵ = tensile strength (300 kg/mm²)/elastic modulus (20 x 10³ kg/mm²) x 100 = 0.15%). A brittle interface would initiate a crack on loading only when its fracture strain is lower than that for the fibre¹³⁹.

On heat treatment both the eutectic phase and the Cu-rich layer around the SiC fibre were diffused into the matrix, Figure 51. This indicated that this layer (Cu-rich) was not stable at the heat treatment temperature (solution treatment at 545°C for 2 hours). A layer formed by the suggested mechanism would diffuse into the matrix on heat treatment.

EPMA analysis of the interface region of the Al-Mg/Al₂O₃ composite showed no distinctive variation of the elements (Al, Mg) distribution or concentration in that region, when the fibres were exposed to the melt (Al-3.75 Mg at 730-740°C) for up to 36 minutes. C G Levi et al¹¹¹, reported the presence of Mg-rich layer (reaction product) surrounding alumina fibres incorporated in a semi-solid slurry of Al-Mg alloy. The composite was solidified, then remelted and cast. However, in their experiments fibres were exposed to the alloy for a prolonged time. For liquid metal with a composition of Al-4.3 Mg*, fibres were exposed to the liquid metal for 145 minutes. Such a long exposure time of the fibres to the melt could have produced a severe reaction, resulting in the concentration of a reaction product at the interface (Mg-rich), whereas at the shorter exposure time used in the present investigation, Mg concentration at the fibre/matrix interface was not observed. Taking into account the variation of Mg concentration in the matrix itself (Figure 52), unless a significant concentration of Mg is present at the interface, it would be difficult to detect, particularly for elements of low atomic number such as Mg. The formation of a significant concentration of Mg around the fibre, by the proposed mechanism, is not expected at 3.75% Mg content (by

* This composition of liquid corresponds to the nominal alloy composition of Al-2 Mg, where liquid was enriched in Mg due to the presence of solid α -Al.

weight) in aluminium due to the relatively high solubility of Mg in Al, compared with the solubility of Cu in Al, see Figure 87. This could occur at higher Mg content in the alloy.

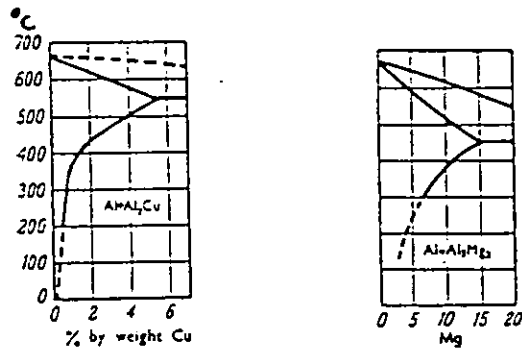


FIGURE 87: Equilibrium diagram of Al-Mg and Al-Cu alloys.
Ref. 138

6.5 METHOD OF COMPOSITE PRODUCTION

During the initial attempts to successfully produce composites of sound quality, certain difficulties were met such as wetting of fibres (SiC and Al₂O₃); fibre separation and dispersion; and melt oxidation etc. These difficulties were discussed in 3.2.1-3.3.2.

6.5.1 Viability of the Method of Production

The viability of the method of composite production used in the present investigation is best judged by the quality of the product (composites) and its cost effectiveness.

It was demonstrated that the composites produced were of sound quality, see 6.4. Composite components retained their integrity when combined together. The good wetting of pretreated fibres by the melt developed

a strong interfacial bonding. Fibres (SiC and Al_2O_3) were uniformly distributed and oriented in the desired random manner (3D). Squeeze casting provided sound matrices (Al-Cu and Al-Mg) of isotropic tensile properties with improved strengths and ductility, see 6.1.

By employing this method of composite production, material cost was kept to a minimum because there was no need to use the more expensive coated fibres or use wetting agents in order to achieve fibre wetting. Commercial alloys containing elements such as Mg and Cu were used. Material cost was further minimized by the full acceptance of fibres in the molten alloy and the high material yield which is achieved by squeeze casting.

The ease and simplicity of processing the material, in addition to the good surface finish and dimensional reproducibility which can be achieved by squeeze casting, results in near net shape/size with little or no machining required with consequent conserving of processing costs. There is no need for expensive equipment for producing the composite castings by this method, which is a further contribution to minimise the final cost of the composites produced.

In addition to the sound quality of the composites produced and the cost effectiveness of the method used for composite production, a wide range of product sizes and shapes can be made by this method.

6.5.2 Volume Content of Fibre

In the present investigation, the maximum volume content of fibres (SiC or Al_2O_3) in the composites was 10%. At higher volume contents of fibre, the 'liquid' composites became viscous and were impractical to squeeze cast because they could not be poured into the die cavity. The fibres formed a skeleton in which liquid metal was entrapped resulting in the restriction of its flow. In addition, mechanically stirring a viscous composite could result in undesirable fibre breakage.

It is believed that higher volume percentages of fibre (with 3D random orientation) could be incorporated in a matrix providing that the fibres are of smaller aspect ratio (l/d). However, aspect ratio should not be lower than that required for the fibres to be loaded up to their fracture strength. Fibre separation was a major difficulty in producing composites with uniformly distributed fibres. Although this difficulty was overcome, as discussed in 3.2.1.II, fibres of smaller aspect ratio could be more readily separated due to fewer mechanical interlocks between fibres. This could make fibre separation easier or possibly unnecessary which would be beneficial in terms of reduced cost. This argument holds only where mechanical interlock is the dominant mechanism of cluster formation with chopped fibre.

6.5.3 Sources of Inclusion

A positive pressure of nitrogen gas cover was maintained inside the furnace in which the melt was held during fabrication of the liquid composite, see 3.5.2. A complete elimination of melt oxidation could not be expected and, therefore, the objective was to minimise oxidation as far as possible and indeed the level of oxide inclusion content in the cast composites was very low.

The vortex in the melt, during the production of the composite, continuously disrupted the protective aluminium oxide film at the melt surface and exposed fresh molten metal to the atmosphere inside the furnace which could not have been completely oxygen-free.

Oxygen could be present due to incomplete replacement of air by nitrogen at the beginning of liquid composite fabrication. In addition, a flame test was used to ensure the existence of a positive pressure of nitrogen inside the furnace by observing outflow of gas at the joint where a gas leak would be expected. However, due to the temperature gradient inside the furnace (gas temperature) a differential

pressure could have been developed (chimney effect) inside the furnace. Although a positive pressure was observed at the top of the furnace, where the joints are, a negative pressure could have existed at the bottom of the furnace and air could have penetrated the refractory lining at that area into the furnace.

A further improvement in the efficiency of the inert gas protective cover could be made by using a gas-tight furnace with provision for inert gas flushing, preferably at the lower part of the furnace. Additional gas flow to assist the gas flow provided through the fibre separation device to maintain a positive pressure of inert gas inside the furnace could also be beneficial. The gas flow through the fibre separation device cannot be replaced or increased (at composite fabrication) because, in addition to providing gas cover, it has other functions which were found to be necessary such as: directing separated fibre onto the melt surface; detaching fibres carried over by the wire brushes; and cooling the device. At a higher gas flow level (5-6 litre/min), fibres were observed to be carried over out of the crucible causing the loss of expensive fibre.

6.5.4 Reaction of the Al-3.75 Mg (LM5) Molten Alloy with Atmosphere

As detailed in 3.8.2, the Al-Mg molten alloy developed some reaction products at the melt surface and the crucible (Mullite grade D/A) periphery when held at 760°C under a nitrogen cover. The reaction products had a cauliflower-like appearance and were covered with what appeared to be a white, non-metallic compound. The same alloy when held under similar conditions in a graphite crucible developed reaction products which accumulated at the melt surface, were different in appearance (see Figure 29) and were present to a reduced extent. By contrast, a normal, protective, oxide-like film was produced at the surface of a melt held in a Mullite crucible when the nitrogen cover was replaced by air introduced at the same rate as the nitrogen (6 litre/min).

The reaction of the melt under a nitrogen cover was found to be temperature and time dependent and the reaction products were of a non-protective nature. At 780°C the reaction products started to accumulate at a high rate within 5-7 minutes, compared to 15 minutes at 760°C, and 40 minutes at 740°C. At 740°C only small amounts of reaction products were detected even after 40 minutes. The following samples were analysed at A.E. Developments, and a report was provided which is included in Appendix II.

Sample 1 - Reaction product skimmed from a melt left under a dry, oxygen-free nitrogen cover for 20 minutes at 760°C in a Mullite crucible

Sample 2 - Reaction products skimmed from a melt kept under the same conditions as sample 1, but in a graphite crucible

Sample 3 - Reaction products skimmed from a melt kept under the same conditions as sample 1, but to which air was introduced at the same rate as the nitrogen in sample 1 (6 litres/minute).

The following conclusions were made:

1. Sample 1 consists of a non-metallic compound, mainly magnesia (71%) and alumina (25%). Oxygen content was three times higher than that for samples 2 and 3. Nitrogen content was 4.5% (weight) compared with 2.5% for samples 2 and 3.
2. Sample 1 contains elements such as Zn (4%), and Cu (1.6%) which are not present, at that level, in the alloy, see Table A2.1. (Table 1, Appendix 2).

A thorough investigation into the thermodynamics of the reaction of the molten (Al-Mg) alloy under different conditions is outside the scope of the present investigation. The observations made and the

analysis of the reaction products could suggest the following:

- a) Under a nitrogen cover (reduced partial pressure of oxygen) the reaction (oxidation mainly) appears to be shifted in favour of the formation of reaction products of a non-protective nature.
- b) Reaction, under nitrogen cover, appears to occur in two stages: an initiation stage, during which the rate of reaction is low (no accumulation of significant reaction product was visually observed); and a propagation stage, in which a rapid accumulation of reaction products occurs. The duration of the first stage and the rate of reaction in the second stage are dependent on the melt temperature. The higher the melt temperature, the sooner the second stage is initiated.

During fabrication of liquid composites with Al-3.75 Mg matrix, the melt temperature was kept below 740°C, usually >730, <740°C, and the total holding time of the melt, at that temperature, was always kept below 40 minutes.

6.6 EFFECT OF THE TIME OF CONTACT BETWEEN THE FIBRE AND THE MOLTEN MATRIX ON THE TENSILE PROPERTIES OF THE Al-Cu/SiC AND Al-Mg/Al₂O₃ COMPOSITES

The vital importance of the achievement of a strong interfacial bond between the fibre and the matrix was discussed in 6.4.III. A strong bond would make load transfer to the fibres possible which is the main objective of the reinforcement of a weak matrix by a strong fibre. In theory, for efficient load transfer from a matrix onto a fibre loaded parallel to its axis, the interfacial shear strength (τ) should be (equation 11, see 2.3.2):

$$\tau \geq \frac{d}{2l} \cdot \sigma_{f.u}$$

Taking the Al-Cu/SiC system as an example, SiC fibre has:

$$d = 10-15 \mu\text{m} \text{ (average } 12.5 \mu\text{m)}$$

$$l = 3 \text{ mm}$$

$$\sigma_{f.u} = 250-300 \text{ kg/mm}^2 \text{ (average } 275 \text{ kg/mm}^2)$$

(See 3.1.1, Table 2)

Therefore $\tau = 0.57 \text{ kg/mm}^2 \text{ (5.6 MPa)}$

It can be seen that this level of interface strength can be achieved in most metal-matrix composites. However, due to internal stresses, at the interface, induced during fabrication of the composite, due to disparity of the thermal expansion of the fibre and the matrix, a higher interfacial bond strength is required. In addition, the formula used to predict the required strength of the interface was derived on the assumption that stresses exist only parallel to the fibre (see 2.3.4), whereas in actual systems, in particular those with 3D random fibre distribution, stresses exist in the radial direction (see Figure 76) which could cause failure at the interface. This would suggest the need for a stronger interface than predicted.

At elevated temperatures the matrix strength is reduced and a stronger interface is needed to permit load transfer to the fibre. Mechanical gripping of the fibre by the matrix will be reduced at elevated temperatures and cannot be relied upon in this case. The efficiency of mechanical bonding at room temperature depends on the fibre aspect ratio and the method of fabrication of composite. However, it is

generally accepted that a certain degree of chemical reaction is necessary in order to develop adequate bonding, although an interface reaction can weaken the fibre in the composite by introducing surface defects into the fibre. The strength of the fibre is dependent upon the severity of the defects, their population and distribution.

Sutton and Feingold¹⁴⁰ have shown that the requirements for strong interfacial bonding and for the fibre to retain their strength tend to oppose each other. In their studies of bonding between nickel and alumina fibre (sapphire), they concluded that surface damage and bonding were related to the amount of interface reaction. Figure 88 shows the competing effects of interface interaction on fibre degradation and improved bonding. Therefore, interface reaction must be controlled so that strong interfacial bonding is developed at an acceptable level of attack on the fibre.

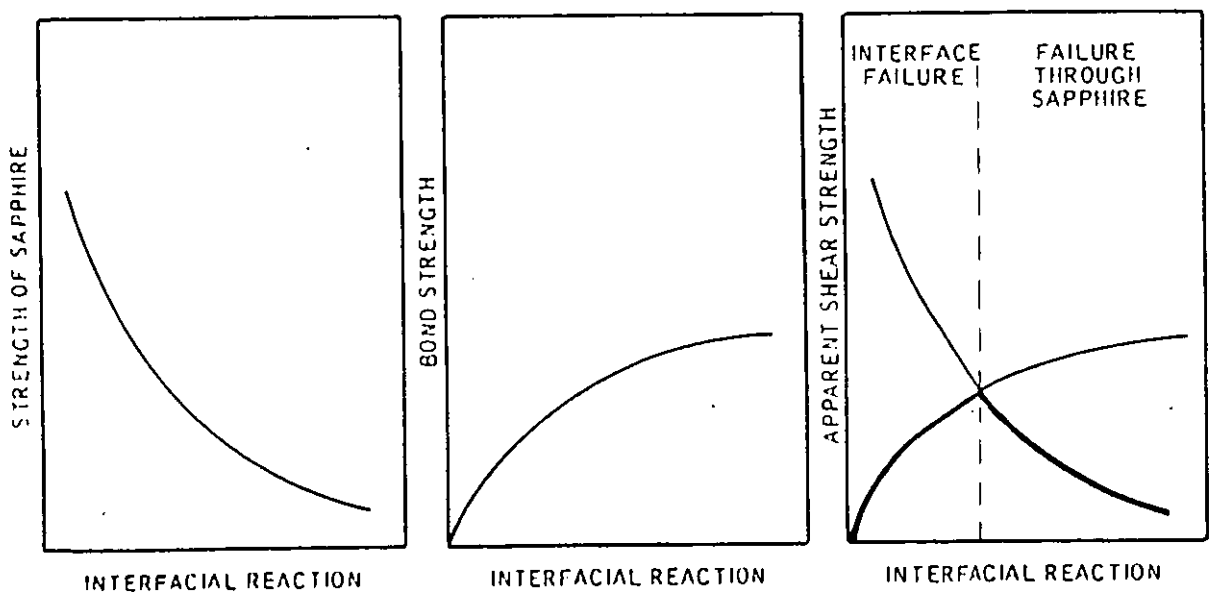
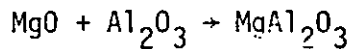


FIGURE 88: Schematic of effects of interfacial reaction on bond strength and fibre (sapphire) degradation (Ref 140)

A further complication arises from the fact that the strength requirement of the interface varies with the orientation of the fibre in relation to load direction. A moderate interfacial strength would permit load transfer on to a fibre stressed parallel to its axis, whereas a stronger interfacial bonding is needed when the fibre is stressed normal to its axis. Khan¹⁴¹ reported axial strength (UTS) of Al/graphite fibre (unidirectionally aligned) composite in agreement with those predicted from the rule-of-mixtures. Although the interfacial bonding was adequate when the composite was tested parallel to the fibre (axial strength), transverse strength was very low ($\sigma_{\text{trans}}/\sigma_{\text{axial}}$ is about 0.06) due to inadequate bonding when the composite was tested in that direction. Yajima et al¹⁰⁸ reported transverse strength less than 10% of the axial strength for Al/SiC composite (unidirectionally aligned fibre) as a result of inadequate bonding when the composite was tested in the transverse direction.

Klein¹⁴² reviewing the different theoretical analyses predicting off-axis strength of composites (unidirectional reinforcement), came to the following conclusion: *"At present there are no theories that have been developed sufficiently to permit prediction of composite off-axis strength from the mechanical properties of the interface, fibre and matrix"*.

In the composite systems considered in this investigation (3D random), the situation is far more complex because fibres are aligned in all possible directions and there is almost no theoretical guidance on the strength requirements of the interface. However, there should be a bonding condition that would yield optimum mechanical properties for a controlled amount of interaction at the interface. Chemical interaction between fibre and matrix can be developed in both composite systems. In the Al-Cu/SiC composite system, molten Al reacts with SiC to form Al_4C_3 , copper does not react with SiC¹²¹. In the Al-Mg/ Al_2O_3 composite, the following reaction was suggested¹¹⁰:



In castings group V (see 3.6, Group V), all factors, other than time of contact, which influence the reaction between the fibres (SiC or Al_2O_3) and the respective molten alloy (Al-Cu, Al-Mg) were kept constant. Composites of both systems (Al-Cu/SiC and Al-Mg/ Al_2O_3), containing a fixed volume content of fibre (4%) were fabricated with variable time of contact between the fibres and the molten alloy in order to develop variable degrees of chemical reaction at the fibre surface, i.e. variable interfacial strength and attack on fibre. The effect of contact time, between the fibre and the respective molten alloy, on the tensile properties of the Al-Cu/SiC and Al-Mg/ Al_2O_3 (4% volume fibre) is shown in Figures 57 and 58 (and in Tables A3.5 and A3.6) respectively.

It can be seen that, for both composite systems, UTS values increase with the increase of the time of contact up to a 'point' (~18 and 15.5 minutes for Al-Cu/SiC and Al-Mg/ Al_2O_3 respectively) due to the effect of improvement in bonding. At longer times of contact, due to the degradation of fibre strength, the composite's strength decreases. The point of maxima possibly represents the situation where the competing effects of interface reaction on fibre strength and improved bonding were balanced to produce maximum strength in that particular composite system. This analysis is confirmed by the observations on fibre fracture and interface behaviour when the composites were fractured (tensile), see Figures 67-69. For composites (Al-Cu/SiC and Al-Mg/ Al_2O_3) with fibre exposed to the molten alloy for a time corresponding to the UTS maxima, adequate bonding was observed as indicated by the absence of interfacial failure and there was no significant fibre degradation. At longer times of contact fibre degradation, indicated by the multi fracture and fragmentation of fibre (see Figures 68 and 69b), became a common feature. At shorter times of contact, interface failure was common when the fibres were near-normal

to the stress (tensile) direction, but those near-parallel to the stress direction showed very few such failures.

Similarly, the elastic modulus showed a maximum value for contact times in the range of 23-30 minutes for the Al-Cu/SiC system and 15-25 minutes for the Al-Mg/Al₂O₃ system. The maximum values of elastic modulus correspond to time of contact longer than that for maximum UTS. Fibres near normal to the stress direction, which require a stronger interfacial bonding, i.e. longer time of contact, contribute little to the strength of the composite (see 2.3.3, Figure 7), whereas their contribution to the value of elastic modulus is more significant. Experimental data, reported by Champion et al⁸⁰, on Al-Li/Al₂O₃ composite (unidirectional reinforcement) are in support of this theoretical view. In composites reinforced with unidirectionally aligned fibre, transverse strength is usually very low compared with their longitudinal strength. By contrast their transverse modulus is only slightly lower than the longitudinal modulus. The ratio of longitudinal/transverse modulus is approximately 3:2¹⁴³. That is because fibre near normal to the stress axis contribute little to the strength of the composite, whereas their contribution to the value of elastic modulus is considerable. The fibres near normal to the axis require a stronger interfacial bonding i.e. longer time of contact. Therefore, in the present investigation, the maximum value of elastic modulus was obtained at time of contact longer than that needed for the maximum UTS. Degradation of fibre strength was less significant because elastic modulus is measured at low stresses. With increased time of contact, the interfacial bonding is stronger but a reduction in fibre strength occurs progressively. A stronger interfacial bonding would result in more constraint on matrix flow. Degradation of fibre strength would reduce the matrix flow necessary to fracture the weakened fibre. This possibly resulted in the observed continuous decrease in the values of percentage elongation (Figures 57 and 58) and reduction in area (Tables A3.5 and A3.6) for both composite systems, with increasing time of contact.

The increase in the measured value of 0.1% offset proof stress, with the increase in time of contact, is possibly a direct result of the improvement in bonding. The increase in the value of 0.1% proof stress was reduced at time of contact near that corresponding to the maxima for elastic modulus. This is possibly due to the effect of degradation of fibre strength, however, because proof stress is measured at lower stress, compared with UTS, the effect of degradation of fibre strength was less pronounced. In addition, the continuous reduction of the capability of the matrices to flow could have contributed toward a higher measured proof stress.

From the foregoing discussion it appears that at a certain degree of chemical reaction between the fibre and the respective molten alloy, maximum values of tensile properties of the composites are achieved. Therefore during the production of composites this reaction needs to be controlled accordingly.

6.7 TENSILE PROPERTIES OF THE SQUEEZE CAST COMPOSITES

The composites produced were grouped under three sections, see 5.8. In 6.6 the effects of contact time, between the fibres and the respective molten alloy, on the tensile properties of the composites of Section II were discussed. Therefore discussion here will be limited to the composites of sections I and III.

6.7.1 The Tensile Properties (Room Temperature) of the Composites of Section I (Casting Groups III, IV)

This includes the initial squeeze cast composites for which the time of contact between the fibre and the molten matrix during fabrication was not controlled. This section includes two groups of composites, groups III and IV.

Casting group III:

In this group of squeeze cast composites, Al-4.5Cu matrix was reinforced with either SiC or Al₂O₃ fibre. Composites were fully heat treated. The room temperature tensile properties of both composite systems are shown in Table 11. The results indicate a reduction in the values of the tensile properties as a result of the presence of fibre, the reduction increasing with the increase in the fibre content in the matrix.

The observed poor bonding and distribution of alumina fibre in Al-Cu/Al₂O₃ composite (see Figure 78 and A4.4) could have contributed to produce poor tensile properties. However, good fibre bonding and distribution was observed in the Al-Cu/SiC composites.

The poor tensile properties of Al-Cu/SiC composite could not have been a result of uncontrolled time of contact between the fibre and the molten matrix, at fabrication, because:

1. Fibres could not have been greatly under-exposed to the melt because a strong interfacial bonding was observed, see Figure 79. Also the high reduction in the values of percentage elongation and reduction in area, as a result of the presence of fibre, could not be produced unless a strong interface was developed. Indeed, in the case of Al-Cu/Al₂O₃ where poor bonding was observed, there was hardly any reduction in the values of percentage elongation or reduction in area. Due to practical limitations, composites containing 4% (volume) fibre could not be produced with fibre exposed to the melt for less than 8 minutes, see 3.6, Group V. A longer time is needed to produce composites with fibre content higher than 4% (volume).

The results of the tensile tests in Group V indicate that composite castings (as-cast Al-Cu/SiC) with fibre exposed to the melt for 8 minutes have 0.1% proof stress higher than that measured for

the matrix alloy (Al-Cu) casting. Increasing the contact time beyond 8 minutes shows progressive improvements in all the properties up to the time when corresponding peak values are reached in those properties. By contrast, composite castings (heat treated) of group III had tensile properties lower than those for the matrix alloy.

2. Fibres could not have been greatly over exposed to the melt either for all group IV castings because fibre degradation was observed only in the composite containing 10% (volume) fibre. In addition long times of contact, as can be seen in Figure 57, would produce higher values of proof stress and possibly (depending on how long is the time of contact) improved elastic modulus which is not the case here. Therefore, the reduced tensile properties of the composite casting, of Group III (heat treated) should be attributed to reasons other than time of contact, although the latter could have contributed in reducing the strength of the composites.

Two effects of heat treatment of the Al-Cu/SiC composites were observed:

- The Cu-rich layer which was observed around the fibre was diffused into the matrix, see Figures 49 and 51.
- The ductility of the matrix was reduced, the heat treated matrix had a 4-5% elongation and reduction in area (see Table 11), compared with ~15% for the as-cast matrix.

The diffusion of the Cu surrounding fibres into the matrix did not appear to affect the integrity of the fibre/matrix interface and there is no evidence to suggest an interface controlled failure of the composite. For composites reinforced with short fibres high ductility of the matrix is a property of particular importance because:

- matrix flow, under stress, is essential in order to make load transfer onto the fibre possible
- matrix of high ductility is more capable of accommodating differences in thermal expansions of the fibres and the matrix. Therefore during fabrication, lower internal stress at fibre/matrix interface will develop on cooling from the fabrication temperature when the matrix is ductile
- on loading a composite, a high stress (shear) concentration is expected to develop at the fibre ends (see 2.3.4). Therefore unless the matrix is ductile enough and able to redistribute stresses, through elastic and plastic deformation, stresses could build up (locally) to the failure stress level of the matrix which would result in cracks at the fibre ends and, consequently, a premature failure of the composite. Cracks have a drastic effect on elastic modulus of composites¹⁴⁴.

The poor properties of the heat treated Al-Cu/SiC composites are most likely to be a result of the low ductility of the matrix which could have resulted in inefficient load transfer onto fibres, development of high internal stresses at the interface and stress concentration at the fibre ends during fabrication, and the build up of high stress concentration at fibre ends on loading. These effects combined together could have resulted in the measured poor properties (tensile) of the composites. This analysis is supported by the observed negligible plastic flow of the matrix in the close vicinity of the fibres when the composites were fractured (tensile), see Figure 79. In addition, the same composite in the as-cast state showed substantial improvement in certain tensile properties such as proof stress and elastic modulus, see Figure 53.

In the case of the Al-Cu/Al₂O₃ (heat treated) composites where the reduction in the values of tensile properties was less severe (see

Table 11), the poor bonding possibly limited the adverse effects of low ductility of the matrix by failure of the interface on loading.

Fukunaga et al¹¹⁴, reported a significant improvement in tensile strength, both at room and elevated temperatures, of composites with a highly ductile matrix (Al) reinforced (2D random) with β -spodumene ($\text{Li}_2\text{O} \cdot \text{Al}_2\text{O}_3 \cdot 4\text{SiO}_2$) short fibre. A preform of fibre was infiltrated by the molten matrix alloy, "squeeze infiltration". However, composites with matrix (Al, 2.7 Cu, 9.8 Si, 1.25 Ni) of "low ductility" (not specified), similarly fabricated and reinforced with the same fibre, had much lower tensile strength at room temperature than the matrix alloy. At 350°C the composite had a strength equal to that of the matrix at the temperature, possibly due to increased ductility of the matrix at that temperature, see Figure 89. They explained the poor composite strength at room temperature by the difficulty in redistribution of stresses because of the low ductility of the matrix.

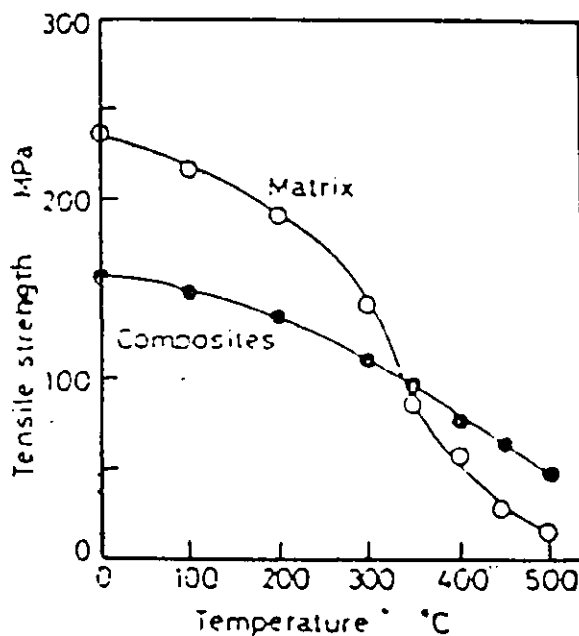


FIGURE 89: High temperature tensile strength of a composite with matrix of low ductility and the matrix alloy (Ref 114)

Dean⁸⁴, reported improved tensile strength, at 1100°C, of composite of a nickel alloy reinforced with tungsten wire (continuous). Composites were fabricated by hot pressing. However, below 1100°C, the strength of the composite was always less than that of the matrix, and below 900°C the yield stress was less than that of the matrix. The worst case was at room temperature when the matrix alloy yielded at 700 MPa but the composite yielded at only 310 MPa. This was attributed to internal tensile stress set up in the matrix by differential shrinkage on cooling from the fabrication temperature.

Casting Group IV

This group includes as-cast composites of Al-Cu/SiC and Al-Mg/Al₂O₃. The tensile properties of the Al-Cu/SiC composites are shown in Figures 53 and 54 (and in Table A3.3). As can be seen with the increase in the volume content of fibre in the matrix, tensile strength decreases whereas 0.1% proof stress significantly increases. Elastic modulus shows substantial improvement with up to 6% (volume) fibre, at higher fibre content no significant improvement was measured (slight increase at 8% fibre). By comparing these results with the results obtained when the time of contact between the fibre and the molten matrix was controlled, i.e. results for casting group VI (or VII) see Figure 59, and keeping in mind the effects of time of contact (see Figure 57) it is possible to conclude that in these composites (Al-Cu/SiC group IV), fibres were exposed to the melt for a time longer than that found to produce maximum UTS values (~ 18 minutes, see Figure 57). Time of contact between the fibres and the melt could have varied from one casting to another (for castings in group IV). Usually, the higher the fibre content in the matrix the longer is the processing time for the composite (liquid) which normally accounts for a high percentage of the total time of contact.

If we compare the tensile properties of an Al-Cu/SiC composite, for example group IV casting containing 4% (volume) fibre (Table A3.3),

with the tensile properties of similar composites in group VI (Table A3.7), it can be seen that the composites of group IV have a lower UTS, percentage elongation and reduction in area and a higher elastic modulus (0.1% PS is slightly higher). This is in agreement with the expected effects of a longer time of contact for composites in group IV (see Figure 57).

The lack of further improvement of the elastic modulus with fibre content higher than 6% is possibly due to even longer times of contact between the fibre and the melt. This is possibly because the processing time of composites (liquid composite) is longer when a higher content of fibre is introduced into the melt. The properties of the composite with 8 and 10% fibre could suggest that the fibres were kept in contact with the melt for a longer time than that necessary to produce the maximum value of elastic modulus (Figure 57). This is supported by the observed severe degradation of fibres in composites containing 8% and 10% (volume) fibre, see Figure 76.

In a similar method of analysis, the tensile properties of the Al-Mg/ Al_2O_3 which are shown in Figures 55 and 56 and in Table A3.4, can be explained by fibre being exposed to the melt, during fabrication, for a short time and less than that which was found necessary to produce a maximum value of UTS (see Figure 58). This resulted in the observed inadequate bonding as shown in Figure 77.

6.7.2 The Tensile Properties of the Composites (as-cast) of Section III, Casting Groups VI and VII (Controlled Time of Contact), at Room and Elevated Temperatures

This section of castings includes two groups of squeeze cast composites, groups VI and VII, where the time of contact between the fibres and the respective molten alloy was controlled, each group contains composites of Al-Cu/SiC and Al-Mg/ Al_2O_3 . SiC fibres were exposed to the melt for

18 minutes (average). Al_2O_3 fibres were exposed to the melt for 15.5 minutes (average).

Castings in Group VI were made first to examine the tensile properties (room temperature) of these composites before producing the final group. Group VII was produced for making the final assessment of certain properties. The final group of castings (Group VII) also provide a measure of the reproducibility of the composites and their properties.

Composites of Group VI were tested (tensile) at room temperature, whereas composites of Group VII were tested at both room and elevated temperatures.

Castings Group VI

The tensile properties (room temperature) are shown in Figure 59 and Table A3.7 for the Al-Cu/SiC composites and in Figure 60 and Table A3.7 for the Al-Mg/ Al_2O_3 composites. It can be seen that, when the chemical reaction at fibre interface is controlled in order to develop a strong interfacial bonding at an acceptable degree of chemical attack on the fibres (see 6.6), the objective of matrix reinforcement is achieved.

For both composite systems the increase in the values of both elastic modulus and 0.1% proof stress is substantial. For example Al-Cu/SiC composite, with 10% (volume) fibre, had elastic modulus and 0.1% proof stress values of 82 GPa and 184 MPa respectively, compared with 70.5 GPa and 106.7 MPa (respectively) for the squeeze cast matrix alloys, see Table A3.7.

However, the tensile properties of the squeeze cast matrix alloys were already improved over those for castings produced at atmospheric pressure (sand and gravity die cast).

The increase in the values of UTS and 0.1% offset proof stress of squeeze cast composites containing 10% (volume) fibre over those for the same matrix alloy gravity die cast is 53% and 164% respectively in the case of Al-Cu/SiC composite system, and 41% and 104% respectively in the case of Al-Mg/Al₂O₃ composites.

The moderate improvement in tensile strength (UTS), for both composite systems when reinforced with fibre, is no surprise because of the relatively low volume content of fibre. In addition, because fibres are oriented in 3D random manner, their reinforcement effect will be reduced. Fukuda and Chou²³, theoretically predicted the value of orientation factor for 3D random orientation to be 1/8. Cox²⁴ and Christensen²⁵ predicted a value of 1/6, see 2.3.5. These values for orientation factor should be compared with 1 for a composite reinforced with unidirectionally aligned fibre. However, the composites produced (3D) provide isotropic properties (tensile), see Tables 9 and 10, whereas composites reinforced with aligned fibre (unidirectional) suffer from a major hindrance to their practical use because of poor transverse strength¹⁴¹.

The improvement in the elastic modulus, for both composite systems, was more significant than that of the tensile strength because all fibres at all orientations contribute towards higher elastic modulus. However, the contribution of fibre aligned at near normal to the tensile stress direction to the value of tensile strength (UTS) is very limited and could be negative (depends on bonding), see 6.6.

The decrease in the values of percentage elongation and reduction in area for both composite systems, see Tables A3.7 and A3.8, as a result

of the presence of fibre in the matrix is a natural result of the constraint imposed on matrix flow by brittle fibres well bonded to the matrix. However, composites with 10% fibre still have percentage elongation and reduction in area (ductility) in the range of 3-4%. This level of ductility would satisfy the designer's requirement, unlike composites with unidirectional reinforcement¹⁴⁵, for structural materials to have ductility around 5%¹⁴⁵.

The achievement of a substantial improvement in tensile properties for both composite systems (Al-Cu/SiC and Al-Mg/Al₂O₃) compared with the matrix alloys, is attributed most of all to the sound structural quality of the composites, high ductility of the matrix alloys, and controlled interfacial reaction between the fibres and the respective molten alloy during fabrication.

Castings Group VII

The measured tensile properties at room and elevated temperatures are shown in Figures 61-63 and Table A3.9 for the Al-Cu/SiC composites, and in Figures 64-66 and Table A3.10 for the Al-Mg/Al₂O₃ composites. Tensile properties are plotted against the volume content of fibre for each test temperature.

The tensile properties at room temperature, for both composite systems are well in agreement with those for the same composites of group VI, see Tables A3.7 and A3.8, and Tables A3.9 and A3.10. This implies that the production method provides reproducibility of the composites and their properties.

The reinforcement of the matrix alloys was retained at elevated temperatures. For both composite systems the strengthening efficiency (UTS composite/UTS matrix) was increased at 200°C. In the case of the Al-Mg/Al₂O₃ composite the increase was slight. This increase is

possibly due to the relief, at that temperature, of the internal stresses in the matrix and at the fibre/matrix interface, which would be expected to develop by differential shrinkage on cooling from the fabrication temperature.

The 0.1% proof stress of the Al-Cu/SiC composites and the matrix showed little decrease up to 200°C. At 250°C, both the matrix and the composite showed a larger decrease possibly due to softening of the matrix. The decrease in the values of 0.1% proof stress for Al-Mg/Al₂O₃ composite and the matrix is more gradual up to 250°C, at 300°C, a rapid decrease took place for both the matrix and the composites. Therefore the decrease in tensile properties of the composite at elevated temperatures appears to be due to softening of the matrix. However, at 250°C both composite systems still have elastic modulus and 0.1% proof stress values comparable with those for the squeeze cast matrix at room temperature.

SEM examinations of fractured composites of groups VI and VII indicated that a strong interfacial bonding led to the fracture of fibres at both room and elevated temperatures with no interface failure and no significant degradation of fibre, see Figures 70-74.

This indicates a successful control of the reaction between the fibre and the molten matrix during fabrication of the composites. The high ductility of the matrix, see Figure 75, allowed a high degree of plastic deformation of the matrix to occur around the fibre (Figures 70-74) which is, as discussed in 6.7.1 - Group III, essential for effective reinforcement of the matrix.

The increase in the values of the tensile properties (UTS, 0.1% PS and elastic modulus) for both composite systems (groups VI and VII) appears to have a linear relationship with the increase in fibre volume content in the matrix at both room and elevated temperatures. Therefore a higher

percentage of fibre would result in further improvement in tensile properties. In the present investigation it was not practically possible to incorporate more than 10% (volume) fibre, see 6.5.2. It might be possible to incorporate a higher percentage of fibre (3D random) in a matrix by choosing fibre of a smaller aspect ratio (l/d), provided that the aspect ratio is not less than that required to load the fibres to their fracture strength, at working temperature, for a given interface strength.

6.7.3 Comparison of the Experimental Results with the Theoretical Prediction of Composite Tensile Properties

The theoretical principles of composite reinforcement were briefly reviewed in Chapter 2 (2.3).

For short fibre composites the modified rule-of-mixtures takes the general form

$$\sigma_{Cu} = \sigma_{f.u.} V_f \cdot F(l_c/l) \cdot C_o + \sigma_m' (1 - V_f) \quad (24)$$

where C_o is the orientation factor, Fukuda²³ suggested that for a composite with fibre randomly oriented in three dimensions, $C_o = 1/8$, whereas Cox²⁴ and Christensen²⁵ suggested $C_o = 1/6$.

$F(l_c/l)$ is a function of fibre length in relation to the critical length of fibre (l_c).

Subscripts c, f, m and u refer to composite, fibre, matrix and ultimate value.

σ_m' is the stress on the matrix at a strain equal to the fibre strain at fracture¹². If we consider the brittle fibres to be fully elastic

up to their fracture, then σ_m' is the stress on the matrix at strain $\epsilon_f = \sigma_{f.u}/E_f$.

l_c can be calculated from equation 11 (see 2.3.2), $l_c/d = \sigma_{f.u}/2\tau$.

τ is the shear strength of the interface, which can be taken to equal half the yield strength of the matrix¹⁴.

Riley¹⁸, taking into consideration fibre length and stress distribution at fibre ends, modified the rule of mixtures to the form (see 2.3.4, unidirectional alignment):

$$\sigma_{c.u} = \frac{6/7}{1+(5l_c/7l)} \cdot \sigma_{f.u} \cdot V_f + \sigma_m'(1-V_f) \quad (22)$$

Because fibre in the composites in this investigation are of 3D random orientation, an orientation factor (C_o) should be used, using $C_o = 1/6$, equation 22 is modified to:

$$\sigma_{c.u}(3D) = 1/6 \cdot \frac{6/7}{1+(5l_c/7l)} \cdot \sigma_{f.u} V_f + \sigma_m'(1-V_f) \quad (22-3D)$$

Christensen²⁵ suggested the following equation to predict the elastic modulus of composites with fibre oriented in a 3D random manner (see 2.3.5), for $V_f < 0.2$:

$$E_{3D} = \frac{V_f}{6} \cdot E_f + [1 + (1+\nu_m)V_f]E_m \quad (26)$$

ν_m is the Poisson's ratio for the matrix.

The value of properties needed to calculate the tensile strength and the elastic modulus of both composite systems are tabulated in Table 17.

TABLE 17: Data Needed for Calculation in Equations 22 and 26

Property (average)	Source	Al-Cu/SiC	Al-Mg/Al ₂ O ₃
d (μm)	Tables 1 and 2	12	3
ℓ (μm)	Tables 1 and 2	3000	500
σ _{fU} (MPa)	Tables 1 and 2	2700	2000
E _f (GPa)	Tables 1 and 2)	190	300
E _m (GPa)	Tables A3.7,A3.8	70.5	70.9
0.1% PS (matrix) MPa	Tables A3.7,A3.8	106	146
ν _m	Ref 146	0.31	0.31
ε _f = σ _{fU} /E _f	-	0.0142	0.0066
ℓ _c (μm)	Equation 11	305	41
σ _m ' (MPa) at strain = ε _f	Experiment	127	166

From equations 22(3D), 26 and data in Table 17:

- For Al-Cu/SiC composites

$$\sigma_{cu} = 127 + 232.56 (V_f) \quad (6.1)$$

$$E_{3D} = 70.5 + 124 (V_f) \quad (6.2)$$

- For Al-Mg/Al₂O₃ composites

$$\sigma_{cu} = 166 + 103.9 (V_f) \quad (6.3)$$

$$E_{3D} = 70.9 + 142.8 (V_f) \quad (6.4)$$

The theoretical prediction of the values of elastic modulus and UTS are plotted against the volume percentage of fibre, in comparison with the experimental results (composites of Group VI), in Figure 90 for the Al-Cu/SiC composite system and in Figure 91 for the Al-Mg/Al₂O₃ composite system.

For both composite systems, the theoretical prediction of the values of UTS are much lower than the experimental results. However, it is of interest to note that in both Figures 90 and 91 the lines which represent the experimental results and the theoretical prediction are approximately parallel. The difference in values is $\sim \sigma_{mu} - \sigma_m'$, this means that experimental results will be in better agreement with the theoretically predicted values if the term σ_m' in equation 24, is replaced by σ_{mu} . In addition, unless σ_m' is replaced by σ_{mu} , equation 24 (as in other modifications of the rule-of-mixtures) would not satisfy the boundary conditions. For example, at $V_f = 0$ (i.e. fibre-free matrix) $\sigma_{cu} = \sigma_m'$ which simply cannot be true, at $V_f = 0$, σ_{cu} must be equal to σ_{mu} (UTS of the matrix).

A common feature between the different modifications of the rule-of-mixtures is that all were concerned with the modification of the first term of the rule-of-mixtures ($\sigma_{cu} = \sigma_{fu} \cdot V_f + \sigma_m' (1 - V_f)$.) i.e. $\sigma_{fu} \cdot V_f$, in particular the introduction of different formulae of the function $F(\lambda_c/\lambda)$, whereas the second term, $\sigma_m' (1 - V_f)$, was assumed to be applicable. The term σ_m' was first introduced into the rule-

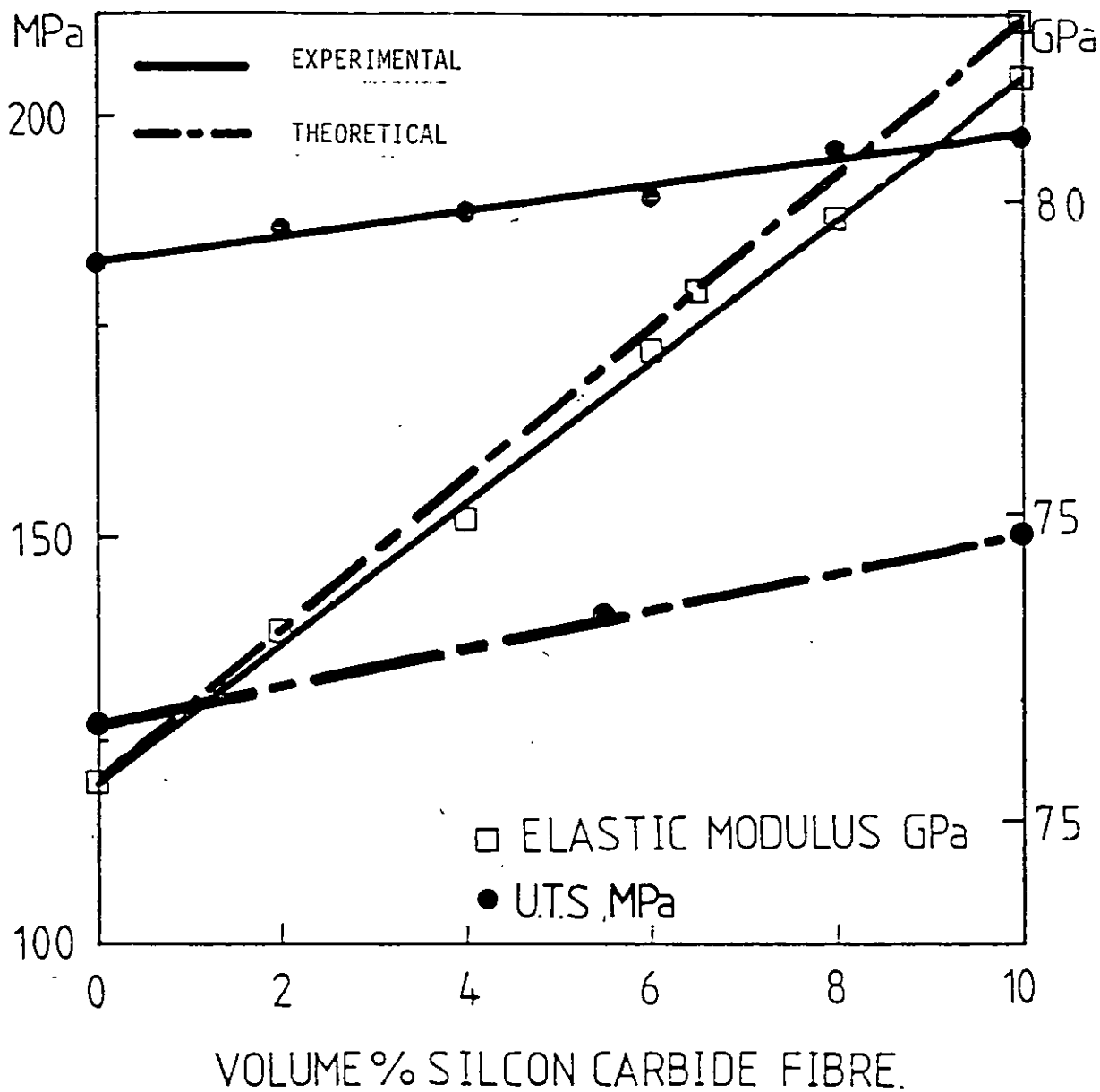


FIGURE 90: Experimental results in comparison with the theoretical prediction of the elastic modulus and UTS of the Al-4.5 Cu/SiC composite system

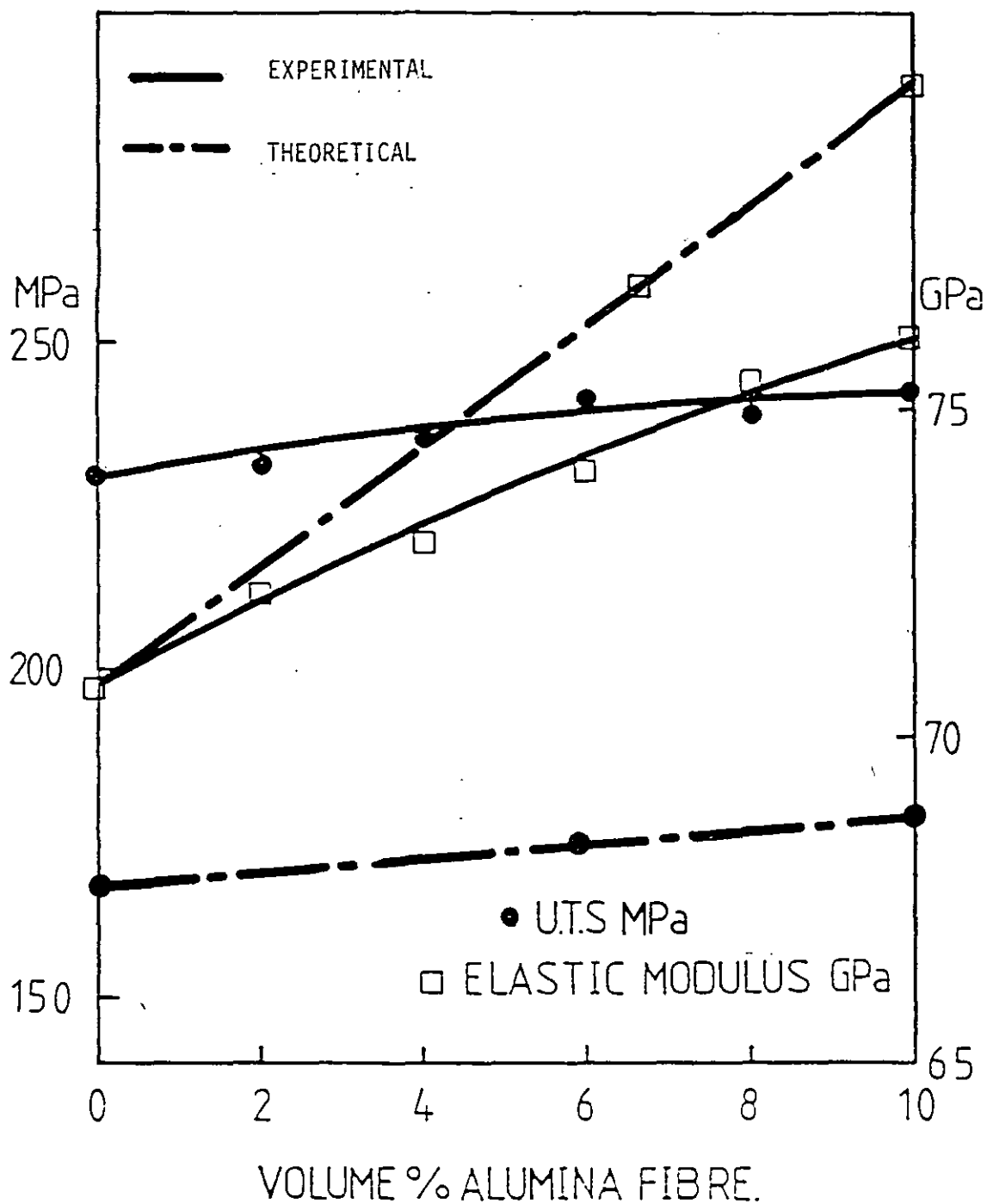


FIGURE 91: Experimental results in comparison with the theoretical prediction of the elastic modulus and UTS of the Al-3.75 Mg/ Al_2O_3 composite system

of-mixtures for composites reinforced with continuous fibre, at the conditions of equal strain in the fibre and the matrix, and that composite failure results when the fibres fail.

The assumption of equal strain in fibre and matrix cannot be made in the case of composites similar to those in this investigation, possibly not even before loading. Composite failure could not have resulted from failure of the fibre because at this condition:

$$\sigma_{cu} = \sigma_{mu} (1 - V_f) \quad (4)$$

Experimentally σ_{cu} was always $> \sigma_{mu}(1 - V_f)$, (which is the requirement for the rule-of-mixtures to be applicable). In fact it was always $> \sigma_{mu}$, i.e. fibres strengthen the matrix and their contribution should be added to the term $\sigma_{mu}(1 - V_f)$ (see 2.3.1).

From the foregoing discussion, it is suggested that equation 24 should be modified to

$$\sigma_{cu} = \sigma_{fu} \cdot V_f \cdot F(\ell_c/\ell) \cdot C_0 + \sigma_{mu}(1 - V_f) \quad (28)$$

Accordingly the Riley solution (equation 22) has been modified and, using $C_0 = 1/6$, we get

$$\sigma_{cu(3D)} = \frac{1}{6} \cdot \frac{6/7}{1 + (5\ell_c/7\ell)} \cdot \sigma_{fu} \cdot V_f + \sigma_{mu}(1 - V_f) \quad (29)$$

With this modification, experimental results and theoretical predictions of the values of UTS are in better agreement.

For the Al-Cu/SiC composite system, the theoretical value of UTS at a fibre volume content of 10% will be ($\sigma_{mu} = 183$ MPa, Table A3.7) $\sigma_{cu} = 200.6$ MPa, compared with an experimental value of 197 MPa.

In this calculation $\sigma_{fu} = 2700$ MPa as the average specified strength of SiC fibre (see 3.1.1 Table 1) was used. However it was found that the fibres lost some of their strength when heated (900°C for 2 hrs) as a pretreatment, this will be discussed in 6.11. The average measured strength of heat treated SiC fibre (see Table 16, Cycle 1) was 1825 MPa. Using this value for SiC fibre strength, from equation 29 at 10% volume fibre, $\sigma_{cu} = 189$ MPa in comparison with the experimental value of 197 MPa.

For Al-Mg/Al₂O₃ composites, the theoretical value of UTS (σ_{cu}) at a fibre volume content of 10% from equation 29 ($\sigma_{mu} = 230$ MPa) will be $\sigma_{cu} = 234$ MPa, compared with the experimentally measured value of 243 MPa.

For both composite systems, the experimental values of the strength of composites were slightly higher than those theoretically predicted. The difference is insignificant and could be attributed to strain hardening of the matrix on loading at fibre ends and channels between fibres¹⁴⁷ and constraint of the matrix¹⁴.

The experimental values of σ_{cu} , for both composite systems, were always higher than those for the fibre-free castings, i.e. $\sigma_{cu} > \sigma_{mu}$. This implies the non-existence of either V_{crit} or V_{min} . However, the condition for the rule-of-mixtures to be applicable ($\sigma_{cu} > \sigma_{mu}(1-V_f)$) is satisfied, for all volume percentages used during this investigation.

The concepts of V_{\min} and V_{crit} were introduced during theoretical analysis of composites reinforced with continuous fibre. Strain was assumed to be equal in both phases (fibre and matrix). According to this analysis, at fibre content level less than V_{\min} , $\sigma_{\text{cu}} = \sigma_{\text{mu}}(1-V_f)$. This will occur only if all fibres simultaneously fracture at one plane and therefore they do not contribute to the strength of the composite. In a real situation, regardless of the volume content of fibre, fibre would be expected to fracture, under load, at various planes and load would be transferred to fibre fragments simulating composite reinforced with short fibre. Therefore, fibres are expected to contribute to the final strength of composite, even after their fracture, at all levels of fibre content, i.e. $\sigma_{\text{cu}} > \sigma_{\text{mu}}$, provided that the matrix is ductile enough to allow load transfer.

The concepts of V_{crit} and V_{\min} are not discussed in available theoretical analysis of composite reinforced with short fibre. However, at $V_f = V_{\text{crit}}$, $\sigma_{\text{cu}} = \sigma_{\text{mu}}$.

Substituting σ_{cu} by its value as in equation 24:

$$\sigma_{\text{fu}} \cdot V_f \cdot F(l/l_c) \cdot C_0 + \sigma_{\text{m}'} (1-V_f) = \sigma_{\text{mu}}$$

$$\therefore V_{\text{crit}} = \frac{\sigma_{\text{mu}} - \sigma_{\text{m}'}}{\sigma_{\text{fu}} \cdot F(l/l_0) \cdot C_0 - \sigma_{\text{m}'}}$$

Earlier in the discussion, it was suggested that $\sigma_{\text{m}'}$ should be replaced by σ_{mu} for the modified rule-of-mixtures to be applicable. For this condition, from equation 30, $V_{\text{crit}} = 0$, which is in support of the experimental finding.

The theoretically predicted values of elastic modulus (equation 26) for the Al-Cu/SiC composite are well in agreement with those measured experimentally (see Figure 90). At 10% volume content of fibre the theoretical value is 82.9 GPa (see equation 6.2) compared with 82 GPa (see Table A3.7).

The measured (experimental) values of the elastic modulus for Al-Mg/ Al_2O_3 composites are lower than the theoretical prediction, see Figure 91. At 10% (volume) fibre, from equation 6.4, $E_{3D} = 85.15$ GPa compared with the experimentally measured value of 75.9 GPa (see Table A3.8).

Ceramic fibres, such as SiC and Al_2O_3 are brittle and stiff (high elastic modulus). Therefore they usually fracture on bending and, because of their high stiffness, handling fibres of small diameter causes discomfort, fibres tend to penetrate skin rather than bend. The alumina fibres used, unlike SiC fibres, tend to curl and on handling, they ball-up and cause no discomfort. They can be bent over at small radius without fracture. Therefore, their stiffness is questionable. Their specified value of elastic modulus is 300 GPa (see 3.1.1, Table 2). This value of elastic modulus could have been produced on a laboratory scale. However, these fibres are still in their early stage of development and the received fibres do not appear to be of that level of stiffness. This might explain the disagreement between the experimental results and the theoretical prediction.

6.8 THE EFFECT OF THERMAL CYCLING ON THE TENSILE PROPERTIES OF THE COMPOSITES

The tensile properties of the thermally cycled Al-Cu/SiC and Al-Mg/ Al_2O_3 composites are shown in Tables 12 and 13 respectively.

The results indicated that thermal cycling, between room temperature and 350°C , had no significant effect on the tensile properties of the composites. UTS values for composites with 8% or 10% (volume) fibre were slightly reduced during the first few cycles (5 cycles). Further cycling (up to 20 cycles) produced no further reduction in UTS values. The reduction in UTS values was less than 5% for composites with 10% fibre. cycling had no observable effect on the fracture behaviour of the interface.

Khan¹⁴¹ reported ~18% reduction in the strength of a Al/graphite (continuous) fibre) composite when it was subjected to thermal cycling between room temperature and 500°C, reduction in strength occurred during the first few cycles. Metals usually have a thermal expansion coefficient much higher than that for the reinforcement fibre (ceramics) (see 4.2.5). Therefore, during thermal cycling stresses and strains are expected to develop and concentrate at the fibre/matrix interface. Unless the interfacial bond is strong enough to withstand the developed stresses, interface failure would be expected which would adversely affect the mechanical properties of the composite. In the present investigation, at test conditions, the strong interfacial bonding between the fibre and the matrix, and the high ductility of the matrix alloys, which make them capable of accommodating high strains, are possibly the main factors contributing to the composite's resistance to thermal cycling. In addition, certain levels of stresses and strains are expected to have developed mainly at interfaces, on cooling from fabrication temperature, by differential shrinkage. Therefore, on heating up during cycling, differential expansion would not be expected (at test conditions) to produce drastic effects.

6.9 FATIGUE LIFE OF THE COMPOSITES

The results of the fatigue tests (rotating bend, reverse bending stress was 95 MPa) are shown in Table 14.

As was discussed in 6.1, matrix alloys (Al-Cu and Al-Mg) had a longer fatigue life when they were squeeze cast compared with those produced by sand or gravity die casting. For both composite systems, results show a substantial improvement in fatigue life of the squeeze cast matrix when reinforced with fibre. Fatigue life increased with the increase in the volume content of fibre.

The increase in fatigue life of Al-Cu/SiC and Al-Mg/Al₂O₃ composites with 10% (volume) fibre was 68% and 43% respectively compared with the

fatigue life of the squeeze cast matrix alloy, whereas when compared with the gravity die cast matrix alloy the increase was 119% and 53% respectively. This significant improvement in fatigue life is possibly due to a reduced rate of fatigue crack propagation when the matrix is reinforced with fibre. This is despite the fact that fibres provide potential sites for crack initiation.

Hancock¹⁴⁸ suggested that in composites, fatigue cracks can initiate at the fibre/matrix interface in addition to those initiating at the free surfaces. Fractured fibres or fibre ends are also possible sites for crack initiation. Therefore crack initiation is easier in composites. However, under fatigue loading the stress in the matrix of a composite is lower than that which would occur in the unreinforced matrix, since the fibres carry more than a proportional share of the load. This is expected to delay crack initiation in the matrix. The actual ease of crack initiation will depend on the relative contributions made by the above-mentioned factors, and it is known that on the whole crack initiation is easier in composite materials. At the propagation stage, cracks are impeded and deflected by the fibre/matrix interface. A weak interface extends composite fatigue life* because failure will occur at the interface instead of the matrix resulting in crack branching¹⁴⁸. Plastic flow of a ductile, low-yielding matrix also blunts the crack's tip and minimises crack tip stresses. These factors act together to reduce the rate of crack propagation in composites. Hancock stated that *"most of the fatigue life of the composite appears to be spent growing cracks"*.

Forsyth et al¹¹⁸ reported a ten-fold reduction in the rate of crack propagation in a hot-rolled composite of Al/steel wire (14% volume). They also found that the most effective angle for the wires was 45° to the crack, not 90°.

* Axial fatigue life of composite reinforced with unidirectionally aligned continuous fibre.

Therefore in the present investigation random orientation of fibre, unlike its effect on tensile strength, would be expected to contribute more to improve fatigue life which might explain the high increase in fatigue life of the composites. The high ductility of the matrix alloys is also beneficial. For composites with 3D random fibre, the optimum strength of the interface is not clear. Although a weak interface is desired for fibres aligned near normal to the crack, fibres with weak interface in the plane of a fatigue crack could offer a low resistance path for the crack to propagate through. In addition, in the composites of the present investigation (short fibres) a weak interface would make crack initiation at fibre ends or at the interface easier. Hancock¹⁴⁸ described the ideal fatigue-resistant composite, reinforced with unidirectionally aligned continuous fibre, to be the one having a low-yield strength ductile matrix, and a high-yield strength brittle fibre, and a weak interface. With the exception of the strength of interface, which could be different for a 3D composite, the composite systems tested in the present investigation appear to fit Hancock's description of fatigue-resistant composites.

The strength of interfacial bonding, in the present investigation, was controlled to maximise the tensile properties (UTS). A similar investigation to optimise fatigue life of the composite could be the subject of a further investigation. During fracture studies there was no evidence of crack re-direction by interface failure, however, fatigue crack arrest or redirection by a fibre was occasionally observed, see Figures 8.1a and 8.2a.

The results in Table 14 for fatigue life of both composite systems, when graphically represented as in Figure 92, show an interesting feature. Composites with 2% (volume) fibre have a fatigue life comparable with that for the matrix, the increase in fatigue life appears to be proportional to the further increase in fibre content. Although this might be a mere typical fatigue scatter, it might be because at low content of fibre (2%), fibres were not capable of significantly

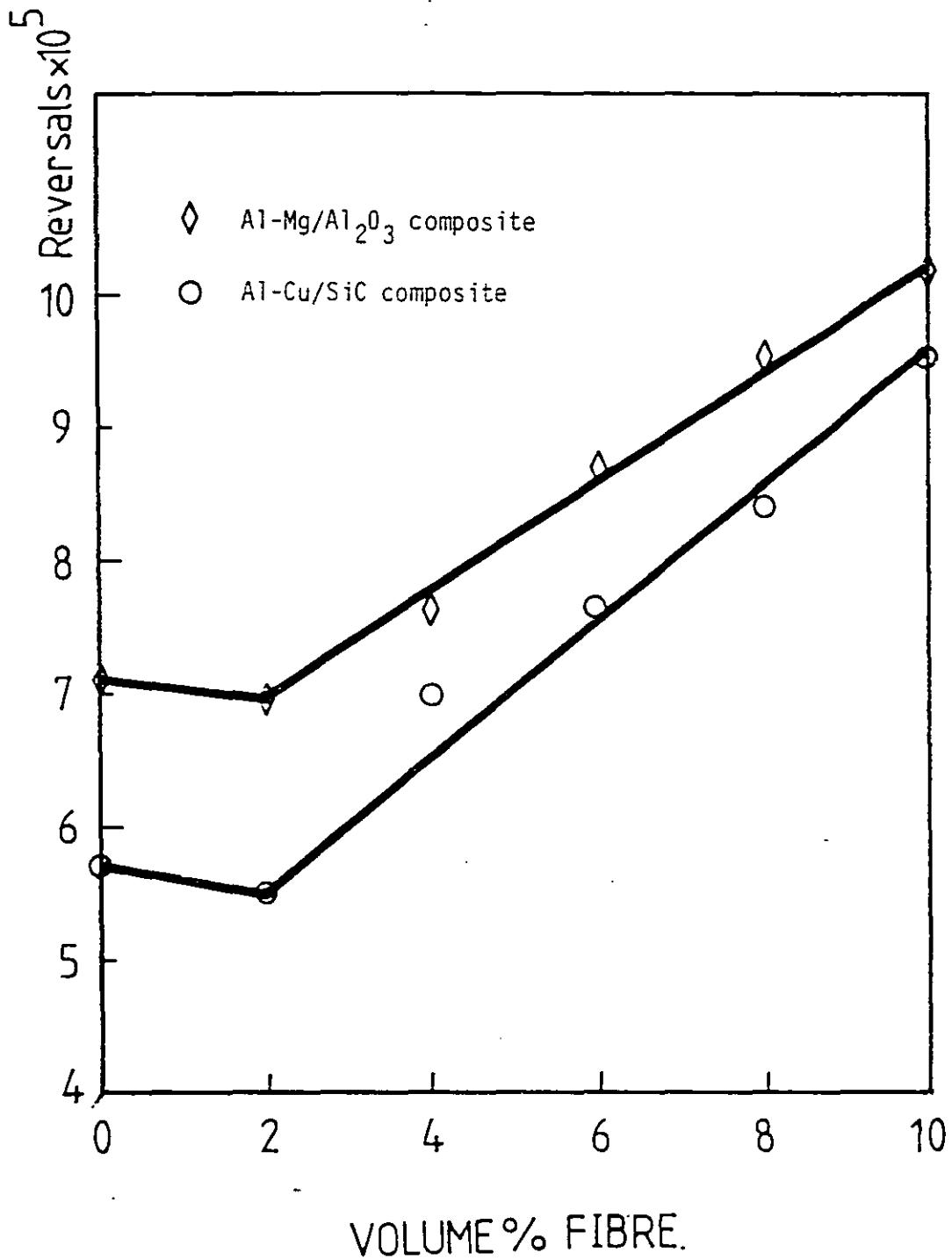


FIGURE 92: Effect of fibre volume percent on fatigue life of Al-Cu/SiC and Al-Mg/ Al_2O_3 composites

affecting the crack propagation rates. Nevertheless they provide a large number of possible sites for crack initiation. At higher contents of fibre, crack propagation would be severely restricted.

Although the number of possible initiation sites would increase with increasing fibre content, it is doubtful if there would be any increase in the number of cracks initiated or if there would be any acceleration of the process of cracks initiation.

6.10 TOOL WEAR

The results of the tool wear tests, on machining specimens of both Al-Cu/SiC and Al-Mg/Al₂O₃ composites, are shown in Figures 83 and 84 respectively and in Table 15. The increased tool wear when machining composites, compared with tool wear when machining the matrix alloys, is a direct result of the presence of the hard abrasive phase, i.e. fibre. The higher the content of that phase in the matrix, as results show, the higher is the wear of the machining tool as would be expected. It must be realised that this test was carried out in order to study the effect of the presence of fibre on tool wear, as a separate factor, and not to study tool life. In addition, cutting conditions (including tool geometry) were selected (see 4.2.10) for optimum surface finish rather than tool life. Therefore, tool wear can be reduced by selecting more suitable cutting conditions to optimise tool life and machining cost.

The approach to optimise machining conditions of composites might have to be different from that for conventional metals. Composites are different materials and need to be dealt with as such. A high feed rate and depth of cut combined with negative angles on a single point tool might reduce tool wear when machining composites. Squeeze casting usually produces a good surface finish and dimensional accuracy, therefore the need for machining a squeeze cast composite is reduced and, for some squeeze cast components, can be limited to the working surfaces. Therefore, although it is important to be aware of the machining difficulty of composites and to deal with this, it should not hinder their practical usefulness.

6.11 THERMAL STABILITY OF NICALON^(R) SiC FIBRE

The results of the tensile tests (room temperature) of Nicalon^(R) SiC fibre, when subjected to different heating cycles, are shown in Table 16. The measured average tensile strength of the as-received fibres was (273 kg/mm²) within the specified value of 250-300 kg/mm² (see 3.4, Table 1). This confirms the adequacy of the method used for testing (tensile) the fibre strength.

The tensile strength results for fibres exhibited some scatter. Strength of fibres decreased with an increase in fibre diameter. This phenomenon has been reported by Andersson and Warren¹²⁴, and Yajima et al¹²⁵. The scatter in tensile strength is usual for brittle solids, and in this case is possibly due to defects in the fibre such as the observed surface defects, see Figure 41a.

Andersson suggested that because fibres of higher purity, at production conditions, are produced when their diameter is small, their strength is higher. Yajima attributed this to residual carbon in fibres of larger diameter which reduces their strength.

Because of the observed scatter in fibre tensile strength and its variation with fibre diameter, comparison between certain heating cycles could not be made.

The results indicate that the tensile strength of fibres is reduced as a result of heating using all the heating cycle conditions. The reduction in strength was not dependent, at test conditions, on atmosphere (see cycles 3 and 5, in air and in vacuum). Higher reduction was measured at longer heating times, see cycles 1 and 2. Fibres heated using cycles 2 and 3 had a similar strength, therefore thermal shock was not a cause of reduction in fibre strength (see also cycles 6 and 7).

The Nicalon^(R) SiC fibre (polycrystalline β -SiC) were developed in Japan by Yajima and co-workers at the Mippon Carbon Co Ltd¹⁰⁸.

Andersson and Warren¹²⁴ schematically summarised the main stages in fibre production as shown in Figure 93.

At the final stage of fibre production, the polymer fibres (polycarbosilane) is converted to inorganic SiC. In the first stage of conversion, occurring during heating, organometallic and organic bonds, for example, Si-CH₃ and C-H, decompose, so that the polycarbosilane is converted into a material containing mainly Si-C bonds¹⁴⁹. Decomposition occurs gradually above 300°C and is completed at about 800°C¹⁴⁹, at this stage the structure is amorphous¹²⁴. In the second stage, on heating at above 800°C, crystallisation to β -SiC takes place. Crystallisation of β -SiC is accompanied by carbon precipitation.

Yajima et al¹²³ studied the relationship between the tensile strength of the SiC fibre produced and the heating temperature of the polycarbosilane at the final stage of production, their results are shown in Figure 94. Heating at a temperature higher than 1200°C causes the tensile strength to drop. This is accompanied by an increase in the volume fraction of crystallised β -SiC. They concluded that the tensile strength drops with further crystallisation of β -SiC because of the precipitation of carbon. Fibres produced by heating at 1500°C had a very low strength, a larger fraction of crystallised β -SiC and an "unexpectedly large quantity of excess carbon".

Therefore during production of SiC fibre, the mechanical properties of SiC are optimised by heating the polycarbosilane (100°C/hr) at the final stage of production, to about 1200°C¹²³.

This means that crystallisation of β -SiC, which can take place at \sim 800°C, is not complete. Thus, post-heating of these fibres at temperatures above \sim 800°C, as is the case in the present investigation, would make it possible

FIGURE 93:

Schematic diagram showing the main stages in the production of Nicalon SiC fibre (Ref 124)

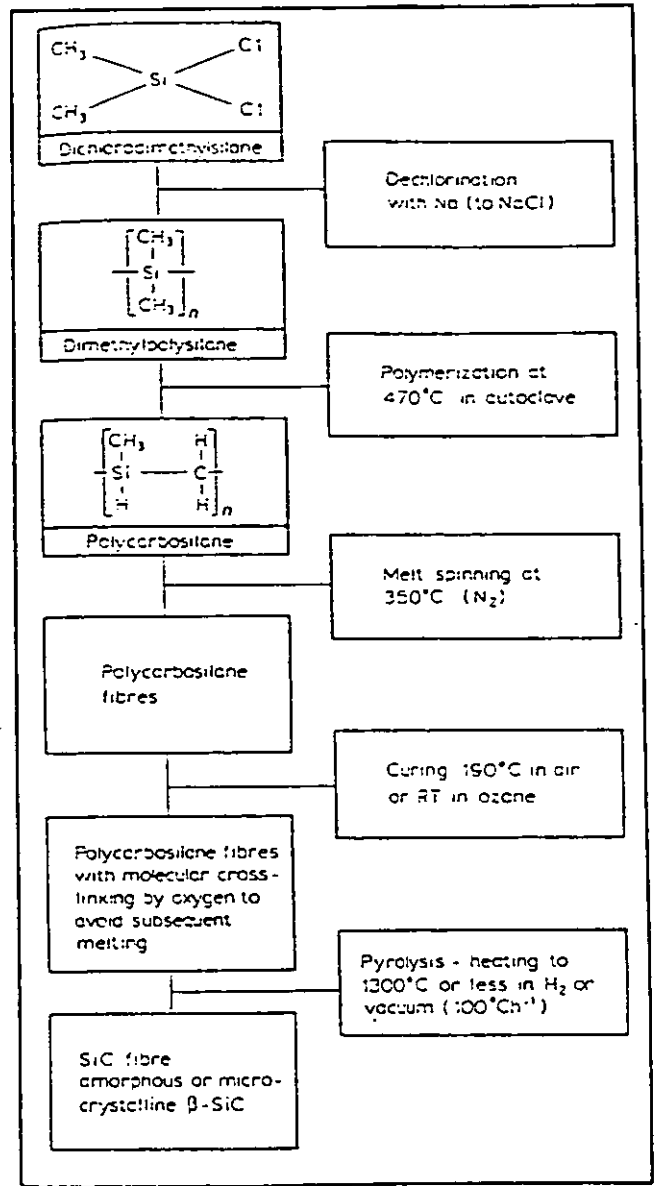
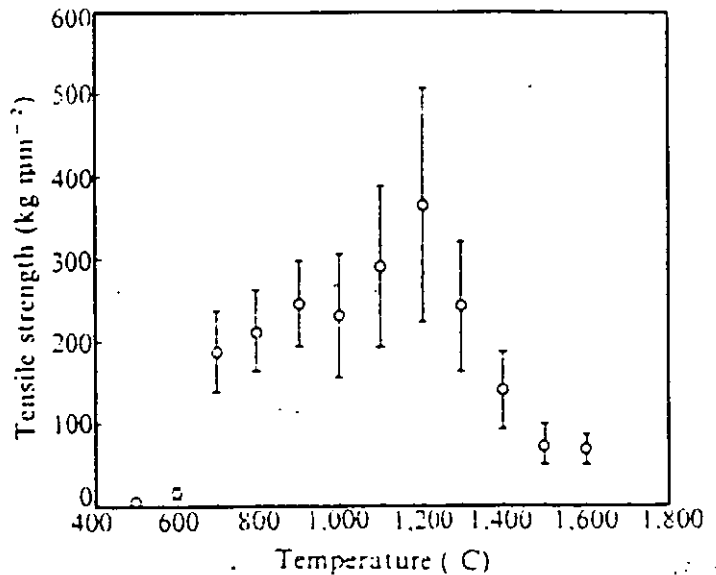


FIGURE 94:

Variation of the tensile strength of SiC fibre with heat-treatment temperature of the polycarbosilane fibre at the final stage of production (Ref 123)



for crystallisation of β -SiC to proceed resulting in precipitation of carbon and consequently reduced tensile strength. This is possibly the cause of the measured reduced strength of SiC fibre when heated, regardless of heating cycle or conditions. In support of this, the DTA analysis, Figure 85, showed a reaction peak at 1025°C , the reaction starts at $\sim 800^{\circ}\text{C}$.

CHAPTER VII

CONCLUSIONS

CHAPTER 7CONCLUSIONS

The concluding remarks refer to both Al-Cu/SiC and Al-Mg/Al₂O₃ composite systems unless otherwise stated.

1. Squeeze Casting

- i) Squeeze casting produced pore-free and fine equiaxed structures in both the Al-4.5 Cu and Al-3.75 Mg alloys.
- ii) The tensile strength and proof stress (0.1% offset) are substantially improved for both alloys when they are squeeze cast. At a solidification pressure of 188 MPa, the values of UTS and 0.1% proof stress are 60% and 35% (Al-Mg), 50% and 60% (Al-Cu) respectively higher than those for the gravity die cast alloys. The increase in ductility is more than two-fold.
- iii) The Al-Cu alloy has a 30% longer fatigue life when squeeze cast. Only 7% improvement in fatigue life is produced when the Al-Mg alloy is squeeze cast.
- iv) The properties of the squeeze cast matrix alloys are isotropic.
- v) Squeeze casting provided the structure and properties desired for short fibre reinforcement in 3D.
- vi) The time of solution treatment of the squeeze cast Al-4.5 Cu alloy was shorter compared with the time recommended (British Standard) for the equivalent gravity die cast alloy. However, further investigation is needed for this to be confirmed on a quantitative basis.

2. Composite Production

- i) Pretreatment of the fibres was necessary to remove the surface contamination so that the molten alloys wet the fibres.
- ii) Magnesium appeared to be a stronger wetting agent than copper for the system in which alumina fibres were used.
- iii) The presence of powdered material, released from the stirrer, consistently caused rejection of fibre from the melt.
- iv) It is not necessary to use coated fibres or employ special wetting agents in order to produce composites of enhanced quality by the method used in the present investigation. Commercial casting alloys of aluminium containing elements such as copper and magnesium provide adequate wetting for good interface bonds to be developed.
- v) During production of the composites, the chemical reaction between the fibre and the respective molten alloy must be controlled so that the maximum reinforcement of the matrix by the fibre is achieved.
- vi) A device was necessary to separate the matted fibre before their introduction into the melt.
- vii) The simple and cost effective method of composite production used in the present investigation yielded castings of sound structural quality with a uniform distribution of fibre, randomly oriented in three dimensions and with no significant fibre damage.
- viii) The structure and properties obtained in the squeeze cast composites have good reproducibility.

- ix) The method of fabrication has the potential for production of a wide range of component sizes and shapes.
- x) The arrangement for the inert-gas cover used during introduction of the fibres to the melt requires further development to ensure composite quality.

3. Composite characteristics

- i) Poor tensile properties were produced in the heat-treated composite castings of group III, most likely because of the reduced ductility of the matrix.
- ii) A thin copper-rich layer was observed around individual SiC fibres in the matrix of the Al-4.5 Cu/SiC composites. In addition, most fibres appeared to be associated with the α -Al/CuAl₂ eutectic phase.
- iii) The copper enrichment around the SiC fibre is thought to be due to solute rejection during solidification, helped by the hot zone at the metal/fibre interface.
- iv) The squeeze cast composites have pore-free matrices of fine equiaxed structure.

4. Properties of Composites with Controlled Contact Time

- i) A strong interfacial bond is developed between the fibres and the respective matrix alloy with minimum fibre degradation.
- ii) The addition of fibres results in substantial improvement in the tensile properties (room temperature) of the squeeze cast composites over and above that of the squeeze cast matrix alloy in particular, elastic modulus and proof stress (0.1% offset).

- iii) The increase in tensile property values is linearly proportional to the volume of fibre in the matrix.
- iv) Further improvement in tensile, and other properties, are highly likely by increasing the amount of fibre beyond the 10% by volume used in the present investigation.
- v) Thermal cycling, under the test conditions, had no significant effect on the tensile properties of the composites.
- vi) Fatigue life was significantly improved as a result of fibre addition over and above the initial improvement observed by squeeze casting the matrix alloy.
- vii) The reinforcement due to fibre addition was maintained at higher temperatures. At 250°C, both the composite systems with 10% volume fibre had elastic modulus and proof stress (0.1% offset) values comparable with those for the respective squeeze cast matrix at room temperature.

5. Theoretical Prediction of the Tensile Properties of the Composites

- i) The predicted values of composite strength obtained by using the equation for the modified rule-of-mixtures were found to be much lower than the actual experimental results.
- ii) A further modification of the modified rule-of-mixtures is proposed for predicting the strength of composites reinforced with short fibres.
- iii) The tensile strength values of the squeeze cast composites are in reasonable agreement (slightly higher) with the theoretical predictions when the modified rule-of-mixtures is further modified as proposed.

- iv) The measured values of the elastic modulus of the Al-Cu/SiC composites are in good agreement with the theoretical prediction of Christensen²⁵. The Al-Mg/Al₂O₃ composites had lower elastic modulus values than theoretically predicted, possibly because the actual elastic modulus of Al₂O₃ fibre is lower than the value quoted by the suppliers.

6. Machinability of Composites

- i) The presence of the hard and abrasive reinforcement fibres in the matrix alloys adversely affected the wear of the cutting tools.

7. Thermal Stability of Nicalon^(R) SiC Fibre

- i) The tensile strength of SiC fibre can be measured using a simple method which produced results that were in good agreement with the values quoted by the supplier.
- ii) The tensile strength (room temperature) of Nicalon^(R) SiC fibre is reduced when heated for 2 hours or more at 800°C or higher (900°C).

CHAPTER VIII

SUGGESTIONS FOR FURTHER WORK

CHAPTER 8SUGGESTIONS FOR FURTHER WORK

Metal matrix composites, in particular those reinforced with short fibre, are far from being completely understood and a great deal of research work is still needed. The following suggestions for further work are made in order of priority:

1. In the present investigation, composite castings with up to 10% (volume) fibre were produced. At higher fibre contents the 'liquid' composite became viscous and it was difficult to pour into the die cavity. Physically, the smaller the aspect ratio (λ/d) of the fibre, the higher is the fibre volume percentage that can be incorporated in a matrix (fibres randomly oriented in 3D). Higher contents of fibre would be expected to produce further improvement in the mechanical properties of the composites. However, the aspect ratio of the fibres should not be less than that required for the fibres to be loaded to their fracture strength at service conditions. With this point of view, it would be of interest to investigate the possibility of producing composites with increased amounts of fibre (3D) beyond the 10% (volume) used in the present investigation. These composites would be produced by the same technique and their properties examined.
2. It was found that pre-treatment (heating) of SiC fibre was necessary so that the fibres can be wet by the molten alloy. Because of the observed reduction of fibre strength on heating, it is important to investigate an alternative pre-treatment of these fibres to avoid the loss of fibre strength. Acid vapour pickling is a possible alternative that could be evaluated.
3. In the present investigation, it was shown that the fatigue life of the composite castings was substantially improved due to fibre

additions. However, fatigue life was determined at a fixed level of reverse-bend stress. Because fatigue life is possibly the most important single property of a material, since it is often stated that fatigue accounts for at least 90% of all service failures due to mechanical causes, it is essential to have more information and a better understanding of fatigue in composites (3D). Investigation of the following two aspects is considered to be a priority:

- i) The requirement of the level of bond strength (fibre/matrix) which would produce the maximum fatigue life for a composite (3D) has not been determined in the present investigation. Therefore it is suggested that the strength of fibre/matrix bonds which would produce the maximum fatigue life for composite castings with a given volume content of fibre should be investigated. Optimisation can be carried out in a similar manner to that reported in this investigation for tensile properties (see 3.6, Group V).
 - ii) Establish the S-N curve for composite castings and its variation with fibre content. This will provide designers with the necessary information.
4. Static loading is rarely experienced in actual service conditions, dynamic loading is more predominant. Investigation into the fracture toughness of composites is of particular importance. The toughness of a material indicates its capability to resist fracture under dynamic, as well as static, loading by inhibiting crack propagation. In addition, toughness (fracture surface energy) is often used as a design parameter to calculate the strength of structural components under service conditions in the presence of the inevitable flaws in materials.
 5. Investigations into the ideal fibre/matrix combination in order to optimise the final composite properties by the selection of alloying

elements and their concentration in the alloy. For example, Fukunaga et al¹¹⁵ reported that maximum tensile strength was obtained for an Al/SiC composite at a copper concentration of 1%. For a similar system Kohora¹⁵⁰ reported that the presence of silicon as an alloying element reduces the chemical attack on the fibre (SiC) by the molten aluminium and consequently degradation of fibre strength. Ideally the alloy (to be reinforced with short ceramic fibre) should be both strong and highly ductile. In the molten state it should wet and react with the fibres at a low rate so that strong bonds can be developed with minimal degradation of the fibres. A low rate of reaction (between the fibre and the melt) will also extend the permissible time of contact between the two phases which would be beneficial for composite production.

REFERENCES

REFERENCES

1. Javitz, A.E.
Design, January 1965, 18, p64.
2. Berghezan, A.
Composites, 1972, 3, (5), p200.
3. Kelly, A.
Sci. American, 1967, 217, (B), p161.
4. Berghezan, A.
Nucleus, 1966, 8, (5), 1. (Nucleus S.A. Editeur: 1 Rue Chalgrin, Paris, 16e).
5. Berghezan, A.
Conf. faite au stage d'etudes: les Materiaux Nouveaux, Paris, CPT 80, Av. 18 Juin 1940-92500 Rueil-Malmaison.
6. McDaniels, D.L. et al.
Metal Progress, 1960, 78, (5), p118.
7. Dietz, A.G.H.
Int. Science and Technology, August 1964, p58.
8. Kelly, A. and Tyson, W.R.
'Fibre Strengthened Materials", Second International Materials Symposium, Univ. Calif. June 1964.
9. McDaniels, D.L. et al
Stress-strain behaviour of tungsten fibre-reinforced copper composites, 1963a, NASA TND 1881.

10. Kelly, A. and Davies, G.J.
Met. Rev., 1965, 10, (37), p1.
11. Piehler, H.R.
Trans. AIME, 1965, 233, p12.
12. Kreider, K.G.
Composite Materials, Vol IV, Ed. K.G. Kreider, Academic Press,
1974, pp 1-35.
13. Cox, H.L.
Brit. J. App. Phys., 1952, 3, p72.
14. Kelly, A. and Tyson, W.R.
High strength materials. Ed. V.F. Zakay, J. Wiley and Sons,
1965, pp 578-602.
15. Sun, C.T. et al.
Advances and Trends in Structures and Dynamics Symposium. Univ.
Florida, 1984.
16. Pih, H. and Sutlitt, D.R.
Developments in Theoretical and Applied Mechanics. April 1970,
5, p88.
17. Norio, S. et al.
J. Mater. Sci., 1984, 19, p1145.
18. Riley, V.R.
J. Compos. Mater. 1968, 2, p436.
19. Fukuda, H. and Chou, T.
J. Mater. Sci., 1981, 16, p1088.

20. Sun, C.T. and Wu, J.K.
J. of Reinforced Plastics and Composites. 1984 (April), 3,
p130.
21. Bowyer, W.H. and Bader, M.G.
J. Mater. Sci., 1972, 7, p1315.
22. Curtis, P.T. et al.
J. Mater. Sci., 1978, 13, p377.
23. Fukuda, H. and Chou, T.
J. Mater. Sci., 1982, 17, p1003.
24. Cox, H.L.
Brit. J. Appl. Phys. 1952, 3, p72.
25. Christenssen, R.M. and Waals, F.M.
J. Compos. Mater. July 1972, 6, p402.
26. Lee, L.H.
Polymer Eng. Sci., 1969, 9, p213.
27. Krieder, K.G.
Composite Materials, Vol IV, Academic Press, 1974, p30.
28. Hikami, F. and Chou, T.
J. Mater. Sci., 1984, 19, p1805.
29. Levitt, A.P.
Whisker Technology, ed. Wiley Interscience, N.Y., 1970, p245.
30. Divecha, A. et al.
Maipar Incorporated, Report on Silicon Carbide Whisker-Metal Matrix
Composites, Contract AF33 (615) 531, 1967 (January).

31. Landis, H. et al.
SAMPE, July 1981, p19.
32. Warnes, L.A.
Ministry of Aviation, Explosive Research and Development Establishment, Report ERDE 17/R/65, July 1965.
33. Sutton, W.H. and Feingold, E.
General Electric Company, Materials Science Research, Vol. 3, Plenus Press, 1966.
34. Wolf, S.M. et al.
Army Materials and Mechanics Research Centre, AMRA, TR66-19, July 1966.
35. Warren, R. and Andersson C.H.
Composites, April 1984, 18, (2), p101.
36. Chorne, J. et al.
General Electric Company, Contract No. W66-0443-d, January 1967.
37. Cheskis, H.P. and Heckel, R.W.
Dresel Institute of Technology, 70th Annual Meeting of the ASTM, June 1966.
38. Mullin, J. et al.
J. Compos. Mater. January 1968, 2, (1), p82.
39. Davis, L.W.
ASTM STP 427, 1967, p69.
40. Parratt, N.J.
ERDE Waltham Abbey, England, 58th Annual Meeting.

41. Petrasek, D.W. and Weeton, J.W.
Trans. Met. Soc., 1964, 230 (8), p977.
42. Delai, A.J. et al.
Am. Ceramic Soc., 68th Annual Meeting, May 1966.
43. Shaver, R.G. and Withers, J.C.
10th Refractory Compos. Working Group Meeting, Atlanta, 1965.
44. Alexander, J.A. et al.
Proc. 10th SAMPE Symp., San Diego.
45. Rajagopal, S.
J. Applied Metal Working, ASM, 1981, 1, (4), p3.
46. Plyatskii, V.M.
Extrusion Casting, ed. Adolph W., New York, Primary Sources,
1965.
47. Kaneko, Y. et al.
Die Cast Eng., May-June 1979, p26.
48. Anon.
Engineering (London), February 1984, 224, (2), p94.
49. McGuire, M.F.
Diesel and Gas Turbine Progress, September 1979, p59.
50. Anon.
Foundry Trade Journal, March 14th, 1985, p164.
51. Franklin, J.R. and Das, A.A.
Brit. Foun. April 1984, 77, (3), p150.

52. Das, A.A. and Chatterjee, S.
The Metallurgist and Materials Technologist, March 1981, p137.
53. Benedyk, J.C.
SME, Technical Paper No. CM71-840, 1971.
54. Chatterjee, S. and Das, A.A.
The British Foundryman, November 1984, 65, p420.
55. Chatterjee, S. and Das, A.A.
Ibid., 1973, 66, p118.
56. Williams, G. and Fisher, K.M.
Metal Technology, July 1981, 8, (263), Paper No. 24.
57. Bidulya, P.N.
Russ. Cast. Prod., 1964, 396, p150.
58. Weinberg, F.
Met. Soc., Univ. Warwick, 15-17 Sept. 1980, Paper 23.
59. Lipehin, T.N. and Bykov, P.V.
Russ. Cast Prod. 1973, 109
60. Kaneko, Y. et al.
Foundry Trade Journal 1980, 148, 397.
61. Epanchintsev, O.G.
Russ. Cast Prod., January 1972, p34.
62. Livey, D.T. and Murray, P.
Plainsee Proc., 2nd Seminar, 1956, p325.
63. Carnahan, R.D. et al.
J. Amer. Ceram. Soc., 1958, 41, p343.

64. Prabriputaloong, K. and Piggott M.R.
Surface Sci., 1974, 44, p585.
65. Nicholas, M.
J. Mater. Sci., 1968, 3, p571.
66. Wolf, S.M. et al.
Chem. Eng. Progr., 1966, 62, p74.
67. Champion, J.A. et al.
J. Mater. Sci., 1969, 4, p39.
68. Brennan, J. and Pask, J.A.
J. Amer. Ceram. Soc., 1968, 51, p569.
69. Allen, B.C.
Trans. AIME, 1963, 227, p1175.
70. Kohler, W.
Aluminium, 1975, 51, p443.
71. Calow, C.A. and Wakelin, R.J.
J. Inst. Metals, 1968, 96, p147.
72. Mehrabian, R. et al.
Metallurgical Transactions, August 1974, 5, p1899.
73. Mahar, R.L. et al.
Technical Report AFML-TR-68-100, May 1968.
74. Mehan, R.L. and Feingold, E.
J. Mater., 1967, 2, p239.
75. Mehan, R.L.
ASTM, STP438, 1968, p29.

76. Mehan, R.L.
J. Comp. Mater., 1970, 4, p90.
77. Calow, C.A. and Moore, A.
Inst. of Metallurgists, Practical Metallic Composite, Spring Meeting, March 1974, 70-174Y, Series 3, pB17.
78. Gelderloos, D.G. and Karasek, K.R.
J. Mater. Sci. Letters, 1984, 3, p232.
79. Imich, G.
United States Patent, No. 2,793,949, May 1957.
80. Champion, A.R. et al.
2nd Int. Conf. Compos. Mater., Toronto, Canada, April 16-20, 1978.
81. Levi, C.G. et al.
Metallurgical Trans. A., May 1978, 9A, p697.
82. Pai, B.C. et al.
Mater. Sci. and Engineering, 1976, 24, p31.
83. Mortimer, D.A. and Nicholas, M.
J. Mater. Sci., 1970, 5, p149.
84. Dean, A.V.
J. Inst. Met., 1967, 95, p79.
85. Alexander, J.A. and Stuhrke, W.F.
ASTM Spec. Tech. Pub. No. 427, 1967, p34.
86. Calow, C.A. and Moore, A.
J. Mater. Sci., 1972, 7, p543.

87. Jech, R.W. et al.
Reactive Metals, 2nd Edition, Ed. W.R. Clough, Interscience,
New York, 1959, p109.
88. Shimizu, H. et al.
SAE Meeting, Los Angeles, October 2-6, 1967, Paper 670861.
89. Freedman, A.H.S.M.E.
ASM Westec Conf. March 1970.
90. Hamilton, C.H.S.M.E./A.S.M.
Ibid.
91. Tressler, R.E. and Moore, T.L.
SME/ASM Westec Conf., March 1970.
92. House, L.
MSc Thesis, The George Washington Tinanium, May 1979.
93. Metacalfe, A. and Klein, M.
Composite Materials, Vol. 1, Academic Press, New York, 1974,
pp 127-158.
94. Shorshorov, M.
J. Mater. Sci., 1979, 14, p1850.
95. Ochiai, S. and Murakami, Y.
Ibid., p831.
96. Landis, H. et al.
SAMPE, July 1981, p19.
97. Cratchley, D. and Baker, A. A.
Metallurgia, 1964, 69, p153.

98. Kreider, K.G. and Baker, A.A.
Metallurgia, 1964, 69, p153.
99. Anon.
Foundry Trade Journal, February 2, 1984, p62.
100. Anon.
Automotive Engineer, Oct/Nov. 1982, 7, (5), p50.
101. A.E. PLC, UK Patent GB2 135 222A, 1984.
102. A.E. PLC, UK Patent, GB2 106 433A, 1983.
103. A.E. PLC, UK Patent, GB2 133 330A, 1984.
104. Imperial Clevite Inc.
GB 2 090 779A, 1982.
105. Imperial Clevite Inc.
GB 2 090 780A, 1982.
106. Champion, A.R. et al.
2nd Int. Conf. Compos. Mater. Toronto, Canada, April 16-20, 1978.
107. Ohingra, A.K et al.
Proceedings of the First Metal Matrix Composite Workshop,
Inst. Defence Analysis, Washington, September 1975, p C-501.
108. Yajima, S. et al.
Composite Materials, Ed. Kawata, K. and Akasaka, T., Proc. Japan-
US Conference, Tokyo, 1981.
109. Lloyd, D.J.
J. Mater. Sci., 1984, 19, p2488.

110. Levi, C.G. et al.
Rheocasting, Proceedings of a Workshop, Army Materials and Mechanics Research Centre, 3-4 February 1977, MCIC Report No. 78-35, Columbus, Ohio 43201, Columbus Laboratories 505, King Avenue, Ed. French, R.D. and Hodi, F.S. 1978, p41.
111. Levi, C.G. et al.
Metallurgical Transactions A, May 1978, 9A, p697.
112. Surappa, M.K. and Rohatgi, P.K.
J. Mater. Sci., 1981, 16, p983.
113. Fukunaga, H. and Kuriyama, M.
Bulletin of the JSME, May 1982, 25, (203), p842.
114. Fukunaga, H. and Komatsu, S.
Bulletin of the JSME, October 1983, 26, (22), p730.
115. Fukunaga, H. and Ohde, T.
Proc. 47th Int. Conf. Compos. Mater., Progress in Science and Engineering Composites, Tokyo, 1982, p1443.
116. Fukunaga, H. and Ohde, T.
Progress in Science and Engineering of Composites, Tokyo, 1982, 2, pp 1443-1450.
117. Nakata, E. et al.
Rept. Cast. Res. Lab. Wasda University, 1983, 34, p27.
118. Forsyth, P.J.E. et al.
Appl. Mater. Res. 1964, 3, p223.
119. Baker, A.A.
J. Mater. Sci., 1968, 3, p412.

120. Mordike, B.L. et al.
Conf. Metallurgy of Light Alloys, Inst. of Metallurgists,
24-26 March 1983, Loughborough University, p65.
121. Warren, R. and Andersson, C.H.
Part. II, Composites, April 1984, 15 (2), p101.
122. Gibson, P.R.
PhD Thesis, Loughborough University, 1984, p342.
123. Yajima, S. et al.
Nature, June 21, 1979, 279, p706.
124. Warren, R. and Andersson, V.H.
Part I, Composites, January 1984, 15, (1), p16.
125. Yajima, S. et al.
Am. Ceram. Soc. Bull. 1976, 55, p1065.
126. Epanchintsev, O.G.
Russ. Cast Prod., 1972, p34.
127. Lipchin, T.N. and Tominskaya, M.A.
Metalloved Term Obraka, Metal., October 1980, 10, p37.
128. Epanchintsev, O.G.
Russ. Cast Prod. 197, p34.
129. Campbell, J.
Iron and Steel Inst. Spec. Report, 1968, 110, p18.
130. Asaeda, T. et al.
Bull. JSME, April 1977, 20, (142), p489.

131. Nomoto, M. et al.
J. Jpn. Inst. Light Met., April 1980, 30, (4), p212.
132. Kaneko, Y. et al.
Foundry Trade Journal, February 28, 1980, p397.
133. Cohen, W. and Ishai, O.
J. Compos. Mater. 1967, 1, p390
134. Fukunaga, H. and Goda, K.
Bull. JSME, January 1985, 25, (235), p1.
135. Kondic, V.
Metallurgical Principles of Founding, Edward Arnold Ltd.,
London, 1968, pp 83-84.
136. Marshall, R.C. et al.
Silicon Carbide, Proc. 3rd Int. Conf. on Silicon Carbide,
Miami, Florida, 17-20 September 1973, pp 669-671.
137. Carpenter, H. and Robertson, J.M.
Metals, Vol. I, Oxford University Press, London, New York,
Toronto, 1939, p29.
138. Zeeleder, A.V.
The Technology of Aluminium and its Light Alloys, High Duty
Alloys Ltd., Slough, Bucks, 1948, p92.
139. Shorshorov, M. Kh. et al.
J. Mater. Sci., 1979, 14, p1850.
140. Sutton, W.H. and Feingold, E.
Mater. Sci. Res., 1966, 3, p577.

141. Khan, I.H.
Metallurgical Trans. A., September 1976, 7A, p1281.
142. Klein, M.J.
Composite Materials, Vol. I, Ed. A.G. Metcalfe, Academic Press,
New York and London, 1974, p208.
143. Kreider, K.G. and Prewo, K.M.
Composite Materials, Vol. 4, Ed. K.G. Kreider, Academic Press,
New York and London, 1974, p430.
144. Takao, Y. et al.
Int. J. Solids Structures, 1982, 18, (8), p723.
145. Divecha, A.P. and Fishman, S.G.
Conf. Mechanical Behaviour of Materials, 20-24 August 1979,
Vol. 3, ICM3, Cambridge, England, p351.
146. Dieter, G.
Mechanical Metallurgy, 2nd Ed. McGraw-Hill, Kogakusha Ltd.,
1976, p51.
147. Sutton, W.H. and Chorne, J.
Fibre Composite Materials, ASM, Metals Park, Ohio, 1965, p178.
148. Hancock, J.R.
Composite Materials, Vol. 5, Ed. Lawrence J. Broutman, Academic
Press, 1974, pp 371-417.
149. Yajima, S. et al.
Nature, June 24, 1976, 261, p683.
150. Kohara, S.
"Composite Materials", K. Kawata and T. Akasaka, Eds.,
Proc. Japan-US Conference, Tokyo, 1981, p 224.

APPENDICES

A P P E N D I X I

APPENDIX IA1.1 PRESS LOAD TEST

A 50 tons single action hydraulic press (Turner press) with facility for load adjustment was used for squeeze casting. Press load is shown on a dial. A test was carried out to examine the functioning of the press at variable load setting. A load cell (NCB/MRE Type 440) of 10 volts input and output of 24 mV corresponding to 1000 kN was used to measure the actual press load. Input to the load cell was provided by a stabilised power supply unit (Farnell Type E30/2). The load cell output was measured using a chart recorder which was first calibrated.

Test results can be summarised as follow:

Press Load (tons)	
Set	Measured
10	0.63
15	15.09
20	19.98
30	29.7
40	39.7
>40	Press failed to function

Outside the range 15 tons - 40 tons the press failed to function properly and was used only at loads within that range.

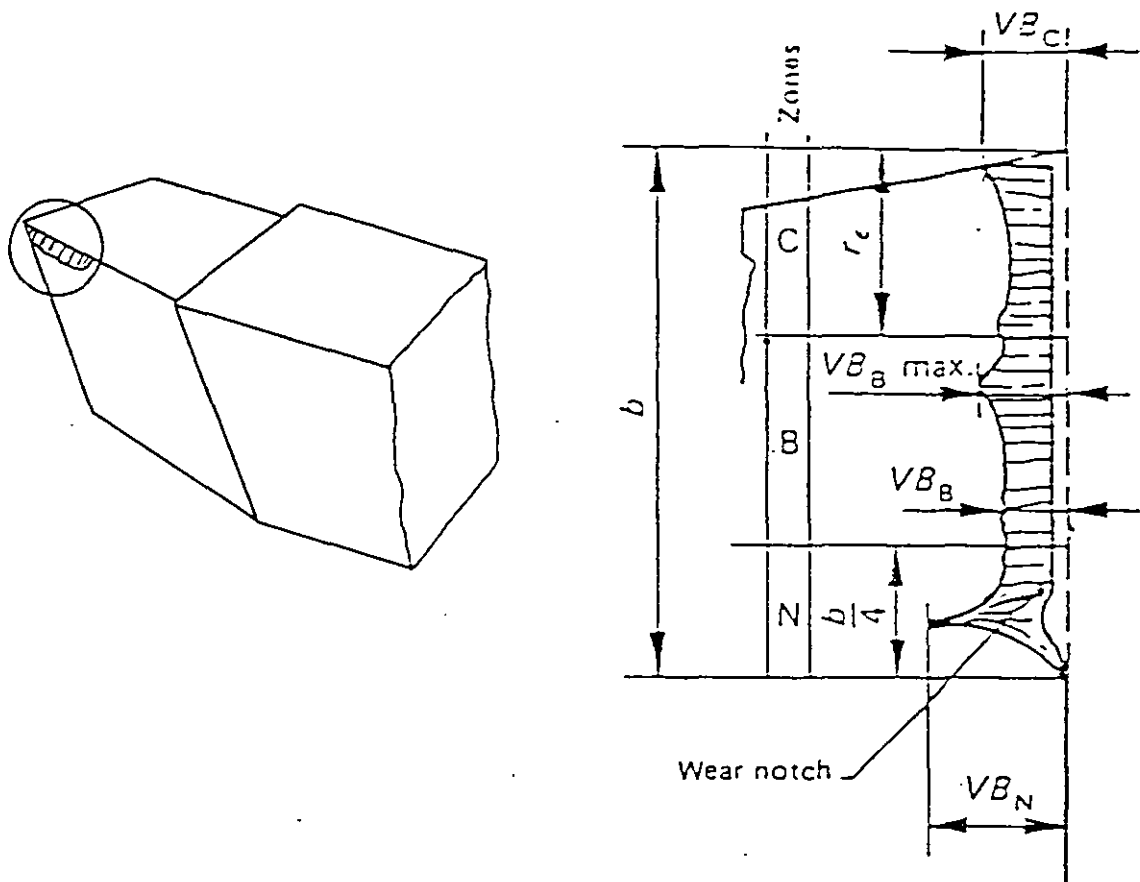


FIGURE A1.1 FLANK WEAR ON A SINGLE-POINT TOOL (TURNING)

A1.2 FLANK WEAR OF A TURNING TOOL*

Flank wear is a type of tool wear that takes place at the major flank surface of cutting tools as shown in Figure A1.1. VB_B is the average width of the flank wear land and can be taken as a tool life criteria if the flank wear land is considered to be regularly worn in zone B. $VB_B = 0.3 \text{ mm}$ for sintered carbide tools.

* Extracted from: BS 5623:1979
ISO 3685:1977

VB_{Bmax} is the maximum width of the flank wear land and can be taken as tool life criteria if the flank wear is irregularly worn.

$VB_{Bmax} = 0.6 \text{ mm}$ for sintered carbide tools.

A P P E N D I X I I

AE Developments Ltd Memorandum

From J.R.M. Hood

Reference JRME/MEC

To A.J. Clegg
cc A.R. Baker

Date 20.12.84

Project No. 76612

SEM EXAMINATION OF THREE LMS MELT SAMPLES

Three samples scooped from the top of LMS melts were supplied as follows:-

- Sample 1 - Reaction product scummed from a melt left under a dry, oxygen-free nitrogen cover for 20 minutes at 760°C in an amolite crucible.
- Sample 2 - Material from a melt kept under the same conditions as sample 1, but in a graphite crucible.
- Sample 3 - Material from a melt kept under the same conditions as sample 1, but to which air was introduced at the same rate as nitrogen in sample 1 (6 litres/minute).

Sample 1 consisted of a white compound of non-metallic appearance. Samples 2 and 3 had the appearance of thin oxide coatings on the melt.

The three samples were analysed in the scanning electron microscope by means of energy-dispersive and wavelength dispersive X-ray spectroscopy.

Energy Dispersive Spectroscopy

The energy dispersive equipment at AED is capable of analysing elements of atomic number greater than 9. Therefore, any analyses performed in this way neglect the presence of elements such as oxygen, nitrogen and carbon.

The analyses spectra obtained for samples 1, 2, 3 and a section through sample 3 are illustrated in Figures 1-4 respectively. It is evident from these figures that sample 1 contains a very high level of magnesium compared with the LMS melt alloy. Quantitative analyses of these spectra are listed in Table I. The analysis of the melt alloy conforms approximately to that carried out at Loughborough. All of the samples supplied exhibit increased concentrations of magnesium on the surface.

Wavelength Dispersive Analysis

The energy dispersive analysis facility at AED is augmented by wavelength dispersive equipment capable of analysing boron, carbon, nitrogen and oxygen. The three samples were each analysed for carbon, nitrogen and oxygen.

Each of the samples was found to contain a small amount of carbon. However, since the scanning electron beam deposits some carbon at high currents the amount detected was not considered to be significant.

Small amounts of nitrogen were detected in each sample, approximately 2.5% by weight in samples 2 and 3 and 4.5% in sample 1. These figures were obtained by comparison with a known sample of titanium nitride. A typical spectrum for nitrogen (obtained from sample 3) is illustrated in Figure 5. The amounts detected are consistent with the melts having been kept in contact with nitrogen.

- 2 -

Significant amounts of oxygen were also detected in each of the samples, sample 1 containing approximately three times the amount found in samples 2 and 3. The low specimen current in sample 1 (1.8×10^{-7} Amps.) compared with samples 2 and 3 (12×10^{-7} Amps.) for a beam current of 15×10^{-7} Amps. indicates that the first sample consists entirely of non-metallic compounds, mostly oxides. The approximate amount of oxygen in sample 1 can, therefore, be calculated by stoichiometry, Table II.

Conclusions

Sample 1 consists mainly of magnesia (71%) and alumina (25%). Samples 2 and 3 exhibit oxide coatings which are magnesium rich. Small amounts of nitrogen were detected in each sample.

JRM Hood.

J. R. M. HOOD

TABLE I
ENERGY DISPERSIVE X-RAY ANALYSES

Element	Sample 1	Sample 2	Sample 3	Alloy (LHS)		LHS Specification
				AED	Toughborough	
Hg	65.1	8.1	14.9	3.1	3.75	3.0 - 6.0
Al	28.3	87.3	81.0	93.5	Rem.	Rem.
Si	0.1	2.1	3.1	2.2	-	0.3 max.
Mn	0.2	0.7	1.0	0.6	0.67	0.3 - 0.7
Fe	0.6	1.8	2.4	0.5	0.27	0.6 max.
Cu	1.6	0.0	0.3	0.0	-	0.1 max.
Zn	4.0	0.0	0.4	0.2	-	0.1 max.

TABLE IICOMPOSITION OF SAMPLE 3

Oxide	% by weight
Mgo	71.0
Al ₂ O ₃	24.6
Others eg FeO, MnO	4.4

FIGURE 1

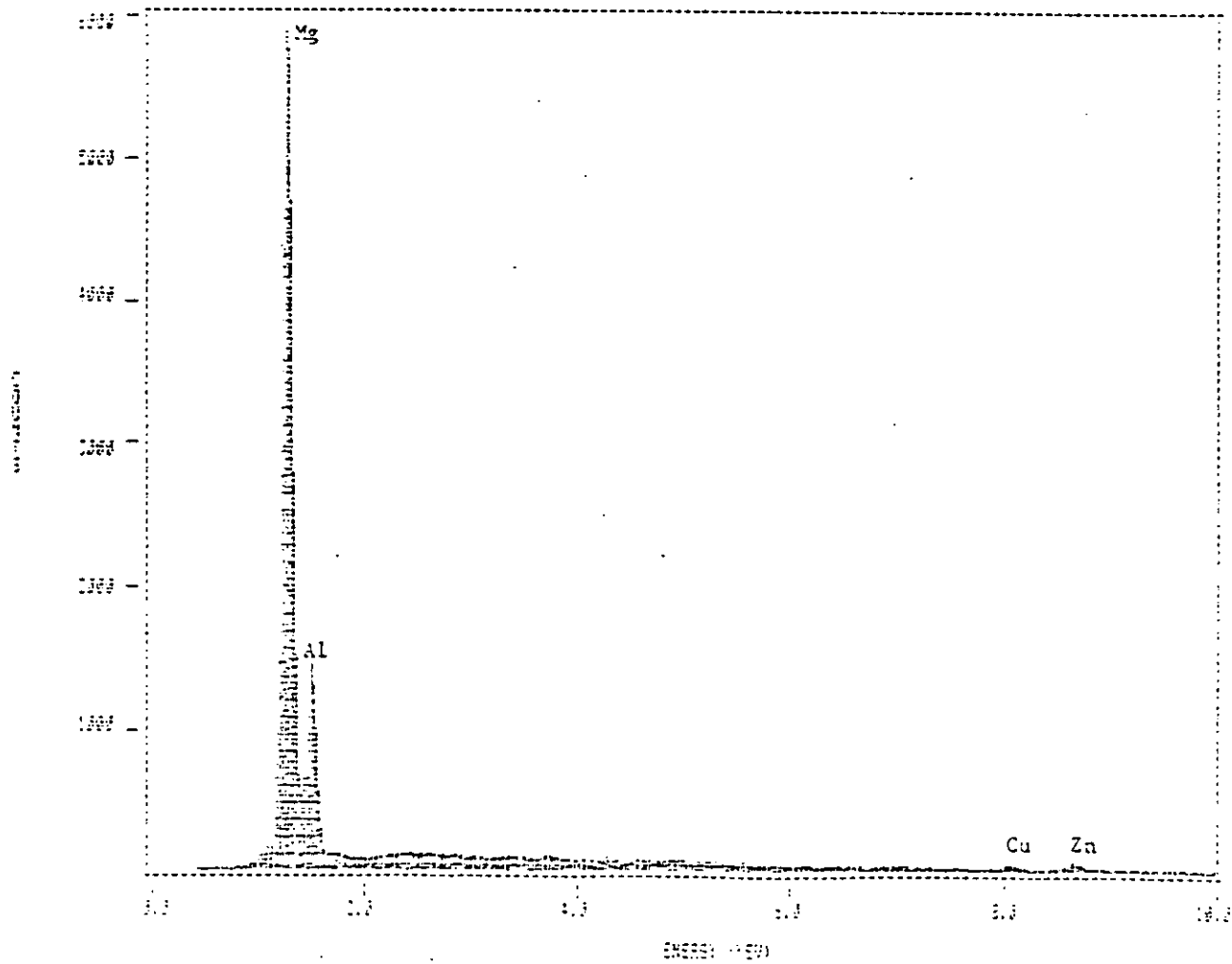
SAMPLE 1

PROGRAM NAME

SYSTEM FILE NAME

==

==



0) PIGTI

FIGURE 2

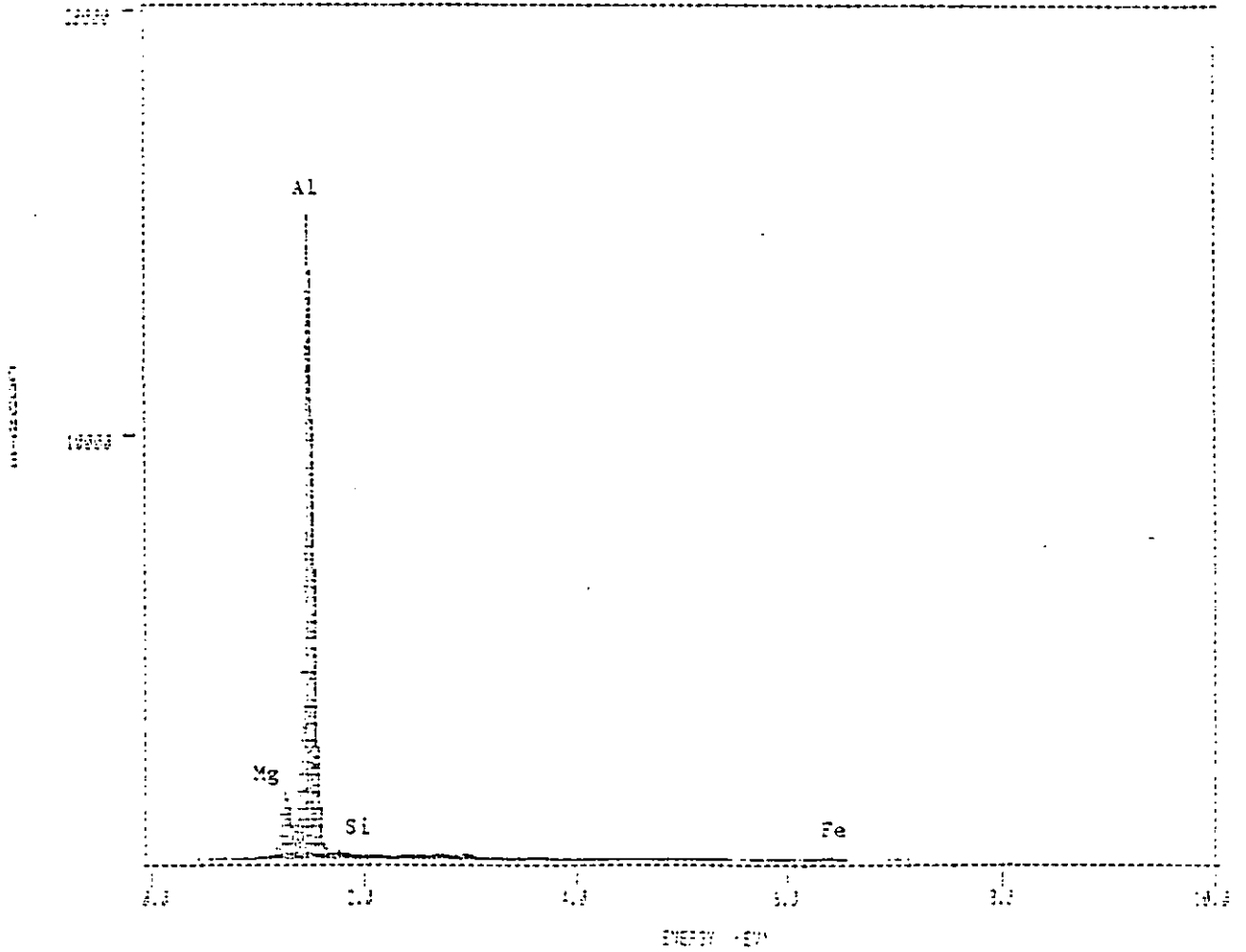
SAMPLE 2

SPECTRUM LABEL

SPECTRUM FILE NAME

12

12



CP16111

FIGURE 3

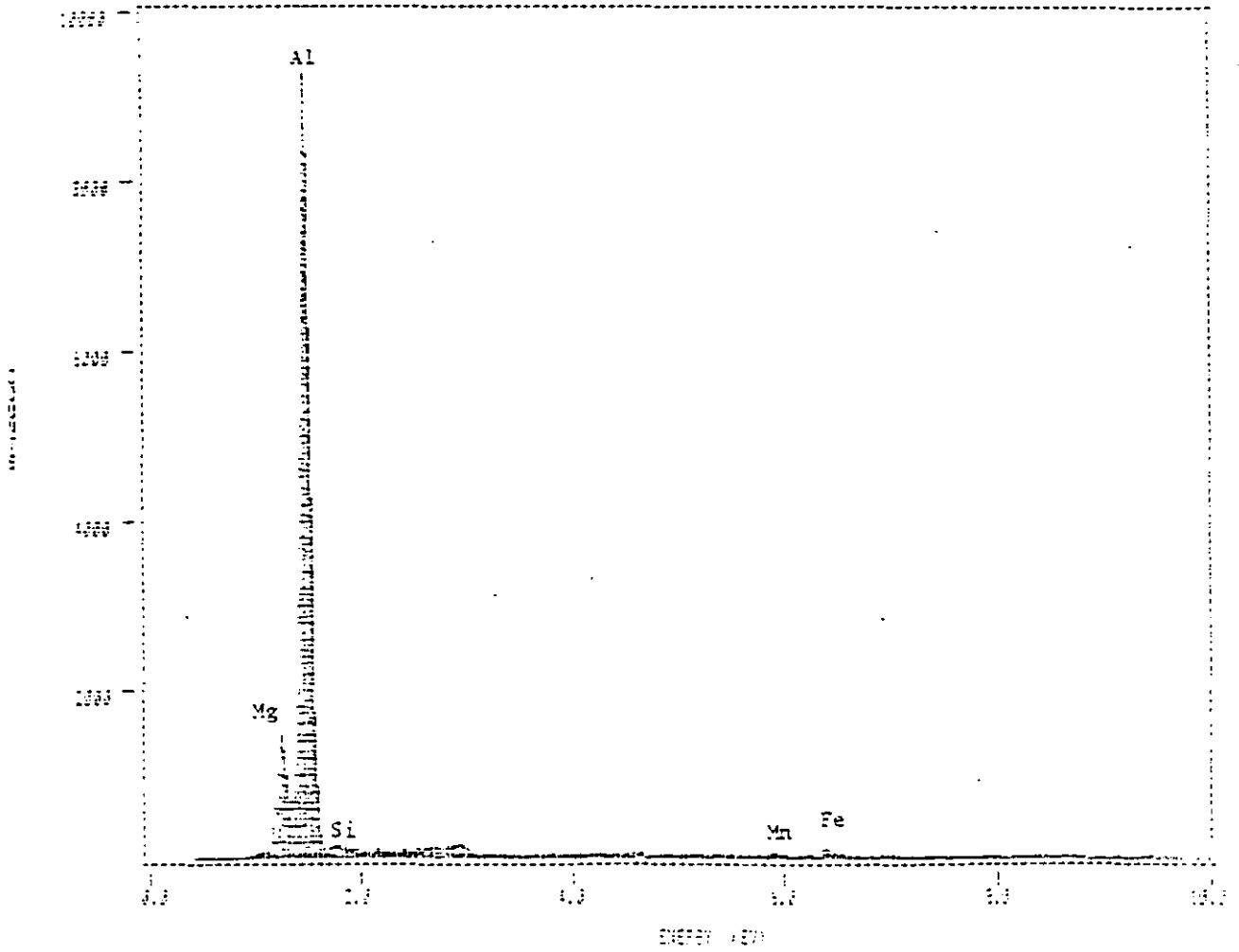
SAMPLE 3

SPECTRUM LINE

SPECTRUM FILE NAME

11

01 71



OF DIGIT

FIGURE 4

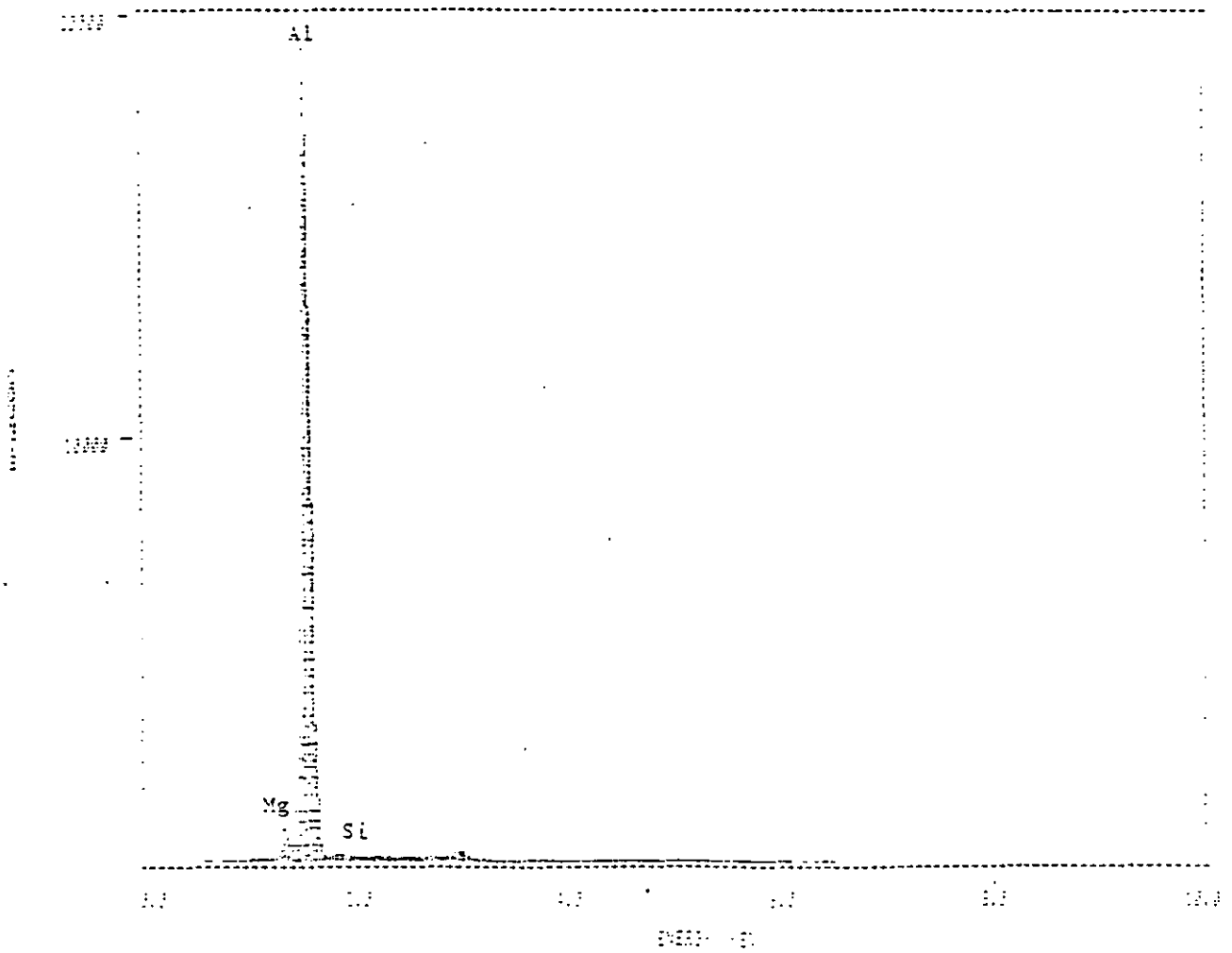
MOLT (EXAMPLE 3)

METER LANE

SPECTRA FILE NAME

M

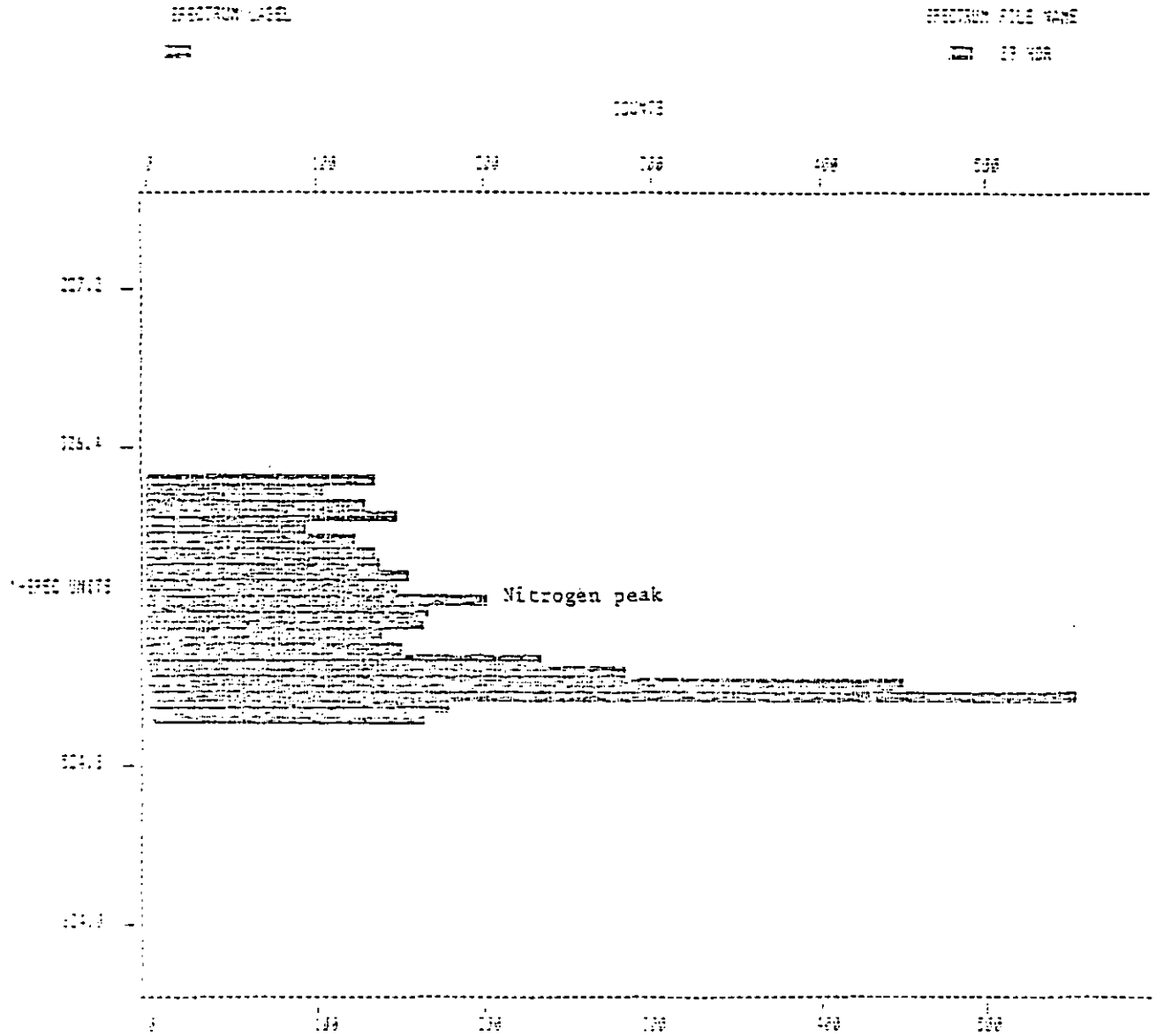
M 7



3 DIGIT

FIGURE 3

NITROGEN SPECTRUM FOR SAMPLE 3



(X-RAY)

A P P E N D I X I I I

TABLE A3.1: Effect of solidification pressure on the tensile properties of the cast Al-4.5 Cu matrix alloy (room temperature)
(Values in brackets represent the averages)

Solidification Pressure MPa	UTS MPa	0.1% PS MPa	Elastic Modulus GPa	Elongation %	Reduction in Area %	Remarks
0.1 (gravity die cast)	131	69		7.5	7	
	128	72		7	6.5	
	128	68		6.5	6	
	129	70		7	6.5	
	(129)	(69.75)		(7)	(6.5)	
70	168	92		11	11	
	165	88		11	10.5	
	164	89		12.5	11.5	
	166	90		12.5	11	
	(165.75)	(89.75)		(12)	(11)	
94	178	99		13	12.5	
	176	101		13.5	13	
	179	98		13	12.5	
	176	97		13.7	13	
	(177.25)	(98.75)		(13.3)	(12.75)	
140	191	108		16	15	
	190	107		15.5	15	
	187	106		14.5	14	
	189	107		15	14.5	
	(189.75)	(107)		(15.25)	(14.6)	
188	195	112		16	15.5	
	192	110		15.5	15	
	194	109		14.5	14	
	192	111		16	15	
	(193.25)	(110.5)		15.5)	(14.9)	
(Sand cast)	107	65		5	4	
	106	64		5.5	4.5	
	108	53		6	5	
	104	67		5.5	4	
	(106.25)	(64.75)		(5.5)	(4.35)	

TABLE A3.2: Effect of solidification pressure on the tensile properties of the cast Al-3.75 Mg matrix alloy (room temperature)

(Values in brackets represent the average)

Solidification Pressure MPa	UTS MPa	0.1% PS MPa	Elastic Modulus GPa	Elongation %	Reduction in Area %	Remarks
0.1 (Gravity die cast)	174 173 172 171 (172.5)	93 92 91 90 (91.5)		8 7.5 7.5 8 (7.75)	7.5 7 6.5 7 (7)	
70	207 206 205 205 (205.75)	121 120 119 119 (119.75)		15 14.5 14 14 (14.4)	14 13.5 13 13 (13.4)	
94	219 220 221 218 (219.5)	128 127 129 130 (128.5)		16 15.5 15 15.5 (15.5)	15.5 15 14 15 (14.9)	
140	231 229 230 228 (229.5)	142 139 138 141 (140)		18 17 16.5 16.5 (17)	16.5 16 15.5 15.5 (15.9)	
188	236 234 233 236 (234.7)	145 146 143 142 (144)		18.5 18 17.5 17.5 (17.9)	17 17 16.5 16.5 (16.7)	
Sand cast	146 144 143 147 (145)	86 84 85 87 (85.5)		6.5 6 5.5 6 (6)	6 5.5 5 5.5 (5.5)	

TABLE A3.3: Tensile properties of the Al-4.5 Cu matrix/SiC fibre, composite. Castings group IV.

(Values in brackets represent the average)

Volume % Fibre	UTS MPa	0.1% PS MPa	Elastic Modulus GPa	Elongation %	Reduction in Area %	Remarks
0	182	109	70.9	16	14.5	
	183	107	70.5	15	14	
	186	107	70.6	15.5	14	
	185	108	70.4	14.5	13.5	
	(184)	(107.7)	(70.6)	(15.2)	(14)	
2	185	125	75	4.5	8.5	
	187	123	74	9	8	
	182	122	73.5	8.5	7.5	
	186	126	73.5	9	8	
	(185)	(124)	(74)	(9)	(8)	
4	181	143	80	6	5	
	179	144	78	5.5	4.5	
	183	141	79	4.5	4	
	185	140	78.5	5	4	
	(182)	(142)	(78.9)	(5.2)	(4.4)	
6	180	158	83	5	4	
	177	157	81	4.5	3.5	
	177	155	80	5	3	
	182	153	82	4.5	3.5	
	(179)	(155.7)	(81.5)	(4.75)	(3.5)	
8	177	165	84	6	5.5	
	174	166	83	5	4	
	176	162	81.5	5.5	4	
	173	161	83.5	5	3.5	
	(175)	(163.5)	(83)	(5.4)	(4)	
10	174	171	83	3	2	
	168	168	81.5	2	1	
	172	167	83	2.5	2	
	174	170	81.5	2.5	2	
	(172)	(169)	(82)	(2.5)	(1.7)	

TABLE A3.4: Tensile properties of the Al-3.75 Mg matrix/ Al_2O_3 fibre composite. Casting group IV.

(Values in brackets represent the average).

Volume % Fibre	UTS MPa	0.1% PS MPa	Elastic Modulus GPa	Elongation %	Reduction in Area %	Remarks
0	233 229 228 231 (230.2)	147 145 144 148 (146)	72 70.5 71 70.5 (71)	17 17.5 18 16 (17.1)	16 16 16.5 15 (15.9)	
2	229 226 225 228 (227)	164 162 160 162.5 (162.1)	71 70.5 70 71.5 (70.7)	10 9 8.5 9.5 (9.2)	8 7.5 6 7 (7.1)	
4	225 221 223 223 (223)	176 172 175 173 (174)	71 71.5 70 70.5 (70.7)	6 5 5 4.5 (5.1)	5 4 4 3.5 (4.1)	
6	219 216 215 220 (217.5)	184 181 178 183 (182)	71 71.5 70 71 (70.9)	4 3 3.5 3 (3.4)	3.5 2.5 2.5 2 (2.6)	
8	211 217 212 216 (214)	190 186 184 188 (187)	72 71.5 70.5 71 (71.2)	3.5 3 2.5 3 (3)	3 2 2 2.5 (2.4)	
10	209 204 201 206 (205)	197 192 187 196 (193)	72 71.5 70 69 (70.6)	2.5 2 2.5 1.5 (2.1)	2 1 1.5 1 (1.4)	

TABLE A3.5: Effect of contact time between silicon carbide fibre and the Al-4.5 Cu matrix alloy on the room temperature tensile properties of squeeze cast composites containing 4 volume percent fibre

(Values in brackets represent the average)

Contact Time Mins	UTS MPa	0.1% PS MPa	Elastic Modulus GPa	Elongation %	Reduction in Area %	Remarks
8	185 186 188 188 (186.7)	114 112 111 111 (112)	73 71 72 72 (72.2)	13 12 12 12.5 (12.4)	12 11 11 11.5 (11.4)	
13	194 192 193 191 (192.5)	130 129 127 127 (128.2)	74 73 74 75 (74)	12.5 12 11.5 12 (12)	11.5 11 11 10.5 (11)	
18	194 195 196 195 (195)	140 138 137 139 (138.5)	76 75 74 76.5 (75.4)	11.5 11 11 11.5 (11.2)	10 10 9 10 (9.7)	
28.5	184 181 182 183 (182.5)	149 150 148 146 (148.2)	78 77 76 78 (77.2)	10 9 8.5 9 (9.1)	8.5 7.5 7 8 (7.7)	
39	171 170 174 173 (172)	153 152 151 151 (151.7)	76 75 74 74 (74.7)	6.5 7 6 5.5 (6.2)	5 5.5 5 4.5 (5)	

TABLE A3.6: Effect of contact time between alumina fibre and the Al-3.75 matrix alloy on the room temperature tensile properties of squeeze cast composites containing 4 volume percent fibre

(Values in brackets represent the average).

Contact Time Mins	UTS MPa	0.1% PS MPa	Elastic Modulus GPa	Elongation %	Reduction in Area %	Remarks
6.5	225	147	71	15	14	
	219	141	70	14	13	
	218	146	68	14.5	13	
	222	145	68	13.5	12.5	
	(221)	(144.7)	(69.2)	(14.2)	(13.1)	
11.5	221	157	73	13	12	
	224	161	72	12.5	11	
	222	160	71.5	12	11	
	225	158	71.5	11.5	10.5	
	(223)	(159)	(72)	(12.2)	(11.1)	
15.5	228	167	73.5	12.5	12	
	224	164	73	12	11.5	
	223	161	72	11.5	10.5	
	229	166	73.5	11	10.5	
	(226)	(164.5)	(73)	(11.7)	(11.1)	
26.5	219	174	72.5	10	9	
	216	170	73	9	8	
	215	169	73.5	9	8	
	218	171	71	8.5	7.5	
	(217)	(171)	(72.5)	(9.1)	(8.6)	
36.5	205	180	72.5	5.5	5	
	197	176	70.5	5	4.5	
	198	175	70	5	4.5	
	204	177	71	4.5	4	
	(201)	(177)	(71)	(5)	(4.5)	

TABLE A3.7: Room temperature tensile properties of squeeze cast composites with up to 10 volume percent of silicon carbide fibre matrix alloy Al-4.5 Cu. Castings group VI.
(Values in brackets represent the average)

Volume % Fibre	UTS MPa	0.1% PS MPa	Elastic Modulus GPa	Elongation %	Reduction in Area %	Remarks
0	184 185 182 181 (183)	108 107 106 106 (106.7)	71 70 72 69 (70.5)	18 17 16 17.5 (17.1)	16.5 16 14 15.5 (15.5)	
2	188 186 185 187 (186.5)	124 122 121 124 (122.7)	74 72 73 71 (72.5)	14 13 15 12 (13.5)	12.5 12 13 11 (12.1)	
4	189 190 187 187 (188.2)	143 140 139 138 (140)	76 75 74 74.5 (74.8)	11 10.5 10 9.5 (10.2)	10 9 8.5 8 (8.9)	
6	192 188 187 192.5 (190)	157 155 154 157 (155.7)	78 77 77.5 76.5 (77.2)	6 7 5.5 5 (5.9)	5 5.5 4 4 (4.6)	
8	197 196 195 193 (195.2)	171 169 168 172 (170)	80.5 79 78.5 79.5 (79.4)	4.5 4 3.5 3.5 (3.9)	4 3 3 2.5 (3.1)	
10	201 196 197 195 (197.2)	186 183 185 184 (184.5)	83 81.5 82 81.5 (82)	3.5 3 3 2.5 (3)	3 2.5 2.5 2 (2.5)	

TABLE A3.8: Room temperature tensile properties of squeeze cast composites, with up to 10 volume percent of alumina fibre. Matrix alloy Al-3.75 Mg. Casting group VI
(Values in brackets represent the average).

Volume % Fibre	UTS MPa	0.1% PS MPa	Elastic Modulus GPa	Elongation %	Reduction in Area %	Remarks
0	228 227 232 234 (230.2)	144 145 147 148 (146)	70.5 70 71 72 (70.9)	17.5 18 16 16.5 (17)	16.5 16.5 15 15.5 (15.7)	
2	234 231 230 233 (232)	159 152 155 154 (155)	73 72 71.5 71.5 (72)	14 13.5 13 13.5 (13.5)	13 12.5 12 12 (12.4)	
4	238 234 235 237 (236)	166 163 163 162 (163.7)	74 72.5 73 72.5 (73)	11.5 11 11 10.5 (11)	10.5 10 9.5 9 (9.7)	
6	245 241 239 243 (242)	179 176 174 179 (177)	75 73.5 72.5 76.5 (74.4)	8.5 9 7.5 8 (8.1)	7.5 8 6.5 7 (7.2)	
8	243 239 238 241 (240.2)	183 179 178 181 (180.2)	76.5 75 74.5 75.5 (75.4)	7 6 5.5 5.5 (6)	6 5 5 4.5 (5.1)	
10	244 245 238 245 (243)	186.5 187 184 188 (186.4)	75 77 76 75.5 (75.9)	4.5 4 3.5 4 (4)	4 3.5 3 4 (3.6)	

TABLE A3.9: Room and elevated temperatures tensile properties of the squeeze cast Al-4.5 Cu matrix/SiC fibre composite. Casting group VII.

(Values in brackets represent the average)

Volume % Fibre	UTS MPa	0.1% PS MPa	Elastic Modulus GPa	Elongation %	Reduction in Area %	Remarks
0	184	107	71	17	15	
	183	105	70	16	15	
	181	104	70.5	15	13	
	182	105	71.5	16	14	
	(182.5)	(105.2)	(70.7)	(16)	(14.2)	
Room Temperature						
2	186	123	74	13	12	
	184	121	73.5	12	11	
	182	119	73	12	11	
	183	121	73	11	10.5	
	(183.7)	(121)	(73.4)	(12)	(11.1)	
4	188	137	76	10	9	
	187	135	75	9	8	
	186	135	74.5	8.5	7.5	
	191	137	76.5	8.5	7.5	
	(188)	(136)	(75.5)	(9)	(8)	
6	194	154	79	6	5	
	191	151	78	5	4.5	
	192	152	77.5	4.5	4	
	191	155	78	5	4.5	
	(192)	(153)	(78.1)	(5.1)	(4.5)	
8	196	168	80	4	3	
	194	167	80.5	4.5	3	
	194	165	79	3.5	3	
	197	167	79.5	4	3	
	(195.2)	(166.7)	(79.7)	(4)	(3)	
10	198	185	81.5	3.5	3	
	200	187	83.5	3	2.5	
	196	182	82	2.5	2	
	197	183	81.5	3	2.5	
	(197.7)	(184.2)	(82.1)	(3)	(2.5)	

/Continued...

TABLE A3.9: continued

Volume % Fibre	UTS MPa	0.1% PS MPa	Elastic Modulus GPa	Elongation %	Reduction in Area %	Remarks
0	167	95	150°C 66	27	25	
	165	94	64	26	25	
	164	93.5	67	25	24	
	166	93.5	64	26	24	
	(165.5)	(94)	(65.2)	(26)	(24.5)	
2	173	113	71	21	19.5	
	171	112	70.5	19	18	
	168	110	69	18	17	
	169	111	69.5	19	17.5	
	(170.2)	(111.5)	(70)	(19)	(18)	
4	175	123	74.5	14	12.5	
	172	121	73	12	11	
	173	120	72.5	11	10.5	
	176	124	73.5	12	11	
	(174)	(122)	(73.4)	(12.2)	(11.5)	
6	183	146	77	9	8	
	179	144	76	8	7.5	
	180	143	75.5	8.5	7	
	182	146	76.5	8	7.5	
	(151)	(144.7)	(76.2)	(8.5)	(7.5)	
8	187	160	80	7	6	
	186	162	78	5.5	5	
	188	161	78.5	6	5.5	
	185	162.5	79.5	5.5	5	
	(156.5)	(161.4)	(79)	(6)	(5.5)	
10	191	178	82.5	4	4	
	190.5	175.5	81	4.5	4	
	188.5	176	81.5	4	3.5	
	189	178.5	81.5	3.4	3.5	
	(189.7)	(177)	(81.6)	(4)	(3.7)	

/Continued...

TABLE A3.9: continued

Volume % Fibre	UTS MPa	0.1% PS MPa	Elastic Modulus GPa	Elongation %	Reduction in Area %	Remarks
0	124	93	2000C 63	33	34	
	121	91	62	29	30	
	117	88	81	31	29	
	118	89	62	33	32	
	(120)	(90.2)	(62)	(31.5)	(31.2)	
2	133	109	68	24	22	
	129	105	67.5	21	19	
	128	104	67	23	22	
	134	110	67.5	20	19	
	(131)	(107)	(67.5)	(22)	(20.5)	
4	136	117	70	17	16	
	141	122	71	16	15	
	142	121	71.5	15	14	
	140	120	71	15.5	14	
	(139.7)	(120)	(70.5)	(15.9)	(14.7)	
6	152	136	72.5	13	12	
	144	133	73	11	10	
	148	133	73.5	12	11	
	151	135	74.5	12	11	
	(150)	(135.2)	(73.4)	(12)	(11)	
8	158	150	75.5	9	8	
	159	149	76	8	7	
	161	152	76.5	7	6	
	162	153	76	8	6	
	(160)	(151)	(76.1)	(8)	(6.7)	
10	168	162	79	7	6	
	172	165	77.5	8	6	
	173	166	78.5	7	6	
	170	163	78	6	5	
	(171)	(164)	(78.2)	(7)	(5.75)	

/Continued...

TABLE A3.9: continued

Volume % Fibre	UTS MPa	0.1% PS MPa	Elastic Modulus GPa	Elongation %	Reduction in Area %	Remarks
0	78	73	58	38	40	
	76	72	57	35	38	
	77	75	57.5	34	35	
	77.5	76	57	40	44	
	(77.1)	(64)	(57.4)	(36.7)	(39.2)	
2	87	71	63	28	24	
	83	67	61.5	24	21	
	86	70	62	26	23	
	88	72	63	29	26	
	(86)	(70)	(62.4)	(26.7)	(23.5)	
4	88	80	66	20	17	
	93	81	64	18	16	
	90	78	65	16	15	
	93	77	67	19	17	
	(91)	(79)	(65.5)	(18.2)	(16.2)	
6	98	92	69	16	14	
	93	88	67.5	14	12	
	97	91	68.5	15	12	
	96	90	68	14	12	
	(96)	(90.2)	(68.2)	(14.7)	(12.5)	
8	107	96	71	10	9	
	102	93	70	9	8	
	104	94	70.5	8	8	
	103	93	69	9	7	
	(104)	(94)	(70.1)	(9)	(8)	
10	113	107	72	7	6	
	107	105	71	6	5	
	108	103	70.5	6	5	
	109	103	72.5	5	5	
	(109.2)	(104.5)	(71.5)	(6)	(5.2)	

/Continued..

TABLE A3.9: continued

Volume % Fibre	UTS MPa	0.1% PS MPa	Elastic Modulus GPa	Elongation %	Reduction in Area %	Remarks
0	51	35	300 ^o C	46	51	
	47	32		41	48	
	46	33		38	45	
	49	33		47	54	
	(48.2)	(33.2)		(43)	(49.5)	
2	53	38		33	26	
	48	34		29	23	
	52	37		31	25	
	51	38		28	22	
	(51)	(36.7)		(30.2)	(24)	
4	57	38		23	19	
	51	33		17	16	
	53	36		18	16	
	55	34		22	18	
	(54)	(35.2)		(20)	(17.2)	
6	59	48		19	17	
	54	43		18	16	
	53	44		15	14	
	58	46		16	15	
	(56)	(45.2)		(17)	(15.5)	
8	63	45		12	11	
	60	42		9	9	
	58	41		10	10	
	63	44		9	9	
	(61)	(43)		(10)	(9.7)	
10	63	47		8	7	
	67	51		7	6	
	65	50		6	5	
	66	49		7	7	
	(65.2)	(49.2)		(7)	(6.2)	

TABLE A3.10: Room and elevated temperature tensile properties of the squeeze cast Al-3.75 Mg matrix/ Al_2O_3 fibre composite. Casting group VII

(Values in brackets represent the average).

Volume % Fibre	UTS MPa	0.1% PS MPa	Elastic Modulus GPa)	Elongation %	Reduction in Area %	Remarks
Room temperature						
0	236	148	71.5	19	17	
	229	143	70.5	18	16	
	227	147	70	17	15	
	232	146	71.5	20	17	
	(231)	(146)	(70.9)	(18.5)	(16.2)	
2	236	161	72	13	11	
	231	155	71	15	13	
	228	154	71.5	13	12	
	237	158	71	15	13	
	(233)	(157)	(71.4)	(14)	(12.2)	
4	234	162	73	12	11	
	238	166	72.5	11	10	
	237	167	73.5	11	11	
	235	161	72.5	12	11	
	(236)	(164)	(72.9)	(11.5)	(10.7)	
6	243	178	74	9	8	
	240	177	73.5	8	8	
	238	175	73	9.5	9	
	239	174	74	10	9	
	(240)	(176)	(73.6)	(9.1)	(8.5)	
8	244	177	74	7	6	
	238	180	75	6	5.5	
	241	179	76	6.5	6	
	237	176	76	5.5	5	
	(240)	(178)	(75.2)	(6.2)	(5.6)	
10	247	189	76	5	4	
	244	167	75	5.5	4	
	242	184	75.5	6	4.5	
	243	184	76	4	3	
	(244)	(186)	(75.6)	(5.1)	(3.9)	

/Continued..

TABLE A3.10: continued

Volume % Fibre	UTS MPa	0.1% PS MPa	Elastic Modulus GPa	Elongation %	Reduction in Area %	Remarks
0			150°C			
	215	131	66	28	26	
	209	128	65	24	22	
	210	130	64.5	25	23	
	210	127	68	27	25	
	(211)	(129)	(65.9)	(26)	(24)	
2	211	141	70	22	20	
	214	143	68	19	16	
	213	138	69	20	18	
	212	138	68.5	23	21	
		(212.5)	(140)	(68.9)	(21)	(19.2)
4	212	145	71	15	13.5	
	216	149	70.5	13	12	
	213	146	70	12	11	
	215	148	70	14	12.5	
		(214)	(147)	(70.4)	(13.5)	(122)
6	217	159	71.5	10	9	
	221	163	72.5	9	8	
	223	162	73	8	7	
	215	160	71	9	7	
		(219)	(161)	(72)	(9)	(7.7)
8	223	171	74	7	6	
	219	167	73	6	5.5	
	220	170	73.5	6	5.5	
	222	166	74	7	7	
		(221)	(168.5)	(73.6)	(6.5)	(6)
10	221	178	75	6	5.5	
	225	182	75.5	4.5	5	
	226	181	74	5	4.5	
	220	179	74.5	5	5	
		(223)	(180)	(74.7)	(5.1)	(5)

/Continued...

TABLE A3.10: continued

Volume % Fibre	UTS MPa	0.1% PS MPa	Elastic Modulus GPa	Elongation %	Reduction in Area %	Remarks
0	176	115	63	37	39	
	179	119	64	33	34	
	181	117	63.5	36	38	
	176	118	63	34	37	
	(178)	(117.2)	(63.4)	(35)	(37)	
2	188	129	67	27	23	
	185	127	66	23	19	
	186	126	65	25	21	
	185	130	66	21	17	
	(186)	(128)	(66)	(24)	(20)	
4	193	139	69	17	15	
	191	135	67	18	15.5	
	186	133	67.5	19	16	
	190	137	68.5	19	17	
	(190)	(136)	(68)	(18.25)	(15.9)	
6	196	155	71	14	12	
	191	149	70	12	10	
	192	150	70.5	12	11	
	193	150	70	13	10	
	(193)	(151)	(70.4)	(12.7)	(10.7)	
8	203	164	72	9	8	
	202	162	71	10	9	
	198	160	70.5	12	10	
	205	166	72.5	9	8	
	(202)	(163)	(71.5)	(10)	(8.7)	
10	201	170	73	8	7	
	206	173	74	7	7	
	207	175	72	6	6	
	202	171	74.5	8	7.5	
	(204)	(172.2)	(73.4)	(7.25)	(6.9)	

/Continued...

TABLE A3.10: continued

Volume % Fibre	UTS MPa	0.1% PS MPa	Elastic Modulus GPa	Elongation %	Reduction in Area %	Remarks
0	127	106	250 ^o C 60	44	47	
	126	104	58	40	44	
	125	102	57.5	43	46	
	128	100	60.5	45	47	
	(126.5)	(103)	(59)	(43)	(46)	
2	131	112	62	36	32	
	137	116	63	33	28	
	138	117	63	32	27	
	134	115	61	35	31	
	(135)	(115)	(62.2)	(34)	(29.5)	
4	141	125	65	23	20	
	138	122	64	19	16	
	137	121	64.5	22	18	
	140	126	65	24	20	
	(139)	(123.5)	(64.6)	(22)	(18.5)	
6	145	131	68	18	17	
	149	134	67	17	16	
	151	137	67.5	16	15	
	147	130	66.5	16	16	
	(148)	(133)	(67.2)	(16.7)	(16)	
8	154	148	70	10	9	
	156	147	69	12	11.5	
	150	144	68	11	10	
	152	145	69	12	10.5	
	(153)	(146)	(69)	(11.2)	(10.2)	
10	161	155	70.5	8	7	
	165	157	71.5	6	5	
	164	156	71	6	6	
	162	158	72	7	6	
	(163)	(156.5)	(71.2)	(6.7)	(6)	

/Continued...

TABLE A3.10: continued

Volume % Fibre	UTS MPa	0.1% PS MPa	Elastic Modulus GPa	Elongation %	Reduction in Area %	Remarks
0	83 99 97 95 (96)	54 58 57 55 (56)	300°C	54 48 49 53 (51)	58 33 54 58 (55.7)	
2	101 108 106 105 (105)	67 69 70 70 (69)		43 38 39 44 (41)	39 36 35 41 (37.7)	
4	105 111 109 107 (108)	81 80.5 80 80.5 (80.5)		34 29 30 35 (32)	26 20 19 24 (22.2)	
6	112 115 112 116 (113.7)	92 95 91 94 (93)		20 22 19 22 (20.7)	15 16 13 15 (14.7)	
8	125 122 121 126 (123.5)	112 108 107 113 (110)		13 11 11 12 (11.7)	11 8 9 10 (9.5)	
10	131 135 132 136 (133.5)	122 124 123 125 (123.5)		10 9 8 8 (8.75)	8 9 7 7 (7.7)	

A P P E N D I X I V

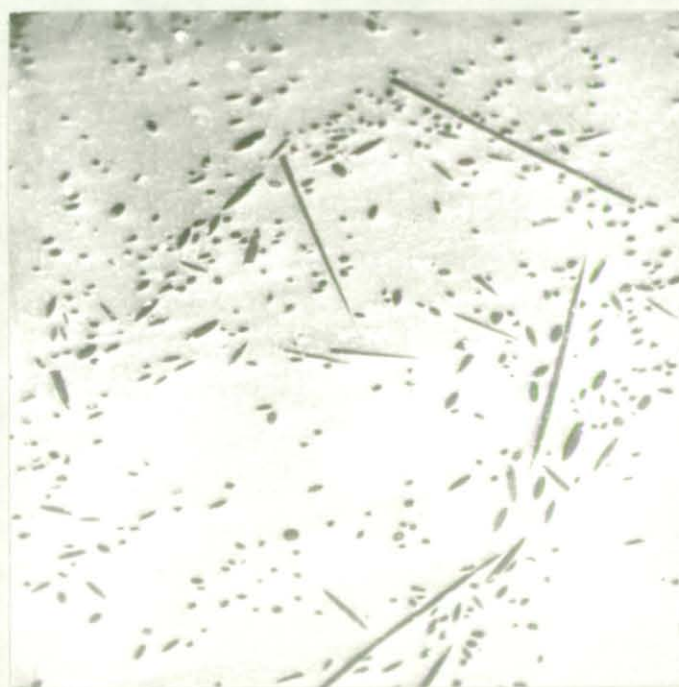


FIGURE A4.1: Fibre distribution and orientation (Al-4.5 Cu/SiC composite)
Silicon carbide fibre at two perpendicular planes x80

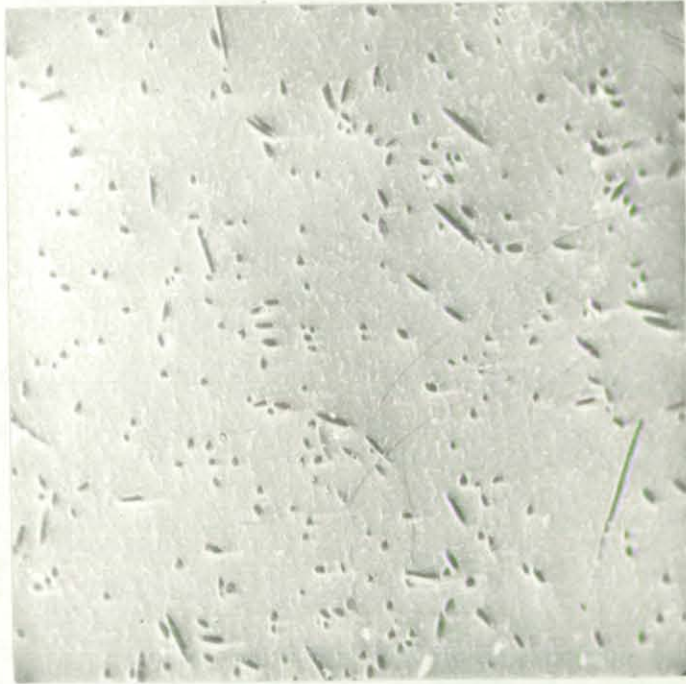
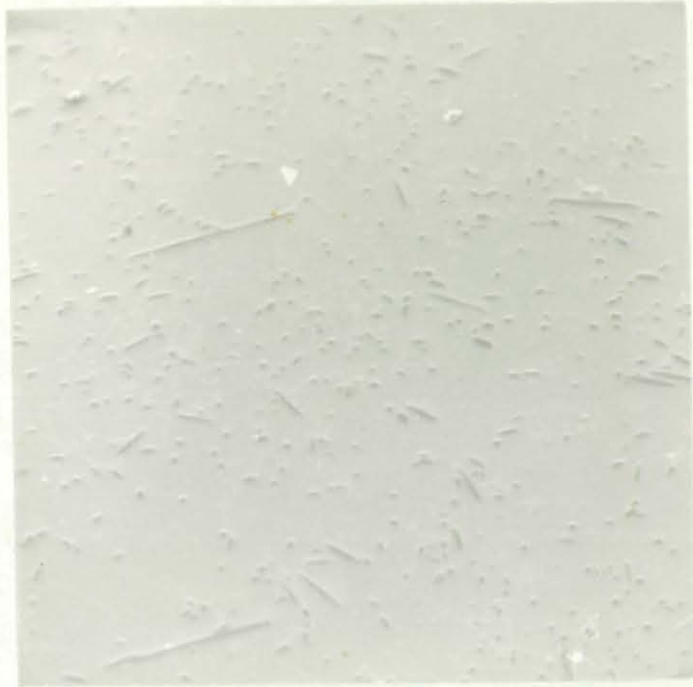


FIGURE A4.2: Fibre distribution and orientation (Al-4.5 Cu/SiC composite)

- a) 8% v/v silicon carbide fibre x50
- b) 6% v/v silicon carbide fibre x80

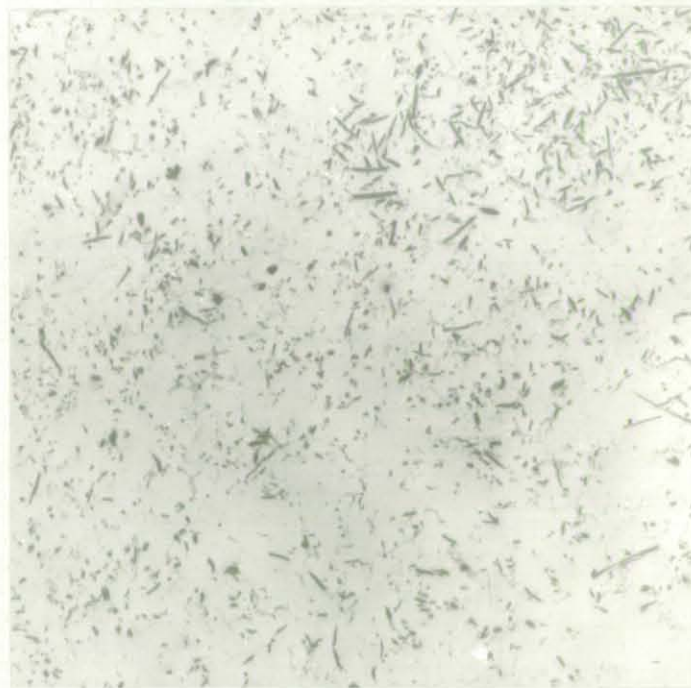
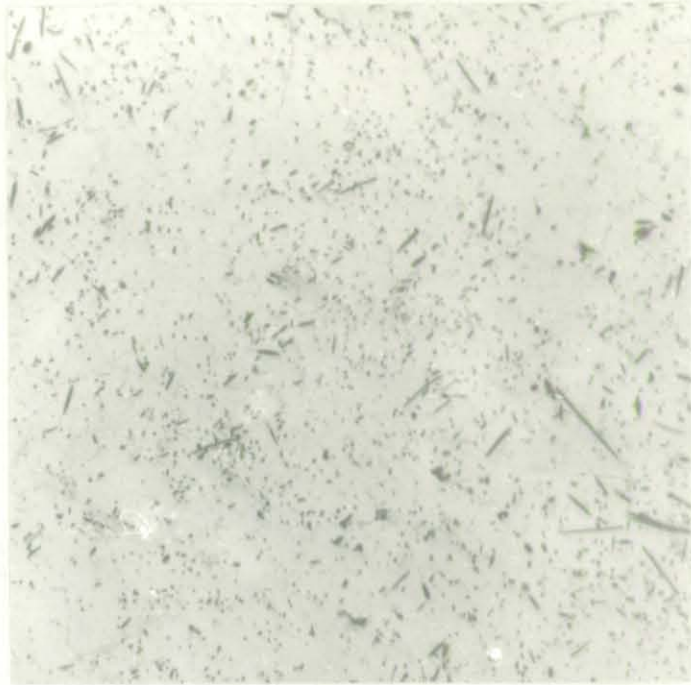


FIGURE A4.3: Fibre distribution and orientation ($\text{Al-3.76 Mg/Al}_2\text{O}_3$ composite).

Alumina fibre at two perpendicular planes x100 (10% v/v)

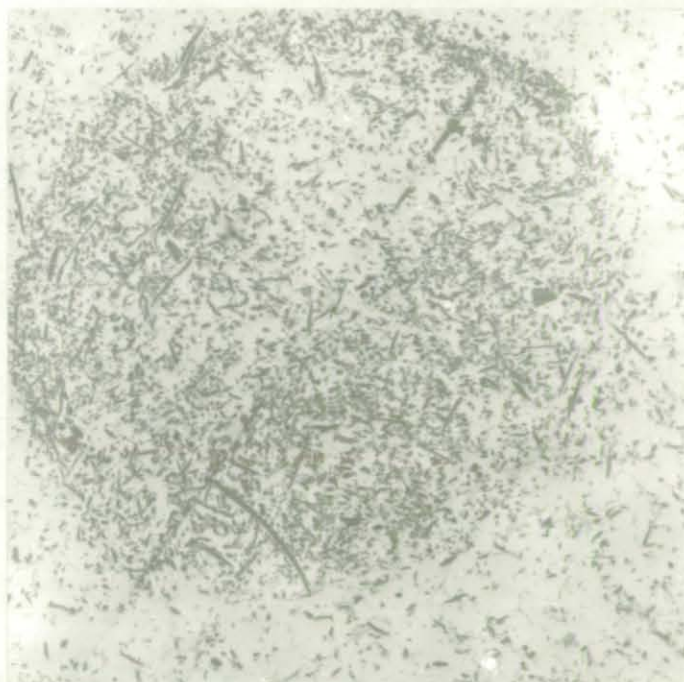


FIGURE A4.4: Fibre distribution.

Poor dispersion of alumina fibre in the Al-4.5 Cu matrix (castings group III). 10% v/v fibre

